The background is a textured oil painting. A woman with dark, curly hair stands in the center-right, wearing a purple dress and a bright orange shawl. To her left is a large, brown, segmented, worm-like creature that curves around her. The landscape is a mix of brown and green fields under a sky with a prominent rainbow. The overall style is expressive and somewhat somber.

**BIOGEOCHEMICAL
INTERACTIONS**
in DELTA SYSTEMS:
present state and future challenges

Dunia Rios Yunes

*Biogeochemical interactions in
delta systems: present state
and future challenges*

ISBN: 978-94-6469-786-5

DOI: 10.33540/2139

Cover design by Stefanie van den Herik

This research was conducted at the Royal Netherlands Institute for Sea Research and was financially supported by the Royal Netherlands Academy of Arts and Sciences (KNAW) with project number PSA-SA-E-02.

Printed in The Netherlands

Copyright © 2024 Dunia Rios Yunes

All rights reserved. No part of this publication may be reproduced in any form, by print or photo print, microfilm, or any other.

Biogeochemical interactions in delta systems: present state and future challenges

Biogeochemische interacties in deltasystemen: huidige stand
en toekomstige uitdagingen

(met een samenvatting in het Nederlands)

Interacciones biogeoquímicas en sistemas deltaicos: estado
presente y futuros desafíos

(con un resumen en Español)

Proefschrift

ter verkrijging van de graad van doctor aan de
Universiteit Utrecht
op gezag van de
rector magnificus, prof. dr. H.R.B.M. Kummeling,
ingevolge het besluit van het college voor promoties
in het openbaar te verdedigen op

vrijdag 1 maart 2024 des middags te 2.15 uur

door

Dunia Rios Yunes

geboren op 27 augustus 1992
te Mexico-Stad, Mexico

Promotor:

Prof. dr. K.E.R. Soetaert

Copromotor:

Dr. Dick van Oevelen

Dr. Tom Ysebaert †

Beoordelingscommissie:

Prof. dr. Tjeerd Bouma

Prof. dr. Ulrike Braeckman

Prof. dr. Jack Middelburg

Prof. dr. ir. Katja Philippart

Dr. Christophe Rabouille

Dit proefschrift werd (mede) mogelijk gemaakt met financiële steun van de Koninklijke Nederlandse Akademie van Wetenschappen (KNAW) met project no. PSA-SA-E-02.

Acknowledgements

I would not be able to start my acknowledgements without thanking the people who gave me the opportunity of doing a PhD at NIOZ. Prof. Dr. Karline Soetaert and Dr. Tom Ysebaert. When I think about the day of my interview for this position, I always remember it was a very pleasant and fun conversation that left me with a very nice feeling. A feeling that has remained throughout my PhD. Thank you for believing in me.

The success of a PhD is highly determined by the supervisors. In my case, I have been very lucky to have been guided by Karline, Dr. Dick van Oevelen, and Tom. Your supervision and guidance allowed me to develop as an independent researcher and to find my voice in my own terms. Above all, you contributed to making my PhD a very enjoyable and challenging learning experience.

Karline, one of the things that I liked the most about our meetings was that there was always space for laughter in between all the science and complicated biogeochemistry talk. I always felt encouraged by you, even when it took me some time to wrap my head around some complicated concepts. I also liked that you challenged my ideas and perceptions and were critical about my lines of thought. Over time, this pushed me to develop sound and substantiated arguments that would satisfy one of my most thorough critics. Although most of our interaction occurred in the office, you also had the opportunity to assess and direct my field work technique. For instance, in China, where you were observing me, crawling in the mud, while standing clean on the salt marsh... I guess this is one of the perks that comes with being a great supervisor! I have learnt a lot from you as a person and as a colleague. I will forever be thankful to you for choosing me as your student and I consider myself very lucky to have developed myself as a researcher under your guidance.

Dick, we started working together a little over a year after my PhD started and I can only thank you for accepting to supervise me. You were a great supervisor not only because you gave me crucial support during (several) complicated times, but also because you are always happy to discuss topics that extended beyond the PhD project. You have had a substantial contribution to the quality of this thesis by providing a different, fresh, and critical perspective on this work.

Tom, you were one of the people that chose me to embark on this adventure. One of the things that I remember the most is how keen you were on collaboration and cooperation; you understood that great things cannot be accomplished alone. You were one of the master minds behind the PSA project, a project that would enhance Sino-Dutch cooperation, develop coastal science, and touch the lives of many researchers and students. Although our collaboration was unfortunately cut short, I will always remember

you as an inquisitive, sharp, encouraging, and friendly supervisor. Above all, I will always remember you as one of the most influential people of my career.

(soon Dr.) Tim Grandjean, my friend, we started our PhD at the same time in the same project and we have lived through so many things together. In the beginning of our PhD, I remember you used to come say “hi” to my office every day. This is something that over time became a daily ritual that I looked forward to. We also went to China together, and that was such a fun experience full of beautiful memories. We would start the days eating steamed buns with hot soy milk before going to the field and getting completely covered in mud. Then, we would return to the lab, make a mess, clean it, sleep in a sofa until someone came to pick us up, and we would end the day with delicious Chinese food. One of my fondest memories of what also turned out to be a culinary adventure is how you said you would NEVER eat one of the animals (turtle, snake, etc.) from the restaurant’s aquarium. But little did you know that the dish you so much liked was indeed frog! The face you made when this information was disclosed was absolutely priceless! Our memories together are not only confined to our Chinese trip. We have also had our share of adventure in The Netherlands, like that time when you pulled me on a sledge in the mudflat because I didn’t bring my boots, or when you had to crawl out of the mud because you were SUPER stuck, or that other time when you almost killed me of hypothermia in the field. The cherry on top of all these beautiful memories, is that we have also created a very nice friendship. Sharing my PhD journey with you has been a wonderful experience!

Dr. Justin Tiano, you were also in that job interview, but little did I know about how important you would be during my PhD. One thing I vividly remember is that during my first days at De Keete you came and told me that I had been chosen for the PhD position “not because of my knowledge, but because of my potential...”. You couldn’t have chosen a better better way to make me feel at ease! This comment, naturally, stayed with me during the PhD. And it assured me that I had the “something” and the skills that made me the right person for this position. In addition to being a great colleague, you (and Alex) became my friends. Whenever I had to spend time- often endless hours- with you in the lab, I knew it was going to be fun and full of very interesting and engaging conversations that lasted for hours on end, and sometimes even longer than the lab work itself... I must confess I miss it. We collaborated in many interesting projects, but the most memorable of them all was when we had to carry hundreds of kilos of sand for our experiment. That was intense work! and it even made me wonder if I was instead doing a PhD in the art of carrying sand.

Dr. Olivier Beauchard I would like to thank you because even when you are extremely busy you were ready to lend a helping hand and give constructive feedback and ideas. You were always supportive and willing to help, not only me, but also all those lost PhD students that come to you in search for some light in the darkness of statistics. It has been great collaborating with you.

Dr. Emil De Borger, Prof. Dr. Tjeerd Bouma, Prof. Dr. Johan van de Koppel, Prof. Dr. Peter Herman, thank you for the valuable input, interesting conversations, discussions, and all the challenging questions you raised about my research. You pushed me to think, reassess my thought process, and to polish my ideas.

Special thanks to the technicians Anton, Daniel, Lennart, Peter, Pieter, Jan, Jeroen, Jurian and Yvonne, they were an integral and fundamental part of my PhD thesis. We spent some nice times in the field and in the lab. Thank you for your support and ideas and ensuring the quality of my results. I would like to especially thank Pieter van Rijkswijk, Anton Tramper and Jeroen van Dalen for teaching me the techniques that I would use for the rest of my PhD and helping me in all my very intensive sampling campaigns. Also, thanks to Peter van Breugel for being always eager to help and engage in fun conversations at lunch, or at the corridor, or anywhere really. And Jan Peene for always having a very positive attitude and making people smile. Thank you to Jan Megens for making sure that everything ran smoothly and we always had enough coffee for fuel and to Christine de Zeeuw for always greeting us with a friendly face at the reception.

Thanks to “my” students Bo Bosschaart, Hasan Al Yamani, Ivory Maast, Nicole Brackenborough, Sietse de Wal, Sophia Suvacarov, Thiri Naing, Ymke Temmerman and Naomi Bakken. Collaborating with you was a great experience. We had to work through some difficult and uncertain times, and in some cases our projects had to be completely changed due to the coronavirus pandemic restrictions. Some of you even had to be supervised 100% online and we never had the opportunity to meet in person. Nevertheless, we managed to overcome these difficulties and produce good results. I hope you keep on working hard and have a successful future.

Aditi, Archontoula, Coco, Eleonora, Loreta, Pieter, Stef, Ricky and Zhengquan your friendship has been the sprinkles of my PhD. I am so happy to have you as friends and for all the fun times we have spent together. Thanks to all the other PhD's and BOZ people Alena, Alice, Carolina, Celine, Chiu, Colin, Evert, Jaco, Lander, Lauren, Lixia, Marte, Mingxuan, Mo, Rosanna, Tim H., Ting, Tori, and many others for the nice conversations, pick nicks, pool nights, runs and fun outings.

Mamá, Papá y Tiano aunque estemos físicamente lejos, nuestros corazones estan juntos. Muchas gracias por siempre darme su apoyo y aliento incondicional y por impulsarme a conseguir lo que me propongo. Sin ustedes yo no hubiera logrado llegar hasta aquí. Los quiero mucho.

Zach, you have been a crucial person for the completion and success of this project. You were with me every step of the way and unconditionally supported me through the good, the bad, and the ugly. Thanks a lot for your patience and understanding. My success has been in great part linked to you having been there by my side.

Last, but not least, I want to thank myself for all the hard work, endurance, discipline, and perseverance that I put into this project. And most importantly for always believing in myself.

“It is a curious situation that the sea, from which life first arose should now be threatened by the activities of one form of that life. But the sea, though changed in a sinister way, will continue to exist; the threat is rather to life itself.”

Rachel Carson, *The Sea Around Us*, 1961

Contents

Chapter 1	Introduction	I
Chapter 2	Long-term changes in ecosystem functioning of a coastal bay expected from a shifting balance between intertidal and subtidal habitats	21
Chapter 3	Annual biogeochemical cycling in intertidal sediments of a restored estuary reveals dependence of N, P, C and Si cycles to temperature and water column properties	49
Chapter 4	Influence of benthic fauna on intertidal sediment biogeochemistry along the estuarine salinity gradient	73
Chapter 5	Sediment resuspension enhances nutrient exchange in intertidal mudflats	97
Appendix A	How do estuaries improve water quality?	131
	Summary	137
	Sammenvating	139
	Resumen	141
	Short Curriculum Vitae	143
	Bibliography	145

Chapter I *Introduction*

1.1 Estuaries

Estuaries are transition zones that connect terrestrial and marine ecosystems. They are dynamic environments with high spatiotemporal variability in their physical, chemical, and biological characteristics (Heip et al., 1995; Mateus et al., 2008). The main defining feature of an estuary is the longitudinal salinity gradient that originates from the mixing of riverine and marine water and determines the biogeochemical processes and biological communities that exist within (Ysebaert et al., 1998; Bianchi, 2007; Rios-Yunes et al., 2023b). Salinity is the main factor used to differentiate between the three main parts of an estuary (Bianchi, 2007): the freshwater zone is the area closest to land, it is fluvial-dominated and carries sediments and fresh water from upstream; the brackish zone, also known as the "body of the estuary", is where freshwater from rivers and streams mixes with marine water, and it is typically influenced by riverine, tidal, and wave processes; the marine zone, or "the mouth of the estuary", is where the estuary connects with the sea and the salinity is marine (Figure 1.1A).

Estuaries also have a vertical gradient that is determined by elevation, inundation, and tidal range. The estuarine coast is divided into three zones: the supratidal, the intertidal, and the subtidal (Figure 1.1B). The intertidal zone comprises the area between the highest high-water mark and the lowest low-water mark (Dipper, 2022) and is subject to intermittent exposure and inundation with each tidal cycle. These areas are under the constant influence of waves, currents, tides, precipitation, wind, light irradiance, desiccation, drainage, air intrusion, temperature changes, and freshwater runoff (Baugh et al., 1990; Falcão and Vale, 1998; Rocha and Cabral, 1998; Mateus et al., 2008; Fagherazzi et al., 2017). The confluence of these factors makes the intertidal zone one of the most dynamic areas of an estuary.

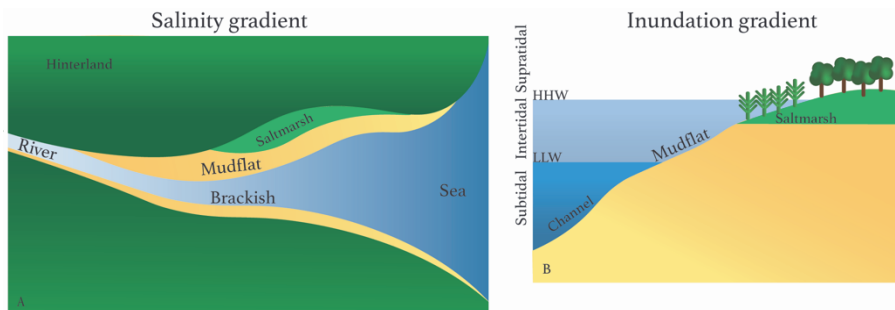


Figure 1.1 Panel A shows the horizontal salinity gradient from riverine freshwater to brackish and marine areas. The vertical gradient of the supratidal, intertidal, and subtidal zone is shown in panel B and depicts the high high-water (HHW) mark as the upper most boundary of the intertidal area and the low low-water (LLW) mark as the lowest boundary.

1.2 Mudflats

Mudflats form in sheltered intertidal areas where fine sediments deposit (Dyer, 1998; Friedrichs, 2011). They are composed of cohesive sediments with a higher content of mud to sand particles and are usually bordered in the upper boundary by a saltmarsh (Mateus et al., 2008; Friedrichs, 2011). Vertical structures like mud mounds, vegetation and conspicuous fauna are typically absent. Nevertheless, these areas support rich biological assemblages and are habitat to microphytobenthos, macroalgae, infauna and epifauna (Ysebaert et al., 1998; Mateus et al., 2008).

In addition to their biological relevance, mudflats are unique systems with a constant and important coupling between sedimentary, physical, chemical, and biological processes (Dyer, 1998). In fact, mudflats are amongst some of the most productive and biogeochemically active areas in the world (Yoshino et al., 2012; Byun et al., 2019; Serôdio and Paterson, 2021). As such, they play a crucial role in the global nutrient cycles as centres of not only transformation and recycling of organic matter (OM) and nutrients, but also nutrient exchange between sediments and the water column (i.e. benthic-pelagic nutrient exchange) (Serôdio and Paterson, 2021; Rios-Yunes et al., 2023b, 2023c).

1.2.1 *Mudflat biota*

The distribution of primary producers and fauna along the estuary is determined by their capacity to regulate and tolerate the different metabolic requirements imposed by changes in salinity (i.e. osmoregulation) (Dahl, 1956; Peterson and Ross, 1991; Rivera-Ingraham and Lignot, 2017), and results in a progression from freshwater to more marine species (Ysebaert et al., 1993; Soetaert et al., 1994a; Maris and Meire, 2017). The primary producers in mudflats include microphytobenthos and, to a lesser degree, macroalgae (Mateus et al., 2008). The microphytobenthos community in freshwater areas is usually dominated by euglenoids, green algae and freshwater diatoms, while marine diatoms gain dominance in the brackish and marine zones (Kromkamp and Peene, 1995a; Muylaert et al., 2002; Maris and Meire, 2017). The community structure of primary producers is typically influenced by seasonal fluctuations in light irradiance, turbidity, nutrient concentrations, and temperature (Soetaert et al., 1994a; Underwood et al., 1998; Maris and Meire, 2017). Notwithstanding, the microphytobenthos community of mudflats exhibits low temporal variability and a rather stable production independent of seasonality (Ysebaert et al., 1993, 1998; Terai et al., 2000; Rios-Yunes et al., 2023b).

Mudflats are also habitat to microbes (viruses, fungi, and bacteria), microbenthos (< 38µm), meiobenthos (32µm – 500µm), macrobenthos (500µm – 1 cm), and megabenthos (> 1cm) (Fenchel, 1978; Stratmann et al., 2020). The macrobenthos, which includes invertebrates such as polychaetes, oligochaetes, molluscs, and crustaceans (Queirós et al.,

Chapter 1

2013), live within or on the sediment, and are crucial to the mudflat ecosystem since they are the main food source for vertebrates such as mammals and migrating birds (Baugh et al., 1990; Ysebaert et al., 1993, 1998; Mateus et al., 2008).

In addition to being an important component of the estuarine trophic chain, macrobenthic organisms play a relevant role in the biogeochemical dynamics of mudflat sediments and estuarine ecosystems. Their bioturbating and bioirrigating activity has the potential to alter the sediment stability (Widdows et al., 2000a; Widdows and Brinsley, 2002; Dairain et al., 2020), influence the microbial community (Pelegrí and Blackburn, 1994; Deng et al., 2022), promote oxic conditions (Thoms et al., 2018), modify the benthic concentration of OM, chl a, and nutrients (Aller, 1982; Meysman et al., 2006; de Backer et al., 2011; Kristensen et al., 2012; Queirós et al., 2013), and even aid in sediment restoration (Lam-Gordillo et al., 2022). Thus, the activities of macrobenthos can have far reaching consequences for the biogeochemistry of mudflat sediments.

1.3 Benthic biogeochemistry

Biogeochemistry is the scientific discipline that explores the physical, chemical, biological, and geological processes and reactions that govern the composition of and control the structure and function of ecosystems (Box 1.1). It focuses on the analysis of the diverse and interlinked chemical cycles that are either driven by or have an impact on biological activity such as those of, for example, carbon, nitrogen, silicate, and phosphorus (Tartowski and Howarth, 2013).

Box 1.1 Transfer of nitrogen, phosphorus, and silicon between the atmosphere, lithosphere, hydrosphere, and biosphere.

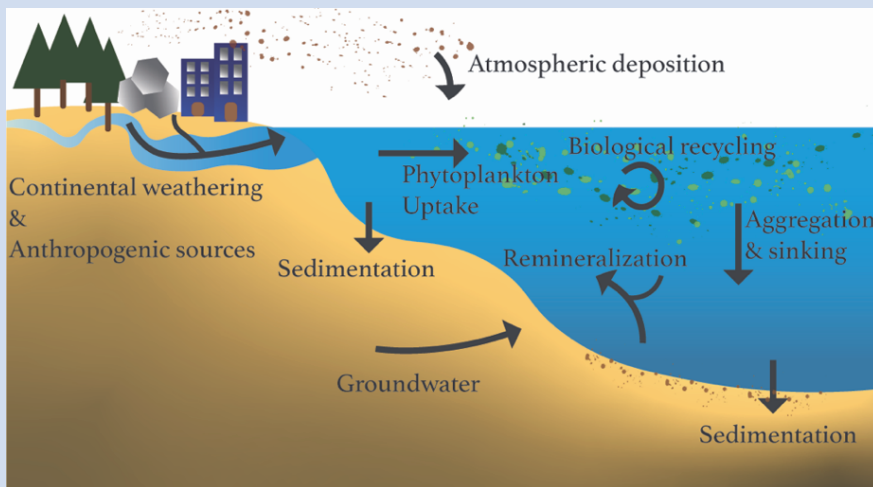
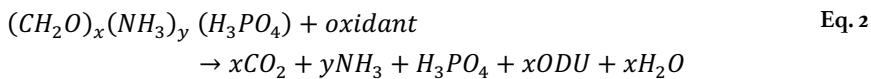
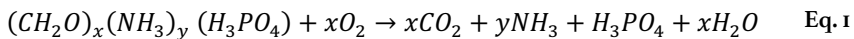


Figure 1.2 The transfer of nutrients between the lithosphere, atmosphere, hydrosphere, and biosphere is crucial for the nutrient cycles. The main sources of nutrients to the world's

oceans are terrestrial input, including anthropogenic input, groundwater, and atmospheric deposition. The atmosphere is the main sink for nitrogen, while the lithosphere is the main sink for phosphate and silicon. The remineralization of organic matter in the water column and the sediment enables the recycling of nutrients for biological consumption. Benthic remineralization in shallow systems and coastal areas has a relatively greater impact on pelagic primary production compared to the open ocean. This is because benthic processes influence a smaller volume of water in shallow areas. Image adapted from Tréguer et al. (1995); Slomp et al. (1996); Paytan and McLaughlin (2007); Slomp (2011).

Mudflats receive organic matter from autochthonous sources, e.g. microphytobenthos, and allochthonous sources, including input from rivers and seas and those of terrestrial origin such as debris, sewage, and fertilizers (Heip et al., 1995; Syvitski et al., 2005; Soetaert et al., 2006; Gilbert et al., 2007). After the OM deposits on the mudflat, it is incorporated into the sediment by, for example, sedimentation, tidal action, or macrobenthic activity. Thereafter, heterotrophs oxidize the OM in the oxic layer of the sediment by using oxygen (O_2) as an electron acceptor or oxidant (Eq. 1). Once the available O_2 has been utilized, alternative electron acceptors such as nitrite (NO_2^-), nitrate (NO_3^-), manganese(IV) (Mn^{4+}), iron(III) (Fe^{3+}), sulphate (SO_4^{2-}) and oxygen bound to OM are used in sequential order to obtain energy (Eq. 2, Figure 1.3, (Heip et al., 1995; Soetaert et al., 1996a; Canfield and Thamdrup, 2009; Arndt et al., 2013).



Where ODU stands for oxygen demand units associated with reduced substances produced during anoxic remineralization.

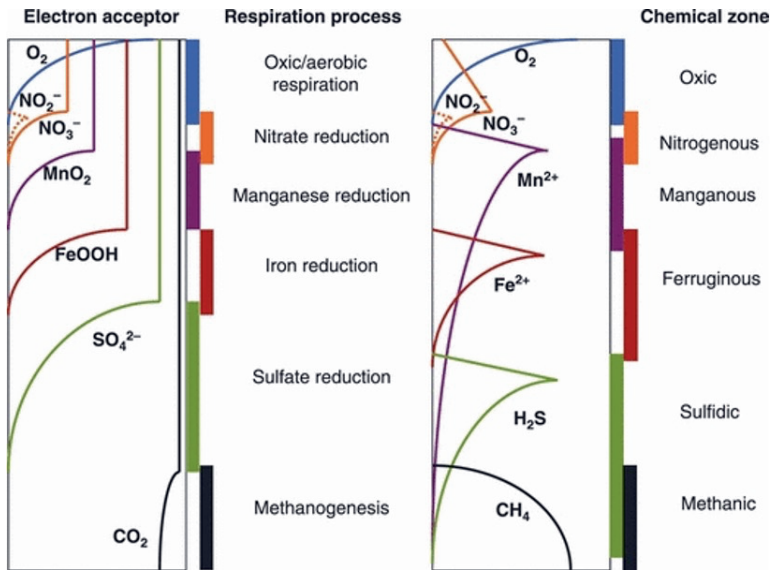


Figure 1.3 On the right, a scheme of the depth distribution of electron acceptors within the sediment and the main biogeochemical reactions consuming these oxidants. On the right, the name of the chemical zonation in which these reactions occur. Note that this is an abstraction and may not accurately represent the profiles and depth distribution found in nature. Schematic extracted from Canfield and Thamdrup (2009).

The remineralization of OM in mudflat sediments controls the recycling of inorganic carbon and nutrients. It is influenced by abiotic factors such as salinity, temperature, and OM reactivity (Arndt et al., 2013; Lessin et al., 2018; Tee et al., 2021; Rios-Yunes et al., 2023b), but also by biotic factors like benthic microbial and macrofauna activity (Braeckman et al., 2010a; De Berger et al., 2020). The magnitude of these influences can determine the efficiency in OM storage (Byun et al., 2019; Rios-Yunes et al., 2023c) and nutrient retention of different sediments and coastal environments (Rios-Yunes et al., 2023c, 2023a).

Chemical substances like carbon dioxide (CO_2), dissolved inorganic nitrogen (ammonium (NH_4^+), NO_2^- and NO_3^-), phosphate (PO_4^{3-}) and dissolved silicon (DSi) are released into the porewaters as products of oxic and anoxic remineralization. Thereafter, the nutrients can either remain stored within the sediment (Slomp et al., 1996; Herbert, 1999; Jordan et al., 2008; Rios-Yunes et al., 2023a); reach the sediment surface and the water column to be recycled and consumed by primary producers (Heip et al., 1995); or be removed by water currents. The benthopelagic exchange of nutrients, also known as flux, is essential for primary production and the overall productivity of coastal ecosystems as it can affect the water column concentration of NH_4^+ (Falcão and Vale, 1995; Cabrita et al., 1999), NO_2^- and NO_3^- (Koch et al., 1992; Usui et al., 1998), PO_4^{3-} (van der Zee et al., 2007; Jordan et al., 2008) and DSi (Yamada and D'Elia, 1984). Nevertheless, the efficiency of this exchange may be affected by changes in the macrobenthic community (Raffaelli et al., 2003), but also by

increased mudflat erosion and sediment resuspension derived from climate change and coastal management (e.g. dredging) (Kalnejais et al., 2010; Niemistö and Lund-Hansen, 2019; Rios-Yunes et al., 2023a).

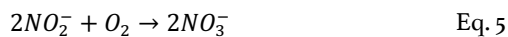
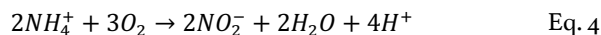
1.3.1 Nitrogen cycle

The aquatic nitrogen (N) cycle can be divided in three main parts: the incorporation of atmospheric nitrogen into the aquatic cycle; the retention, transformation, and recycling of biologically available nitrogen species; and the removal of nitrogen back into the atmosphere (Figure 1.4, Herbert, 1999; Thamdrup and Dalsgaard, 2002; Dedieu et al., 2007; Decleyre et al., 2015; Hutchins and Capone, 2022). The atmosphere is the greatest reservoir of nitrogen in the planet. However, this nitrogen exists primarily as molecular nitrogen (N_2), which cannot be easily assimilated by living organisms. Hence, it needs to be incorporated into organic compounds by a process called nitrogen fixation.

Nitrogen fixation is the first part of the nitrogen cycle, and it occurs naturally through the activities of specialized archaea and bacteria. These microorganisms convert N_2 from the atmosphere into biologically available nitrogen, incorporating it into their own tissues and subsequently integrating it into the food chain (Eq. 3). Nitrogen fixation can also be done artificially by industrial processes such as the Haber-Bosch process, commonly used to produce fertilizers. The significance of fertilizer production for humanity is so immense that industrial nitrogen fixation has emerged as the primary nitrogen input to the global N-cycle (Swaney et al., 2012; Hutchins and Capone, 2022).



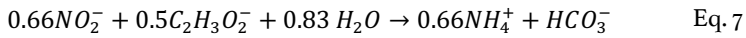
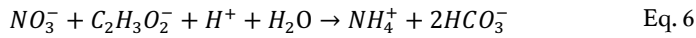
After the atmospheric nitrogen is fixed, it becomes a component of OM and undergoes a series of transformations between biologically available forms. The first is *Ammonification*, which involves the release of NH_4^+ from organisms by either the excretion of substances and waste, or the remineralization of OM when they die. Thereafter, the released NH_4^+ either becomes available for uptake by primary producers or is utilized by nitrifying bacteria as an electron acceptor to obtain energy. *Nitrification* is an aerobic two-step process. The first step involves the conversion of NH_4^+ into NO_2^- by ammonium-oxidizing bacteria and archaea (Eq. 4), while the second step involves the conversion of NO_2^- into NO_3^- by nitrite-oxidizing bacteria (Eq. 5). Nitrification is the main source of nitrate to marine environments (Dedieu et al., 2007)



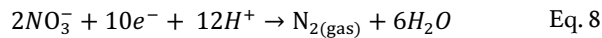
The NO_3^- produced during nitrification can either be returned into the water column, utilized for dissimilatory nitrate/nitrite reduction to ammonium (DNRA), or used by

Chapter 1

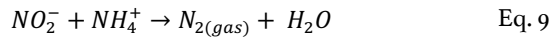
denitrifiers as electron acceptor. The *DNRA* is a two-step anaerobic process that reduces NO_3^- (Eq. 6) or NO_2^- (Eq. 7) to NH_4^+ , thereby retaining nitrogen in a biologically available form (Lam and Kuypers, 2011; Decleyre et al., 2015).



The last part of the nitrogen cycle involves the removal of nitrogen from the system and its return to the atmosphere, the main nitrogen sink. Denitrification is an anaerobic process conducted primarily by prokaryotes that remove bioavailable NO_3^- (Eq. 8) by converting it to $\text{N}_{2(\text{gas})}$ with nitrous oxide being produced at an intermediate step ($\text{NO}_3^- \rightarrow \text{NO}_2^- \rightarrow \text{NO} + \text{N}_2\text{O} \rightarrow \text{N}_{2(\text{gas})}$). Denitrification is an important process controlling the concentration of nitrogen available for primary producers in coastal marine systems (Herbert, 1999; Dedieu et al., 2007)



Anammox, or anaerobic ammonium oxidation, is an alternative biologically mediated removal process that also produces $\text{N}_{2(\text{gas})}$ from the oxidation of NH_4^+ . However, unlike denitrification, which utilizes NO_3^- , anammox relies on NO_2^- as the electron acceptor (Eq. 9, Thamdrup and Dalsgaard, 2002; Lam and Kuypers, 2011). Regarding nitrogen removal in coastal sediments, denitrification is considered a more important process than anammox (Thamdrup and Dalsgaard, 2002).



In addition to depending on the availability of OM and the concentration of oxygen and nitrogen compounds, the nitrogen cycle is influenced by various physical, chemical, and biological factors such as temperature, salinity, pH, light and macrofaunal activity (Rysgaard et al., 1994; Herbert, 1999; Dedieu et al., 2007; Hutchins and Capone, 2022). For example, the growth and activity of nitrifying and denitrifying bacteria are affected by temperature (Herbert, 1999). Similarly, the lower salinity of freshwater and brackish areas promotes growth of nitrifying bacteria, and thus nitrification (Rysgaard et al., 1999). In contrast, nitrification and denitrification decrease in marine areas where the higher salinity not only promotes desorption of NH_4^+ from sediment particles eventually causing NH_4^+ limitation to nitrifying bacteria, but it also inhibits the activity of denitrifiers due to the high concentration of sulphide in marine sediments (Herbert, 1999; Rysgaard et al., 1999; An and Gardner, 2002). It is noteworthy that the anthropogenic input of nitrogen to marine environments in the form of fertilizers and urban, agricultural, and industrial run-off has become another, if not, the most important factor controlling the global nitrogen cycle (Herbert, 1999; Swaney et al., 2012).

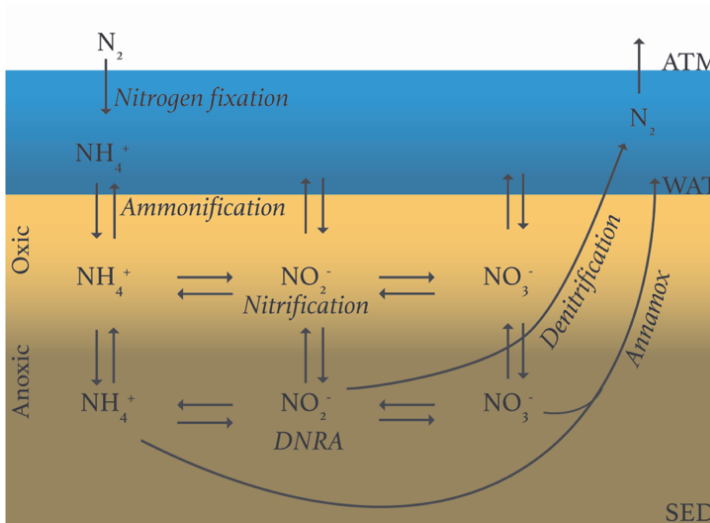


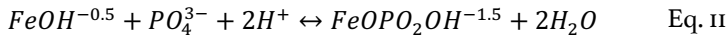
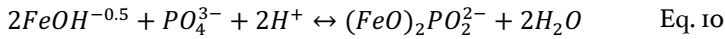
Figure 1.4 Simplified scheme of the benthic nitrogen cycle (A adapted from Herbert, 1999; Hutchins and Capone, 2022). Depicted are the atmosphere (ATM), water column (WAT) and both the oxic and anoxic layers of the sediment (SED).

1.3.2 Phosphorus cycle

Phosphorus (P) is an essential nutrient that regulates the ocean's productivity. The P cycle is closely associated with geological processes (Figure 1.5). The inorganic mineral apatite [$(Ca_5PO_4)_3(F, Cl, OH)$] is the most abundant mineral containing phosphorus in the Earth's crust (Paytan and McLaughlin, 2007). Continental input in the form of weathering of minerals, rocks and soils and from anthropogenic activities (e.g. fertilizer runoff and sewage) is the main source of phosphate (dissolved and particulate) to the ocean (Figure 1.5, Slomp, 2011). Although most P reaches the ocean by fluvial transport, there are other alternative inputs such as atmospheric deposition of volcanic ash, aerosols and mineral dust also deliver P to marine environments, albeit to a lesser degree (Benitez-Nelson, 2000; Paytan and McLaughlin, 2007; Slomp, 2011).

Particulate inorganic phosphorus is associated with particles containing minerals like apatite and iron oxyhydroxides ($FeOOH$) (Paytan and McLaughlin, 2007; Jordan et al., 2008). Most of the particulate P, especially that associated with apatite, is quickly retained in estuarine sediments and in the coastal shelf (Benitez-Nelson, 2000; Paytan and McLaughlin, 2007). However, inorganic phosphorous in the form of phosphate (PO_4^{3-}) can also sorb to iron oxides on the surface of clay particles in freshwater conditions (Jordan et al., 2008). These particles can eventually be transported to high salinity areas, where the PO_4^{3-} can be subsequently released and contribute to the pool of biologically available phosphorus (Eq. 10 and Eq. 11, Paytan and McLaughlin, 2007; Weng et al., 2012).

Chapter 1



The phosphate associated with OM, iron oxides, and authigenic minerals is in a reactive and biologically available form (Paytan and McLaughlin, 2007; Slomp, 2011). Primary producers can assimilate biologically available PO_4^{3-} and incorporate it into their tissues as organic P (Paytan and McLaughlin, 2007). This organic P can subsequently be passed into the trophic chain and biologically recycled (Paytan and McLaughlin, 2007). Phosphate is released back into the environment as dissolved PO_4^{3-} by biological excretion, cellular lysis, or by the oxic and anoxic remineralization of OM (Paytan and McLaughlin, 2007). The dissolved PO_4^{3-} can follow two paths: it can either be reassimilated by organisms or undergo a series of transformations, transitioning from a dissolved to a particulate form. Such transformations may include sorption to particulate matter which leads to deposition and the subsequent re-entry of P into the sediment through burial and sedimentation (Paytan and McLaughlin, 2007; Ruttenger, 2019). The burial of authigenic phosphate minerals is the ultimate major sink of oceanic P (Benitez-Nelson, 2000; Ruttenger, 2019).

Once in the sediment, the dissolved PO_4^{3-} can diffuse into the overlying water or be incorporated as PO_4^{3-} bound to FeOOH in sediment particles as long as oxic conditions are present (Slomp, 2011). When these particles reach anoxic sediments in freshwater areas, the FeOOH is reduced to Fe^{2+} and the PO_4^{3-} released; thereafter, both the Fe^{2+} and PO_4^{3-} can diffuse upwards into oxic layers where FeOOH can form again and bind PO_4^{3-} , thereby repeating the cycle in a process known as the “P-shuttle” (Figure 1.5, Slomp et al., 1996; Jordan et al., 2008). In marine areas, however, sulphides are also formed in the anoxic layer (Jordan et al., 2008). This sulphide can precipitate Fe^{2+} and effectively prevent it from binding to PO_4^{3-} , which results in the accumulation of PO_4^{3-} in porewaters and its return to the overlying water either by molecular diffusion or bioirrigation (Jordan et al., 2008; Wallmann, 2010; Slomp, 2011). Nevertheless, the released PO_4^{3-} in anoxic sediments can also follow an alternative path and re-enter the geological cycle by precipitating and forming authigenic minerals such as carbonate fluorapatite ($Ca_5(PO_4)_3CO_3$), abbreviated as: CFA (Slomp et al., 1996; Benitez-Nelson, 2000; Ruttenger, 2019).

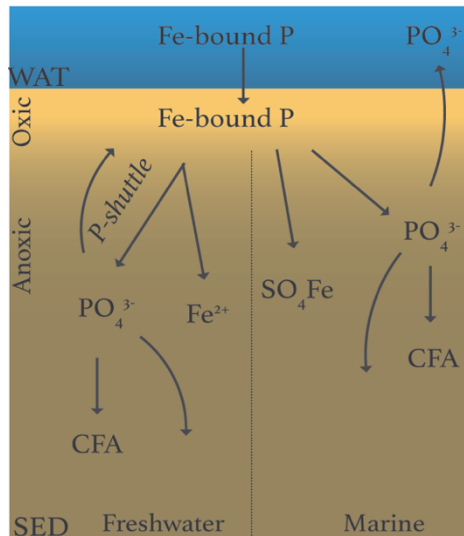


Figure 1.5 Simplified scheme of the benthic phosphate cycle adapted from Slomp et al. (1996); Paytan and McLaughlin (2007); Jordan et al. (2008). Depicted are the atmosphere (ATM), water column (WAT) and both the oxic and anoxic layers of the sediment (SED). CFA refers to carbonate fluorapatite.

Human activities such as fertilizer use, sewage disposal, deforestation and aquaculture have disrupted the global phosphorus cycle by increasing transport to the marine environment between 50 and 300% (Slomp, 2011; Ruttenger, 2019). This has led to a disruption of coastal biogeochemistry and the onset of eutrophic conditions that promote harmful algal blooms and anoxia (Ruttenger, 2019).

1.3.3 Silica cycle

Silicon (Si), the most abundant element on the earth's crust, is mobilized through rock weathering. It is subsequently transported to the ocean in particulate or dissolved form through various pathways, including rivers and estuaries, atmospheric deposition, hydrothermal inputs and the dissolution of marine sediments and basalt (Figure 1.2, Tréguer and de La Rocha, 2013). Silicon is an important nutrient utilized by organisms, such as terrestrial siliceous plants and diatoms, to produce hard structures made of biogenic silica (BSi) (Struyf and Conley, 2009; Tréguer and de La Rocha, 2013). Most of the marine production of BSi is attributed to diatoms with other organisms like siliceous sponges, radiolarians, and silicoflagellates having a smaller contribution (Tréguer and de La Rocha, 2013).

Once a siliceous organism dies, its BSi starts dissolving and regenerating DSi as it settles to the seafloor (Tréguer et al., 1995). The undissolved BSi that deposits on the sediment is buried and continues to dissolve into the porewater (Figure 1.6, Tréguer et al., 1995; Struyf

et al., 2005b). The DSi in the porewaters subsequently diffuses to the sediment surface and enters the water column where it can be reutilized. However, not all DSi escapes the sediment. Both BSi and DSi can accumulate in porewaters, and the BSi can also be immobilized through early diagenetic processes involving the adsorption of aluminium, iron, and other cations to form authigenic aluminosilicate minerals (Michalopoulos et al., 2000; Dixit, 2003; Struyf et al., 2005b; Tréguer and de La Rocha, 2013). In both cases the silicate is removed by re-entering the geological cycle.

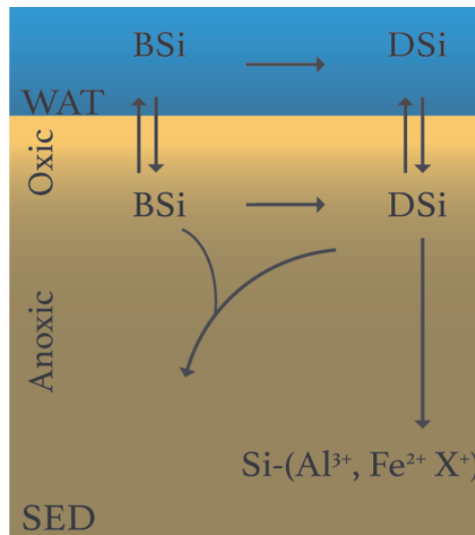


Figure 1.6 Simplified scheme of the benthic silicon cycle adapted from Tréguer et al. (1995). Depicted are the atmosphere (ATM), water column (WAT) and both the oxidic and anoxic layers of the sediment (SED). BSi to biogenic silicate; and DSi to dissolved silicate.

1.4 Estuaries, mudflats, and humanity

Estuaries are important areas that support biodiversity and biogeochemical processes and have been at the centre of human societies for millennia. They have been traditionally utilized for a wide range of activities including fishing, hunting, shellfish harvesting, aquaculture, as well as for cultural and religious events (Bailey et al., 2020; López-Romero et al., 2021; NSW Department of Planning and Environment, 2021). Estuaries continue to play a significant role in modern society, providing multiple invaluable intangible and tangible ecosystem services.

Intangible services are those that enhance our quality of life such as recreation, cultural heritage, and aesthetics (Vejre et al., 2010; Small et al., 2017). Meanwhile, tangible services have a measurable economic value and provide benefits that support our health, livelihoods, and the functioning of our society (Costanza et al., 2014). The tangible services

offered by estuaries include sources of raw materials, areas for housing, commercial fishing, and aquaculture; waterways for transport and shipping; habitat for pelagic, benthic, and migratory species; and environmental functions such as carbon storage; nutrient retention and recycling; coastal protection; erosion control; and water purification (Barbier et al., 2011; Ysebaert et al., 2016).

Due to our close relationship with estuaries, these areas are subject to intense anthropogenic influence. Among all human activities, land use change for farmland, industrial, or urban use poses the greatest threat to estuaries. The construction of cities, ports, and related infrastructure like dams and dikes, results in the degradation or permanent loss of intertidal areas and coastal ecosystems (OSPAR, 2008a; Stauber et al., 2016). For instance, land reclamation has far-reaching consequences in coastal ecosystems. It causes changes to tidal regimes, coastal currents, sediment loads, deposition rates, freshwater run off, and salinity gradients, and reduces coastal fishing grounds (OSPAR, 2008a; Reed et al., 2009). Dredging for maintenance of shipping routes and ports has a similarly negative impact. The reworking and resuspension of sediments not only releases pollutants and nutrients into the water column, but it also smoothens benthic features or buries habitats of bottom-dwelling organisms, thereby affecting photosynthetic, benthic, and pelagic organisms (OSPAR, 2008b, 2008a; Stauber et al., 2016).

Physical alterations of the coastline are not the only threats to estuaries. Nearby human settlements and economic activities also change the chemical characteristics of estuarine systems. Inputs from sewage, farm runoff, and wastewater contribute to an increase in pollutants and nutrients in the water column, which can negatively affect marine life and decrease water quality (Gilbert et al., 2007). The increased concentration of nutrients in estuaries can lead to eutrophication and water column anoxia, subsequently altering the biological community and biogeochemical characteristics of the water column and the sediment (Soetaert and Herman, 1995b). Furthermore, the indirect impacts of climate change, such as sea level rise, coastal erosion, heatwaves, increased storm frequency, and ocean acidification, also pose a significant threat to estuarine systems and their biogeochemical functionality (Harley et al., 2006; Rios-Yunes et al., 2023a, 2023c).

Within estuaries, the intertidal zone, including its salt marshes and mudflats, is the most impacted area by human activities and climate change. The loss and degradation of intertidal areas globally is a pressing problem. It is estimated that 22,000 km² of intertidal area has been lost since 1984, and, alarmingly, more than 80% of these ecosystems are subject to high human pressure (Murray et al., 2019; Williams et al., 2022). Mudflats are particularly vulnerable as they have been historically regarded as waste land and are often buried by sand dumping from dredging and land reclamation activities. Furthermore, the increased threat of coastal erosion and sea level rise means that these areas, and their associated ecosystem services, will be the first to disappear.

Chapter 1

It is difficult to fathom the extent of anthropogenic impact on coastal areas, but it becomes a little clearer when it is highlighted that 20 of the world's largest cities and seven of the ten largest ports are located near estuaries. Moreover, around 40 % of the world's population, which exceeded 8 billion people in 2022, resides in coastal areas (Figure 1.7, Small et al., 2003). This implies that approximately 3.2 billion people live within 100 km of the coast. Therefore, it is unsurprising that estuaries are subjected to immense pressures and widespread degradation, with only 15 % of the world's coastal regions remaining intact, mostly in the arctic region (Reed et al., 2009; Barbier et al., 2011; Williams et al., 2022).

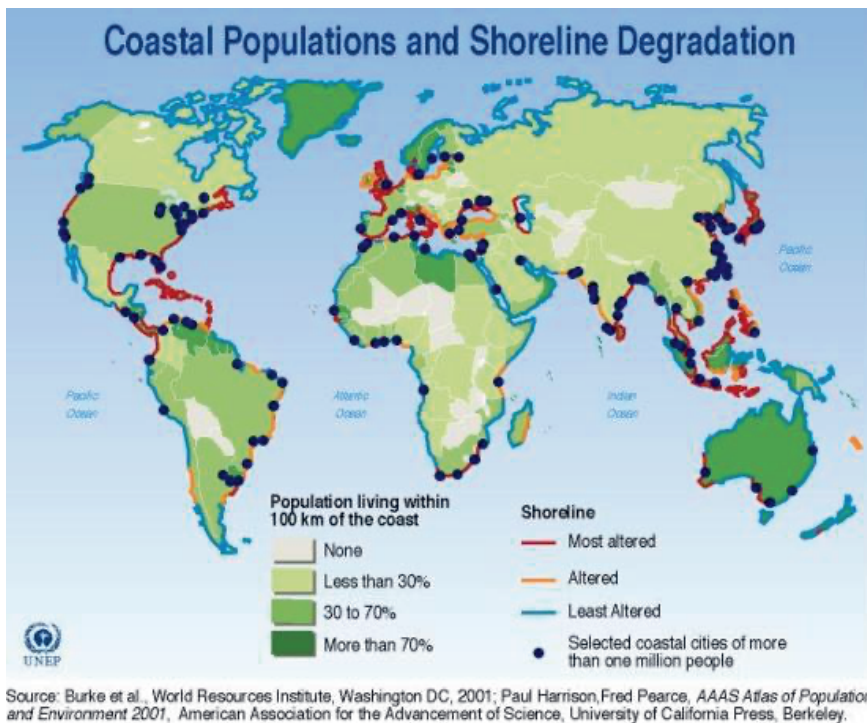


Figure 1.7 Proportion of a country's population living within 100 km of the coast, represented in different shades of green. Coastal cities with more than one million inhabitants marked with dots. The degree of human alteration of the coastal zone is indicated by the different colours of the coastline. Image obtained from www.grida.no/resources/5542 Cartographer: This

The importance of estuaries and mudflats and their ecosystem services is gaining attention in the global stage. Currently, several initiatives intended to limit their degradation, and to potentiate their use as centres for carbon storage (i.e. Blue carbon) are being discussed at the national and international level (Krauss et al., 2018; Bulmer et al., 2020; Hilmi et al., 2021). Nevertheless, more information regarding the processes occurring in these areas, such as, for example, their biogeochemical function, is still needed to better understand the challenges that these systems are facing and to improve their protection.

1.5 The Dutch coast

The Dutch coastline has undergone extensive morphological transformations since the Quaternary period, with natural factors such as glacial and interglacial periods leading to changes in sea-level and episodes of land erosion and accretion (Gerritsen, 2005; VanKoningsveld et al., 2008). The Netherlands is located in a low elevation area and is therefore susceptible to flooding and sea-level rise. The constant threat posed by the sea sparked the development and implementation of technological advances for coastal defence systems as early as 500 DC (VanKoningsveld et al., 2008). However, it was not until the XIII century that dikes were extensively introduced to protect the coastline (VanKoningsveld et al., 2008). Since then, land reclamation and the construction and maintenance of protective structures became commonplace continuing well into the XXI century (VanKoningsveld et al., 2008).

The flood disaster of 1953 marked a turning point, leading to the creation of the "Delta Plan", which has been the most extensive modification of the Dutch coastline, involving the closure of all sea inlets in the southwest of the country except for those serving the ports of Rotterdam and Antwerp (Gerritsen, 2005; VanKoningsveld et al., 2008). The implementation of the Delta Plan has understandably brought about profound changes that are still ongoing and will continue to be felt for decades to come on the hydrodynamics, morphology, and biology of the affected areas (Ysebaert et al., 2016; Rios-Yunes et al., 2023c). It is, thus, undeniable that the Dutch coast has undergone unprecedented anthropogenic changes, so much that an old saying goes¹: "God created the world, but the Dutch created The Netherlands".

1.5.1 *Eastern Scheldt tidal bay*

The Eastern Scheldt (ES) tidal bay, former estuary, is a notable example of a system that was greatly modified by the Delta Plan. The Eastern Scheldt estuary was one of the branches of the delta for the rivers Meuse, Scheldt, and Rhine. However, after the construction of river dams, the Eastern Scheldt was disconnected from these rivers and transformed into a tidal bay (Smaal and Nienhuis, 1992). Currently, the ES is only connected to the North Sea through a barrier that allows seawater exchange except during bad weather when it is closed (Smaal and Nienhuis, 1992).

The transformation of the Eastern Scheldt into a tidal bay led to significant changes in its morphology, biogeochemistry, and biology. The closure of the ES resulted in the loss of its salinity gradient causing various changes including a reduction in suspended organic

¹ Contended attribution to Scottish physician Archibald Pitcairne or theologian James Fraser <https://rijksmuseumboerhaave.nl/collectie/verhalen/herkomst-spreuk-ontrafeld/>

Chapter 1

matter, tidal currents, water volume and turbidity, as well as a shift of the biological community (Smaal and Nienhuis, 1992; Nienhuis and Smaal, 1994; Wetsteyn and Kromkamp, 1994). One of the enduring and concerning consequences of the ES closure is the phenomenon of “sand starvation”. Which occurs due to a deficit of sediments caused by reduced riverine input and weaker tidal currents that leads to the continuous erosion of intertidal areas (van Zanten and Adriaanse, 2008; Ysebaert et al., 2016). The problem of sand starvation in the ES is a concerning issue, with estimates suggesting that by 2001, the ES had already lost 8% (equivalent to 870 ha) of intertidal areas at a rate of ~0.5 km² per year (van Zanten and Adriaanse, 2008). To this day, the ES is still undergoing geomorphological changes and losing intertidal mudflats (Smaal and Nienhuis, 1992; Ysebaert et al., 2016). This not only threatens shellfish aquaculture and fisheries (Smaal and Nienhuis, 1992), but also affects ecosystem functionality by, for example, decreasing the area where biogeochemical processes such as nutrient retention can occur (Rios-Yunes et al., 2023c).

1.5.2 *Western Scheldt estuary*

The Western Scheldt (WS) estuary is the only remaining branch of the Meuse, Scheldt, and Rhine rivers’ delta (Heip, 1989). Its main tributary is the Scheldt River that originates in France, flows through Belgium, and eventually discharges into the Western Scheldt near Antwerp. Unlike the Eastern Scheldt, the Western Scheldt was not closed off by the Delta Plan and retained its natural connection to the Scheldt River and the North Sea to maintain unrestricted shipping traffic to the Port of Antwerp (VanKoningsveld et al., 2008). Situated in one of the most densely populated and industrialized regions of Europe, the WS basin receives urban and industrial sewage as well as agricultural runoff from the surrounding lands (Wollast and Peters, 1978; Gilbert et al., 2007).

By the early 1970s, the WS was severely hypereutrophic, exhibiting oxygen depletion and denitrification in the water column due to high levels of pollutants and nutrients entering the estuary (Wollast and Peters, 1978; Heip, 1989; Soetaert et al., 2006). Consequently, a series of policies were implemented to limit the influx of pollutants, raw sewage, and fertilizers and to restore the ecological health of the estuary (Soetaert et al., 2006). By the late 1990s, pollution levels were successfully reduced, resulting in predominantly oxic conditions in the water column (Soetaert et al., 2006; Cox et al., 2009). More recently, the establishment of the Brussels-North wastewater treatment plant in 2007 further contributed to the improvement of the water quality in the estuary (Brion et al., 2015).

Currently, the WS exhibits year-round oxic conditions, and recent reports indicate that the implementation of restoration policies has successfully improved the water quality of this former hypereutrophic estuary (Cox et al., 2009; Rios-Yunes et al., 2023b). Nevertheless, sewage, farmland run-off and maintenance dredging of the main channel

to maintain shipping access remain as periodical stressors (Meire et al., 2005; Gilbert et al., 2007).

It is clear that the Eastern Scheldt tidal bay and the Western Scheldt estuary have experienced significant alterations in their morphological and chemical properties, while also facing substantial anthropogenic pressures. These tidal areas are among the most extensively studied worldwide, providing ample information on their morphological, chemical, and biological characteristics (refer to Box 1.2 for details on the benthic community). The combination of extensive modifications and the abundance of available data renders the ES and WS systems interesting systems for exploring the biogeochemical dynamics within highly disturbed tidal areas.

Box 1.2 Main taxa of the macrobenthic community of the Western and Eastern Scheldt:

Oligochaetes

Oligochaetes dominate freshwater sediments (Ysebaert et al., 1993; Seys et al., 1999). These organisms are found in oligo- and mesohaline areas within the first 5 cm of fine sediments with an abundant supply of organic matter (Giere and Pfannkuche, 1982; McCann and Evin, 1989). They respire via transdermal oxygen diffusion, so their vertical distribution is strongly influenced by the concentration of oxygen (van Hoven, 1975). Oligochaetes exhibit diverse life strategies with some species being interannual and others breeding year-round or following seasonality (Giere and Pfannkuche, 1982; Giere, 2006). They move freely in the sediment matrix by crawling, burrowing, or conveying and act as biodiffusors (Beauchard et al., 2012; Queirós et al., 2013). Oligochaetes feed by non-selective detritivory, deposit feeding, bacterivory, and transepidermal or transintestinal uptake of dissolved substances (Giere and Pfannkuche, 1982; Giere, 2006; Queirós et al., 2013). They are known water quality indicators because of their high resistance to pollution (Kownacki and Szarek-Gwiazda, 2022).

***Corophium volutator* (Pallas, 1766)**

The amphipod *Corophium volutator* is a deposit feeder typically found in the mesohaline areas (Ysebaert et al., 1998). It exhibits limited movement and lives in “U”-shaped burrows between 2 and 6 cm deep which are constantly irrigated during high tide (Pelegri et al., 1994; De Backer et al., 2010; Queirós et al., 2013). *C. volutator* is an important biodiffusor and bioturbator whose particle burial activities mix approximately $1 \text{ cm}^2 \text{ y}^{-1}$ (Mermillod-Blondin et al., 2004; de Backer et al., 2011; Queirós et al., 2013). However, it does not induce non-local transport (Mermillod-Blondin et al., 2004; de Backer et al., 2011). At high densities ($> 15,000 \text{ ind. m}^{-2}$), the flushing activities of *C. volutator* enhance oxygen consumption, OM transformation and nutrient recycling (De Backer et al., 2010;

de Backer et al., 2011), as well as nitrification- denitrification and benthic nutrient release (Pelegrí and Blackburn, 1994).

***Hediste (Nereis) diversicolor* (O.F. Müller, 1776) and *Alitta succinea* (Leuckart, 1847)**

The polychaetes *Hediste diversicolor* and *Alitta succinea* occur in brackish and marine sediments, but *H. diversicolor* prefers lower salinities than *A. succinea* (Kristensen, 1988; Fong, 1991). They live in “U”-shaped burrows (Nielsen et al., 1995) and move freely within the sediment acting as biodiffusers and inducing non-local transport (Mermillod-Blondin et al., 2004; Queirós et al., 2013). For instance, the bioturbating and bioirrigating activity of *H. diversicolor* has been detected up to 9 cm depth (Mermillod-Blondin et al., 2004). Both polychaetes have an omnivorous diet, but *A. succinea* is a non-selective deposit feeder (Fong, 1987), while *H. diversicolor* exhibits more varied feeding habits that include predation of, for example, *C. volutator* and *M. balthica* (Rönn et al., 1988); scavenging of the top sediment layer; or filtration for phytoplankton (Nielsen et al., 1995). The bioturbating activity of *H. diversicolor* has been observed to influence nitrogen fluxes (Thoms et al., 2018).

***Heteromastus filiformis* (Claparède, 1864)**

The polychaete *Heteromastus filiformis* lives in muddy sediments of brackish and marine areas (Wolff, 1973; Ysebaert et al., 1998). It exhibits slow free movement within the sediment matrix (Queirós et al., 2013) and creates vertical burrows between 10 and 30 cm deep (Cadée, 1979). The population of *H. filiformis* fluctuates intra and inter annually and does not recruit every year (Cadée, 1979). *H. filiformis* is a non-selective deposit feeder that utilizes an upward conveyor belt feeding strategy, in which it feeds at depth and releases faecal pellets on the sediment surface that are highly resistant to bacterial degradation (Cadée, 1979; Queirós et al., 2013). *H. filiformis* is an important sediment reworker and surface modifier (Cadée, 1979).

Bivalves

Bivalves are typically found in marine, and to a lesser extent, in brackish areas. They exhibit limited movement within the sediment matrix and are surface modifiers (Queirós et al., 2013). Bivalves have a "U" shaped body with syphons through which they inhale and exhale water. Water exchange occurs within the animals' body, preventing contact between the pumped oxygen-rich water and the sediment. As a result, their pumping activity has limited influence on the chemical conditions of the sediment (Mermillod-Blondin et al., 2004).

The cockle *Cerastoderma edule* (Linnaeus, 1758) is a suspension feeder commonly found in marine and brackish areas (Wolff, 1973; Ysebaert et al., 1998, 2003a). *C. edule* is a commercially exploited species that lives between 2 to 7 cm depth in a large range of

sediment types provided that the hydrodynamical conditions are favourable (Wolff, 1973; Mermillod-Blondin et al., 2004). They are particularly sensitive to extreme temperature fluctuations with their populations being decimated by extreme cold (Wolff, 1973), and more recently, by extreme heat (Burdon et al., 2014; Zhou et al., 2022).

The clam *Macoma balthica* (Linnaeus, 1758) is tolerant to different salinities inhabiting marine and brackish areas (Wolff, 1973; Ysebaert et al., 1998). *M. balthica* is a selective deposit-feeder and suspension-feeder (in high tide) commonly found in fine muddy sand sediments (Wolff, 1973).

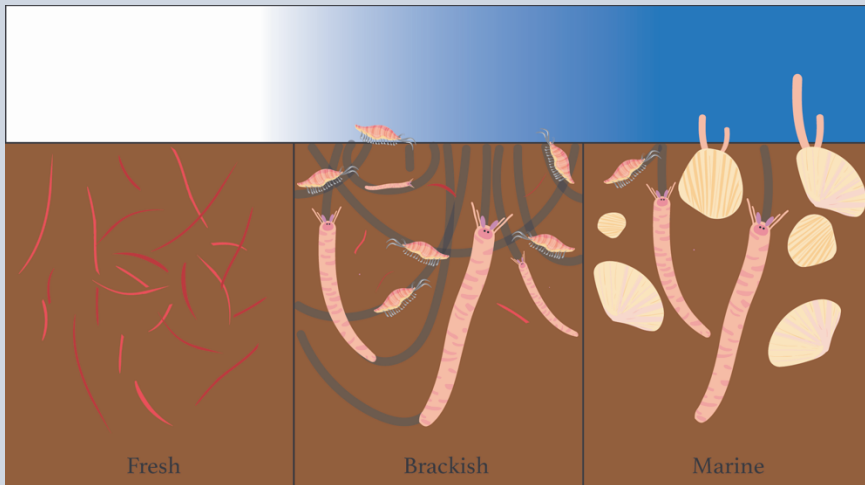


Figure 1.8 Representation of the different communities found along the salinity gradient of the Western Scheldt and in the Eastern Scheldt

1.6 Thesis aim and scope

This PhD project was part of a Sino-Dutch cooperation initiative aiming at investigating the historical and future fluctuations in sediment and nutrient flows across the river, estuary, and sea continuum, while also examining the potential regime shifts in the Yangtze Delta in China and the Rhine-Meuse-Scheldt-Ems Deltas in The Netherlands. The primary objective of this project was to compare the biogeochemical dynamics between these systems. However, the outbreak of the coronavirus pandemic and subsequent travel restrictions caused major modifications to the initial plan and made it impossible to continue our research in China. Nevertheless, the motivation to understand the biogeochemical dynamics of tidal mudflats and the potential modifications associated with climate change remained unchanged.

Chapter 1

The focus of this PhD project was to investigate the biogeochemical dynamics of intertidal mudflats in the Western and the Eastern Scheldt and to understand the relation between biogeochemical functionality and anthropogenic stressors. The main questions addressed in this thesis surrounded three main topics: First, what are the differences in biogeochemical functionality between intertidal and subtidal sediments, what is their relative contribution for coastal biogeochemical functionality and what are the potential implications for coastal management? Second, how does the biogeochemistry of intertidal sediments differ along the salinity gradient and seasonally, and what is the effect of macrobenthos activity on the nutrient dynamics observed? Last, what happens to the biogeochemical dynamics of intertidal sediments during a resuspension event, and how does this affect sedimentary nutrient storage?

To answer these questions, we first looked at the differences in ecosystem functionality between subtidal and intertidal systems in the Eastern Scheldt tidal bay as shown in **Chapter 2**. The nutrient retention in the intertidal and subtidal areas was quantified to determine the contribution of each area to the total nutrient retention of the tidal bay. Moreover, the potential consequences of intertidal area loss due to coastal erosion and sand starvation were evaluated, and it was determined that losing these areas would result in a net decrease in nutrient removal capacity of the ES tidal bay.

The factors controlling biogeochemical dynamics seasonally and along the salinity gradient of an estuarine system are addressed in **Chapter 3**, which explores the monthly biogeochemical processes occurring along the salinity gradient of the Western Scheldt estuary and their dependence to local environmental factors. **Chapter 4** builds upon this knowledge and investigates the effect of the benthic community and their bioturbating activity on the biogeochemical dynamics observed along the WS.

Chapter 5 studies the potential consequences of resuspension events for biogeochemical processes in coastal areas. The inspiration for this topic arose from a trip to China in the summer of 2019. A week before our arrival, Typhoon Lekima had caused tremendous damage to the coast close to Shanghai and had resuspended massive quantities of sediment. This chapter explores the consequences of sediment resuspension on the concentration of nutrients in the water column and in porewaters. To this end, sediment resuspension experiments were conducted in different mudflats in the Western Scheldt and the Eastern Scheldt. It was demonstrated that sediment resuspension changed the concentration of nutrients in the water column with potential consequences for the water quality of coastal systems.

Appendix A provides version of chapter 2 that targets an audience of 10 years and older and is not a part of the scientific contents of this thesis.

Chapter 2 *Long-term changes in ecosystem functioning of a coastal bay expected from a shifting balance between intertidal and subtidal habitats*

Dunia Rios-Yunes; Justin C. Tiano; Pieter van Rijswijk; Emil De Borger;
Dick van Oevelen and Karline Soetaert

Dunia Rios-Yunes and Justin C. Tiano contributed equally to this work.

Published in Continental Shelf Research (2023)

DOI: [10.1016/j.csr.2022.104904](https://doi.org/10.1016/j.csr.2022.104904)

2.1 Abstract

Coastal areas are subjected to several anthropogenic stressors with much of the world's intertidal areas receding due to human activities, coastal erosion, and sea level rise. The Dutch Eastern Scheldt (ES) has been predicted to lose around 35 % of intertidal areas by 2060. This study investigates differences between biogeochemical fluxes of intertidal and subtidal sediments of the ES and assesses how ongoing erosion may modify the sedimentary ecosystem functioning of this coastal bay in the coming decades. Monthly fluxes and porewater concentrations of dissolved inorganic nitrogen (DIN), phosphorous (DIP), silica (DSi), carbon (DIC) and oxygen (O_2) as well as organic matter (OM) characteristics were measured from intertidal and subtidal sediments from June 2016 – December 2017. Compared to subtidal stations, OM was significantly more reactive in intertidal samples and exhibited 37 % higher O_2 fluxes, suggesting a strong influence from microphytobenthos. Subtidal sediments exhibited an average efflux of nitrates ($0.28 \text{ mmol m}^{-2} \text{ d}^{-1}$) and phosphates ($0.09 \text{ mmol m}^{-2} \text{ d}^{-1}$) into the water column, while intertidal areas displayed average influxes (nitrates = $-1.2 \text{ mmol m}^{-2} \text{ d}^{-1}$, phosphates = $-0.03 \text{ mmol m}^{-2} \text{ d}^{-1}$) directed into the sediment. The calculated removal of total DIN and DIP from the water column was 34 – 38 % higher in intertidal compared to subtidal samples suggesting stronger denitrification and phosphorus adsorption to solid particles from intertidal sediments. As an upscaling exercise, we estimate potential erosion induced changes if the ES stations are representative for the system. With this assumption, we estimate 11 % and 8 % reductions for respective nitrogen and phosphorus removal in the entire ES by 2060. Given the global observations of eroding intertidal areas and rising sea levels, we suggest that the predicted habitat loss may cause significant changes for coastal biogeochemistry and should be investigated further to understand its potential consequences.

2.2 Introduction

Coastal sediments are well known for their high primary production and importance in global biogeochemical cycling (Woodward, 2007). These habitats receive OM and nutrients from autochthonous (e.g., local algal blooms) and allochthonous sources (e.g., terrestrial including sewage and fertilizers; Gilbert et al. [2007]) which enter the sediment by tidal action, sedimentation, and sediment reworking by benthic organisms (Arndt et al., 2013; Kang et al., 2015). Other essential ecosystem functions mediated by coastal sediments include the mineralization of organic matter (OM), benthic-pelagic nutrient exchange, as well as the cycling, and the export and/or removal of inorganic nutrients (Magalhães et al., 2002; Khalil et al., 2013; Lessin et al., 2018).

Nutrient exchange between the water column and the sediment is different between intertidal and subtidal regions. In intertidal sediments tidal flushing during inundation causes the release of porewater nutrients into the water column (Falcão and Vale, 1998; Rocha and Cabral, 1998; Cabrita et al., 1999), while nutrient exchange in permanently subtidal sediments is governed primarily by molecular diffusion (Falcão and Vale, 1995), faunal-induced sediment reworking and irrigation (Laverock et al., 2011; Kristensen et al., 2012), and wave-mediated advective transport (“subtidal pump”, Riedl et al. [1972]). The difference in biogeochemical cycling between intertidal and subtidal coastal areas may lead to distinct ecological functions allocated to each zone (De Borger et al., 2020). Moreover, there are ecosystem-specific differences (Herbert, 1999) that should be considered as for example subtidal denitrification has been reported to be higher than in the intertidal in some systems (Joye and Paerl, 1993; Eyre et al., 2011) and lower in others (Piehler and Smyth, 2011). The input of OM in intertidal sediments is mostly associated with local microphytobenthic blooms, while OM influxes in subtidal sediments rely more on pelagic deposition leading to potential differences in OM quality and carbon characteristics between tidal zones.

Coastal habitats have been gaining attention as areas for “Blue carbon” storage (i.e. organic carbon) (Laffoley et al., 2014; Byun et al., 2019; Hilmi et al., 2021; IUCN, 2021). Most of the focus, however, has been placed on vegetated areas and less is known about the role of pure sedimentary ecosystems. Reports of high organic carbon stocks stored in mudflats (Byun et al., 2019; Bulmer et al., 2020; Douglas et al., 2022) suggest the importance of certain sedimentary habitats for long term carbon sequestration. However, dynamics between tidal zones and the possible threat of coastal erosion and/or sea level rise (SLR) remains largely unexplored.

The balance between intertidal and subtidal sediments in coastal areas is in constant change. However, the extent of intertidal areas is decreasing worldwide as a consequence of land reclamation, land-use change, SLR, coastal hardening, coastal erosion, and reduced sediment supply (Murray et al., 2019). Notably, erosion, decreased sediment

Chapter 2

input, and SLR will determine the loss of intertidal area and its conversion to subtidal areas (Ysebaert et al., 2016; Murray et al., 2019). This conversion may alter the ecosystem functions and services provided by these areas (e.g. nutrient recycling, export, and removal), with potentially wider consequences to regional biogeochemistry.

An ongoing example of changing intertidal-subtidal dynamics can be found in the Eastern Scheldt (ES) tidal bay located in the southwest of The Netherlands. The ES was transformed from an estuary into a fully saline tidal bay upon the construction of a “storm-surge barrier” (Delta Works project) at its mouth and several riverine dams in 1986 (Smaal and Nienhuis, 1992). These developments decreased the likelihood of local flooding but drastically reduced natural sediment deposition while altering the biological, abiotic, morphodynamic and biogeochemical characteristics of the ES (Smaal and Nienhuis, 1992; Nienhuis and Smaal, 1994; ten Brinke, 1994; Wetsteyn et al., 2003). Decreased water column nutrient concentrations led to increased nutrient limitation to primary production (Wetsteyn and Kromkamp, 1994; Wetsteyn et al., 2003; Smaal et al., 2013) while the reduced sedimentation resulted in a loss of intertidal surface area (Smaal and Nienhuis, 1992).

A condition known as “sand starvation” is currently exhibited in the ES resulting from continuous erosion of intertidal areas, lower riverine input of sediments and weaker tidal currents that fail to replenish tidal flat sediments (van Zanten and Adriaanse, 2008; Ysebaert et al., 2016). By 2001, it was estimated that the ES had lost 8% (870 ha) of intertidal areas accounting for ~0.5 km² per year (van Zanten and Adriaanse, 2008). The ES continues to experience geomorphological and biogeochemical changes (Smaal and Nienhuis, 1992; Ysebaert et al., 2016) including the ongoing loss of intertidal flats (and associated ecosystem functions) and their conversion to subtidal areas.

The aim of this study was to assess biogeochemical characteristics of intertidal and subtidal ES sediments and to predict changes to ecosystem functions due to the expected conversion of intertidal to subtidal areas as a consequence of sand starvation. OM mineralization and nutrient fluxes were estimated for intertidal and subtidal sediments by conducting monthly sediment incubations over a period of 1.5 years.

2.3 Methods

2.3.1 Study area

The Eastern Scheldt is a tidal bay and former estuary located in the southwest of The Netherlands with a mean depth of 8.84 m. Its sedimentary habitats cover an area of 350 km², ~110 km² of which being intertidal areas (Jiang et al., 2019). It remains connected to the North Sea through sluices, resulting in a tidal flush dominated system (~2 x 10⁴ m³ s⁻¹) with a decreasing landward gradient of suspended chlorophyll *a* (chl *a*), nutrient

concentrations, suspended sediment, and turbidity (Smaal and Nienhuis, 1992; Wetsteyn and Kromkamp, 1994). Riverine input in the ES is negligible (4.3 m s^{-1}) (Jiang et al., 2019).

Sampling was conducted in three sedimentary sites from the ES intertidal: Zandkreek (ZK), Olzendenpolder (OP), and Dortsman (DT) and three sites from the subtidal: Hammen (HM), Viane (VN), and Lodijkse gat (LG). Intertidal samples from ZK (51.55354° N , 3.87278° E) exhibited silty sediments (median grain size under $62.5 \mu\text{m}$) while OP (51.46694° N , 4.072694° E) and DT (51.56804° N , 4.01425° E) were characterized by very fine sand ($62.5\text{--}125 \mu\text{m}$) and fine sand ($125\text{--}250 \mu\text{m}$), respectively. Samples from HM (51.65607° N , 3.858717° E) displayed the coarsest sediments in the study and were taken from a depth of 7 m. The muddy subtidal site VN (51.60675° N , 3.98501° E) lies within a bathymetric depression (13 m depth) adjacent to intertidal areas (Figure 2.1). LG (51.48463° N , 4.166001° E ; 17 m depth) was the most inland location and exhibited very fine sand (Figure 2.1)

The granulometric, and bioirrigation (the faunal mediated exchange of solutes into the sediment) characteristics, as well as detailed information about macrofauna assemblages from these samples are documented in De Borger et al. (2020). Macrofaunal species densities at intertidal sites averaged 1 326, 1 955, 15 384 ind. m^{-2} corresponding to 17.0, 14.3, 7.3 g (ash free dry weight [AFDW]) of biomass per m^2 for sites ZK, OP and DT respectively. Abundances at intertidal sites were dominated numerically by *Hediste diversicolor* in ZK, *Peringia ulvae* in OP and *Corophium volutator* in DT. In comparison, subtidal sites HM, VN and LG all featured lower average densities (931, 168, and 580 ind. m^{-2}), but sandy stations (HM and LG) had higher biomass (36.4, 46.9 g AFDW m^{-2}) than VN (2.7 g AFDW m^{-2} ; (De Borger et al., 2020). The numerically dominant species in the subtidal site HM was *Mytilus edulis*, while *Crepidula fornicata* and *Ophiura ophiura* displayed the highest abundances at LG and VN respectively.

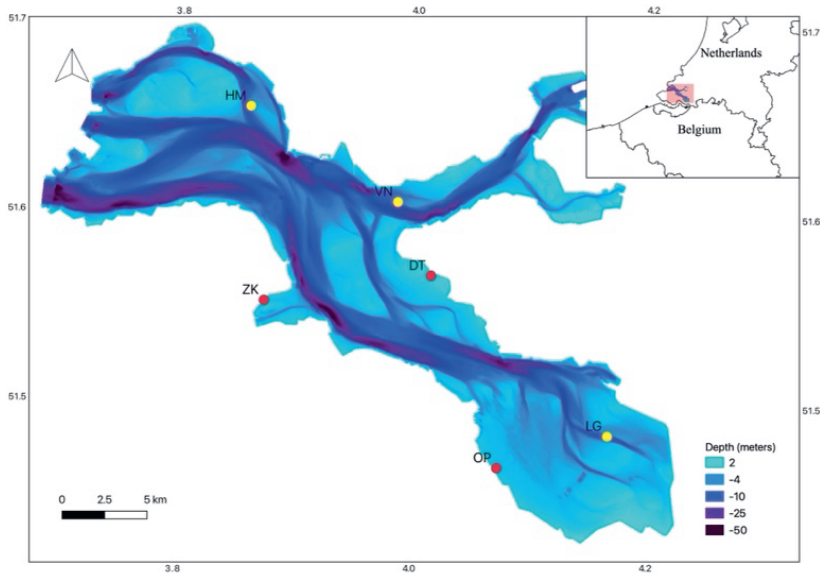


Figure 2.1 Bathymetric map of the Eastern Scheldt showing sampling points in the intertidal (red): Zandkreek (ZK), Olzenderpolder (OP) and Dortsman (DT) and subtidal (yellow): Hammen (HM), Viane (VN) and Lodijkse gat (LG) zones.

2.3.2 Sample Collection

Intact sediment core samples were collected monthly between June 2016 to December 2017 (exact sampling dates can be found in Supplementary Table A 2.1 and Table A 2.2) and used for porewater extraction and flux measurements of oxygen (O_2) and nutrients. Duplicate samples were taken for both intertidal and subtidal stations amounting to 114 and 102 cores from the intertidal and subtidal zones, respectively, as subtidal sampling was not possible in January and February of 2017 due to logistic constraints (Supplementary Table A 2.1). Sandy and muddy sites in the subtidal and intertidal stations were chosen to cover different sediments in contrasting environments.

Intertidal sediments were sampled during low tide and were defined between -2 to 2 m Normal Amsterdam Water Level ('NAP'; Kuijper and Lescinski, 2013). Cores for flux measurements were collected by inserting a cylindrical 14.5 cm diameter (\varnothing) by 30 cm (height) transparent PVC pipe into the sediment at a depth of 15 – 20 cm and carefully extracting the sediment without disturbing or tilting the core. Subtidal samples were collected using a cylindrical box corer (30 cm \varnothing , 55 cm height) deployed from the RV *Delta*, from which subcores were obtained and ~30 L of surface water were pumped from each subtidal site for later use in the laboratory.

Additional cylindrical PVC cores (3 cm \varnothing , 20 cm height) were collected for porewater nutrient extraction (all months), dry sediment parameters (median grain size, carbon and nitrogen content, porosity; June and December of 2016), and solid phase phosphorus (solid-P) and iron (solid-Fe) (July and December of 2016 and 2017). These cores were inserted 10+ cm into the sediment to obtain two segments: shallow from 0 – 5 and deep from 5 – 10 cm depth. Samples for chl a, phaeophorbide, and phaeophytin measurements were extracted from the upper 1 cm of the sediment using a cut-off syringe (all months).

2.3.3 *Dry sediment parameters*

Details regarding the laboratory analysis of sediment grain size parameters, organic carbon (OC) and total nitrogen (TN) content, porosity calculation, and pigment extraction can be found in De Borger et al. (2020). Sediment data previously reported in De Borger et al. (2020) were combined with additional samples from the monitoring period and recalculated for the current study. Organic carbon percentages were combined with bulk density measurements to obtain OC stocks in the upper 10 cm of sediment.

The ratio chl a/ (chl a + phaeophytin) was used as a proxy for organic matter reactivity as assessed with sediment pigments (Jodo et al., 1992; Pastor et al., 2011; Bonifácio et al., 2014; Lamarque et al., 2021). For solid-P and solid-Fe extraction, a ~500 mg subsample of sediment was obtained within an anaerobic glove box. These samples were exposed to 10 mL of 65 % nitric acid (HNO₃) and placed in a microwave to heat the sample (microwave energy is absorbed by the liquid surrounding the sample) while monitoring the temperature. The metals present were converted into soluble salts by the nitric acid and the high temperature (205°C), to prepare them for measurement via Inductive Coupled Plasma – Optical Emission Spectrometry (ICP-OES).

2.3.4 *Porewater nutrients*

Immediately after arrival to the lab, the porewater cores were placed inside an anaerobic glove box (Coy lab products, USA) to prevent aerobic chemical reactions prior to extraction. Thereafter, sediment from shallow and deep segments was collected in 50 mL centrifuge tubes (polypropylene; TPP, Switzerland). Porewater was extracted by centrifugation (10 min, 5000 rpm) (Sigma 3-18KS, Sigma Laborzentrifugen GmbH, Germany). Extracted porewater (500 μ L) was placed back in the anaerobic glove box and filtered (0.45 μ m) into 6 mL plastic vials to be stored at -20°C for 2-5 days until analysis. For porewater phosphate, a separate 100 μ L sample was acidified with 10 μ L of hydrogen sulphide (H₂S) to inhibit sorption of PO₄³⁻ to other materials. Upon thawing, samples for NH₄⁺, NO₂⁻, NO₃⁻, PO₄³⁻, and DSi were analysed by a SEAL QuAAtro segmented flow analyser (Jodo et al., 1992). Detection limits were: 0.05 mmol m⁻³ for NH₄⁺ and DSi, 0.03 mmol m⁻³ for NO₃⁻ and PO₄³⁻ and 0.01 mmol m⁻³ for NO₂⁻.

2.3.5 Flux measurements

After collection, the 14.5 cm \varnothing sediment cores were brought to a climate-controlled chamber at The Royal Netherlands Institute for Sea Research, Yerseke (NIOZ- Yerseke) which was set to represent the ambient water temperature (7-20 °C) in the Eastern Scheldt. Water temperatures in the ES were obtained from the Dutch Directorate-General for Public Works and Water Management (Rijkswaterstaat, n.d.). Each core was placed in a thermostatic bath, aerated, and left to acclimatize for 16-18 h in the dark. Overlying water was carefully added to each sediment core preventing resuspension and was continuously homogenized with a central stirring mechanism attached to the lid of each core which functioned during the entire incubation. Intertidal incubations used overlying unfiltered water pumped directly from the Eastern Scheldt at the institute which is located in relatively close proximity to the intertidal sites. The water collected at subtidal sampling stations was used as overlying unfiltered water for subtidal samples. In ideal circumstances, representative water directly from intertidal sample sites would have been collected, however, logistic time-constraints prevented this from happening.

Upon the addition of overlying water, aeration was stopped, a T_o water sample was taken, and the cores were sealed airtight and dark O_2 incubations were started. Optode sensors (FireSting O_2 , Pyroscience) were used to measure oxygen concentrations in the overlying water at an interval of 30 s during the incubation period. After 4 h, the cores were opened and re-aerated for ensuing nutrient flux incubations in the dark. Water samples were collected at 4, 8, and 22 h after the start of the incubation period (after the T_o water sample), filtered (0.45 μ m; GF/F Whatman) into 6 ml polystyrene vials, and frozen (-20 °C) for nutrient analysis. Determination of nutrients followed the same procedure used for porewater nutrient samples.

All flux calculations across the sediment-water interface were obtained by fitting a linear regression on the concentration changes over time and multiplying the regression coefficient with the height of the overlying water column. A positive flux denotes an efflux or release from the sediment to the water column, and a negative flux an influx, or consumption of the solute by the sediment.

Organic matter mineralization was calculated assuming a molar ratio 1:1 carbon (C) to O_2 fluxes. Phosphorus (P) and nitrogen (N) mineralization were calculated from Redfield ratios 106:1 (C:P) and 106:16 (C: DIN), respectively.

$$DIN\ remineralization = O_2\ Flux * \frac{16}{106}$$

$$P\ remineralization = O_2\ Flux * \frac{1}{106}$$

The percentage of mineralized N and P removed from the system was calculated with the following equations:

$$DIN\ removed = \left(1 - \frac{DIN\ Flux}{DIN\ remineralization}\right) * 100$$

$$P\ removed = \left(1 - \frac{PO_4^{3-}\ Flux}{P\ remineralization}\right) * 100$$

Values over 100 % imply an influx of solutes into sediment, so that nutrient removal is higher than the nutrients generated by mineralization. The nutrients removed in addition to those mineralized are taken up from the water column.

2.3.6 Statistical analysis

All statistical analyses for this study were performed using R (R Core Team, 2020). To assess statistically significant differences between intertidal and subtidal samples, generalized linear mixed models (GLMM) were used (Bolker et al., 2009) using ‘zone’ (intertidal or subtidal) and ‘temperature’ as fixed effects and ‘station’ and ‘replicate’ as random effect variables. GLMM’s were created using the *glmer*-function in the R package “lme4” (Bates et al., 2015). For each parameter a full model (fixed and random effect variables) was run against a reduced model with only random effects using a partial F-Test. The residual error structure of the response variables featured gamma distributions which was incorporated in the GLMM’s. A log link function was specified to account for non-linearity between predictor and mean response variables. Additional information on the statistical models used can be found in Table 2.1. Water column concentrations (2016-2017) and sediment type distribution in the ES (2016) was obtained from Rijkswaterstaat (Rijkswaterstaat, 2016). Geospatial analysis was done with the program QGIS (QGIS Development Team, 2021).

2.4 Results

2.4.1 Environmental conditions and dry sediment parameters

Water temperature ranged from 7.1 – 9.9 °C in the winter to 16.9 – 19.7 °C in the summer months (Supplementary Figure B 2.1 to Figure B 2.6). Mean organic carbon stocks from intertidal stations OP (sandy) and DT (sandy), and ZK (muddy), accounted for 0.55, 0.10

Chapter 2

and 0.79 kg C m⁻² (equivalent to 46.1, 8.1 and 66.2 mol m⁻²) in the upper 10 cm of the sediment, respectively. Organic carbon stocks for subtidal HM (sandy), VN (muddy) and LG (sandy) measured 0.23, 0.98, and 0.93 kg m⁻² (19.6, 82.0 and 77.5 mol m⁻²), respectively.

On average, intertidal stations displayed lower OC percentages and higher chl a concentration compared to subtidal sites (Table 2.2). Muddy stations (ZK/VN) had the highest concentrations of OC, TN, and phytopigments (chl a, pheophorbide, pheophytin), while their OM reactivity scores (chl a/ [chl a + Phaeophytin]), were lower than those of sandy stations within their respective zones (Table 2.2). Overall, OM reactivity was significantly higher (19%) in the intertidal compared to the subtidal samples ($p < 0.05$). Details for seasonal chl a concentration in the intertidal/subtidal and macrofauna assemblages are documented in De Borger et al. (2020). Solid-P and solid-Fe were highest, on average, in the muddy stations but showed high variability for all stations except for DT, which displayed the lowest solid-P and solid-Fe values in the study (Table 2.2).

Table 2.1 Results from Generalized Linear Mixed Effects Models (GLMM) used to test differences between intertidal and subtidal samples. For each parameter a full model containing fixed and random effects was run against a reduced model which contained only random effects using a partial F-Test. Fixed effects included ‘Zone’ (intertidal or subtidal) and ‘Temperature’. Random effects included ‘Station’ (sampling location) and ‘Replicate’.

Models		
Full model:	Parameter ~ Zone + Temperature + ϵ (Station) + ϵ (Replicate)	
Reduced model:	Parameter ~ ϵ (Station) + ϵ (Replicate)	
Parameter	χ^2 (df = 2)	p – value
<i>Dry sediment parameters</i>		
Median grain size (um)	0.680	0.712
OC (%)	0.916	0.632
TN (%)	1.97	0.373
chl a	4.67	0.0965
Phaeophorbide	4.86	0.088
Phaeophytin	2.05	0.358
OM reactivity score (chl a/ [chl a + Phaeophytin])	9.03	p≤0.05
<i>Biogeochemical Fluxes</i>		
O ₂ flux	44.2	p≤0.05
NH ₄ ⁺	64.1	p≤0.05
NO ₂ ⁻	6.05	p≤0.05
NO ₃ ⁻	13.8	p≤0.05
PO ₄ ³⁻	29.1	p≤0.05
DSi	79.3	p≤0.05
DIN flux	52.9	p≤0.05
<i>Nutrient removal</i>		
Nitrogen removal	37.3	p≤0.05
Phosphorus removal	41.4	p≤0.05
% Nitrogen removal	27.8	p≤0.05

Subtidal vs intertidal biogeochemistry

% Phosphorus removal	18.1	$p \leq 0.05$
<hr/> <i>Porewater Nutrients</i> <hr/>		
NH ₄ ⁺	10.2	$p \leq 0.05$
NO ₂ ⁻	4.11	0.128
NO ₃ ⁻	14.5	$p \leq 0.05$
PO ₄ ³⁻	1.57	0.456
DSi	5.12	0.077
DIN	11.5	$p \leq 0.05$

Table 2.2 Dry sediment parameters for Eastern Scheldt stations: median grain size (D50; μm), porosity, organic carbon (OC; %) and total nitrogen (TN; %), chlorophyll a (chl a; $\mu\text{g g}^{-1}$), pheophorbide ($\mu\text{g g}^{-1}$), pheophytin ($\mu\text{g g}^{-1}$), OM reactivity score ($\text{chl a}/(\text{chl a} + \text{Pheophytin})$), solid phase phosphorus (solid-P; mol m⁻³ bulk solid) and iron (solid-Fe; mol m⁻³ bulk solid). Measurements were averaged for samples taken within 0 and 5 cm depths in the sediment. Significant figures are reported differently in accordance with the parameter.

	ZK	OP	DT	Combined Intertidal	VN	LG	HM	Combined Subtidal
D50*	56.0±16.4	124±10.8	139±1.92	106±38.6	65.3±71.6	117±8.3	195±45.3	126±72.0
Porosity*	0.52±0.08	0.46±0.12	0.40±0.09	0.46±0.10	0.60±0.06	0.42±0.05	0.34±0.05	0.46±0.12
OC*	0.83±0.40	0.17±0.04	0.06±0.01	0.34±0.41	1.1±0.42	0.56±0.14	0.37±0.07	0.67±0.39
TN	0.10±0.04	0.02±0.002	0.01±0.002	0.04±0.05	0.13±0.06	0.05±0.01	0.04±0.01	0.07±0.05
chl a*	22±3.5	11±2.7	9.3±2.5	14±6.4	13±6.7	6.1±4.2	5.8±4.5	8.4±6.3
pheophorbide	1.0±0.73	0.48±0.38	0.07±0.08	0.53±0.62	3.4±2.0	0.89±0.78	1.7±1.9	2.0±1.9
pheophytin	3.3±1.6	1.1±2.3	0.31±0.25	1.6±2.0	5.3±3.7	1.6±1.4	1.5±1.4	2.8±3.0
OM reactivity	0.88±0.04	0.92±0.07	0.97±0.01	0.92±0.06	0.70±0.10	0.80±0.08	0.81±0.07	0.77±0.09
solid-P	8.6±9.2	3.0±3.2	1.7±1.9	4.5±6.3	8.0±10.6	5.0±6.1	3.2±3.6	5.4±7.3
solid-Fe	145±156	47.9±51.3	28.4±30.4	73.7±106	149±187	73.8±79.0	92.5±117	105±133

* Recalculated from De Berger et al. (2020) with additional data.

2.4.2 Sediment-water exchange fluxes

Solute fluxes (O_2 , NH_4^+ , NO_2^- , NO_3^- , PO_4^{3-} , and DSi) were seasonally variable with an increase in fluxes in warmer months (Figure 2.2; Supplementary Figure B 2.1 to Figure B 2.6). Maximum O_2 influxes (fluxes directed into the sediment) in the intertidal incubations were observed in August 2017 ($-78.8 \text{ mmol m}^{-2} \text{ d}^{-1}$) while maximum O_2 influxes in the subtidal incubations occurred in August 2016 ($-63.9 \text{ mmol m}^{-2} \text{ d}^{-1}$; Figure 2.2). The maximum for ammonium effluxes (fluxes directed out of the sediment) was observed in the subtidal incubations in August 2016 at $4.0 \text{ mmol m}^{-2} \text{ d}^{-1}$ while maximum values for NH_4^+ effluxes in the intertidal samples were observed in September 2016 at $5.5 \text{ mmol m}^{-2} \text{ d}^{-1}$. Nitrate fluxes in intertidal samples were almost always directed into the sediment with the highest mean influxes occurring in September 2016 ($-3.2 \text{ mmol m}^{-2} \text{ d}^{-1}$). Subtidal NO_3^- displayed effluxes with a maximum of $0.79 \text{ mmol m}^{-2} \text{ d}^{-1}$ in November 2017. Phosphate fluxes in intertidal and subtidal samples fluctuated within 0.6 and $-0.4 \text{ mmol m}^{-2} \text{ d}^{-1}$ displaying an average influx for intertidal incubations throughout most of the sampling period apart from the warmer months (June – October) of 2017, while effluxes from subtidal samples were higher in the summer months for both years. Mean DSi effluxes were highest in subtidal samples reaching a maximum in July 2016 at $7.1 \text{ mmol m}^{-2} \text{ d}^{-1}$ (Figure 2.2).

Mean O_2 ($p < 0.001$), PO_4^{3-} ($p < 0.001$) and NO_3^- ($p < 0.01$), had significantly greater influxes in the intertidal samples and the latter two solutes showed an efflux in subtidal stations (Figure 2.2, Table 2.3). Subtidal stations displayed significantly higher total DIN, and DSi effluxes compared to intertidal stations ($p < 0.001$). Details for temporal fluxes at individual stations can be found in Supplementary Figure B 2.1 and Figure B 2.6.

Intertidal sediments in ZK, DT and OP mineralized 21.1 , 16.6 and $10.8 \text{ mol C m}^{-2} \text{ y}^{-1}$ compared to 14.0 , 13.4 and $8.1 \text{ mol C m}^{-2} \text{ y}^{-1}$ at subtidal sites LG, HM, and VN, respectively. ZK (muddy intertidal) exhibited the strongest fluxes of O_2 , NH_4^+ , NO_3^- , and DSi. The muddy subtidal site VN displayed the weakest fluxes for O_2 and NH_4^+ (Table 2.3). Intertidal sediments had higher macrofaunal abundance but lower biomass than subtidal sites (De Borger et al., 2020).

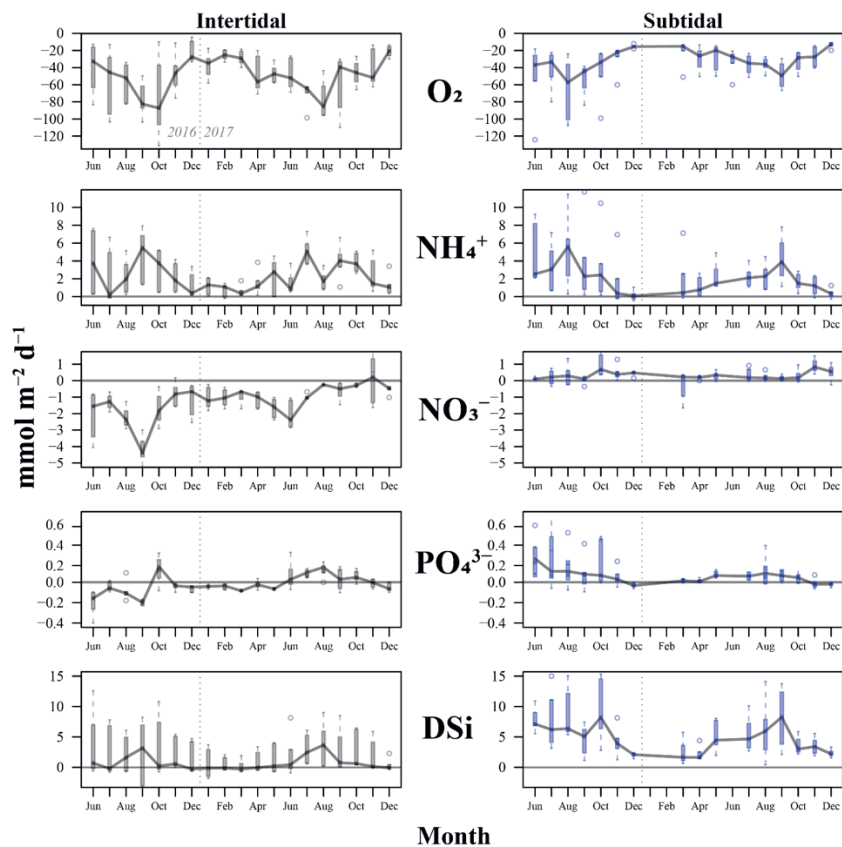


Figure 2.2 Temporal comparison of sediment water exchange fluxes for oxygen and inorganic nutrient between subtidal and intertidal stations. The dark line represents the monthly median flux value with boxplots representing the monthly distribution of the data (minimum/maximum, interquartile range). Negative values denote an influx from the overlying water directed into the sediment.

Table 2.3 Annually averaged mean (\pm standard deviation) daily sediment-water exchange fluxes for oxygen, ammonium, nitrite, nitrate, phosphate, silica, calculated nitrogen (N) and phosphorus (P) mineralization, and the calculated removal of N and P (all units in: $\text{mmol m}^{-2} \text{d}^{-1}$). Negative fluxes indicate sediment influx and positive are sediment effluxes. Significant figures are reported differently in accordance with the parameter.

	ZK	OP	DT	Combined Intertidal	VN	LG	HM	Combined Subtidal
O ₂	-59.7 \pm 23.2	-30.3 \pm 14.8	-48.9 \pm 18.1	-46.3 \pm 22.4	-24.7 \pm 9.7	-40.2 \pm 19.6	-36.7 \pm 8.6	-33.9 \pm 17.6
NH ₄ ⁺	3.5 \pm 1.7	1.9 \pm 1.6	1.0 \pm 1.2	2.1 \pm 1.8	1.1 \pm 0.91	3.3 \pm 2.3	2.7 \pm 2.7	2.4 \pm 2.3
NO ₂ ⁻	0.16 \pm 0.08	0.05 \pm 0.07	0.12 \pm 0.21	0.11 \pm 0.15	0.19 \pm 0.21	0.26 \pm 0.19	0.13 \pm 0.17	0.19 \pm 0.19
NO ₃ ⁻	-1.8 \pm 0.55	-0.99 \pm 0.62	-0.96 \pm 0.84	-1.24 \pm 0.77	0.48 \pm 0.38	0.14 \pm 0.56	0.24 \pm 0.28	0.28 \pm 0.44
PO ₄ ³⁻	0.001 \pm 0.06	-0.04 \pm 0.07	-0.04 \pm 0.06	-0.03 \pm 0.07	0.06 \pm 0.07	0.07 \pm 0.10	0.13 \pm 0.22	0.09 \pm 0.14
DSi	4.5 \pm 2.2	0.72 \pm 1.5	-0.53 \pm 0.56	1.6 \pm 2.6	4.5 \pm 2.4	5.5 \pm 2.8	5.2 \pm 4.0	5.1 \pm 3.1
N mineralized	9.0 \pm 3.5	4.6 \pm 2.2	7.4 \pm 2.7	6.7 \pm 3.8	3.7 \pm 1.5	6.1 \pm 3.0	5.5 \pm 2.8	5.1 \pm 2.7
P mineralized	0.56 \pm 0.21	0.29 \pm 0.14	0.46 \pm 0.16	0.44 \pm 0.21	0.23 \pm 0.08	0.38 \pm 0.16	0.35 \pm 0.23	0.32 \pm 0.17
N removed	7.1 \pm 2.7	3.6 \pm 1.6	7.2 \pm 2.4	6.0 \pm 2.8	2.0 \pm 0.89	2.3 \pm 1.2	2.4 \pm 1.1	2.3 \pm 1.0
P removed	0.44 \pm 0.17	0.23 \pm 0.10	0.45 \pm 0.15	0.37 \pm 0.17	0.12 \pm 0.05	0.15 \pm 0.07	0.15 \pm 0.07	0.14 \pm 0.06
% N removed *	80.4 \pm 13.7	82.7 \pm 23.7	99.8 \pm 14.6	87.7 \pm 19.7	55.5 \pm 16.9	42.6 \pm 19.4	50.7 \pm 21.0	49.6 \pm 19.6
% P removed *	103 \pm 12.3	125 \pm 33.3	111 \pm 13.7	113 \pm 23.5	77.5 \pm 28.1	83.5 \pm 22.2	74.6 \pm 38.3	78.5 \pm 30.0

*Values over 100 % imply the that the sediment influx is higher than the nutrients generated by mineralization. The additional influx is taken up from the water column.

Chapter 2

Measured nutrient fluxes deviated considerably from the fluxes based on OC mineralization, and assuming Redfield stoichiometric ratios. C: DIN flux ratios from intertidal samples were, on average, higher but more variable than those from the subtidal stations (Figure 2.3). In intertidal samples, the deviations from Redfield were lowest for station OP and highest for station DT. On average the DIN:DIP ratio of fluxes exceeded Redfield (16:1), indicating that phosphorus was more efficiently removed than nitrogen for most stations (Figure 2.3).

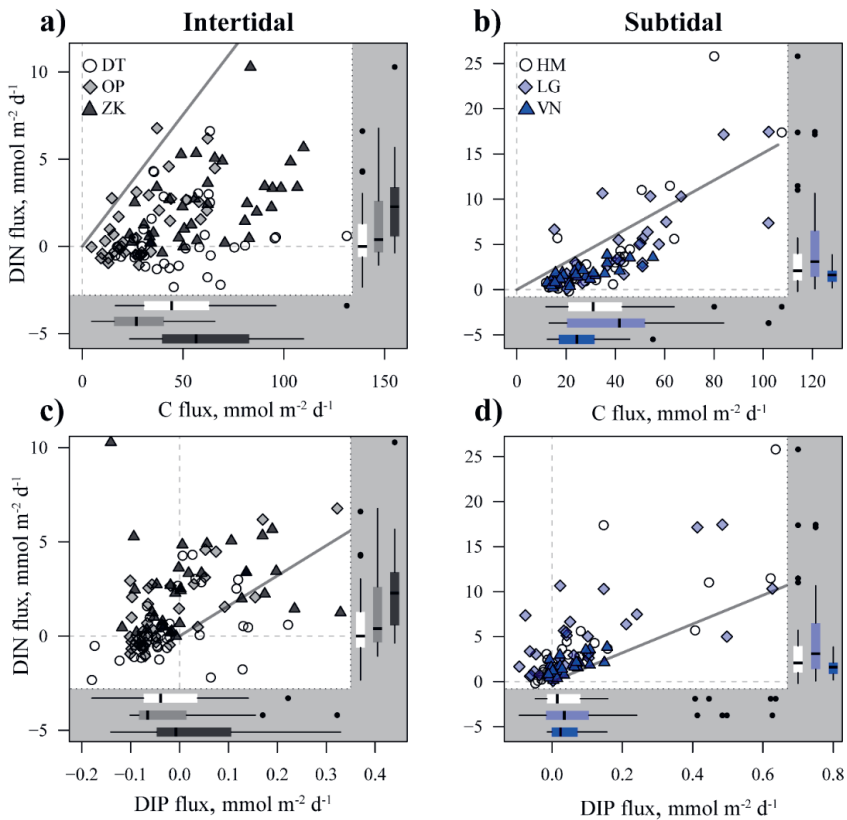


Figure 2.3 Relation between dissolved inorganic nitrogen (DIN) and organic carbon (C) fluxes (a-b), DIN and dissolved inorganic phosphorus (DIP) fluxes (c-d). The dark line represents the Redfield (C: N:P = 106:16:1) ratio.

2.4.3 Porewater nutrients

In contrast to nutrient fluxes, porewater nutrients did not show noticeable levels of seasonality in either zone and were therefore pooled for further analysis. Mean porewater concentrations (0 – 10 cm depth) of NH_4^+ ($p < 0.01$) were significantly higher in subtidal

($299 \pm 209 \text{ mmol m}^{-3}$) compared to intertidal ($83.4 \pm 45.4 \text{ mmol m}^{-3}$) stations. NO_3^- concentrations were higher in the intertidal ($5.1 \pm 5.7 \text{ mmol m}^{-3}$) than in subtidal ($3.9 \pm 3.7 \text{ mmol m}^{-3}$; $p < 0.001$) sediments. The highest concentrations of phosphate were found in the muddy stations of the intertidal (ZK; $86.4 \pm 79.3 \text{ mmol m}^{-3}$) and subtidal (VN; $100 \pm 35.6 \text{ mmol m}^{-3}$). VN also displayed the highest mean NH_4^+ ($512 \pm 172 \text{ mmol m}^{-3}$), and DSi ($745 \pm 162 \text{ mmol m}^{-3}$) concentrations (Figure 2.4). The sandy intertidal DT station had the lowest concentration of DSi ($23.8 \pm 12.5 \text{ mmol m}^{-3}$), NH_4^+ ($44.3 \pm 22.8 \text{ mmol m}^{-3}$), and PO_4^{3-} ($12.5 \pm 8.3 \text{ mmol m}^{-3}$), but also exhibited the highest concentrations of NO_3^- ($7.7 \pm 6.9 \text{ mmol m}^{-3}$) mostly relegated to its upper (0-5cm depth) sediment layers (Figure 2.4). Sediment porewater contained more phosphorus than expected from the N:P Redfield ratio (16:1; Figure 2.5). Data from the sandy intertidal and subtidal stations OP and HM, was the closest to the Redfield N:P proportion while other stations were skewed towards lower ratios. The DIN:DIP ratio of the sandy intertidal and subtidal stations was close to Redfield, while other stations were lower.

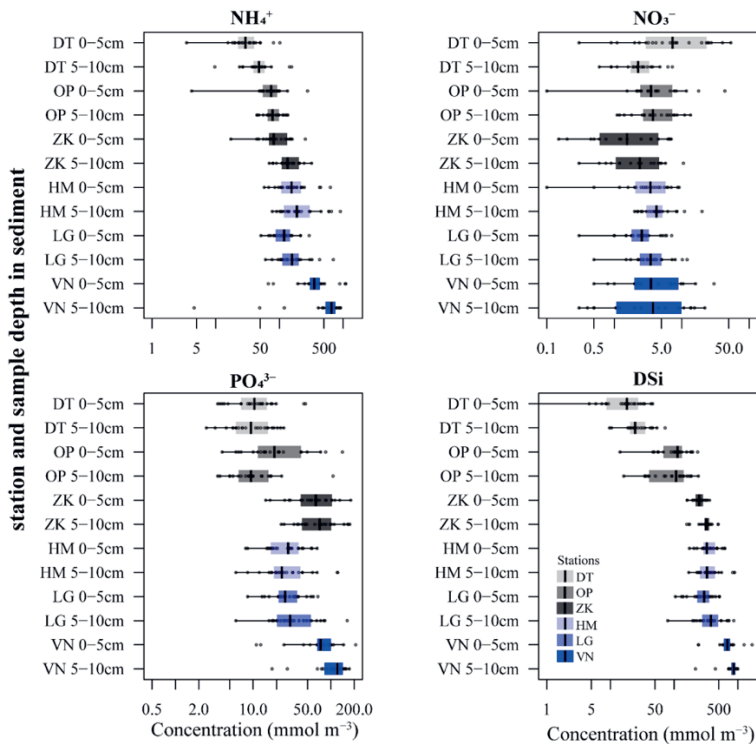


Figure 2.4 Porewater nutrient concentrations shown in logarithmic scale for ammonium (NH_4^+) nitrate (NO_3^-), phosphate (PO_4^{3-}) and dissolved silicate (DSi) in the top (0-5 cm) and bottom (5-10 cm) slices per station. Intertidal stations are shown in grey and subtidal in blue. Note differences in x-axis scale.

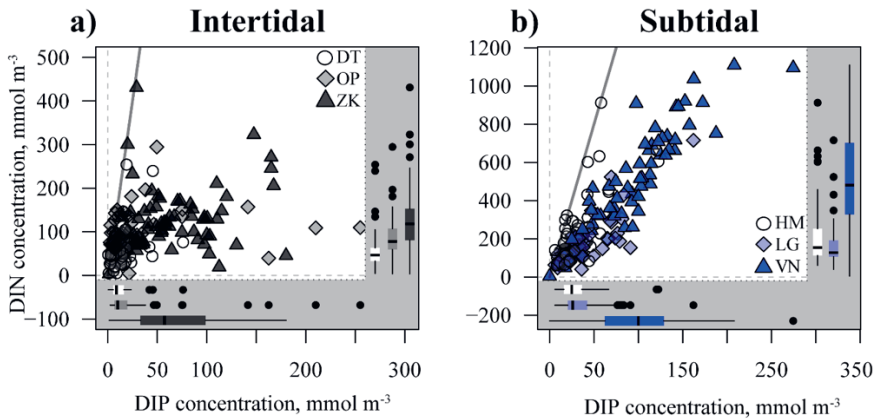


Figure 2.5 The DIN: DIP relation in the sediment porewater (a and b) in subtidal and intertidal stations. The dark line represents the expected Redfield (C: N:P = 106:16:1) ratio.

2.4.4 Nutrient removal

Nutrient removal refers to the processes through which inorganic nutrients released from mineralization become unavailable for primary production. This may occur, for example, through denitrification (bioavailable nitrogen converted to gaseous nitrogen), burial or sediment sorption (bioavailable nutrients which are isolated within the sediment). Combined incubations from intertidal stations removed a significantly higher percentage of total inorganic nitrogen (N) and phosphorus (P) (87.7 % and 113 %, respectively) after mineralization ($p < 0.001$) compared to combined incubations from subtidal stations (49.6 % and 78.5 %, respectively; Table 2.3). The percentage of inorganic N or P removed during incubations from intertidal sediments regularly exceeded 100%. This indicates that nutrient removal was higher than nutrient release from mineralization and thus additional solutes from the overlying water were utilized. Over the 1.5-year monitoring period, a nutrient removal rate exceeding 100% for N and P was observed in 31 % and 75 % of incubations from intertidal sites, while in subtidal sites N removal was never observed and P removal occurred in 18% of the incubations.

In subtidal incubations, percentage P removal was highest in the sandy LG station. In intertidal sediments, the observed percentage N removal capacity was highest at the sandy site DT (Table 2.3). Bioavailable phosphorus was preferentially trapped in intertidal sediments where over 100 % of P was removed after mineralization. The total N and P removal per meter squared was also significantly higher in the intertidal compared to the subtidal ($p < 0.001$) with the highest values for N and P removal coming from DT in the intertidal and the lowest values exhibited in subtidal VN (Table 2.3).

2.5 Discussion

Our results reveal disparities in OM quality, sediment-water exchange fluxes, porewater solute concentrations and the nutrient removal capacity between specific intertidal and subtidal stations in the Eastern Scheldt. Overall, intertidal samples exhibited higher rates of OM cycling and nutrient removal compared to subtidal sediments. The conversion of intertidal to subtidal areas resulting from ongoing intertidal erosion may affect the biogeochemical dynamics of coastal areas and adjacent water bodies. Here we discuss the potential importance of each tidal zone for sedimentary carbon, the mechanisms behind ES nutrient dynamics, and end with an upscaling exercise to explore how future biogeochemical functioning may change based on the expected loss of intertidal surface area in the ES.

2.5.1 Carbon characteristics of Eastern Scheldt intertidal and subtidal areas

Our results suggest that microphytobenthos activity is a determining factor for carbon degradation and other biogeochemical dynamics. Intertidal sediments exhibit a higher chl *a* concentration and are characterized by high microphytobenthos densities (Serôdio and Paterson, 2021), compared to subtidal sediments. This is likely to be one of the factors contributing to the higher OM reactivity and enhanced rates of OM degradation (as inferred from measured O₂ fluxes) in intertidal compared to subtidal samples. Growth of microphytobenthos on ES intertidal flats may provide enough input of fresh OM to maintain a high reactivity score while fuelling increased levels of carbon degradation. This pattern of more reactive OM in shallow vs deep marine habitats has also been found on continental shelf sediments surrounding the United Kingdom and France (Lamarque et al., 2021; Smeaton and Austin, 2022). Reduced DSi concentrations found in intertidal (vs. subtidal) porewater samples (Figure 2.4) provide further evidence of diatom (microphytobenthos) uptake of DSi.

De Borger et al. (2020) describes the relationship between macrobenthos and bioirrigation in the Eastern Scheldt and combined with results from the current study can give valuable insight on how ES fauna affects carbon cycling. ES intertidal sites are associated with prominent bioirrigators with DT being dominated by burrowing amphipods (*Corophium sp.*, *Bathyporeia sp.*) while OP and ZK assemblages are linked with the large polychaetes *Arenicola marina* and *Hediste diversicolor* (De Borger et al., 2020). In contrast, subtidal ES sites are associated with epifaunal assemblages (species residing on the sediment surface) except for LG where the tube building polychaete *Lanice conchilega* is commonly found in the cooler months of the year (De Borger et al., 2020). Our results of higher O₂ consumption (and estimated carbon mineralization) from ES intertidal samples (Table

Chapter 2

2.3) are consistent with De Borger et al. (2020)'s observations of 'deeper' bioirrigation in ES intertidal versus subtidal sediments. This suggests that ES faunal assemblages that cause solute exchange within deeper portions of the sediment, such as those found in the intertidal sites, may facilitate higher rates of organic carbon mineralization (De Borger et al., 2020).

Temperate coastal environments in other parts of the world display higher percentages of organic carbon compared to the ES (Falcão and Vale, 1998; Byun et al., 2019; Douglas et al., 2022). This difference could be related to the reduced input of sedimentary OM to the ES due to the almost absent riverine input; and to the net export of sediments and sedimentary OM to the North Sea created after flood mitigation developments (Wetsteyn et al., 2003; van Zanten and Adriaanse, 2008; Jiang et al., 2020a). The construction of the storm surge barrier in the ES has also reduced water column nutrient concentrations by limiting riverine input (Smaal and Nienhuis, 1992). Understanding the tight coupling between OM production and inorganic nutrients in the ES involves knowledge of biogeochemical processes affecting nutrient availability.

2.5.2 *Nutrient dynamics and removal in the Eastern Scheldt*

Inorganic nutrient concentrations in porewater, sediment-water exchange fluxes, and benthic removal processes (the long-term sequestration of bioavailable nutrients) depend on abiotic variables such as sediment type (Precht et al., 2004) and biotic variables including the presence of microphytobenthos and/or benthic faunal activity (de Backer et al., 2010; De Borger et al., 2020). Our study highlights fundamental disparities in nutrient removal functions between subtidal and intertidal sediments, which were detected upon the analysis of porewater nutrients and the exchange fluxes of NO_3^- and PO_4^{3-} .

Coarse sediments promote nitrification, nutrient release and porewater advection (Precht et al., 2004), and typically exhibit low concentrations of porewater nutrients (De Borger et al., 2021). Muddy ES sediments (ZK and VN) indeed hold higher NH_4^+ and PO_4^{3-} concentrations (Figure 2.4), compared to adjacent sandy sites, a pattern consistent with other temperate sedimentary systems (Falcão and Vale, 1998; Berthold et al., 2018). Small sediment particles exhibit an increased PO_4^{3-} sorption capacity compared to bigger sand particles (Borggaard, 1983). Moreover, muddy sediments have a lower oxygen content which facilitates the desorption of PO_4^{3-} from iron oxides at depth promoting the release of bioavailable phosphorus in porewater (Slomp et al., 1996). This eventually translates in higher concentrations of PO_4^{3-} at depth, like those observed in ZK and VN.

Subtidal sediments displayed relatively high porewater concentrations of NH_4^+ , PO_4^{3-} and DSi, possibly resulting from the lower levels of bioirrigation which have been found at these sites (De Borger et al., 2020). Bioirrigation can increase the oxygenation of sediments and can indirectly enhance nutrient removal processes such as denitrification

(Braeckman et al., 2010b, 2014). Less bioirrigation leads to lower removal and flushing of nutrients causing their accumulation in porewaters and subsequent release to the water column by diffusion, as suggested by the prevalent efflux NH_4^+ , PO_4^{3-} and DSi (Figure 2.2) in the subtidal samples.

A higher chl a concentration in intertidal sites (Table 2.2) suggested that microphytobenthic OM helps fuel the rapid mineralization measured in those sites (Table 2.3), and may potentially support denser benthic communities (De Borger et al., 2020) than in the subtidal sites. The relatively low concentrations of OC, TN (Table 2.2), NH_4^+ , DSi and PO_4^{3-} , and higher NO_3^- (Figure 2.4) observed in intertidal sites porewater may result from higher mineralization, bioirrigation (de Backer et al., 2010; De Borger et al., 2020), tidal flushing (Falcão and Vale, 1998) and/or porewater advection (Precht et al., 2004). These factors facilitate processes that decrease porewater solutes such as nitrification-denitrification, nutrient flushing, and the sorption of phosphates. Influxes of NO_3^- and PO_4^{3-} (as opposed to effluxes; Figure 2.2) observed in the intertidal incubations suggest enhanced sorption of phosphate to sediment particles and higher denitrification than in the subtidal samples; results in agreement with other studies (Piehler and Smyth, 2011). Furthermore, intertidal samples removed on average 80% of mineralized dissolved inorganic nitrogen (DIN) and at least 100% of mineralized dissolved inorganic phosphorus (DIP) (Table 2.3). Intertidal nutrient influxes have been observed in other coastal systems (Magalhães et al., 2002; Khalil et al., 2018) but they contrast with observations from the adjacent Western Scheldt estuary (Rios-Yunes et al., 2023b) where an efflux of DIN and DIP was observed in brackish and marine intertidal mudflats.

The comparisons of the flux ratios with Redfield proportions (Figure 2.3 a and 3 b) show the removal of bioavailable nitrogen, as the flux ratios of C:DIN exceed Redfield (C: N; 106:16). All ES sites also exhibited lower average DIN:DIP flux ratios compared to Redfield (N:P; 16:1) suggesting a proportionally greater sedimentary removal of P compared to N (Figure 2.3 and 3d, Table 2.3) similar to patterns observed in the Douro River estuary in Portugal (Magalhães et al., 2002). While nitrogen is lost from sediments as nitrogen gas, phosphorus is removed by burial in the sediment, often sorbed to solids. Moreover, the comparison between porewater concentration ratios with Redfield (Figure 2.5 a and b) evidenced the preferential removal of DIP over DIN of intertidal and subtidal sediments in this study. Particularly in the intertidal sediments, the DIN: DIP concentration ratio may strongly exceed Redfield (16:1), often leading to PO_4^{3-} concentrations that are as high as DIN (Figure 2.5a). Most of the burial of P is in solid form, as evidenced by the iron-bound phosphorus which measured over two orders of magnitude higher than porewater concentrations indicating high sorption of PO_4^{3-} in ES sediments (solid phase phosphorous in Table 2.2 in mol m^{-3}). By extrapolating information on nutrient removal to total surface areas in the ES, we may be able to roughly predict the impact of future changes to the intertidal-subtidal dynamic.

2.5.3 *Spatial analysis and future implications*

Our study considers six sampling locations within the Eastern Scheldt tidal bay, and we acknowledge that extrapolating from these stations may not lead to a completely accurate representation of biogeochemical dynamics within the system, particularly if certain important areas are underrepresented. Nevertheless, to gain a better understanding of how sediments may affect biogeochemical functioning in the ES, we conducted an upscaling exercise based on the assumption that the average parameters measured in the stations described in this study are representative of the greater ES system.

Our results were spatially interpolated to understand the overall contribution of each zone and sediment type to nutrient removal of the Eastern Scheldt system. The ES covers an area of 347 km² with 216 km² subtidal and 118 km² intertidal area. Of the intertidal area, 1.6 km² corresponds to muddy and ~117 km² to sandy sediments with the remaining area covered by a rocky bottom or saltmarshes. Yearly averaged system-wide mineralization budgets were calculated by considering the contribution of each sediment type to each tidal area. Currently, our estimates suggest that intertidal areas in the ES remove more nitrogen (2.3×10^8 mol N y⁻¹) than subtidal areas (1.8×10^8 mol N y⁻¹), but P removal seems to be similar between these zones (both with $\sim 1.8 \times 10^7$ mol P y⁻¹). This means that if the ES was a closed system without external nutrient inputs, the average winter concentration of N and P in the water column (Rijkswaterstaat, n.d.) may be depleted in ~ 70 and 20 days, respectively. Assuming dynamic equilibrium for ES nutrient sources and sinks, this suggests a substantial input of nutrients from the North Sea to balance this removal. It is noteworthy that our calculation of nutrient removal may be conservative as it is based on dark respiration processes and no primary production has been considered. Primary production could increase nutrient removal through the biogenic uptake from microphytobenthos (Clavier et al., 2005).

A consequence of the flood mitigation developments in the ES has been the ongoing loss of intertidal areas due to “sand starvation”, and the reduced exchange of nutrients and OM with the North Sea (Wetsteyn et al., 2003; van Zanten and Adriaanse, 2008). It is estimated that erosion will contribute to a 35 % loss of intertidal areas in the next four decades (Ysebaert et al., 2016). Following Ysebaert et al. (2016)’s estimates, eroding intertidal areas will increase the ES subtidal area by 19 % potentially reducing the total sedimentary (subtidal + intertidal) nutrient removal of the ES. If the measurements from this study are representative of the greater ES region and if they remain consistent over time, we calculate an erosion induced decrease in the total nitrogen removal capacity from 4.1×10^8 mol N y⁻¹ to 3.7×10^8 mol N y⁻¹ (11 %). We also expect that the future removal capacity of phosphorus to decrease from 3.6×10^7 mol P y⁻¹ to 3.3×10^7 mol P y⁻¹ (8 %). The loss of intertidal surface area could compromise areas important for OM mineralization and nutrient cycling and may decrease important ecosystem functions such as

nitrogen/phosphorus removal, potentially increasing the concentration of nutrients available for primary production.

Sea level rise (SLR) presents an additional threat to ES intertidal areas (Fox-Kemper et al., 2021). Estimates for SLR in the North Sea close to the ES predict an increase of ~17.1 cm following the SSP1-1.9 (Paris) scenario and 27.8 cm for the SSP5-8.5 by 2060 (pers. Comm. Aimée Slangen, Fox-Kemper et al. (2021)). The inclusion of SLR estimates for coastal systems is highly complex and is still in its infancy. A study on future SLR in the ES concluded that tidal amplitude would increase, and that the ES would become ebb-dominated (Jiang et al., 2020a). A transition to ebb-dominance in an already sand-starved system like the ES means that erosion of the intertidal zone, and the resulting loss of nutrient removal capacity would be exacerbated in the future.

It is noteworthy that the future estimates we present may be conservative as they do not account for SLR and might be underestimating the potential loss of nutrient removal capacity in the ES. This can be concerning for a system like the ES due to its ecological and cultural importance. Alterations to its biogeochemical regime, nutrients and primary production can affect the local and migratory species and have consequences for economic activities (Zwarts et al., n.d.; Nienhuis and Smaal, 1994; Ysebaert et al., 2016). Studying how SLR and sand starvation could affect intertidal areas and corresponding nutrient removal functions in coastal areas is therefore important to understand future biogeochemical characteristics of these areas.

To conclude, our study shows that the mineralization and bioavailable removal of inorganic nutrients can be significantly higher in intertidal sediments than in subtidal areas. These results are highly relevant since intertidal areas around the world are receding due to coastal development, erosion, and sea-level rise (Murray et al., 2019). Mudflats cover ~127,000 km² worldwide, and their decline may have consequences on local and regional biogeochemical functioning. Therefore, improved understanding of tidal flat ecosystems is essential to manage and/or mitigate potential reductions to their functions and services. In addition, the relevance of investigating the Dutch coastal zone is that it is one of the most extensively engineered areas in the world. Thus, the environmental consequences derived from the loss of intertidal areas in Dutch systems could serve as a case study to guide future coastal protection projects elsewhere, and to some extent, prevent undesirable environmental problems derived from extensive coastal engineering, coastal erosion, and rising sea levels.

2.6 Acknowledgements

We thank Rijkswaterstaat and the crew of their research vessel, the Delta, for making it possible to conduct the subtidal sampling for this study. We also thank various students who have helped with collecting and processing the information for this study. This work

Chapter 2

could not have been done without the help of the NIOZ analytical lab (Peter van Breugel, Yvonne Maas, Jan Peene, Jurian Brassers and more) which processed our sediment and water samples. Dunia Rios Yunes is a doctoral research fellow funded by the Royal Netherlands Academy of Arts and Sciences (KNAW) (project no. PSA-SA-E-02). Justin Tiano was supported by the Netherlands Ministry of Agriculture, Nature, and Food Quality (LNV) and European Maritime and Fisheries Fund (EMFF) (grant no. 1300021172).

2.7 Appendix

2.7.1 Appendix A: Supplementary Tables

Table A 2.1 Sampling details for oxygen and nutrient fluxes, porewater nutrients, dissolved inorganic carbon (DIC) fluxes and total alkalinity (TA) fluxes. An “x” represents samples taken while a “-” represents absence of sampling. Sample dates are in dd/mm/y format.

Date	Season	Zone	Nutrient Flux	Porewater Nutrients	DIC Flux	TA Flux
07/06/2016	Summer	Subtidal	x	x	-	-
22/06/2016	Summer	Intertidal	x	x	-	-
06/07/2016	Summer	Subtidal	x	x	-	-
18/07/2016	Summer	Intertidal	x	x	x	x
01/08/2016	Summer	Subtidal	x	x	x	x
23/08/2016	Summer	Intertidal	x	x	x	x
13/09/2016	Autumn	Subtidal	x	x	x	x
20/09/2016	Autumn	Intertidal	x	x	x	x
11/10/2016	Autumn	Subtidal	x	x	x	x
18/10/2016	Autumn	Intertidal	x	x	x	x
07/11/2016	Autumn	Subtidal	x	x	x	x
22/11/2016	Autumn	Intertidal	x	x	x	x
05/12/2016	Winter	Subtidal	x	x	-	x
12/12/2016	Winter	Intertidal	x	x	-	-
17/01/2017	Winter	Intertidal	x	x	x	x
13/02/2017	Winter	Intertidal	x	x	x	x
13/03/2017	Spring	Intertidal	x	x	x	x
27/03/2017	Spring	Subtidal	x	x	x	x
10/04/2017	Spring	Intertidal	x	x	x	x
24/04/2017	Spring	Subtidal	x	x	x	x
09/05/2017	Spring	Intertidal	x	x	x	x
22/05/2017	Spring	Subtidal	x	x	x	x
06/06/2017	Summer	Subtidal	x	x	x	x
20/06/2017	Summer	Intertidal	x	x	x	x
04/07/2017	Summer	Subtidal	x	x	x	x
24/07/2017	Summer	Intertidal	x	x	x	x
17/08/2017	Summer	Subtidal	x	x	x	x
28/08/2017	Summer	Intertidal	x	x	x	x
12/09/2017	Autumn	Subtidal	x	x	x	x
25/09/2017	Autumn	Intertidal	x	x	x	x
09/10/2017	Autumn	Subtidal	x	x	x	x
23/10/2017	Autumn	Intertidal	x	x	x	x
07/11/2017	Autumn	Subtidal	x	x	x	x
20/11/2017	Autumn	Intertidal	x	x	x	x
04/12/2017	Winter	Subtidal	x	x	x	x
19/12/2017	Winter	Intertidal	x	x	x	x

Table A 2.2 Sampling details for chloropigments in the sediment, particle size and organic carbon (OC) analysis and solid phase iron (Fe) and phosphorus (P) analysis. An “x” represents samples taken while a “-” represents absence of sampling.

Date	Season	Zone	Sediment Pigments	Particle Size & OC	Solid Fe & P
07/06/2016	Summer	Subtidal	x	-	x
22/06/2016	Summer	Intertidal	-	-	x
06/07/2016	Summer	Subtidal	x	x	-
18/07/2016	Summer	Intertidal	x	x	-
01/08/2016	Summer	Subtidal	x	-	-
23/08/2016	Summer	Intertidal	x	-	-
13/09/2016	Autumn	Subtidal	x	-	-
20/09/2016	Autumn	Intertidal	x	-	-
11/10/2016	Autumn	Subtidal	x	-	-
18/10/2016	Autumn	Intertidal	x	-	-
07/11/2016	Autumn	Subtidal	x	-	-
22/11/2016	Autumn	Intertidal	x	-	-
05/12/2016	Winter	Subtidal	x	x	x
12/12/2016	Winter	Intertidal	x	x	x
17/01/2017	Winter	Intertidal	x	-	-
13/02/2017	Winter	Intertidal	x	-	-
13/03/2017	Spring	Intertidal	x	-	-
27/03/2017	Spring	Subtidal	x	-	-
10/04/2017	Spring	Intertidal	x	-	-
24/04/2017	Spring	Subtidal	x	-	-
09/05/2017	Spring	Intertidal	x	-	-
22/05/2017	Spring	Subtidal	x	-	-
06/06/2017	Summer	Subtidal	x	-	-
20/06/2017	Summer	Intertidal	x	-	-
04/07/2017	Summer	Subtidal	x	-	x
24/07/2017	Summer	Intertidal	x	-	x
17/08/2017	Summer	Subtidal	x	-	-
28/08/2017	Summer	Intertidal	x	-	-
12/09/2017	Autumn	Subtidal	x	-	-
25/09/2017	Autumn	Intertidal	x	-	-
09/10/2017	Autumn	Subtidal	-	-	-
23/10/2017	Autumn	Intertidal	-	-	-
07/11/2017	Autumn	Subtidal	x	-	-
20/11/2017	Autumn	Intertidal	x	-	-
04/12/2017	Winter	Subtidal	-	-	x
19/12/2017	Winter	Intertidal	-	-	x

2.7.2 Appendix B: Supplementary Figures

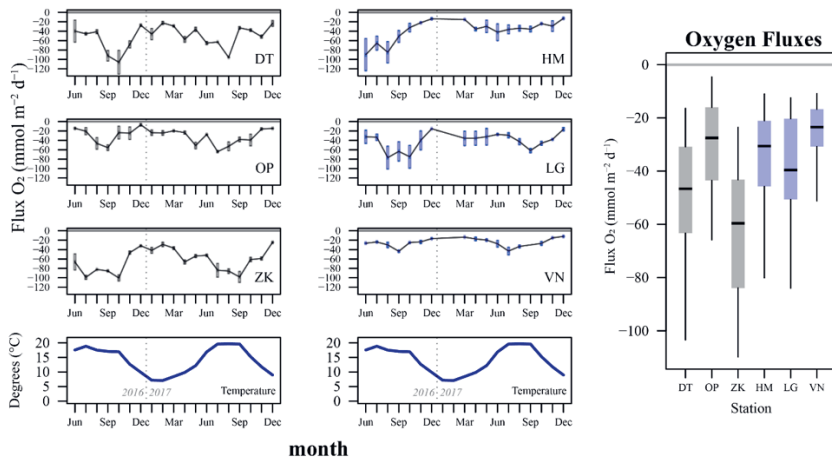


Figure B 2.1 Average monthly oxygen fluxes at each Eastern Scheldt station during the 1.5-year sampling period represented as mmol per m² per day (left). Vertical bars represent standard deviations. The total flux data per station represented as boxplots (mmol m⁻² d⁻¹; right). Intertidal stations are represented in grey and subtidal in blue. Temperature represents the water temperature recorded during incubations which reflected ambient water temperatures in the Eastern Scheldt.

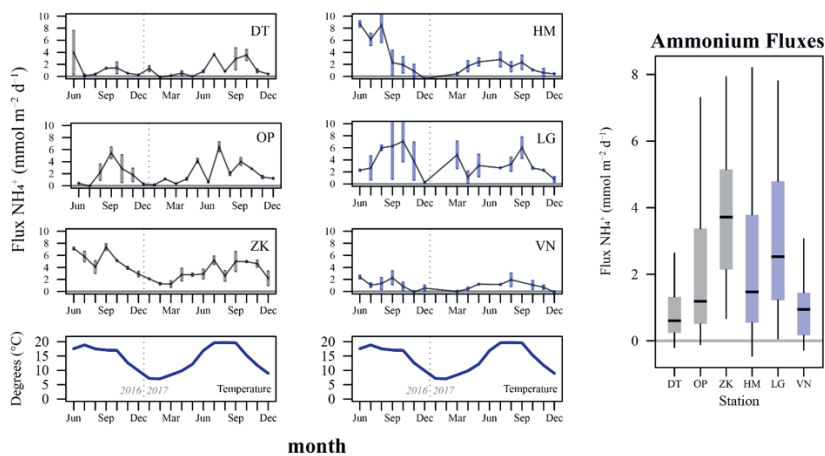


Figure B 2.2 Average monthly ammonium fluxes at each Eastern Scheldt station during the 1.5-year sampling period represented as mmol per m² per day (left). Vertical bars represent standard deviations. The total flux data per station represented as boxplots (mmol m⁻² d⁻¹; right). Intertidal stations are represented in grey and subtidal in blue. Temperature represents the water temperature recorded during incubations which reflected ambient water temperatures in the Eastern Scheldt.

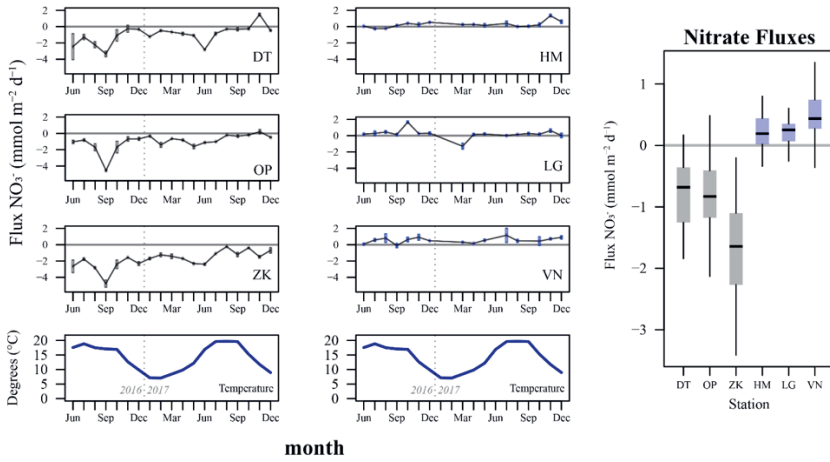


Figure B.2.3 Average monthly nitrate fluxes at each Eastern Scheldt station during the 1.5-year sampling period represented as mmol per m² per day (left). Vertical bars represent standard deviations. The total flux data per station represented as boxplots (mmol m⁻² d⁻¹; right). Intertidal stations are represented in grey and subtidal in blue. Temperature represents the water temperature recorded during incubations which reflected ambient water temperatures in the Eastern Scheldt.

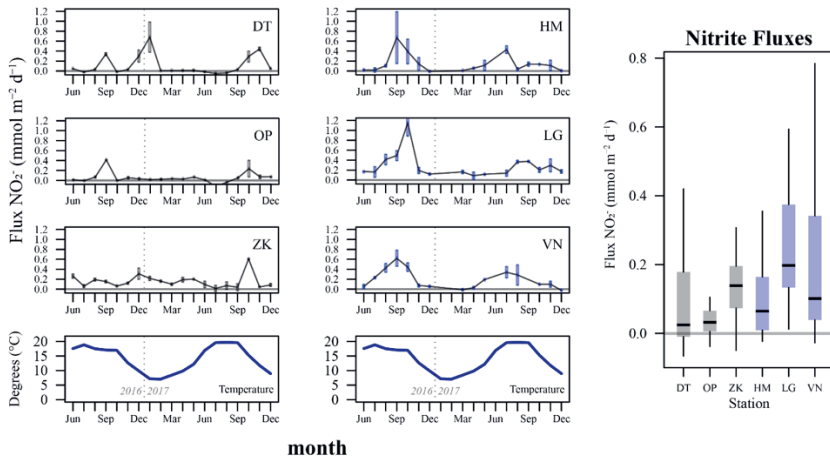


Figure B.2.4 Average monthly nitrite fluxes at each Eastern Scheldt station during the 1.5-year sampling period represented as mmol per m² per day (left). Vertical bars represent standard deviations. The total flux data per station represented as boxplots (mmol m⁻² d⁻¹; right). Intertidal stations are represented in grey and subtidal in blue. Temperature represents the water temperature recorded during incubations which reflected ambient water temperatures in the Eastern Scheldt.

Chapter 2

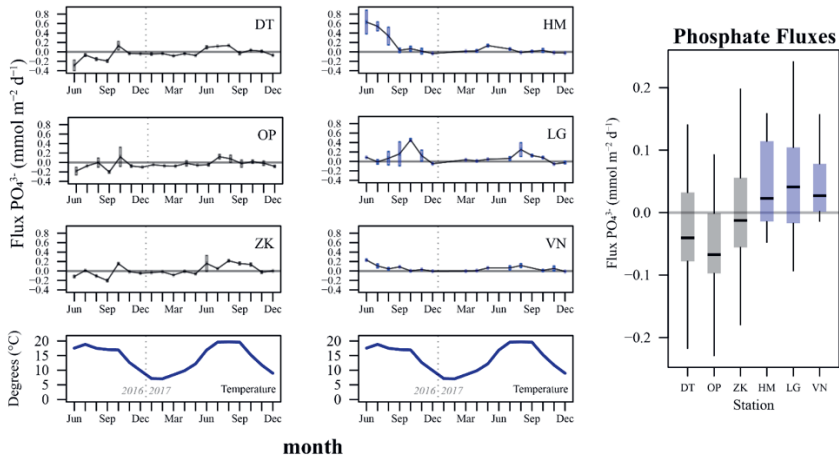


Figure B 2.5 Average monthly phosphate fluxes at each Eastern Scheldt station during the 1.5-year sampling period represented as mmol per m² per day (left). Vertical bars represent standard deviations. The total flux data per station represented as boxplots ($\text{mmol m}^{-2} \text{d}^{-1}$; right). Intertidal stations are represented in grey and subtidal in blue. Temperature represents the water temperature recorded during incubations which reflected ambient water temperatures in the Eastern Scheldt.

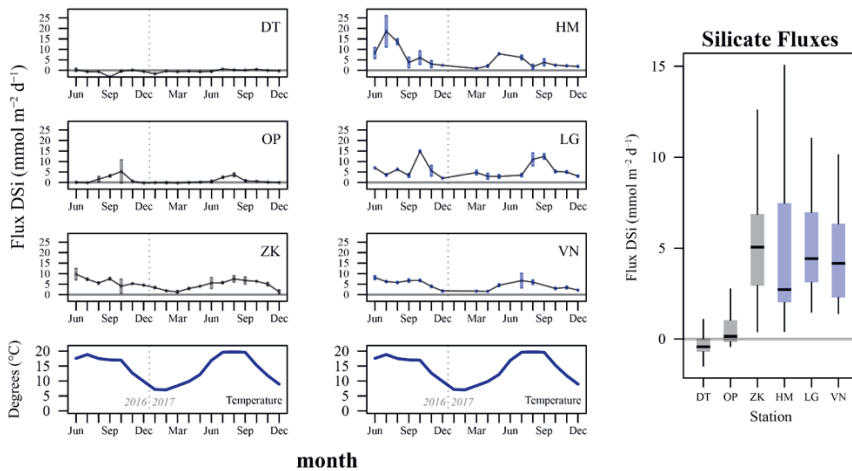


Figure B 2.6 Average monthly dissolved silicate fluxes at each Eastern Scheldt station during the 1.5-year sampling period represented as mmol per m² per day (left). Vertical bars represent standard deviations. The total flux data per station represented as boxplots ($\text{mmol m}^{-2} \text{d}^{-1}$; right). Intertidal stations are represented in grey and subtidal in blue. Temperature represents the water temperature recorded during incubations which reflected ambient water temperatures in the Eastern Scheldt

Chapter 3 *Annual
biogeochemical cycling in
intertidal sediments of a restored
estuary reveals dependence of N,
P, C and Si cycles to
temperature and water column
properties*

Dunia Rios-Yunes; Justin C. Tiano; Dick van Oevelen; Jeroen van Dalen
& Karline Soetaert

Published in Estuarine Coastal and Shelf Science (2023)

DOI: [10.1016/j.ecss.2023.108227](https://doi.org/10.1016/j.ecss.2023.108227)

3.1 Abstract

Estuarine intertidal sediments are important centres for organic matter remineralization and nutrients recycling. Nevertheless, there is limited understanding regarding how these processes occur along the salinity gradient and their seasonality. Here, we report on the seasonal biogeochemical cycles from three types of intertidal sedimentary habitats (freshwater, brackish and marine) located in the Western Scheldt estuary (The Netherlands and Belgium). A full year of solute fluxes, porewater nutrient and sediment pigment concentrations at a monthly resolution revealed clear differences in the biogeochemistry of the three sites, indicating that environmental conditions determined the local nutrient dynamics. Temperature controlled sediment oxygen consumption rates and nutrient fluxes, but also affected pore water nutrient concentrations up to 14 cm deep. Fresh and brackish sediments had a net influx of dissolved inorganic nitrogen (DIN) ($-1.62 \text{ mmol m}^{-2} \text{ d}^{-1}$ and $-2.84 \text{ mmol m}^{-2} \text{ d}^{-1}$, respectively), while only the freshwater sediments showed a net influx of phosphate ($-0.07 \text{ mmol m}^{-2} \text{ d}^{-1}$). We estimated that intertidal sediments remineralized a total of 10,000 t C y^{-1} , with 97% of mineralization occurring in the brackish and marine parts. Overall, sediments removed 11% (1,500 t N y^{-1}) and 15% ($\sim 200 \text{ t P y}^{-1}$) of the total nitrogen and phosphorus entering the estuary from riverine input. Moreover, observations revealed the historical improvement of water quality resulting from water treatment policies. This spatiotemporal study of OM remineralization and early diagenesis in estuarine systems highlights the importance of intertidal sediments for estuarine systems. Our observations can be used in models to predict estuarine biogeochemistry or assess climate change scenarios.

3.2 Introduction

Estuaries are centres of transformation, export, and retention of nutrients from terrestrial sources into coastal waters (Arndt et al., 2009; Statham, 2012a). They exhibit high heterogeneity of biological (e.g. organism activity and species succession), physical (e.g. salinity, morphology, hydrology, light, tidal regime) and biogeochemical properties (e.g. nutrient concentrations, cycling and fluxes) (Magalhães et al., 2002; Middelburg et al., 2005; Arndt et al., 2009; Statham, 2012a). Nutrients entering estuaries have different origins: terrestrial sources such as sewage and fertilizers in the form of ammonium nitrate (NH_4NO_3) and calcium phosphate ($\text{Ca}_3(\text{PO}_4)_2$) (Billen et al., 2005; Soetaert et al., 2006; Gilbert et al., 2007), inputs from other water bodies such as rivers and seas (Gilbert et al., 2007), or inputs from sediment-water exchange (Herbert, 1999). The biogeochemical cycling of nutrients and carbon is ultimately driven by the production and degradation of organic matter (OM) from autochthonous (local microphytobenthos and phytoplankton blooms) or allochthonous (terrestrial) origin (Arndt et al., 2013).

OM and nutrient concentrations typically decrease along the salinity gradient from upstream to downstream areas which resembles a filtering effect (Sharp et al., 1984). The filtering effect traps nutrients in the estuary before reaching the sea; its efficiency depends on OM sources and nutrient cycling processes occurring in the water column along the estuarine salinity gradient (Soetaert et al., 2006; Statham, 2012a), but also on the exchanges between sediment and water column (Magalhães et al., 2002). Examples of such processes include the dilution of riverine water with seawater, *in situ* biogeochemical transformations (Soetaert et al., 2006), uptake by both marine (Pastuszak et al., 2008; Arndt et al., 2009), and terrestrial (siliceous plants in salt marshes) primary producers (Struyf et al., 2005b), and in some cases, wastewater treatment (Brion et al., 2008).

The shallow depth of estuaries together with their high productivity suggest that a great portion of the OM remineralization occurs in the sediment (Jørgensen and Sørensen, 1985). Failing to account for estuarine benthic respiration could overlook around 26% of the global respiration (Middelburg et al., 2005). Furthermore, estuaries provide essential habitats for aquatic and terrestrial organisms and are important centres for nutrient cycling (Lessin et al., 2018) and removal (Magalhães et al., 2002). Research on sediment biogeochemical processes, which fundamentally differ from those occurring in the water column (Cox et al., 2009; Statham, 2012a), is important to complement our understanding of estuarine biogeochemistry.

OM is incorporated into the sediment by deposition, benthic organisms, and tidal action where it is remineralized by heterotrophs that sequentially use different terminal electron acceptors (O_2 , NO_2^- , NO_3^- , Mn^{4+} , Fe^{3+} , SO_4^{2-} , CO_2) to obtain energy (Arndt et al., 2013). Several biogeochemical processes are constrained to occur near the oxic-anoxic interface, notably, nitrification and denitrification, the sorption and desorption of phosphorus

Chapter 3

(PO_4^{3-}) onto sediment particles, and the dissolution of biogenic silica (BSi) (Struyf et al., 2005b). Benthic autotrophic OM production as well as heterotrophic activity associated to OM remineralization are affected by seasonal changes. Seasonality - a driver for environmental variability - induces natural fluctuations in temperature and light irradiance that affect the estuarine biological community, nutrient transformation, and exchange (i.e. flux) rates between the sediment and the water column (Jørgensen and Sørensen, 1985; Soetaert et al., 2006; Arndt et al., 2009; Fang et al., 2019; Mestdagh et al., 2020).

Studying the finer-scale spatiotemporal variability of biogeochemical processes is necessary for a better understanding of estuarine benthic-pelagic processes and to assess their response to climate change (Lessin et al., 2018). Some studies have addressed the seasonality of OM remineralization in estuarine mudflats (Feuillet-Girard et al., 1997; Mortimer et al., 1999; Magalhães et al., 2002; Bally et al., 2004; Cook et al., 2004; van Colen et al., 2012; Khalil et al., 2018; Mestdagh et al., 2020). However, these studies are limited in spatiotemporal resolution (e.g. sampling carried out only once per season or at one station) along the estuarine salinity gradient.

Our study was conducted in the Western Scheldt estuary (WS) between Belgium and The Netherlands. The watershed of the WS and its main tributaries, the Scheldt, Dender, and Rupel rivers, comprises an area of 22,116 km² that is subject to large human influence (e.g. urbanization, farming, and industry) (Soetaert and Herman, 1995b; Middelburg et al., 1996; Gilbert et al., 2007; Maris and Meire, 2017). From the 1960's, the implementation of water quality control policies, and the opening of the Brussels-North wastewater treatment plant (WWTP) have improved water quality, eliminated hypoxia, and reduced the concentration of dissolved inorganic phosphorus (DIP) and nitrogen (DIN) entering the Western Scheldt estuary (Vanderborgh et al., 2007; Hofmann et al., 2008; Cox et al., 2009; Brion et al., 2015).

The WS is therefore a good model for estuarine studies because its water column biogeochemistry has been extensively monitored in its transformation from hyper eutrophication with water column hypoxia supporting denitrification to a eutrophic state with year-round oxic conditions (Soetaert and Herman, 1995a; Middelburg et al., 1996; Soetaert et al., 2006; Arndt et al., 2009; Cox et al., 2009). Nevertheless, the role of intertidal sediments in nutrient dynamics in the WS has not been sufficiently addressed. This study analysed monthly samples from three areas of the WS to i) quantify benthic OM remineralization and biogeochemical cycling, ii) assess whether there have been water quality improvements in the past two decades, and iii) calculate the contribution of intertidal sediments to OM mineralization and nutrient retention.

3.3 Methods

3.3.1 Study area

The Scheldt River originates in France, flows through a brackish water zone in Belgium, and meets marine water in the WS before discharging into the North Sea (Soetaert et al., 1994b). The WS has a typical funnel-shape, narrow in the upstream, freshwater part (average width < 100 m), and then rather abruptly increasing in width past the Belgian-Dutch border until reaching a mean width of 6 km at the mouth (Figure 3.1). Its average depth increases from around 3 m near Ghent to 15 m near the mouth at Vlissingen. The funnel shape morphology gives rise to a longitudinal salinity gradient, with low salinities predominating in the narrow section, and a rather steep salinity gradient in the brackish region where the Scheldt becomes wider. The salinity gradient in the brackish region is also influenced by temporal changes in riverine discharge (Baeyens et al., 1997; Struyf et al., 2004a; Soetaert et al., 2006). For example, a lower riverine discharge in summer causes a salinity increase in the mesohaline area, because there is less dilution and seawater can reach deeper into the estuary. The discharge of tributaries (Schelde, Dender, and Rupel rivers) into the WS is driven by precipitation and is higher during the winter than in the summer with an average yearly discharge of $120 \text{ m}^3 \text{ s}^{-1}$ (Deltares, 2013; Wang et al., 2019). Sampling was conducted in three intertidal mudflats, close to the main channel, with contrasting salinity and 70% dry time (Figure 3.1). The freshwater and brackish sites were adjacent to a reed (*Phragmites australis*) salt marsh.

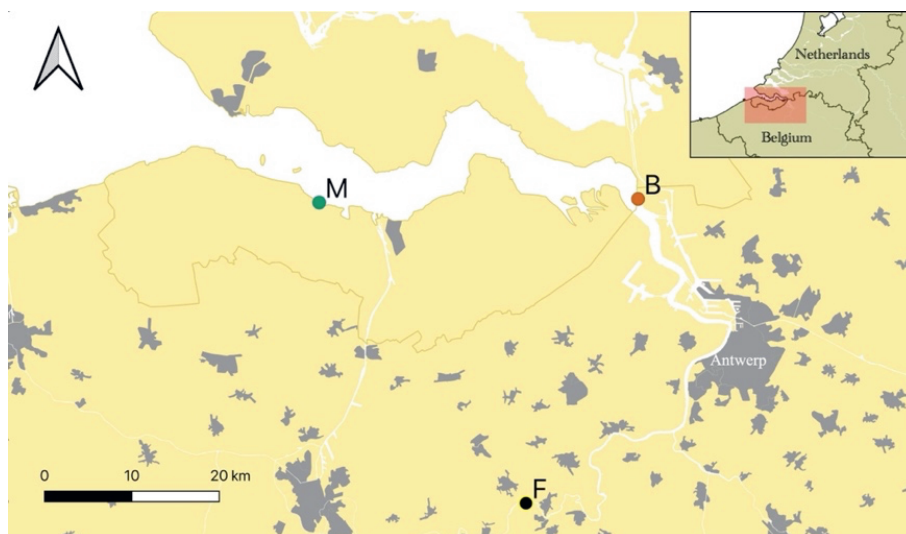


Figure 3.1 Map of the intertidal sampling locations. The freshwater (F) site, at Appels, Belgium (51.04832°N, 4.06934°E) is located in the Scheldt River. The brackish (B) location, at Groot Buitenschoor, Netherlands (51.36337°N, 4.24456 °E), and the marine (M) site, in the Paulina Polder, Netherlands (51.35337°N, 3.72054°E) are in the Western Scheldt. Land use in this area is dominated by farmland apart from cities shown in grey. Maps created with QGIS (QGIS Development Team, 2021).

3.3.2 Sampling method

Sediment core samples from the intertidal sites were taken monthly from March 2019 to February 2020 during low tide. Core samples were taken for incubations (30 cm long, 15 cm inner diameter (\varnothing); filled to half), porewater (30 cm, 10 cm \varnothing), and granulometry (30 cm, 3.5 cm \varnothing). Pigments samples (1 cm³) were sampled by means of a cut-off syringe (1 cm \varnothing) in triplicate from the upper 1 cm of the sediment. At each site, 10 L of water was taken, as close as possible to the sampling location. After collection, the cores were transported to The Royal Netherlands Institute for Sea Research, Yerseke (NIOZ- EDS Yerseke). The incubation cores were kept in a thermostatic bath inside a dark ambient temperature-controlled climate room (representing the ambient water temperatures) until the next day to acclimatize. The porewater was immediately extracted upon arrival to the institute and the pigment samples were frozen at -80°C. The granulometry cores were stored in a 4°C refrigerator until they were processed on the following day.

Additional water column temperature data for the freshwater (station: Dendermonde SF/Dender) and brackish sites (station: Lillo Meetpaal-Onder SF/Zeeschelde) were obtained from the Flemish Environment Agency, Belgium (Flanders Environment

Agency, n.d.), and for the marine site (station: Overloop van Hansweert) from the Dutch Directorate General for Public Works and Water Management (Rijkswaterstaat, n.d.). Water column nutrients from the Ruppel river tributary (Station: 210000) and the Schelde + Dender rivers (Station: 164000) for the sampling period were downloaded from the Geoloket water website (Flanders Environment Agency, n.d.). Discharge values from the Scheldt (station: Dendermonde afw Dender calc/Zeeschelde) and Rupel (station: Wintam Monding calc/Rupel) rivers were obtained from the Flemish Government (Flemish Government, n.d.). Bathymetry data for the year 2021 was provided by Rijkswaterstaat (Rijkswaterstaat, n.d.).

3.3.3 *Experimental methods and calculations*

The porewater was sampled inside an anoxic glove bag using rhizons (CSS 5 cm, Rhizosphere) at 0 (near the sediment-water interface), 1, 2, 3, 5, 10, and 14 cm depth. Of the extracted porewater, an aliquot of 500 μL was sampled for ammonium (NH_4^+), nitrite (NO_2^-), nitrate (NO_3^-), and Dissolved Si (DSi); and one of 100 μL acidified with 10 μL of 1 M sulfuric acid (Merck, No. 100731) for PO_4^{3-} analysis. Photosynthetic marker pigments were analysed following the method described by Zapata et al. (2000). Pigment samples were freeze dried and analysed with HPLC (LC-04, Shimadzu Co., Kyoto, Japan) with a Waters C8 column (150 x 4.6 mm, 3.5 μm particle size, 0.01 μm pore size, nr. WAT200630, Waters Corporation, Milford, MA, USA) connected to a guard cartridge (Symmetry C8 Sentry Guard Cartridge, 100 \AA , 5 μm , 3.9 mm X 20 mm, nr. WAT054250, Waters Corporation, Milford, MA, USA) for separation. The pigments were extracted from 1 g of sediment using 90% acetone (Nanograde, nr. I.00658.2500, Promochem) + APO (β -Apo-8'-carotenal) (10 mL). Following extraction, each sample was homogenised and centrifuged, and 800 μL of the supernatant was injected into the HPLC column.

Sediment incubations were performed in dark conditions, to prevent photosynthesis, at ambient temperature. The cores were filled with pre-bubbled water and hermetically sealed with a lid fitted with a magnetic rotor. Oxygen (O_2) concentration in the overlying water was continuously measured with an oxygen optode (Firesting, Pyroscience). The O_2 measurements were stopped when the concentration reached 70% saturation or after ~7h, after which lids were opened and the overlying water was bubbled. Filtered (Chromdis 0.45 μm , 25 mm, No. 250425) water samples (5 ml) were taken for nutrient (NH_4^+ , NO_2^- , NO_3^- , DSi and PO_4^{3-}) analysis at the start of the incubation, the end of the respiration measurement, and after 23, 31 and 48 hours. The nutrient samples from the incubations and the porewater samples were refrigerated after collection and analysed with a Segmented Flow Analyzer (QuAAtro39 AutoAnalyzer with XY-2 Sampler Autosampler, SEAL Analytical). Fluxes of O_2 and inorganic nutrients (NH_4^+ , NO_2^- , NO_3^- , DSi and PO_4^{3-}) were estimated by fitting a linear regression calculating the change in concentration as a function of time. The fitted slope was multiplied by the height of the overlying water

Chapter 3

column to obtain the flux. To determine the granulometry, slices of 1 cm thickness were taken at 0, 2, and 4 cm, and from 5 – 10 and 10 – 14 cm depth. These slices were freeze dried, and analysed by laser diffraction (MALVERN Mastersizer 2000, No. 34403/139, model APA 2000 with Hydro G 2000 introduction unit). Sediment porosity was calculated from water content and solid-phase measurements accounting for porewater salinity. Organic carbon (OrgC) and N content were determined using an Interscience Flash 2000 organic element analyser.

The temperature coefficient, Q_{10} value, was calculated based on the respiration rates with the following equation.

$$R_2 = R_1 Q_{10}^{\frac{T_2 - T_1}{10}}$$

Where R_1 is the rate of reaction at a first temperature (T_1) and R_2 the rate of reaction at a second temperature (T_2). Graphs and data analysis were created using the computing program R (R Core Team, 2020). The program QGIS was used for geospatial analysis (QGIS Development Team, 2021). Intertidal areas were defined to be between -2 to 2 m NAP (Kuijper and Lescinski, 2013).

3.4 Results

3.4.1 Abiotic conditions of the water column and the sediment

Salinity was stable throughout the year at the different locations (Figure 3.2 A), apart from a slight increase from May to December at the brackish location. The water temperature fluctuated seasonally at all stations (Figure 3.2 B), and for most of the year, was slightly higher at the freshwater and brackish sites compared to the marine site. The water temperature was $\geq 20^\circ\text{C}$ from July to September at all sites.

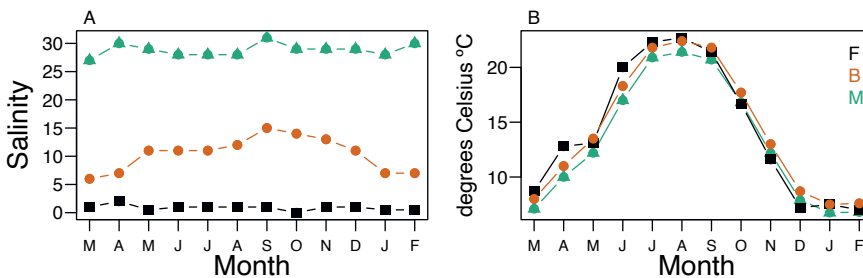


Figure 3.2 Salinity (A) and temperature (B) variations at freshwater (F, black squares), brackish (B, red circles) and marine (M, green triangles) stations of the Western Scheldt along the salinity gradient from March 2019 to February 2020.

Dissolved nutrients varied seasonally (Figure 3.3). The concentration of NH_4^+ in the freshwater site (Figure 3.3A) was highest in winter (March 2019 and December 2019 to February 2020) (mean \pm standard deviation; $22.5 \pm 1.2 \text{ mmol m}^{-3}$) and lowest from April to November 2019 ($4.8 \pm 2.4 \text{ mmol m}^{-3}$). Similar dynamics were observed in the brackish site although the seasonality was less pronounced; here the concentration of NH_4^+ fluctuated around $5.4 \pm 7.0 \text{ mmol m}^{-3}$. In contrast, NH_4^+ values in the marine site peaked during the summer-autumn reaching a maximum of $18.6 \pm 2.4 \text{ mmol m}^{-3}$ in October. NO_2^- showed the lowest concentrations during the summer in all sites (Figure 3.3B), except for one high value in August in the brackish site. Largest fluctuations of NO_2^- were observed in the freshwater site, whereas the seasonality was least pronounced in the marine site. The concentration of NO_3^- changed seasonally (Figure 3.3C), with lowest values in the summer months, and decreasing seawards. The freshwater site had the greatest variation in DSi ranging from a high of $235.7 \text{ mmol m}^{-3}$ in the colder months while remaining below 50 mmol m^{-3} from May to October (Figure 3.3D). A similar seasonality was observed at the brackish site, where the DSi concentration ranged from 38.0 to $161.7 \text{ mmol m}^{-3}$. In contrast, seasonal fluctuations of DSi were minimal at the marine site and ranged between 13.7 mmol m^{-3} and 51.3 mmol m^{-3} . The concentration of PO_4^{3-} only showed seasonality in the freshwater site while concentration values decreased seawards between sites (Figure 3.3E).

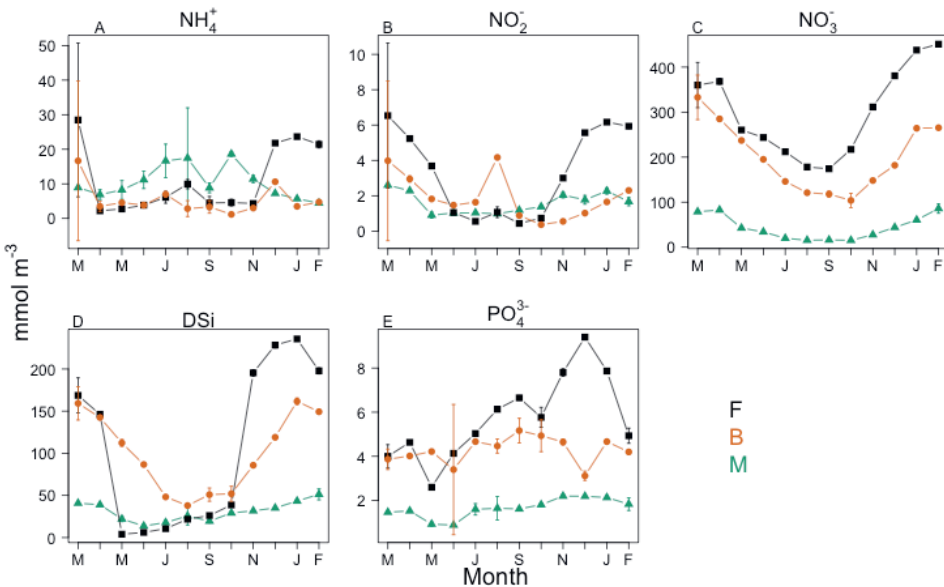


Figure 3.3 Nutrient concentrations of the water column at the freshwater (F, black squares), brackish (B, red circles) and marine (M, green triangles) sites from March 2019 to February 2020. Standard deviation indicated at each point.

The sediment at all sites was muddy with a median grain size (D₅₀) increasing from the fresh ($30.32 \mu\text{m}$) to the marine ($61.51 \mu\text{m}$) part of the estuary (Table 3.1). OrgC was inversely

Chapter 3

related to grain size and porosity that decreased seawards. The sedimentary C:N ratio was highest in the brackish and lowest in the marine part of the estuary.

Table 3.1 Yearly mean \pm standard deviation of physical characteristics of the first 5 cm of the sediment in the fresh, brackish, and marine sites. Median sediment grain size (D₅₀), organic carbon content (OrgC), porosity, and carbon: nitrogen ratio.

	Unit	Freshwater	Brackish	Marine
D ₅₀	μm	30.3 \pm 6.4	48.7 \pm 5.6	61.5 \pm 12.2
OrgC	%	3.1 \pm 0.5	1.1 \pm 0.3	0.6 \pm 0.1
Porosity*	-	0.8 \pm 0.2	0.6 \pm 0.2	0.5 \pm 0.1
C: N	mol: mol	11.3 \pm 0.5	13.2 \pm 1.2	8.7 \pm 0.9

3.4.2 Pigment concentrations in the surface of the sediment

Total pigment concentration was about an order of magnitude higher in the freshwater (Figure 3.4A) compared to the other sites, and the brackish site (Figure 3.4B) had the lowest concentration. A clear summer peak was observed in freshwater site and to a lesser degree in the marine site (Figure 3.4C). In contrast, a spring peak occurred in the brackish part of the estuary. Both the brackish and marine sites had a relatively high concentration in total and in pigments associated with diatoms (Chl c, diadinoxanthin, diatoxanthin, and fucoxanthin [Reuss, 2005]) during January and February.

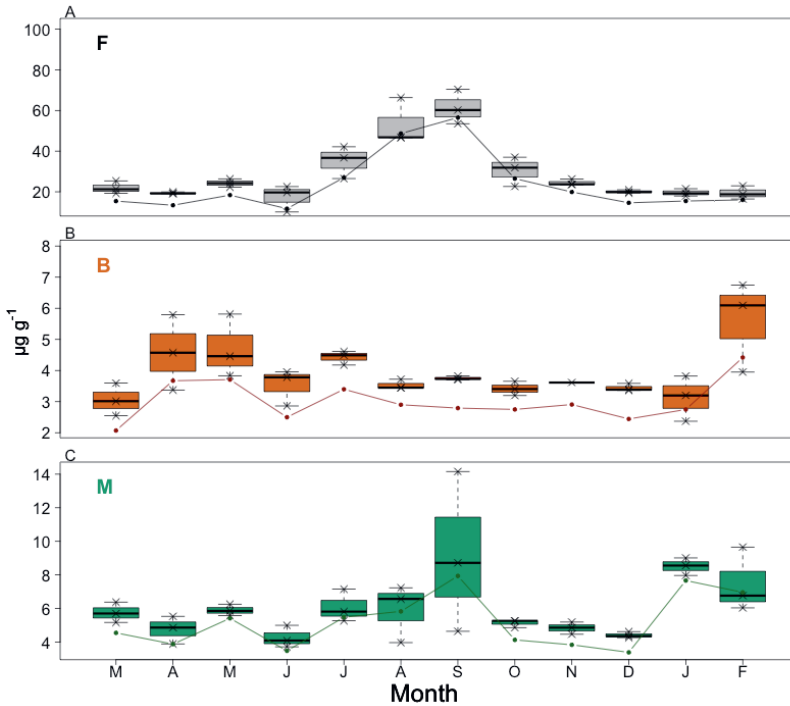


Figure 3.4 Boxplot of seasonal concentrations of all pigments (Alloxanthin, carotene b, Chlorophyllidae a, Chl a, Chl b, Chl c, diadinoxanthin, diatoxanthin, dinoxanthin, fucoxanthin, 19'-hexanoyloxyfucoxanthin, lutein, Mg-2,4-divinyl pheoporpyrin, neoxanthin, peridin, prasinoxanthin, violaxanthin, and zeaxanthin), and line representing the mean of pigments associated to diatoms (Chl c, diadinoxanthin, diatoxanthin, and fucoxanthin [Reuss, 2005]).

3.4.3 Fluxes across the sediment-water interface

Oxygen exchange rates were influenced by temperature and therefore varied seasonally at all stations, peaking in the summer with a maximum of $131.4 \text{ mmol m}^{-2} \text{ d}^{-1}$ in the marine site (Figure 3.5A). The freshwater and brackish sites showed a similar average O_2 exchange rate (38.26 and $43.02 \text{ mmol m}^{-2} \text{ d}^{-1}$, respectively) which was around 40% lower than in the marine part of the estuary ($66.1 \text{ mmol m}^{-2} \text{ d}^{-1}$). Interestingly, the dependence of these rates to temperature, given by Q_{10} values, was lower in the freshwater site (2.55) and higher and similar in the brackish (3.06) and marine (3.01) sites. The freshwater and marine sites had a similar efflux of NH_4^+ that peaked in August ($\sim 12 \text{ mmol m}^{-2} \text{ d}^{-1}$) and appeared directly related to temperature (Figure 3.5B). While the marine site had an efflux of NH_4^+ throughout the year, the freshwater site showed an ammonium efflux only in spring to autumn and an influx in winter. The flux of NH_4^+ observed in the brackish site always fluctuated around zero and did not appear to be affected by seasonal changes in temperature. The flux of NO_2^- in the freshwater site changed seasonally (Figure 3.5C) with

Chapter 3

an efflux in the warmer period of the year, and an influx in the colder period, while the flux observed in the brackish site fluctuated around zero and was a perpetual efflux in the marine site. All sites displayed an influx of NO_3^- throughout the year (Figure 3.5D), with fluxes decreasing with higher salinity. A similar efflux of DSi was observed in the freshwater and brackish site (Figure 3.5E). Nevertheless, the brackish site showed an influx during the winter and spring that was not observed in the freshwater site. The DSi efflux in the marine site was highest in August at $14.0 \text{ mmol m}^{-2} \text{ d}^{-1}$. Overall, the freshwater area exhibited an influx of phosphate with a small efflux observed from August to October (Figure 3.5F), whilst the brackish and marine sites showed an efflux of PO_4^{3-} that peaked in the summer, with a small influx during the cooler months.

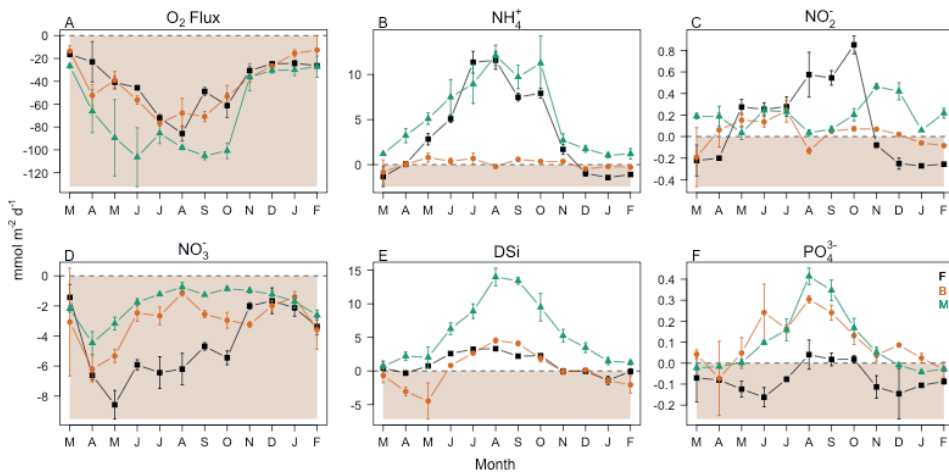


Figure 3.5 Mean \pm standard deviation of O_2 and nutrient fluxes. A negative flux indicates a net nutrient flux from the water column into the sediment (shaded area). Months from March 2019 to February 2020.

The yearly averaged fluxes per site (Figure 3.6) clearly show that i) the freshwater site had a net influx of both DIN ($1.62 \text{ mmol m}^{-2} \text{ d}^{-1}$) and DIP ($0.07 \text{ mmol m}^{-2} \text{ d}^{-1}$), ii) the brackish site exhibited a net influx of DIN ($2.84 \text{ mmol m}^{-2} \text{ d}^{-1}$), but a net efflux of phosphate ($0.1 \text{ mmol m}^{-2} \text{ d}^{-1}$), and iii) the marine site had a net efflux of both DIN ($3.83 \text{ mmol m}^{-2} \text{ d}^{-1}$) and DIP ($0.09 \text{ mmol m}^{-2} \text{ d}^{-1}$). There was an efflux of dissolved silicate at all sites, but mostly in the marine site ($5.71 \text{ mmol m}^{-2} \text{ d}^{-1}$).

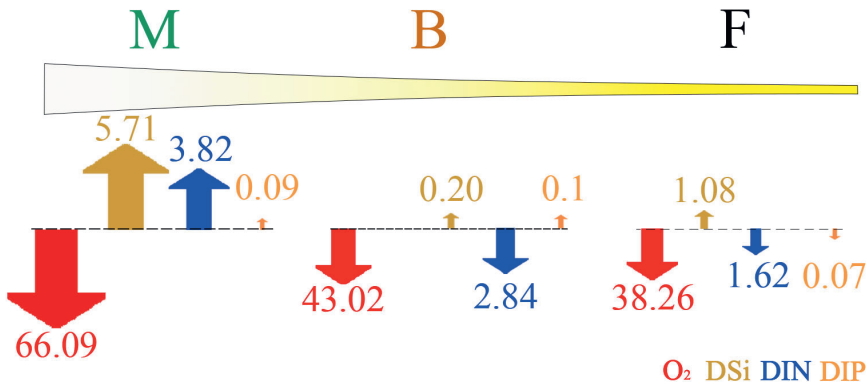


Figure 3.6 Average daily fluxes ($\text{mmol m}^{-2} \text{d}^{-1}$) of oxygen (O_2) in red, dissolved silicate (DSi) in brown, dissolved inorganic nitrogen (DIN) in blue, and dissolved inorganic phosphate (DIP) in orange for the three study sites (freshwater, F; brackish, B; and marine, M). Yellow funnel shape represents the WS and its increasing salinity gradient. The dotted lines represent the sediment-water interface. Arrows pointing down indicate an influx, arrows pointing up an efflux. Image created with Adobe® Photoshop® (23.0.2 release)

3.4.4 Porewater nutrients

Porewater NH_4^+ was highest at the freshwater site (Figure 3.7A) with the average concentration in the deepest layer (14 cm) being about three times as high (720 mmol m^{-3}) than in the brackish and marine sites. In these two latter sites, the general shape of NH_4^+ profiles was different with the marine site exhibiting a more accumulation with depth, but the average concentration of the deepest layer (14 cm) was very similar (Figure 3.7F and K), reaching around 200 mmol m^{-3} . The profiles of NO_2^- and NO_3^- decreased over depth at all sites. The highest concentration of porewater DSi was observed in the freshwater (Figure 3.7D) (601 mmol m^{-3}) and brackish (Figure 3.7I) (560 mmol m^{-3}) sites. The concentration of PO_4^{3-} was greater in the brackish site (Figure 7 J) and lowest in the marine site (Figure 3.7O).

Based on temperature differences, we designated a cooler period, from November to May ($9.5 \pm 2.5 \text{ }^\circ\text{C}$) and a warmer period from June to October ($20.1 \pm 2.2 \text{ }^\circ\text{C}$). Seasonality affected the concentration of the nutrients NH_4^+ , Dsi, and PO_4^{3-} (Figure 3.7A, D, E, F, I, J, K, N and O boxplots) resulting in a higher concentration during the warmer months; this effect was greater in the deeper layers of the sediment. The opposite occurred for NO_2^- and NO_3^- (Figure 3.7B, C, G, H, L and M boxplots) when higher concentrations were observed in the cooler period.

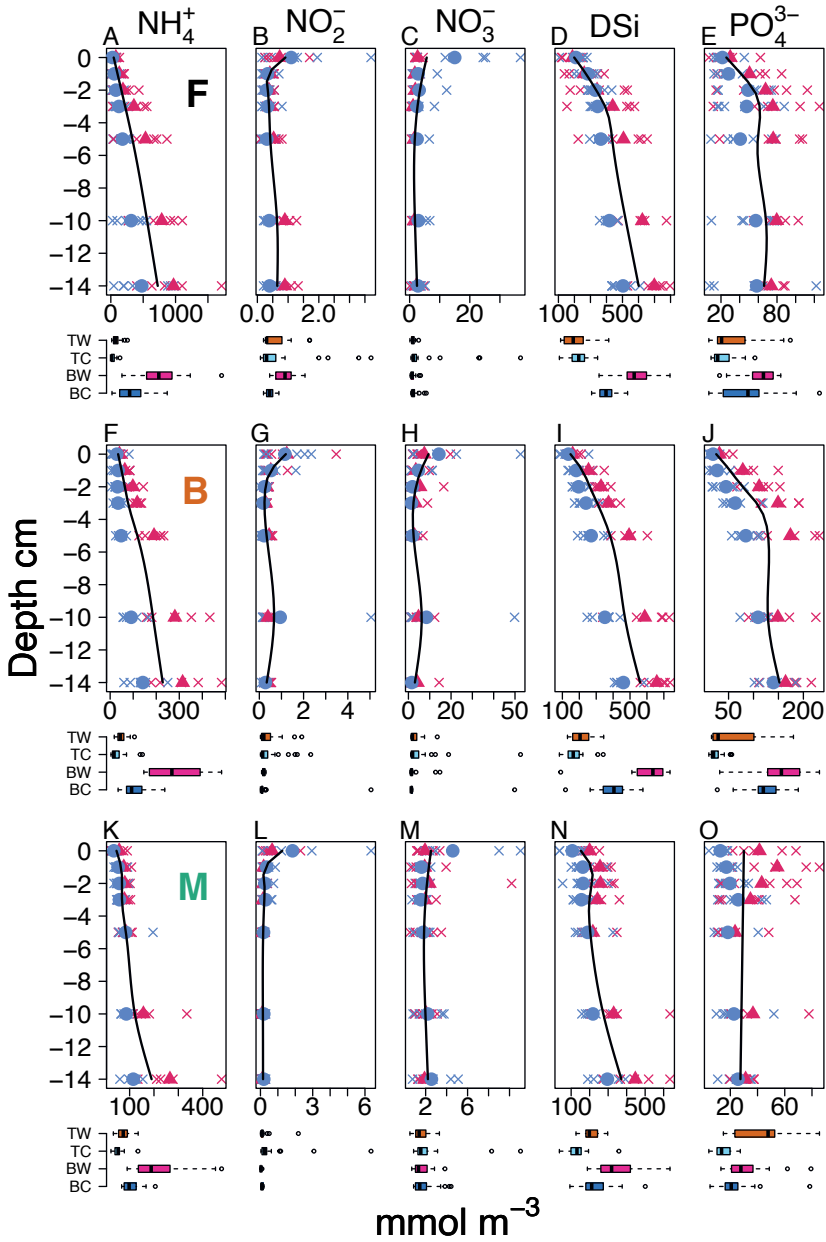


Figure 3.7 Porewater profiles of the freshwater (F), brackish (B) and marine (M) sites, smoothed by means of a cubic spline of the yearly mean (black line). Warmer months (June to October) are represented with red triangles (mean per layer) and red crosses (average per month). Cooler months (March to May and November 2019 to February 2020) are shown with blue circles (mean per layer) and blue crosses (average per month). Note x-scale differences between sites. Boxplots show the comparison of values in the top 1 cm (TC: Top cool and TW: top warm) and 10 to 14 cm (BC: bottom cool and BW: bottom warm) layers.

3.4.5 Nutrient ratios

DIN:DIP ratios (Table 3.2) in the water column (60) of the freshwater site exceeded the Redfield N:P ratio (16:1) almost fourfold, while the obtained DSi: DIP ratio (18) was very close to Redfield (15:1). The DIN:DIP ratio of the water column decreased towards the marine site (36), although remaining well above Redfield, while the DSi: DIP ratio did not change much. In contrast, the sediment average DIN: DIP and DSi: DIP ratios in the pore water were lower than Redfield at all sites.

Table 3.2 Yearly averaged molar ratios of DIN: DIP and DSi: DIP in the water column and porewater.

Site	Water column		Pore water	
	DIN: DIP	DSi: DIP	DIN: DIP	DSi: DIP
Fresh water	60	18	6	12
Brackish	49	24	2	5
Marine	36	19	4	10

3.5 Discussion

Remineralization of OM and early diagenetic processes occurring along the WS estuary show spatial and temporal differences attributable to physical (e.g. temperature), chemical (e.g. salinity, bottom water nutrient concentrations) and biological factors (e.g. algal production). Furthermore, the WS is an example of a restored system where after the implementation of water quality improvement policies the system recovered from hyper eutrophication with water column anoxia to a year-round oxic water column.

3.5.1 Physical characteristics of the water column and the sediment

Salinity fluctuations due to riverine discharge only prevailed in the brackish site, while seasonal temperature variations affected processes in all sites (Figure 3.2). The concentration of nutrients in the water column of the WS was consistently higher in the freshwater portion of the estuary, and decreased with increasing salinity, as previously reported for the area (Middelburg and Nieuwenhuize, 2000; Andersson et al., 2006; Soetaert et al., 2006; Chen et al., 2007; Brion et al., 2008). DIN:DIP ratios exceeding Redfield (Table 3.2) suggested DIP limitation of primary production in the water column for the entire WS. The DSi: DIP ratio was close to the Redfield ratio for diatoms and thus no DSi limitation was detected. A similar observation for this system was reported by Soetaert et al. (2006).

Chapter 3

Despite the potential limitation of P based on nutrient ratios, the concentration of PO_4^{3-} in the water column of the whole estuary was high ($> 1 \text{ mmol m}^{-3}$), and therefore it is unlikely that phosphate was the factor limiting primary production. Instead, it has been reported that the Western Scheldt primary production is limited by light and not by nutrients (Kromkamp and Peene, 1995a; van den Meersche et al., 2011).

The OrgC content of the sediment was highest in the freshwater part of the estuary (around 3%) and decreased downstream (1% in the brackish, 0.5% in the marine site). The C:N ratio of the sedimentary material, an indication of the OM degradability, was high in both the freshwater (11) and brackish (13) sites (Table 3.1). This is probably reflecting the input of refractory OM from allochthonous origin such as detritus derived from terrestrial sources (Boynton and Kemp, 1985; Hopkinson et al., 1999) or the vegetation, reed *Phragmites sp.*, surrounding these areas (Struyf et al., 2005a). Allochthonous OM is by nature less degradable than autochthonous OM (Soetaert et al., 2006). A similar dominance of allochthonous and terrestrial OM upstream has been reported by van den Meersche et al., 2009). In contrast, the low C:N ratio at the marine site indicated a greater proportion of autochthonous OM and higher degradability of OrgC possibly of algal origin e.g. diatoms (Struyf et al., 2005a).

An important source of autochthonous production in intertidal flats comes from microphytobenthos (Underwood and Kromkamp, 1999; Middelburg and Nieuwenhuize, 2000). Seasonality in microphytobenthos production was most pronounced in the freshwater site, which had the highest summer peak, while both the marine and brackish site showed a clear winter peak (January and February) (Figure 3.4) possibly related to lower grazing of microphytobenthos. Photosynthetic pigments varied seasonally by only a factor 2 to 3 between summer and winter indicating a relatively steady microphytobenthic production. This has been reported as typical of microphytobenthic communities as opposed to phytoplankton production with drastic (Terai et al., 2000).

The highest pigment concentrations were observed in the freshwater site; in contrast, they were an order of magnitude lower in the brackish site and slightly increased again towards the marine site. Similar observations have been reported for this system in the 90's (Soetaert et al., 1994a; Kromkamp and Peene, 1995a) and in 2016 (Maris and Meire, 2017). Brackish regions are characterised by a transition from fresh to marine species and experience more prominent salinity fluctuations (Figure 3.2A), which could explain the lower Chl a concentration detected in this part of the estuary (Soetaert et al., 1994a; Kromkamp and Peene, 1995a). The fluctuation in phytopigment concentrations was driven by diatoms (Figure 3.4) which dominate the microphytobenthic community in the WS and have an increasing contribution to the community composition from upstream to downstream areas (Kromkamp and Peene, 1995a; Muylaert et al., 2002; Maris and Meire, 2017).

3.5.2 Sediment respiration

The fate of OM in sediments is to be mineralized and recycled by biogeochemical processes, or to be buried over longer timescales. Daily sediment respiration rates (yearly average) in the dark increased from 38.3 mmol m⁻² d⁻¹ in the freshwater to 66.1 mmol m⁻² d⁻¹ in the marine site (Figure 3.5A), indicating a higher benthic activity towards the mouth of the estuary. While in theory, both higher temperature and OM availability (see algal concentrations in Figure 3.4) in summer may be responsible for the elevated respiration rates, no relationship was found between the respiration rates and Chl a concentration at any site. Instead, the seasonality of respiration closely mirrored seasonal changes in temperature. Temperature, rather than OM availability, seems to be the best descriptor of sediment respiration in the WS, as also observed in other estuaries (Jørgensen and Sørensen, 1985; Hopkinson et al., 1999).

The relationship between respiration and temperature was well described with an exponential, so-called Q₁₀ relationship. The Q₁₀ values, around 3 in the brackish and marine sites indicate a tripling of respiration for an increase in temperature of 10 degrees; the value in the freshwater (2.5) is closer to the theoretical value of 2. The obtained Q₁₀ values are important parameters that quantify the dependence of OM degradation to temperature; and they could be used in models speculating on the effect of rising temperatures on biogeochemical processes in the estuary.

3.5.3 Porewater nutrients

The remineralization of OM releases bioavailable nutrients that can be temporarily stored in pore water, transformed within the sediment, or released into the overlying water column (Herbert, 1999). The shape of the nutrient profiles is influenced by i) the rate at which OM is transported deeper into the sediment (either by advection, mixing, (bio) diffusion and bioturbation), ii) the reactivity of the organic matter (decay products of highly reactive particles do not reach large depths), iii) the intensity of mineralization or dissolution and iv) temperature, which directly affects bacterial mediated processes (e.g. respiration and remineralization) (De Borger et al., 2021). In brief, the nutrients released in the upper layers of the sediment can diffuse into the water column, but those released by dissolution and decay of OM at greater depth cause an increase in the concentration of nutrients such as NH₄⁺, DSi, and –to a lesser extent– PO₄³⁻ (Figure 3.7).

All sites exhibited a gradual increase in the concentration of ammonium (Figure 3.7A, F and K) and a decrease in the concentration of NO₂⁻ and NO₃⁻ (Figure 3.7B, C, G, H, L and M). These dynamics are explained by the release of NH₄⁺ from OM mineralization and its conversion to NO₂⁻ and NO₃⁻ via nitrification. In deeper layers of the sediment NH₄⁺

Chapter 3

accumulates as it is released from OM, and the concentration of NO_2^- and NO_3^- decreases as a consequence of net consumption likely by anammox and denitrification.

The fresh and brackish sites (Figure 3.7D and I) showed a gradual increase in the concentration of DSi. These sites are close to a salt marsh populated by reed (*Phragmites australis*), which accumulates BSi in its tissues in the form of phytoliths (Struyf et al., 2005b). When reed-derived OM is buried into the sediment, the BSi (from phytoliths) dissolves to form DSi (Struyf et al., 2005b) causing its accumulation at depth. In contrast, the DSi profile in the marine site (Figure 3.7N) showed a rapid increase in the upper 5 cm indicating that mineralization and dissolution were restricted to the uppermost layers. This suggests an alternative source of BSi to reed was present in this site, most likely the siliceous frustules of benthic diatoms (Struyf et al., 2005b). Diatom frustules exhibit higher dissolution rates than reed phytoliths (Loucaide et al., 2008) which could result in the rapid increase in DSi concentration observed in this site. The pigment analyses (Figure 3.4) shows that diatoms are an important microphytobenthic group at all sites (Maris and Meire, 2017). However, the green algae *Euglena sp.*, which does not accumulate BSi (Barsanti and Gualtieri, 2020), was dominant in the freshwater site. The main sources of DSi in the WS intertidal sediments are diatom frustules in all sites, and reed phytoliths in the freshwater and brackish sites (Struyf et al., 2005b).

The higher concentration of PO_4^{3-} observed in freshwater and brackish sediments (Figure 3.7E and J) may be associated with sorption of PO_4^{3-} to iron oxides that is promoted in areas with lower salinities (Slomp et al., 1996; Jordan et al., 2008). While the gradual increase in PO_4^{3-} concentration over depth could either result from the P-shuttle transporting iron oxides downwards and desorbing PO_4^{3-} into the anoxic layer as the iron oxides dissolve or from OM degradation releasing PO_4^{3-} (Caraco et al., 1990; Slomp et al., 1996; Jordan et al., 2008). Moreover, high levels of DSi in the pore water, like observed in these sites (Figure 3.7D and I), enhance sorption of PO_4^{3-} to iron oxides and may increase the quantity of PO_4^{3-} entering the sediment and desorbing at depth (Mayer and Jarrell, 2000). In contrast, the marine area exhibited a lower concentration of pore water PO_4^{3-} (Figure 3.6E, J and O) which may be explained by the higher salinity as it reduces sorption of PO_4^{3-} (Caraco et al., 1990; Jordan et al., 2008) and decreases the efficiency of the P-shuttle (Jordan et al., 2008). In areas with a large sulphate concentration (higher salinity), the sulphide (HS^-) produced during sulphate reduction binds to Fe (II) as iron sulphide thereby preventing the formation of FeOOH-PO_4^{3-} compounds; and promoting the desorption of PO_4^{3-} from FeOOH and its release into the water column (Caraco et al., 1990; Jordan et al., 2008).

All sites had sedimentary DIN:DIP ratios that were significantly below Redfield, suggesting that sediments either retained more PO_4^{3-} than DIN and/or had more efficient N compared to P removal processes. This was most prominent at the brackish site, where the DIN:DIP ratio was as low as 1.4 mol: mol at 14 cm (Appendix 3.1), whereas the Redfield ratio is 16. The proportion of DIN relative to DIP being much lower than the N:P ratio of the original organic matter may be a consequence of the build-up of PO_4^{3-} due to

desorption and release at depth, but also of the absence of an equivalent mechanism capturing DIN in the upper layers of the sediment and releasing it at depth. Nevertheless, a lower than Redfield N:P ratio may also arise when the DIN is more efficiently removed from the sediment than DIP through coupled nitrification-denitrification.

3.5.4 Porewater seasonality

The effect of temperature on the concentration of pore water nutrients was detected up to 14 cm depth, however, fluctuations in intertidal muddy sediments have been observed up to 5 m deep (Harrison and Phizacklea, 1987; Beck et al., 2008). The concentration of NH_4^+ at all sites doubled during the warmer months (Figure 3.7A, F and K), possibly as a result of higher decomposition and regeneration rates (Middelburg et al., 1995b; Magni and Montani, 2006) as evidenced by Q_{10} values. In contrast, the difference in the concentration of NO_2^- and NO_3^- between the warm and cool period was more subtle and seemed reversed with lower concentrations in warmer months versus higher in cooler months. While this might suggest a larger net consumption at higher temperature possibly associated with increased denitrification, this may be unlikely. Rather, a higher bottom water concentration of NO_2^- and NO_3^- in the cooler months (Figure 3.3B and C) may have directly influenced their concentration in pore waters (Kemp et al., 1990; Magni and Montani, 2006; Zhang and Huang, 2011) and a deeper O_2 penetration depth in the winter (Sagemann et al., 1996) together with lower OM remineralization rates may have facilitated nitrification, and thus the observed increase in concentration.

The concentration of DSi increased by more than 50% (Figure 3.7D, I and N) in the hotter months. Likely resulting from the increased dissolution of BSi with higher temperature (Kamatani, 1982; Lawson et al., 1978; Struyf et al., 2005b). Similar observations on increasing concentrations of NH_4^+ and DSi with temperature have been reported in other systems (e.g. Kemp et al., 1990; Magni and Montani, 2006; Middelburg et al., 1995a; Sagemann et al., 1996).

Phosphate concentrations were also higher in the warm compared to the cool months, but here the difference appeared to be greatest at intermediate depths (~5 cm) in the freshwater and brackish site, while in the marine site, the fluctuations remained in the sediment surface (~2 cm). Possibly, the effect of temperature was less prominent in the surface sediment because higher temperature increased bioturbation activity and transport of OM and PO_4^{3-} to deeper sediments via the P-shuttle, which together with higher OM mineralization rates caused the release of PO_4^{3-} at depth. Nevertheless, a higher temperature can also enhance sorption of PO_4^{3-} onto sediment particles (Zhang and Huang, 2011), but salinity may be a controlling factor.

3.5.5 Nutrient fluxes

The summer peak observed for the flux of NH_4^+ in the fresh and marine sites likely resulted from higher regeneration rates and OM decomposition (Middelburg et al., 1995a; Magni and Montani, 2006). The range of NH_4^+ fluxes observed in the WS was within values reported for other temperate estuaries ($0.67 - 23.47 \text{ mmol m}^{-2} \text{ d}^{-1}$) (Boynton and Kemp, 1985; Magalhães et al., 2002; Thouzeau et al., 2007). Unexpectedly, the ammonium flux at the brackish site was close to zero (Figure 3.5B), an indication of high NH_4^+ consumption by nitrification in the sediments (Rysgaard et al., 1999; Middelburg and Nieuwenhuize, 2000; Magalhães et al., 2002). It is unlikely that microphytobenthos growth would cause such a trend since i) the Chl a concentration in the brackish part was the lowest of all sites and ii) the yearly pigment fluctuation was similar to that of the marine site where there was a clear efflux during the summer. This, together with the large influx of nitrate (Figure 3.5D) is evidence of the substantial removal of bioavailable nitrogen due to denitrification in the brackish site. A year-round influx of NO_3^- has also been reported in the Douro River estuary (Magalhães et al., 2002), but this is different in other estuaries (Cowan et al., 1996; Thouzeau et al., 2007).

Although both the freshwater and marine sites had a year-round efflux of DSi, the brackish site showed a distinctive influx of DSi in the spring and winter (Figure 3.5E), concurrent with the pigment peaks observed at that time (Figure 3.4B). It is therefore possible that this influx was caused by the uptake of DSi by diatoms (Hopkinson et al., 1999).

The flux of PO_4^{3-} in the freshwater site was generally directed into the sediment (Figure 3.5), except for the three warmest months (August-October) when the sediment was most anoxic, and desorption was promoted. It is unlikely that microphytobenthos uptake affected the influx of PO_4^{3-} in the winter since the pigment concentration was lowest in that period. It therefore seems that sorption was the principal mechanism of P loss in the freshwater site. A similar PO_4^{3-} influx has been observed in other freshwater sediments (Hopkinson et al., 1999), while an efflux, like that of the brackish and marine sites, has also been reported for saline sediments (Cowan et al., 1996; Thouzeau et al., 2007).

The impact of temperature on sediment biogeochemistry was also clear from the nutrient fluxes (Figure 3.5) that showed greater effluxes with higher temperatures for NH_4^+ (freshwater and marine site), NO_2^- (marine), PO_4^{3-} (brackish and marine) and DSi (all stations). In contrast, there was an influx of NO_3^- that consistently peaked in the spring rather than in summer (Figure 3.5D) similar trends have been discussed in Kemp et al. (1990).

3.5.6 Nutrient retention of intertidal sediments

To understand the role of intertidal sediments in the nutrient retention capacity of the Western Scheldt estuary, the nutrient budgets for the fresh, brackish, and marine sites obtained from this study were used to estimate the nutrient budgets for the whole intertidal area of the WS. This approach was based on that of Middelburg et al. (1996) and assumes that the mineralization rates obtained in the fresh, brackish, and marine sites are representative of each zone.

The calculation was based on the yearly-averaged nutrient fluxes (Figure 3.6) of DIN ($\text{NH}_4^+ + \text{NO}_2^- + \text{NO}_3^-$) and PO_4^{3-} . These fluxes were converted to integrated rates and compared to inputs of total nitrogen ($\sim 14,000 \text{ t N y}^{-1}$) and total phosphate ($\sim 1400 \text{ t P y}^{-1}$) from tributaries (Scheldt, Dender, and Rupel rivers), as estimated from riverine water discharge (average $78 \text{ m}^3 \text{ s}^{-1}$) and yearly averaged nutrient concentrations (obtained from Flanders Environment Agency, n.d.). The total area of the freshwater intertidal sediments ($3,413 \text{ km}^2$) was taken from Struyf et al. (2004), and the area of brackish ($28,366 \text{ km}^2$) and marine ($50,271 \text{ km}^2$) intertidal sediments was extracted from recent bathymetry data between -2 and 2 m NAP . To account for the tidal regime of intertidal sediments (12 h emersion), the fluxes were multiplied by 0.5 (Soetaert et al., 1992).

Assuming an O:C ratio in mineralization rate of 1, the intertidal sediments remineralized a total of $10,000 \text{ t C y}^{-1}$ with 97% of mineralization occurring in the brackish (26%) and marine (71%) sections of the estuary. This illustrates that, because of their lower mineralization and relatively small surface area, the contribution of freshwater sediments to estuarine remineralization was negligible (only 3%). The estimated total mineralization was lower than that estimated for the beginning of the 1990's ($16,000 \text{ t C y}^{-1}$, Middelburg et al. [1996]) but was comparable. The difference could be attributed to changes in the total surface area of intertidal sediments from the 1990's, to the consideration of the tidal regime in our calculation, or to the diminution of nutrients and OM discharging into the WS because of water quality management efforts.

OM remineralization and fluxes of DIN and phosphate accounted for a total of $\sim 1500 \text{ t N y}^{-1}$ and $\sim 200 \text{ t P y}^{-1}$, and 11% of nitrogen and 15% of phosphorus from riverine input being removed or retained within the estuary (e.g. by nitrification, denitrification, sorption, or burial). The function of each section and their contribution to nutrients retention resembled a three-step filter. The freshwater area functions as a first barrier for nutrients reaching the estuary, which despite its small area, was a sink of inorganic P (9.0 t P y^{-1}) and N (61.9 t N y^{-1}), as evidenced by the high influxes (Figure 3.6). In contrast, the brackish and marine areas, although with a comparatively less efficient influx per meter squared than the freshwater site, contributed greatly to nutrient retention because of their greater surface area. Nutrient filtration by intertidal sediments is therefore evidenced as an important mechanism decreasing the quantity of nutrients reaching the North Sea and

buffering against eutrophication (Sagemann et al., 1996). Similar findings on the importance of intertidal sediments for estuarine nutrient retention have been reported for other estuaries (Jickells et al., 2000; Magalhães et al., 2002; Liu et al., 2020).

3.5.7 *Historical overview of the state of the Western Scheldt estuary*

The WS has a history of anthropogenic influence that has caused eutrophication and decreased water quality that peaked during the 1970's (Wollast and Peters, 1978; Soetaert et al., 2006). Since then, sanitation schemes to restore ecosystem function and limit the influx of pollutants, raw sewage, and fertilizers have been implemented around the watershed, substantially ameliorating the water quality of the estuary (Soetaert and Herman, 1995b; Brion et al., 2015). For example, the opening of the Brussels-North wastewater treatment plant in 2007, reduced nutrient loads and improved the oxygen saturation of the main tributary of the WS, the Rupel river (Brion et al., 2015). However, there has not been an assessment of the long-term effect of the wastewater treatment plant on the concentration of nutrients in the WS since its implementation.

A comparison of the nutrient concentrations measured in the water column with values reported in early 2000's (Soetaert et al., 2006), demonstrates significant changes in the water quality of the WS. Soetaert et al. (2006) already observed an improvement in the water quality of the WS from 1970 to 2000 regarding lower concentrations of NH_4^+ , NO_2^- , DIP and DSI. While the concentration of NO_3^- and PO_4^{3-} measured in 2019-2020 has remained similar to values reported in 2002, the concentrations of the other nutrients were different to those observed in the beginning of the century. In the early 2000's there was a prominent seaward decrease in NH_4^+ concentration from the freshwater ($\sim 80 \text{ mmol m}^{-3}$) to the marine ($\sim 6 \text{ mmol m}^{-3}$) sector (Soetaert et al., 2006). Currently, the freshwater (11 mmol m^{-3}), marine (10 mmol m^{-3}) and brackish sites (5.4 mmol m^{-3}) have rather similar NH_4^+ concentrations. The largest changes since 2000, are observed in the freshwater site concerning NO_2^- and DSI with the concentration of NO_2^- decreasing from 14 mmol m^{-3} (Soetaert et al., 2006) to 3 mmol m^{-3} currently, and that of DSI decreased from $\sim 190 \text{ mmol m}^{-3}$ (Soetaert et al., 2006) to $\sim 100 \text{ mmol m}^{-3}$. The reduction of nitrite in the freshwater site might be associated to the prevalence of oxic conditions in the water column that have promoted nitrification (Soetaert and Herman, 1995b; van Damme et al., 2005; Cox et al., 2009). In contrast, the NO_2^- concentration at the marine site has remained unchanged, while the concentration of DSI has doubled.

The river discharge has increased over time from $70 \text{ m}^3 \text{ s}^{-1}$ in 2000 (Struyf et al., 2004a) to a long-term (1971 – 2015) mean of $120 \text{ m}^3 \text{ s}^{-1}$ in 2015 (Wang et al., 2019). A higher discharge dilutes nutrient concentrations and would cause lower concentration values, despite the total nutrient loading reaching the WS (Struyf et al., 2004a) being unchanged. However, for the period of our sampling, we obtained average discharge velocities of $78 \text{ m}^3 \text{ s}^{-1}$, so that dilution can be ruled out as an important factor explaining the decrease in concentration.

It is more likely that the reduction in nutrient concentrations (NH_4^+ , NO_2^- , and DSi) reflects the recovery process from eutrophication caused by better sanitation policies such as the implementation of wastewater treatment upstream.

In summary, the processes near the sediment-water interface in estuarine systems depend just as much on seasonality as on the physicochemical characteristics of the study site. Water column properties cause freshwater sites to act as an efficient trap of P and N, while the brackish sites efficiently remove DIN. Temperature was the principal factor affecting overall nutrient fluxes and pore water concentrations of NH_4^+ , DSi and PO_4^{3-} while those of NO_2^- , NO_3^- were mostly influenced by bottom water concentrations. The information obtained in the present study adds to our understanding of the complexity of biogeochemical interactions in estuaries and indicates an important role of intertidal sediments for the biogeochemistry of estuarine systems and adjacent seas. It is relevant for researchers addressing the effects of water treatment policies on estuarine biogeochemistry, the environmental impact of intertidal ecosystem losses or the effects of climate change related stressors on benthic biogeochemistry, among others. Moreover, a positive relationship was recognised between policy and ecosystem functionality restoration where the implementation of policy aimed at improving water quality resulted in sediments regaining their nutrient filter functionality which also ameliorated water quality. This information is important for policy makers and managers as it places emphasis in restoring ecosystem functionality.

3.6 Acknowledgements

This work is funded by the Royal Netherlands Academy of Arts and Sciences (KNAW) (project no. PSA-SA-E-02). Justin C. Tiano is a postdoctoral research fellow funded by BFIAT (Bottom Fishing Impact Assessment Tool) funded by the Netherlands Organization for Scientific Research (NWO), grant No. 18523. We thank the field technicians and laboratory staff, Peter van Breugel, Jan Peene, Anton Tramper, Yvonne van der Maas and Jurian Brasser for their help with sample processing and analysis. Special thanks to our colleague Tim Grandjean and former colleague Pieter Van Rijswijk for their help with sample collection and processing.

Funding: This research was supported by the project 'Coping with deltas in transition' within the Programme of Strategic Scientific Alliances between China and the Netherlands (PSA), financed by the Royal Netherlands Academy of Arts and Sciences (KNAW), Project No. PSA-SA-E-02.

Chapter 3

3.7 Appendix

Appendix 3.1 Porewater Redfield ratios per depth layer. Redfield ratio: DIN: DIP 16, and DSi: DIP 16

Depth	Fresh		Brackish		Marine	
	DIN: DIP	DSi: DIP	DIN: DIP	DSi: DIP	DIN: DIP	DSi: DIP
0	2.8	10.7	2.3	6.9	2.9	7.1
-1	2.6	9.6	1.8	6.6	2.8	8.0
-2	2.8	8.0	1.1	5.1	3.1	8.1
-3	4.3	9.5	0.7	3.5	3.1	8.0
-5	5.3	11.1	0.8	3.3	4.9	11.4
-10	7.7	10.3	1.4	3.7	5.2	12.2
-14	11.8	14.9	1.4	3.7	6.2	13.0

Chapter 4 *Influence of benthic fauna on intertidal sediment biogeochemistry along the estuarine salinity gradient*

Dunia Rios-Yunes; Olivier Beauchard; Emil De Borger; Anton Tramper; Yuan Xu; Tom Ysebaert & Karline Soetaert

In prep.

4.1 Abstract

Intertidal muddy sediments are biogeochemical hotspots exhibiting high levels of oxygen (O₂) consumption, organic matter (OM) remineralization and nutrient recycling. These sediments are inhabited by bioturbating macrobenthos that affect the sediment concentration of chlorophyll a (chl a), O₂, and nutrients as well as the benthopelagic exchange of nutrients. In this study, we studied the benthic community along a well-studied European temperate estuary, the Scheldt Estuary, and investigated its influence on the oxygen penetration depth (OPD), sediment mixing rate, and O₂ and nutrient fluxes; we also explored the relative contribution of the benthos to the observed nutrient fluxes compared to temperature and salinity. We monitored these variables in three intertidal mudflats covering fresh, brackish, and marine habitats. The freshwater habitat was dominated by oligochaetes, the brackish by *Corophium volutator* and *Hediste diversicolor* and the marine site by different polychaetes and bivalves. The bio-irrigation of these communities respectively contributed to 51 %, 84 % and 88 % of total O₂ fluxes. Bioturbation intensity ($Db = 0.22 \text{ cm}^2 \text{ d}^{-1}$) and OPD (max. 7.5 mm) were highest in the brackish habitat. Through variation partitioning, we disentangled the respective contributions of abiotic (temperature and salinity) and faunal components to flux variations. Temperature and salinity together accounted for 45 % of variation, the fauna individual density contributed to 18 %.

4.2 Introduction

Estuarine intertidal sediments receive OM from autochthonous sources in the form of microphytobenthic primary production (Statham, 2012a; Kang et al., 2015; Dagers et al., 2020), and from allochthonous sources such as terrestrial plant debris (Magalhães et al., 2002; Struyf et al., 2006). The organic matter is incorporated into the sediment through burial, sedimentation, tidal action, and sediment mixing by macrobenthic organisms (Meysman et al., 2006; Kristensen et al., 2012). After deposition, the OM is remineralized and transformed by biogeochemical processes; thereafter, the nutrients released are transformed, exchanged with the water column, exported, or removed by the sediment (Magalhães et al., 2002; Rios-Yunes et al., 2023b). The efficiency of these biogeochemical transformations is not only determined by abiotic factors such as temperature (T) (Arndt et al., 2013); salinity (S) (Rysgaard et al., 1999); OM reactivity (Lessin et al., 2018); the sedimentary concentration of oxygen (O₂) (Rysgaard et al., 1994); and nutrient availability; but also by biotic factors including benthic microbial, meio- and macrofaunal activity (Braeckman et al., 2010a).

The interactions between macrofauna (e.g. worms and bivalves) and the physical and biogeochemical characteristics of the sediment have been a subject of fascination and study since Darwin first recognised it well over a century ago (Meysman et al., 2006; Kristensen et al., 2012). Due to their close relation with the sediment, macrobenthic organisms are major contributors to bioturbation, the mixing and irrigation of the sediment (Kristensen et al., 2012). Different types of sediment and water transfer are induced by organism motility through foraging, defecation, and burrow creation (Pearson and Rosenberg, 1977; Aller, 1982; Kristensen et al., 2012). Depending on faunal activity, sediment mixing can be local and random (biodiffusion) or non-local and oriented (bioadvection, upward or downward; François et al., 1997; Soetaert et al., 1996), while water transfer (bioirrigation) can be enhanced by the active ventilation and flushing inside burrows. Local mixing is characterized by small scale mixing, mostly associated with near-the-surface sediment layers, while non-local mixing is due to transport or injection of particles over longer distances, usually resulting in sub-surface peaks associated with feeding behaviour or burrowing of larger animals (Boudreau, 1986). By altering the sediment matrix, macrobenthic activity can change the chemical characteristics of the sediment and water column (Magni and Montani, 2006; Kristensen et al., 2012; Thoms et al., 2018), thereby influencing microbial activity (Pelegri and Blackburn, 1994); early diagenesis (Aller, 1982; Toussaint et al., 2021); benthic-pelagic nutrient exchange (Braeckman et al., 2010a, 2014; de Backer et al., 2011); and even contributing to sediment restoration (Lam-Gordillo et al., 2022).

Despite the abundant literature on bioturbation in estuarine and marine ecology, it is still unclear how it influences benthic biogeochemistry and benthic-pelagic coupling at the water-sediment interface. Previous theoretical works focused on the quantification of

Chapter 4

sediment mixing types (Aller, 1982; François et al., 1997; Soetaert et al., 1996), later enabling empirical studies (e.g. Beauchard et al., 2012; Kristensen and Kostka, 2005; Richard et al., 2023). Concomitantly, other investigators have addressed the relation between sediment bioturbation and benthic biogeochemistry (e.g. Braeckman et al., 2010b; De Borger et al., 2020; Fang et al., 2019). Since benthic estuarine communities are strongly structured by salinity (Ysebaert et al., 1998), expected changes in taxonomic composition might induce functional changes in the sediment. Hence, investigating the relationships between macrofauna and sediment biogeochemistry may provide both a better understanding of ecosystem functioning (Heip et al., 2005), and clues on the potential consequences of biodiversity loss on the functioning of marine ecosystems (Raffaelli et al., 2003).

Previous research has shown considerable differences in the biogeochemical functioning of the intertidal flats of the Western Scheldt estuary, where freshwater sites are net consumers of dissolved inorganic P and N, brackish sites consume dissolved inorganic N, and marine sites release both DIN and DIP (Rios-Yunes et al., 2023b). In this study, we combined the seasonal dataset on sediment biogeochemistry with macrobenthic seasonal data from these three intertidal mudflats of the Western Scheldt estuary, and we tried to disentangle the contribution of various biotic and abiotic factors to benthic-pelagic coupling. This work provides complementary insights to the seasonal patterns of the abiotic component previously reported by Rios-Yunes et al. (2023b).

4.3 Methods

4.3.1 *Study area*

Our study was conducted in the Western Scheldt Estuary, which connects the port of Antwerp in Belgium with the North Sea. Three mudflat locations (Figure 4.1) were visited monthly from March 2019 to February 2020 including the freshwater (F, Appels, Belgium, 51.04832 N, 4.06934 E), the brackish (B, Groot Buitenschoor, Netherlands, 51.36337 N, 4.24456 E) and the marine (M, Paulina Polder, Netherlands, 51.35337 N, 3.72054 E) sections of the estuary. All habitats were sampled during low tide and had a 70 % dry time. The concentration of the water column nutrients: nitrite (NO_2^-), nitrate (NO_3^-), dissolved silicate (DSi), and phosphate (PO_4^{3-}) decreased from the fresh to the brackish and the marine habitat (Table 4.1), while ammonium (NH_4^+) was lowest in the B habitat. The analysis of seasonal fluctuations of water column nutrient concentrations can be found in (Rios-Yunes et al., 2023b).

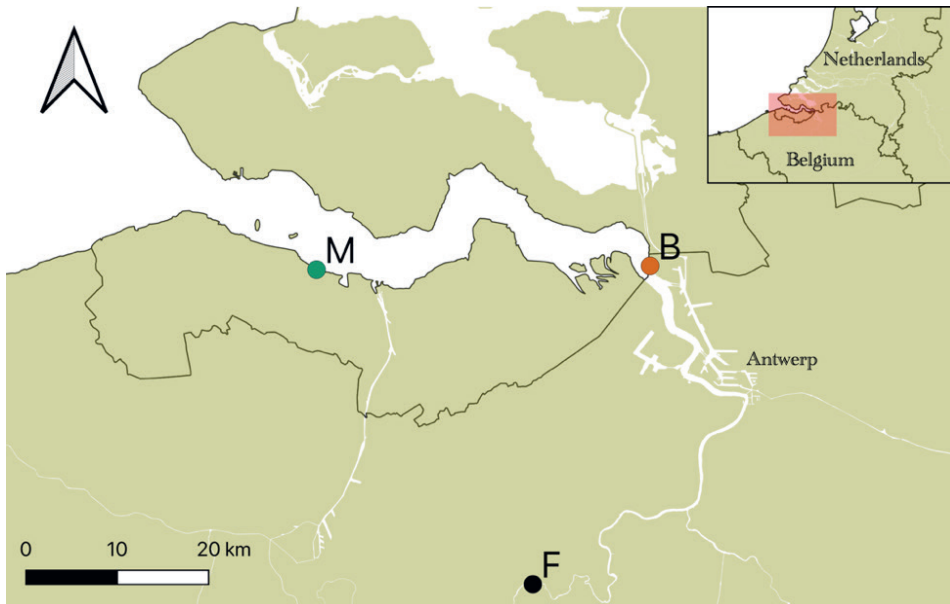


Figure 4.1 Sampling locations in the Scheldt estuary. Freshwater (F), brackish (B) and marine (M) habitats. Maps created with QGIS (QGIS Development Team, 2021).

4.3.2 Sampling method

Sediment core samples were taken in duplicate for macrofauna (30 cm height, 15 cm inner diameter (\varnothing)), grain size, chlorophyll a (chl a) (30 cm height, 3.5 cm \varnothing) and oxygen micro profiling (15 cm height, 6 cm \varnothing). Cores were transported to the Royal Netherlands Institute for Sea Research, Yerseke (NIOZ- EDS Yerseke) immediately after collection. Cores for macrofauna and micro profiling were taken to a dark ambient temperature-controlled climate room and placed in a thermostatic bath and fitted with an aerator. The chl a cores were stored at 4°C until they were processed the next day. For methods regarding core incubations for O₂ and nutrient (NH₄⁺, NO₂⁻, NO₃⁻, DSi and PO₄³⁻) fluxes prior to macrofauna sampling and for the sampling and analysis of grain size and pigments (list of pigments in Appendix 4.1) we refer to Rios-Yunes et al. (2023b).

Chapter 4

Table 4.1 Mean \pm standard deviation of yearly water column concentration (mmol m^{-3}) and fluxes ($\text{mmol m}^{-2} \text{d}^{-1}$) of nutrients ammonium (NH_4^+), nitrite (NO_2^-), nitrate (NO_3^-), phosphate (PO_4^{3-}), dissolved silicate (DSi) as well as oxygen (O_2) consumption rates ($\text{mmol m}^{-2} \text{d}^{-1}$). A negative value indicates an influx into the sediment. Table recalculated from Rios-Yunes et al. (2023b).

	Water column concentration mmol m^{-3}			Fluxes $\text{mmol m}^{-2} \text{d}^{-1}$		
	Fresh	Brackish	Marine	Fresh	Brackish	Marine
O_2	-	-	-	-39.45 ± 20.38	-44.3 ± 22.75	-68.01 ± 35.09
NH_4^+	11.13 ± 10.86	5.40 ± 6.96	10.47 ± 5.98	3.6 ± 4.83	0.1 ± 0.63	5.48 ± 4.24
NO_2^-	3.32 ± 2.59	1.90 ± 1.62	1.59 ± 0.59	0.12 ± 0.39	0.03 ± 0.15	0.2 ± 0.14
NO_3^-	299.56 ± 96.44	199.85 ± 74.46	43.50 ± 26.50	-4.54 ± 2.36	-3.05 ± 1.73	-1.85 ± 1.11
PO_4^{3-}	5.75 ± 1.88	4.28 ± 0.96	1.65 ± 0.45	-0.07 ± 0.08	0.1 ± 0.13	0.09 ± 0.15
DSi	106.61 ± 93.31	100.46 ± 45.41	30.75 ± 11.65	1.08 ± 1.56	0.2 ± 2.8	5.71 ± 4.68

4.3.3 Experimental methods

The chl a cores were sliced per 0.5 cm for the uppermost 3 cm, and then per 1 cm down to a depth of 10 cm. The chl a slices were stored at -80°C and freeze dried before analysis. The chl a was extracted by bead-beating and centrifugation from 1 g of sediment with acetone (No. 1000122500, Merck). The supernatant was measured with a spectrophotometer (Specord 210, Analytik Jena).

Macrobenthos was collected after the sediment cores incubation. The sediment was sieved through 0.5 and 1-mm sieves, and the animals were fixed in formaldehyde 4% with rose Bengal until analysis. Thereafter, the organisms were head-counted, dried at 60°C for 48 h, and incinerated in an ignition oven at 500°C for 3 hours. Ash free dry mass (AFDM) was calculated by subtracting ash weights from dry weights. Taxa were considered for data analysis when they represented at least 1 % of the total density of at least one of the three habitats.

Oxygen micro profiling (~6 micro profiles per core) was done in duplicate cores with an oxygen microsensor (50 mm tip diameter, Ox-50, UNISENSE) at ambient temperature and in dark conditions to prevent influences of the photosynthetic activity of microphytobenthos on the oxygen penetration depth. Microsensors were calibrated with 100% and 0% oxygen saturated seawater to respectively represent oxic and anoxic concentrations. Oxygen concentration readings were taken at 50- μm intervals, starting from approximately ~1000 μm above the sediment water interface (100% O_2 saturation) and ending at the depth at which all oxygen was depleted, which was recorded as the oxygen penetration depth.

4.3.4 Data analysis

All data and statistical analyses were performed with the R software (R Core Team, 2020).

Diffusive fluxes (F_0) across the sediment-water interface ($x=0$) of dissolved oxygen were estimated by applying Fick's law:

$$F_0 = -\frac{\emptyset D_{O_2}}{\theta^2} \left. \frac{\partial O_2}{\partial x} \right|_{x=0}$$

Where D_{O_2} is the diffusion coefficient of oxygen in water, \emptyset is the porosity, θ^2 is the sediment tortuosity, defined as $\theta^2 = 1 - \ln(\emptyset^2)$, as in Boudreau (1996). The oxygen gradient ($\frac{\partial O_2}{\partial x}$) was estimated as the slope of the linear regression of the oxygen concentration versus depth, estimated in the upper 0.5 mm in the sediment. The O_2 diffusion coefficient as a function of temperature and salinity was estimated using the R-package *marelac* (Soetaert et al., 2010). Linear analysis was used to test the relation between OPD and diffusive O_2 fluxes with temperature fluctuations.

The chlorophyll a profiles derived from sediment slices were used to fit a set of 5 biomixing models as described in Soetaert et al. (1996) as implemented in the R package "turbo" (Soetaert and Provoost, 2016). The imposed degradation rate of chl a was 0.02 d^{-1} and it was assumed to be independent of temperature fluctuations (Morys et al., 2016). This fitting procedure determines whether the profiles are dominated by diffusive or nonlocal exchange processes and returns values for the sediment diffusive mixing coefficient (Db , $\text{cm}^2 \text{ d}^{-1}$), injection fluxes (J , $\mu\text{g cm}^{-2} \text{ d}^{-1}$) and the flux to depth of ingested surficial sediment (r , d^{-1}). Differences in chl a concentration between habitats were determined with a Wilcox test ($p \leq 0.05$).

The influence of abiotic components on the sediment O_2 and nutrient (NH_4^+ , NO_2^- , NO_3^- , PO_4^{3-} and DSi) fluxes of the fresh, brackish, and marine habitats has been previously reported by Rios-Yunes et al. (2023b). Variation partitioning (Legendre and Legendre, 2012) was applied to disentangle the effects of salinity, temperature, and benthos individual and biomass densities on flux variations. The significance of the fractions explaining flux variation was tested by permuting matrix rows at random and comparing the observed adjusted- R^2 to simulated ones. The independent effects of the fauna on fluxes were investigated by partial Redundancy Analysis (RDA). This enabled us to explore the relationships between fluxes and taxa while controlling for the abiotic components of salinity and temperature. The significance of the RDA axes was tested by another permutation procedure that compares the successively added axis variance in a step forward way (Legendre et al., 2011). Variation partitioning and RDA were carried out with the R package "vegan" (Oksanen et al., 2020). Ecological traits of the fauna typical of substratum-organism relations such as feeding type, mobility, sediment depth

distribution, mixing type, and burrow type were used to interpret and explain the RDA results, but were not included in the analysis (Fauchald and Jumars, 1979; Beauchard et al., 2023).

4.4 Results

4.4.1 Abiotic conditions of the Western Scheldt estuary

Salinity values were stable throughout the year and increased from the river to the mouth of the estuary (Table 4.2). Temperature was always slightly higher in the fresh than the brackish and marine parts, but overall seasonal fluctuations were similar between habitats. Based on a water temperature threshold of 15 °C, two periods were determined: a cooler period from November to May and a warmer one from June to October with T exceeding 20 °C from July to September.

All habitats had muddy sediments with mean grain size (D₅₀) ranging from 30.32 µm in the fresh to 61.51 µm in the marine area (Table 4.2). Sediment organic carbon (OC) concentration and porosity decreased with increasing salinity. No seasonality was detected for D₅₀, OC or porosity values. The molar Carbon: Nitrogen (C: N) ratio – an indication of carbon lability - was highest in the brackish (~ 13) and lowest in the marine part of the estuary (~9).

Table 4.2 Average yearly values with standard deviation of abiotic parameters from the fresh, brackish, and marine habitats. Salinity (S), temperature (T) and nutrients correspond to the water column and the values of oxygen penetration depth (OPD), sediment mean grain size (D₅₀), organic carbon (OC), C:N ratio of organic matter and porosity are from the first 5 cm of the sediment.

	Unit	Fresh	Brackish	Marine
S	-	0.9±0.5	10.4±2.9	28.8±1.1
T	°C	14.25±5.97	14.27±5.72	13.31±5.63
D ₅₀	µm	30.32±6.40	48.72±5.54	61.51±12.17
OC	%	3.05±0.50	1.05±0.25	0.56±0.13
C: N	mol: mol	11.26±0.52	13.21±1.20	8.73±0.86
Porosity*		0.79±0.23	0.59±0.16	0.54±0.14

*October not included

4.4.2 Oxygen profiles

The O₂ profiles had a typical diffusive shape in the freshwater and in the marine area during summer. Oxygen concentrations showed subsurface peaks, signs of animal ventilation, year-round in the brackish, and during the cooler months in the marine area (Figure 4.2). At all habitats, the O₂ micro profiles exhibited a slightly shallower penetration

during the warmer months of the year (Figure 4.2). Despite these fluctuations, the maximum O₂ penetration depth was rather stable throughout the year in the fresh (3.09 ± 0.1 mm) and marine (3.5 ± 1.5 mm) habitats (Figure 4.2). However, in the brackish habitat the maximum OPD was deeper and decreased linearly ($p < 0.05$) with temperature, becoming shallower in the warm months at around 4.3 ± 1.4 mm and increasing to 7.5 ± 3.8 mm in the cool months (Figure 4.2).

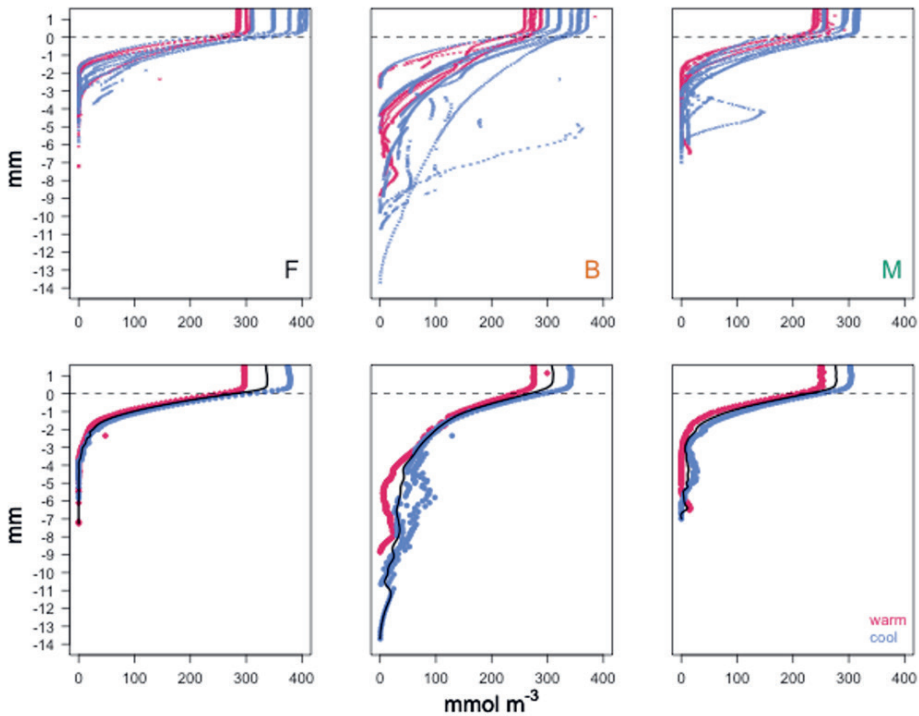


Figure 4.2 top panels showing mean monthly data of oxygen micro profiles for the freshwater (F), brackish (B) and marine (M) habitat. The warmer months (June to October) are represented by red points. The cooler months (March to May and November to February) are shown with blue points. The bottom panels show the mean O₂ penetration in the cooler (blue) and warmer (red) months. Black line is the cubic fitted line of the yearly mean. Horizontal dotted line represents the sediment-water interphase.

The mean diffusive oxygen (DO) fluxes were significantly higher ($p < 0.05$) in the freshwater habitat (15.4 ± 4.8 mmol m⁻² d⁻¹) than in the B and M habitats (respectively 4.9 ± 2.3 mmol m⁻² d⁻¹ and 5.5 ± 2.1 mmol m⁻² d⁻¹; crosses in Figure 4.3A). The DO fluxes increased linearly ($p < 0.05$, $R^2=0.37$) with temperature only in the freshwater habitat. Total O₂ uptake increased from the fresh to the brackish and marine habitats and was higher in the warmer than in the cooler months (points in Figure 4.3A). The ratio between DO fluxes

Chapter 4

and total sediment respiration was calculated (Figure 4.3B). In the F habitat, DO fluxes accounted on average for 49% of the respiration fluxes while in the brackish and marine habitats it amounted to 16% and 12%, respectively.

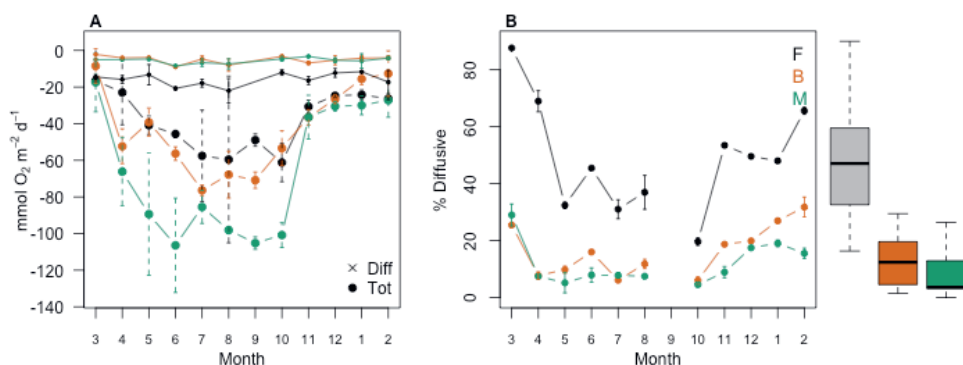


Figure 4.3 Monthly mean of oxygen fluxes (A): total fluxes represented by points and diffusive fluxes by crosses. (B): Monthly percentage of contribution of diffusive oxygen fluxes to total oxygen fluxes. Boxplots represent the mean and standard deviation of the contribution percentage for the fresh (black), brackish (orange) and marine (green) habitats. Vertical lines represent standard deviations.

4.4.3 Sediment Pigments

Ratios of chl c: chl a and chl b: chl a were compared to study the contribution of different microphytobenthos groups to algal organic matter in each habitat (Table 4.3). The higher the chl c: chl a ratio, the greater the contribution of diatoms, while the greater the chl b: chl a ratio, the more important the contribution of green algae and euglenoids to the pigment pool. Benthic diatoms were present in all locations with their contribution increasing from fresh to marine areas (chl b: chl a ratio). The opposite occurred with green algae and euglenoids whose contribution decreased with increasing salinity (chl b: chl a ratio).

Table 4.3 Mean \pm standard deviation of the pigment ratios of chlorophyll (chl) c: chl a and chl b: chl a from the upper 1 cm at each habitat. In both cases, the higher the ratio the greater the contribution of each group.

Habitat	chl c: chl a (diatoms)	chl b: chl a (green algae and euglenoids)
Freshwater	0.03	0.11
Brackish	0.06	0.02
Marine	0.12	0.01

The total monthly concentration of pigments (Appendix 4.1) was compared between habitats (Figure 4.4). The concentration of pigments was significantly different ($p < 0.05$) between the three habitats with the highest values observed in the freshwater habitat and the lowest in the brackish habitat. The freshwater and marine habitats showed a clear summer peak of pigments (Figure 4.4). In contrast, no distinct seasonal peak was observed in the B habitat.

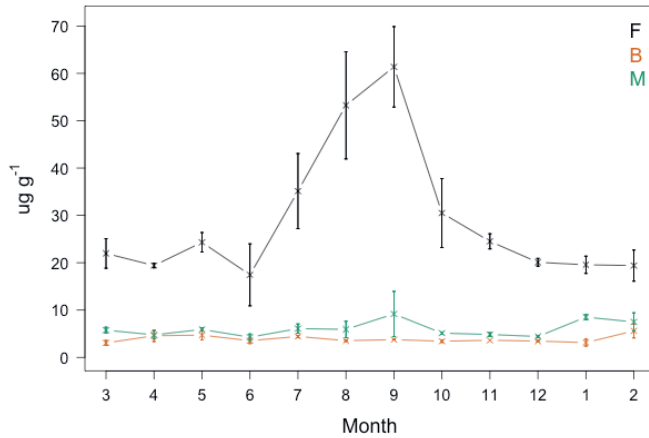


Figure 4.4 Monthly comparison of mean and standard deviation of total pigments concentrations at the freshwater (F), brackish (B), and marine (M) habitats.

The concentration of chl a in the surface (top 4 cm) fluctuated seasonally in all habitats (Figure 4.5). However, in the F and B habitats the seasonal variation was observed down to a depth of 10 cm, and in the case of the F habitat, an increase in chl a concentration at depth occurred during the cool months. In contrast, the chl a concentration in the M habitat converged to low values at depth with no conspicuous seasonality (Figure 4.5).

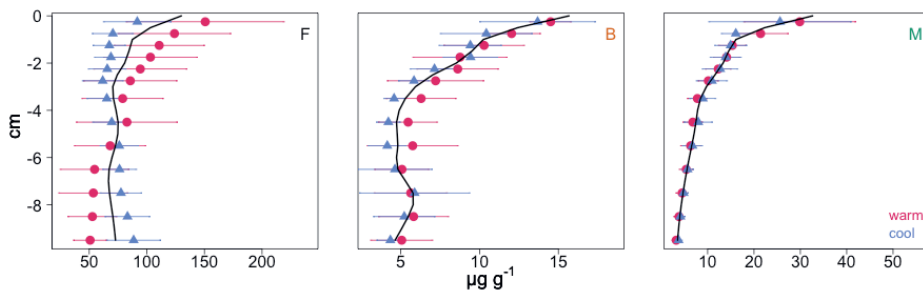


Figure 4.5 Chl a profiles of the freshwater (F), brackish (B) and marine (M) habitats. Black line is the cubic spline of the yearly mean. Blue triangles represent the seasonal average of the cool months (March to May and November 2019 to February 2020) and the red circles that of the warm

Chapter 4

months (June to October). Horizontal lines represent the standard deviation per season in their respective colours. Note x-scale differences between habitats.

The mixing models at the B and M habitats were fitted to the monthly averages of chl a concentrations per depth slice. Both habitats exhibited a combination of diffusive sediment mixing and non-local exchange processes (Appendix 4.2). Non-local exchange processes prevailed throughout the year and occurred in 18 of 24 instances in each site. Mean injection depth and biodiffusion (Db , i.e. local sediment mixing intensity) were greater in the brackish (3.4 ± 3.8 cm and $Db = 0.22$ cm² d⁻¹) than in the marine habitat (1.5 ± 1.6 cm and $Db = 0.14$ cm² d⁻¹). It was not possible to determine the mixing type for the freshwater habitat.

4.4.4 *Macrobenthos*

Clear differences in the macrobenthic community structure were observed along the salinity gradient. The freshwater habitat was dominated by oligochaetes, which were also present in brackish and marine habitats albeit in much lower densities. The brackish habitat abundance (ten taxa) was dominated by the amphipod *Corophium volutator* (68%) and the polychaete *Hediste diversicolor* (8%). The marine habitat was co-dominated by the polychaetes *Alitta succinea* and *Heteromastus filiformis* (each accounting for 31 % of total marine abundance), followed by a few other taxa with each representing less than 10 % and exhibiting variety of ecological traits (Table 4.4). Oligochaetes comprised 99.9 % of the biomass in the freshwater habitat (Table 4.4). But in the B and M habitats there was a higher diversity of taxa contributing to total biomass. In the brackish habitat, *H. diversicolor* had the highest contribution, followed by *C. volutator* and the isopod *Cyathura carinata*. In the marine habitat, the greatest contribution to biomass was associated with the peppery furrow shell *Scrobicularia plana* and the cockle *Cerastoderma edule*, followed by *H. filiformis*.

Table 4.4 Functional description of the fauna. Salinity (F, freshwater; B, brackish; M, marine), percentages of within-habitat total individual density and biomass; T, percentage of total density; Tb, percentage of total biomass. Feeding type: De, deposit-feeding; Su, suspension-feeding; CaSc, carnivory-scavenging. Mobility: S, sessile; L, limited; M, mobile. Depth distribution (cm): depth within the sediment where the presence of the organism is the most likely. Mixing type: Bd, bioturbation; UC, upward conveying; DC, downward conveying. Burrow type: N, none; S, simple (I- or J-shaped); OE, open-ended (anastomosed, Y- or U-shaped) (Beauchard et al., 2023; Fauchald and Jumars, 1979)

Taxon	Individual density (%)				Biomass density (%)				Feeding type			Mobility			Depth distribution			Mixing type			Burrow type		
	F	B	M	T	F	B	M	Tb	De	Su	CaSc	S	L	M	0-5	5-15	>15	Bd	UC	DC	N	S	OE
Oligochaeta	>99.9	9.8	14	72.8	99.8	2.9	0.2	18	x			x			x	x			x				x
<i>Hediste diversicolor</i>	<0.1	8	0.1	1.6	0.2	33.8	0.1	3-4	x			x			x	x			x				x
<i>Abra</i> sp.	<0.1	<0.1	<0.1	<0.1		2.2	I	0.9		x		x			x								x
<i>Alitta succinea</i>	I	3I	I	I		<0.1	7.9	5.7	x			x			x	x							x
Cirratulidae	2	7.8	1.2	1.2		0.1	<0.1	<0.1	x			x			x	x							x
<i>Corophium volutator</i>	67.7	0.3	13.6			26.5	<0.1	2.6	x			x			x	x			x				x
<i>Cyathura carinata</i>	5.6	9.9	2.2			11.9	1.4	2.2	x			x			x	x							x
<i>Heteromastus filiformis</i>	I	3I	3.5			5.7	10.6	8.3	x			x			x	x			x				x
<i>Macoma balthica</i>	1.4	2.7	0.6			8.4	6.5	5.6	x			x			x	x							x
<i>Scrobicularia plana</i>	0.3	5.3	0.6			7.7	52.6	38.9	x			x			x	x			x				x
Spionidae	2.4	8.3	1.4			0.4	0.2	0.2	x			x			x	x			x				x
<i>Cerastoderma edule</i>		3.7	0.4			17.2	12.5		x			x			x								x
<i>Eteone</i> sp.		2.5	0.3			0.1	0.1			x		x			x	x							x
<i>Ruditapes philippinarum</i>		1.8	0.2			0.9	0.6		x			x			x								x

4.4.5 Contribution of fauna to nutrient fluxes

Variation partitioning showed that abiotic and biotic components together explained 70 % of total flux variation; temperature alone accounted for 36 %, salinity for 9 % and faunal individual density for 18 %, confounding effects contributed to a relatively marginal 7 % of the variance (Figure 4.6). The same analysis when representing fauna with biomass density resulted in slightly lower amounts of explained variance (Appendix 4.4).

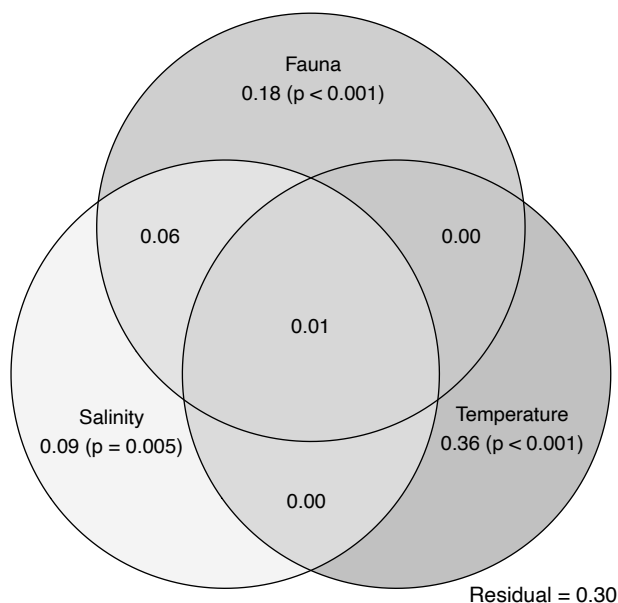


Figure 4.6 Variation partitioning, Venn diagram representing the contribution of explanatory components to flux variance; values are adjusted- R^2 . Salinity, temperature, and faunal individual density explain all together 70 % of total flux variance. Considered independently, each explanatory component has a significant effect on fluxes (p-value < 0.05) while controlling for the two other components (non-overlapping surface areas). Confounding effects (overlaps) have null or low effects.

Partial RDA of faunal-specific effects on fluxes emphasizes the relationships between variables while controlling for salinity and temperature (Figure 4.7). A single axis was found significant, opposing the covariations of the PO_4^{3-} and NO_3^- fluxes and those of DSi , O_2 , NH_4^+ and NO_2^- (Figure 4.7A), as well as those of two opposed groups of taxa (Figure 4.7B). Covariance between variables was determined when these were found on the same side of the axis. A similar pattern was observed with faunal biomass (Appendix 4.5).

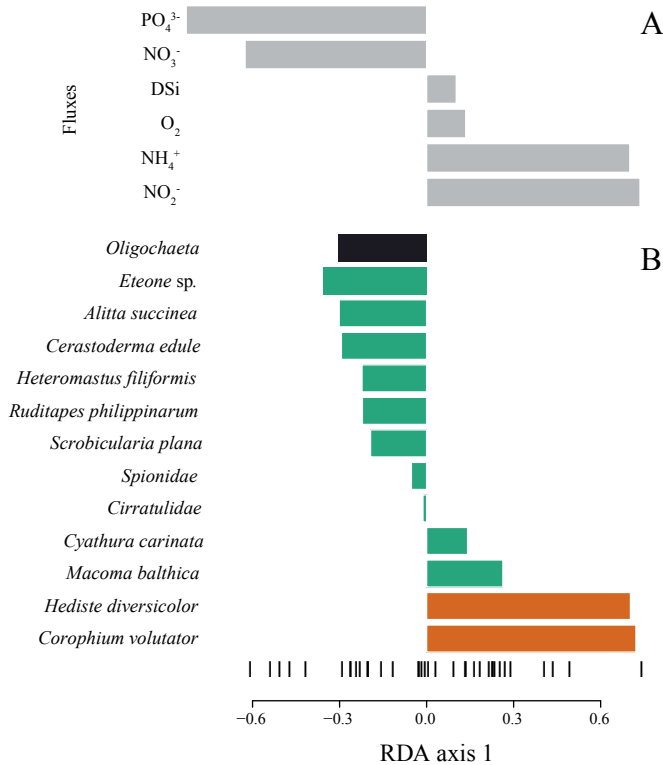


Figure 4.7 Redundancy analysis, first and only significant axis encompassing 49 % of the total multivariate variance. (A) scores of fluxes and (B) scores of taxa individual density. Bar lengths represent the contributions of the variables to the axis variance. Note that these contributions do not necessarily reflect the raw fluxes or organism abundances, instead they show the conditional pattern when controlling for salinity and temperature. Scores of same sign indicate that variables covary positively, and negatively when opposed. Bar colours correspond to the habitats where the taxa are the most abundant: black, freshwater; green, brackish; and orange, marine. Vertical segments at the bottom represent sample positions along the axis; there is no outlier driving the trend.

4.5 Discussion

In this study, we investigated the main driving factors of nutrient fluxes in intertidal sediments in fresh, brackish, and marine habitats of the Western Scheldt estuary. Variation partitioning showed that abiotic and biotic components together explained a high fraction (70 %) of total flux variation, of which more than half was related to seasonal effects (temperature: 36%), 9% to position along the salinity axis, while 18% of variation could be explained by faunal individual density alone (Figure 4.6).

Chapter 4

The three habitats were characterised by distinct macrobenthic communities, with the freshwater habitat having the lowest number of taxa and a strong dominance of oligochaetes, in line with what was previously reported (Wolff, 1973; Ysebaert et al., 1993, 1998; Seys et al., 1999). The pigment ratios (Table 4.3) hinted towards sediments dominated by green algae and euglenoids, as is typically found in freshwater upstream areas (Kromkamp and Peene, 1995b; Muylaert et al., 2002; Maris and Meire, 2017). Nevertheless, microphytobenthos organic matter is not the only source of OM to this sediment. Fragments of vascular plant origin were visually observed during sediment sieving. Thus, it is likely that the chl a found in this sediment not only derived from microphytobenthos, but also from senescent reed (*Phragmites australis*) from the adjacent marsh.

The presence of reed-derived organic matter is probably responsible for the high chlorophyll concentrations in this freshwater sediment, and for the deep penetration of chl a, which displayed even an increasing concentration over depth during the cooler months (Figure 4.5). Unfortunately, the presence of reed derived chlorophyll excludes the application of the mixing models, as they require the input of a chl a degradation rates representative of OM deriving from microphytobenthos and deposited phytoplankton. However, Beauchard et al. (2012) provided evidence of dominant advective mixing in the freshwater area of the estuary. Oligochaetes are indeed known to be upward or downward conveyors that rework several times their own bodyweight in sediment as faeces (Giere and Pfannkuche, 1982; Giere, 2006).

Of all three sites, the freshwater sediment had the smallest total metabolic rate, as measured via the oxygen flux ($39.4 \text{ mmol O}_2 \text{ m}^{-2} \text{ d}^{-1}$). However, it was the only site where diffusive sediment fluxes comprised a significant fraction of the total oxygen flux ($15.4 \text{ mmol m}^{-2} \text{ d}^{-1}$, i.e. 49%), indicating that here sediment-water exchange rates are primarily governed by small-scale processes. With respect to biogeochemistry, Rios-Yunes et al. (2023b) showed this site to be a net consumer of dissolved inorganic phosphate and DIN - albeit to a lesser extent. The RDA analysis also pinpointed Oligochaeta as an important species explaining variation in PO_4^{3-} and NO_3^- fluxes (Figure 4.7).

Total chlorophyll concentration in the *brackish* habitat was an order of magnitude lower than in the freshwater site (Figure 4.4), suggesting a low contribution of reed-derived material, while the pigment ratios suggest that pigments are mainly derived from diatoms (Table 4.3). The major contributors to the macrobenthic community in the brackish habitat are known to be highly specific of this salinity and they were the amphipod *C. volutator*, which is a deposit feeder typically found in high densities in the mesohaline section of the Scheldt Estuary (Ysebaert et al., 1998), and the polychaete *H. diversicolor*, a facultative filter-feeder common in mesohaline areas (Table 4.4; Fong, 1991; Kristensen, 1988). These two species are important bioturbators which may contribute to the vertical movement of chl a through local and non-local mixing (Mermillod-Blondin et al., 2004; de Backer et al., 2011; Queirós et al., 2013; Richard et al., 2023). Sediment bioturbation in this area indeed showed a combination of local and non-local mixing modes, thereby

highlighting the effect of the macrobenthic community activity in these sediments. Furthermore, the brackish habitat exhibited a deeper penetration of chl *a* (Figure 4.5) as well a higher bioturbation intensity than the marine habitat (3.4 cm and $Db = 0.22 \text{ cm}^2 \text{ d}^{-1}$ vs 1.5 cm and $Db = 0.14 \text{ cm}^2 \text{ d}^{-1}$).

In contrast, the diffusive oxygen flux was lowest in the brackish site, only amounting to $4.9 \text{ mmol m}^{-2} \text{ d}^{-1}$, compared to a total oxygen flux of $44.3 \text{ mmol O}_2 \text{ m}^{-2} \text{ d}^{-1}$. The low proportion of diffusive processes to total sediment-water fluxes highlights the importance of burrow ventilation here. This habitat also exhibited the deepest oxygen penetration depth (max. 7.5 mm), and the oxygen concentrations often showed deep maxima (Figure 4.2) that are consistent with the deep bioirrigating activity of *C. volutator* and *H. diversicolor* that flush the sediment with oxygen rich water (Pelegri and Blackburn, 1994; Mermillod-Blondin et al., 2004; Thoms et al., 2018). It is also noteworthy that the brackish habitat showed significant seasonal variation in the OPD (Figure 4.2) that was negatively related to temperature ($R^2 = -0.62, p < 0.05$). This may indicate that the high bioirrigation capacity of *C. volutator* may have not been sufficient to compensate for the enhanced oxygen consumption under higher temperature. With respect to biogeochemistry, the brackish habitat exhibited a net flux of NH_4^+ close to zero ($0.1 \pm 0.6 \text{ mmol m}^{-2} \text{ d}^{-1}$, Table 4.1) and a high benthic influx of NO_3^- ($-3.05 \pm 1.73 \text{ mmol m}^{-2} \text{ d}^{-1}$). This indicates the complete consumption of NH_4^+ released from OM mineralization by benthic nitrification as well as an efficient denitrification that also relied on nitrate from the overlying water. A strong relationship between *C. volutator* and *H. diversicolor* and the fluxes of NH_4^+ and NO_2^- was apparent from the partial RDA (Figure 4.7), assigning a large importance to these two species for the nitrogen removal. This corroborates the results of Pelegri and Blackburn (1994), but contrasts with those from Mermillod-Blondin et al. (2004) and Richard et al. (2023) who observed an increased efflux of NH_4^+ associated with these species in marine conditions. Nitrogen influxes under brackish salinity suggests that, indeed, the bioirrigation activity of *C. volutator* and *H. diversicolor* promotes nitrification and denitrification, but the magnitude of this effect may depend on their abundance (Pelegri et al., 1994; de Backer et al., 2011), multi-species interactions (Raffaelli et al., 2003), and on salinity (Rysgaard et al., 1999). Similarly, the observed efflux of PO_4^{3-} in the brackish habitat (Rios-Yunes et al., 2023b) may be associated with the presence of *C. volutator* (Mermillod-Blondin et al., 2004), although it may also relate to a decrease in PO_4^{3-} sorption to sediment particles at higher salinity (Jordan et al., 2008).

The marine habitat had the highest species richness with a high abundance of polychaetes (*H. filiformis*, *A. succinea*) and bivalves (*C. edule*, *M. balthica*). These data are in line with the increasing proportion of filter-feeders towards the mouth (Pearson and Rosenberg, 1977; Ysebaert et al., 2003b). The dominance of filter-feeding organisms here (Table 4.4) suggests that the marine community is more reliant on phytoplankton-derived OM, which may explain why total O_2 consumption was highest in the marine ($68 \text{ mmol O}_2 \text{ m}^{-2} \text{ d}^{-1}$) habitat (Table 4.1). As diffusive oxygen consumption only contributed 12% to total oxygen

Chapter 4

flux (Figure 4.3), this suggests that, also in this site, macrofaunal activity increases oxygen intake above diffusive processes.

The chlorophyll profiles with sediment depth (Figure 4.5) showed evidence for local mixing as well as non-local processes (Appendix 4.3). Local mixing in the marine habitat may be attributed to the typical biodiffusive nature of the bivalves (Table 4.4, Wolff, 1973; Mermillod-Blondin et al., 2004), while the non-local mixing may be caused by the presence of both *A. succinea* (Queirós et al., 2013) or *H. filiformis*, an upward conveyor (Table 4.4) that feeds in deeper layers and deposits faeces on the sediment surface thereby depleting chl a at depth (Cadée, 1979; Ysebaert et al., 1993; Quintana et al., 2007).

Bivalves, although abundant in the marine habitat, have relatively low influence on the chemical conditions of the sediment pore water (Mermillod-Blondin et al., 2004; Rossi et al., 2008; Queirós et al., 2013). This seems to be at odds with the low contribution of diffusive processes to total oxygen flux (12%), but bivalves ventilate predominantly within their shells, so that the enhanced oxygen exchange has little impact on sedimentary oxygen concentrations. Indeed, while oxygen concentration maxima within sediments are occasionally observed in these sediments, this is much less the case than in the brackish site (Figure 4.2).

It is likely that bivalves affect the sediment-water nutrient fluxes indirectly by increasing the concentration of sedimentary OM (Mermillod-Blondin et al., 2004; Rossi et al., 2008) or by interacting with organisms with a stronger influence on nutrient fluxes (Rossi et al., 2008). This could be supported by the positive covariation between the clam *S. plana* and PO_4^{3-} fluxes (Figure 4.7), as already reported by Richard et al. (2023). The marine habitat displayed a net efflux of NH_4^+ (Table 4.1), probably because the physicochemical and biological aspects that promoted NH_4^+ storage and the high nitrification of the brackish habitat (Rios-Yunes et al., 2023b) were absent. For instance, the efflux of NH_4^+ may have resulted from lowered nitrification due to the inhibitory effect of sulphide on nitrifying bacteria (Rysgaard et al., 1999; Tee et al., 2021); from the low abundance of *C. volutator* that restricted their positive effect on nitrification-denitrification processes (Pelegri and Blackburn, 1994); from the high incidence of *H. filiformis* and *A. succinea* (Table 4.4; Fang et al., 2019); or from increased salinity that promoted desorption of NH_4^+ from sediment particles (Rysgaard et al., 1999). The net efflux of PO_4^{3-} observed in the marine habitat (Table 4.2) and its association with the presence of *A. succinea* (Figure 4.7) contrasts with reports associating the ventilating activity of this species with increased sorption of PO_4^{3-} and reduced effluxes (Swan et al., 2007; Gogina et al., 2018). We suspect that the ventilating activity of *A. succinea* did not sufficiently alter the redox conditions within the sediment to promote sorption of PO_4^{3-} and cause an influx. The observed efflux, however, may have resulted from the higher salinity promoting desorption from sediment particles (Jordan et al., 2008).

Our study confirmed that intertidal biogeochemistry is primarily determined by abiotic factors, such as temperature and salinity, with biotic factors having a lesser, but still important, influence. Similarly, abiotic factors determined the type of OM and macrobenthos found along the estuary. This, in consequence, also affected the benthic biogeochemistry present at each habitat. The bioirrigating activity of macrofauna altered the concentration of OM, oxygen, and nutrients within the sediment. Nevertheless, it was not possible to explain the magnitude of the nutrient fluxes based on macrofauna individual density, biomass density, presence or absence or functional traits. Our study demonstrated the difficulty in providing complete mechanistic links between sediment biogeochemistry and organism behaviour and physiology by means of traditional benthic data. Still, we showed that macrobenthos plays an important role in intertidal sediment biogeochemistry and functional traits may be more important than the specific taxa for ecosystem functionality.

4.6 Acknowledgements

This work is dedicated to the memory of Dr. Tom Ysebaert, a brilliant scientist who devoted a large part of his work to estuarine and coastal environments. Beyond his own research achievements, Dr. Ysebaert relentlessly fostered local and international collaborations, and his legacy of scientific excellence will continue to inspire many of us. We would like to thank the students Sophia Suvacarov, Nicole Brackenborough and Sietse de Wal and the NIOZ analytical lab (Peter van Breugel, Yvonne Maas, Jan Peene, Jurian Brasser and more) for helping processing sediment and water samples. This work is funded by the Royal Netherlands Academy of Arts and Sciences (KNAW) (project no. PSA-SA-E-02).

4.7 Appendix

Appendix 4.1 List of pigments, type of pigment and taxonomic association. The pigment Chl c was studied as the sum of Chl c1, Chl c2, and Chl c3. Table compiled from Foss et al., 1984; Schimek et al., 1994; Reuss, 2005; Sajilata et al., 2008; van Leeuwe et al., 2014; Yilmaz and Gökmen, 2016.

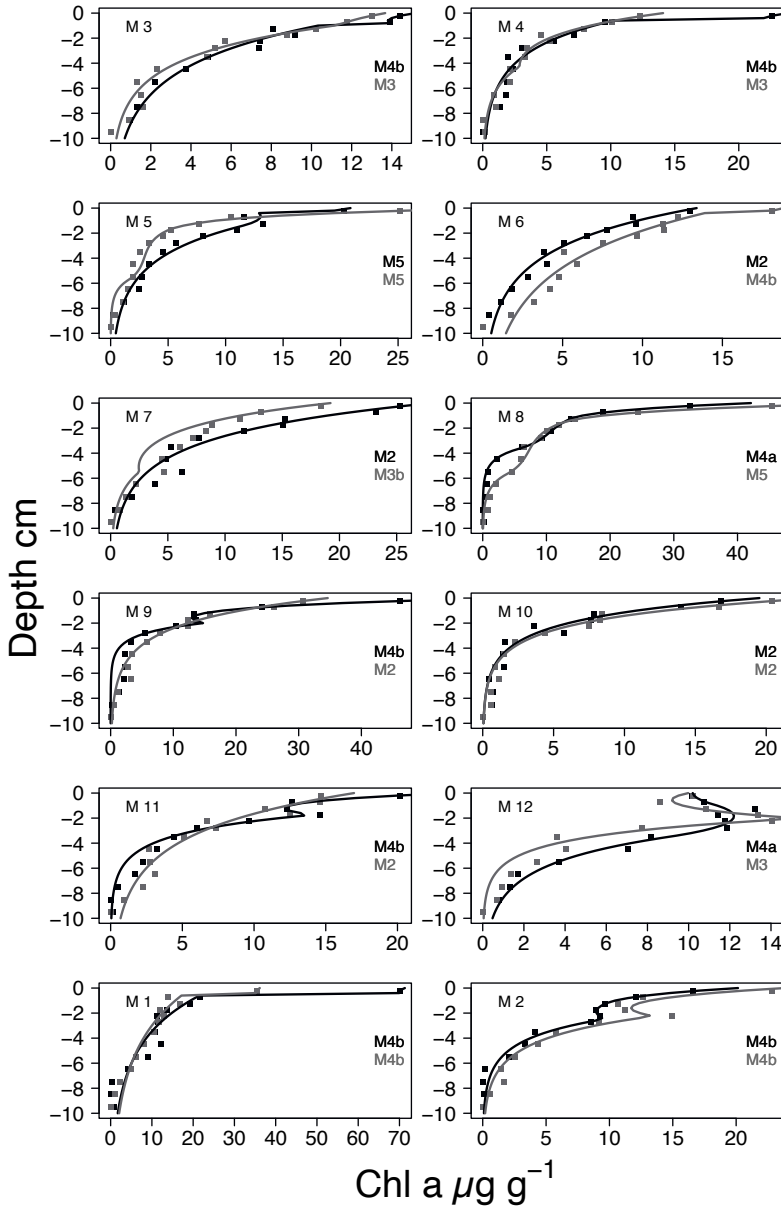
Pigments	Type	Taxonomic association
19-hexanoyoxyfucoxanthin	Pigment	Phaeocystis
Alloxanthin	Pigment	Cryptophytes
Carotene b	Pigment	Most algae
Chl a	Pigment	All photosynthetic algae
Chl b	Pigment	Euglenoids and green algae
Chl c	Pigment	Diatoms
Chlorophyllide a	Pigment	Chl a derivative
Diadinoxanthin	Pigment	Diatoms and euglenoids
Diatoxanthin	Pigment	Diatoms
Fucoxanthin	Pigment	Diatoms
Lutein	Pigment	Euglenoids and green algae

Chapter 4

Pigments	Type	Taxonomic association
Mg-2,4-divinyl pheoporphyrin	Pigment	Cryptophytes
Neoxanthin	Pigment	Euglenoids and green algae
Peridinin	Pigment	Dinoflagellates
Prasinoxanthin	Pigment	Prasinophytes
Zeaxanthin	Pigment	Most algae
Degradation products		
Pheophorbide a	Grazing product	Senescent diatoms
Pheophytin a	Decay product	Chl a derivative
Pheophytin b	Decay product	Chl b derivative

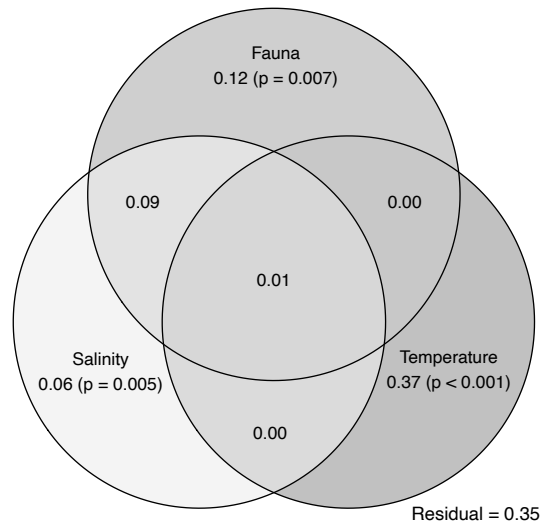
Appendix 4.2 Bioturbation type selection output from the bioturbation model with respective AIC fits per station per sample one and two

Station	Month	Bioturbation type sample 1	Bioturbation type sample 2
B	March	Non-local	Non-local
B	April	Non-local	Non-local
B	May	Non-local	Local
B	June	Local	Local
B	July	Non-local	Non-local
B	August	Non-local	Local
B	September	Non-local	Non-local
B	October	Local	Non-local
B	November	Local	Non-local
B	December	Non-local	Non-local
B	January	Non-local	Non-local
B	February	Non-local	Non-local
M	March	Non-local	Non-local
M	April	Non-local	Non-local
M	May	Non-local	Non-local
M	June	Local	Non-local
M	July	Local	Non-local
M	August	Non-local	Non-local
M	September	Non-local	Local
M	October	Local	Local
M	November	Non-local	Local
M	December	Non-local	Non-local
M	January	Non-local	Non-local
M	February	Non-local	Non-local

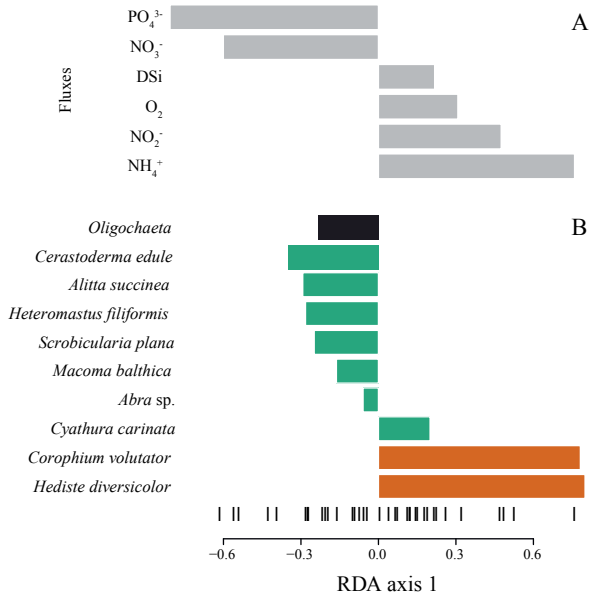


Appendix 4.3 Example of chl a profiles (points) and the fits (lines) obtained from the bioturbation analysis for the marine site. Model M2 indicates diffusive mixing with no non-local exchange, while models M3, M4 and M5 represent non-local bioturbation (Soetaert et al., 1996b). Each of the two samples collected monthly from March 2019 to February 2020 is respectively represented with grey or black.

Chapter 4



Appendix 4.4 Variation partitioning, Venn diagram representing the contribution of explanatory components to flux variance; values are adjusted- R^2 . Salinity, temperature, and fauna biomass density explain all together 65 % of total flux variance. Considered independently, each explanatory component has a significant effect on fluxes ($p < 0.05$) while controlling for the two other components (non-overlapping surface areas). Confounding effects (overlaps) have null or low effects.



Appendix 4.5 Redundancy analysis, first and only significant axis encompassing 59% of the total multivariate variance. (A) scores of fluxes and (B) scores of taxa. Bar lengths represent the contributions of the variables to the axis variance. Note that these contributions do not necessarily reflect the raw fluxes or organism biomass, instead they show the conditional pattern when controlling for salinity and temperature. Scores of same sign indicate that variables covary positively, and negatively when opposed. Bar colours correspond to the habitats where the taxa are the most abundant: black, freshwater; green, brackish; and orange, marine. Vertical segments at the bottom represent sample positions along the axis; there is no outlier driving the trend.

Chapter 4

Chapter 5 *Sediment resuspension enhances nutrient exchange in intertidal mudflats*

Dunia Rios-Yunes, Tim Grandjean, Alena di Primio, Justin Tiano, Tjeerd J. Bouma, Dick van Oevelen & Karline Soetaert

Published in *Frontiers in Marine Science* (2023); Special issue: Solute Transport and Transformation Across the Sediment-Water Interface in Coastal Ecosystems

doi: [10.3389/fmars.2023.1155386](https://doi.org/10.3389/fmars.2023.1155386)

5.1 Abstract

Intertidal coastal sediments are important centres for nutrient transformation, regeneration, and storage. Sediment resuspension, due to wave action or tidal currents, can induce nutrient release to the water column and fuel primary production. Storms and extreme weather events are expected to increase due to climate change in coastal areas, but little is known about their effect on nutrient release from coastal sediments. We have conducted *in-situ* sediment resuspension experiments, in which erosion was simulated by a stepwise increase in current velocities, while measuring nutrient uptake or release in field flumes positioned on intertidal areas of a tidal bay (Eastern Scheldt) and an estuary (Western Scheldt). In both systems, the water column concentration of ammonium (NH_4^+) and nitrite (NO_2^-) increased predictably with greater erosion as estimated from pore water dilution and erosion depth. In contrast, the phosphate (PO_4^{3-}) dynamics were different between systems, and those of nitrate (NO_3^-) were small and variable. Notably, sediment resuspension caused a decrease in the overlying water PO_4^{3-} concentration in the tidal bay, while an increase was observed in the estuarine sediments. Our observations showed that the concentration of PO_4^{3-} in the water column was more intensely affected by resuspension than that of NH_4^+ and NO_2^- . The present study highlights the differential effect of sediment resuspension on nutrient exchange in two contrasting tidal coastal environments.

5.2 Introduction

Intertidal sediments are centres of organic matter (OM) remineralization, nutrient recycling, transformation, and removal (Boynton et al., 2018; Lessin et al., 2018; Rios-Yunes et al., 2023b). Solute exchange between sediments and the water column is crucial for the functioning of coastal ecosystems as it affects the concentration of nutrients available for primary production. This exchange is generally caused by passive diffusion, bioturbation and bioirrigation (Aller, 1982; Braeckman et al., 2010; De Borger et al., 2020), or sediment resuspension from wave and tidal action (Cabrita et al., 1999; Tengberg et al., 2003; Kalnejais et al., 2010). It can also be triggered by human activities such as dredging and bottom trawling (Morin and Morse, 1999; Dounas et al., 2007; Tiano et al., 2021).

Sediment resuspension and coastal erosion are expected to increase due to climate change-related alterations of wind patterns as well as the magnitude and frequency of extreme weather events such as storms and hurricanes (Woth et al., 2006; Statham, 2012b; Chen et al., 2018; Niemistö and Lund-Hansen, 2019). During a resuspension event, nutrients and dissolved OM in the water column can adsorb onto resuspended sediment particles and decrease their concentration in the water column (Tengberg et al., 2003; Tiano et al., 2019). Alternatively, pore water nutrients, whose concentration in the sediment is typically higher than in the water column, may be released into the overlying water at the equivalent of several days of undisturbed fluxes (sum of diffusive and fauna-induced fluxes) (Tiano et al., 2021). An erosion event can also release OM previously stored in sediments resulting in an increase in bacterial mineralization in the water column and higher utilization of dissolved oxygen (DO) (Tengberg et al., 2003).

Enhanced nutrient concentrations in the water column (Kalnejais et al., 2010; Niemistö and Lund-Hansen, 2019; Tengberg et al., 2003) have been observed to harm coastal ecosystems worldwide (Malone and Newton, 2020). The list of detrimental effects includes harmful algal blooms, eutrophication, habitat loss, the disappearance of macrobenthic communities, coastal acidification, deoxygenation, and dead zones (Qin et al., 2004; Breitburg et al., 2018; Chen et al., 2018; Malone and Newton, 2020). Indeed, studies in lacustrine environments have reported eutrophic conditions and algal blooms following resuspension events (Ogilvie and Mitchell, 1998; Qin et al., 2004; Schallenberg and Burns, 2004; Dzialowski et al., 2008). Understanding how sediment resuspension affects nutrient release is important given the current worldwide challenges associated with nutrient dynamics and enrichment in coastal areas (Malone and Newton, 2020). This knowledge could aid eutrophication management efforts by identifying sediments which are sensitive to disturbance-induced nutrient release or areas important for nutrient storage. In addition, it could help identify areas whose nutrient storage capacity could be compromised by increased storm frequency.

Chapter 5

Shallow marine sediments and estuaries may be expected to react similarly to resuspension, however, relatively few studies have been conducted on the topic, and those that did, yielded inconsistent results (Morin and Morse, 1999; Chen et al., 2018; Niemistö and Lund-Hansen, 2019). Local abiotic conditions like salinity, grain size and the concentration and origin of OM in the sediment play an important role in determining the type of biogeochemical reactions occurring in coastal areas (Jordan et al., 2008; Loucaide et al., 2008; Rios-Yunes et al., 2023b). For example, phosphate sorption-desorption depends on salinity, but also on the concentration of DSi (Caraco et al., 1990; Jordan et al., 2008). Similarly, the concentration of OM and pore water nutrients is closely associated with smaller grain sizes (Precht et al., 2004). Therefore, the combination of these parameters may determine the extent of nutrient release in coastal sediments.

We measured nutrient exchange between the sediment and water column following experimentally induced erosion in intertidal sediments from the Western Scheldt estuary (WS) and the Eastern Scheldt (ES) tidal bay, The Netherlands. After extensive engineering, the ES became a tidal bay, while the WS remained an estuary (Smaal and Nienhuis, 1992). The Western Scheldt and Eastern Scheldt are therefore a good case study because they display contrasting biogeochemical characteristics and sediment dynamics despite sharing a similar geological origin (Smaal and Nienhuis, 1992; Jiang et al., 2019; Rios-Yunes et al., 2023b, 2023c). The aim of our study was to quantify instantaneous changes in nutrient concentration by causing sediment resuspension *in-situ*, and to determine its effects in the water column properties of two contrasting ecosystems: an estuary, and a tidal bay. We investigated sites along gradients of inundation time (high tidal zone and low tidal zone), salinity and grain size to define the biogeochemical differences amongst these systems and whether these differences influenced nutrient release due to erosion.

5.3 Methods

5.3.1 Study sites

5.3.1.1 Eastern Scheldt Tidal Bay

The Eastern Scheldt tidal bay is a former estuary in the southwest of The Netherlands (Figure 5.1). The ES has a storm surge barrier, constructed in 1986, that isolates it from tidal exchange with the North Sea only during severe storm conditions. River inflow into the Eastern Scheldt is controlled by multiple sluices resulting in a negligible input of freshwater and sediments ($4.3 \text{ m}^3 \text{ s}^{-1}$) and nearly constant salinity ($S = 30$) (Jiang et al., 2019). Currently, the Eastern Scheldt is a flush-dominated system ($\sim 2 \times 10^4 \text{ m}^3 \text{ s}^{-1}$ tidal exchange over a 12 h tidal cycle) with a decreasing gradient of chlorophyll *a* (chl *a*), nutrient concentrations, suspended sediment, and turbidity from the North Sea in the west to the

eastern section (Smaal and Nienhuis, 1992; Wetsteyn and Kromkamp, 1994; Jiang et al., 2019). The construction of the storm surge barrier and sluices triggered several alterations that ranged from geomorphological including the transformation from an estuary to a tidal bay, reduced sediment input, sand starvation, and constant erosion of intertidal areas (Smaal and Nienhuis, 1992; Nienhuis and Smaal, 1994; ten Brinke, 1994); to biological following the change of benthic species into a fully marine community (Ysebaert et al., 2016); and biogeochemical comprising the loss of the salinity gradient and decreased nutrient concentrations (Wetsteyn and Kromkamp, 1994).

5.3.1.1 Western Scheldt Estuary

The Western Scheldt is a typical funnel-shaped estuary with a longitudinal salinity gradient. The Scheldt River starts in France, runs through Belgium, and ends in The Netherlands. At the Dutch – Belgian border, the Scheldt River becomes wider and mixes with the saline water from the North Sea creating a brackish zone, to finally discharge into the North Sea (Soetaert et al., 1994b) (Figure 5.1). The salinity gradient in the brackish region is influenced by seasonal fluctuations in precipitation and riverine discharge (Baeyens et al., 1997; Struyf et al., 2004b; Soetaert et al., 2006). The Western Scheldt used to be a eutrophic system with water column anoxia, but the implementation of water quality policies since 1970's has improved the water quality (Soetaert et al., 2006; Rios-Yunes et al., 2023b).

5.3.2 Sampling sites

Eight intertidal mudflats were sampled (Figure 5.1), three in the Eastern Scheldt: Dortsman (DT), Rattekaai (RK) and Zandkreek (ZK), and five along the salinity gradient of the Western Scheldt: Appels (AP), Groot Buitenschoor (GBS), Riland (RL), Zuidgors (ZG) and Paulinapolder (PP). At each site, two locations were selected at 25 m (referred to as 'high tidal zone') and 200 m (referred to as 'low tidal zone') from the salt marsh edge, except for the narrow mudflats of Zandkreek (Eastern Scheldt) and Appels (Western Scheldt) where sampling was only done in the high tidal zone (Appendix 5.1). The sites exhibited a range of porosity and median grain sizes from muddy ($D_{50} 24.9 \pm 2.8 \mu\text{m}$) to sandy ($D_{50} 163.5 \pm 8.3 \mu\text{m}$) sediments (Table 5.1). Owing to its greater freshwater inputs, the Western Scheldt estuary generally has higher total dissolved inorganic nitrogen, phosphate and dissolved silica concentrations, though lower ammonium concentrations, than the Eastern Scheldt (Table 5.1).



Figure 5.1 Map of sampling locations indicated with red diamonds. In the Western Scheldt: Appels (AP) in the freshwater, Groot Buitenschoor (GBS) and Rilland (RL) in the brackish, and Zuidgors (ZG) and Paulinapolder (PP) in the marine part. In the Eastern Scheldt: Rattekaai (RK), Dortsman (DT) and Zandkreek (ZK). Coordinates are in Appendix 5.1

Table 5.1 Abiotic characteristics of the sediment (top 5 cm) and water column at the different sites of the Eastern Scheldt and Western Scheldt. Mean standard deviation of median sediment grain size (D50, μm), volumetric porosity (Por), and water-column salinity (S) and concentration of ammonium (NH_4^+), nitrite (NO_2^-), nitrate (NO_3^-), dissolved silicate (DSi) and phosphate (PO_4^{3-}) in mmol m^{-3} . Sites in the Western Scheldt are ordered from upstream to downstream. Numbers marked with a (') represent a significant difference (t-test, $p \leq .05$) between mean values in the WS and ES.

Site	S	High tidal zone D50 μm	Low tidal zone D50 μm	Por	NH_4^+	NO_2^-	NO_3^- mmol m^{-3}	DSi	PO_4^{3-}
Western Scheldt estuary									
AP*	1	24.9 \pm 2.8	-	0.8 \pm 0*	47.5 \pm 1.5	12.2 \pm 0.2	291.2 \pm 1.3	144.7 \pm 4.6	8.1 \pm 0.4
GBS	9	48.1 \pm 9.6	48.9 \pm 3.4	0.8 \pm 0.2	0.9 \pm 0.9	0.3 \pm 0	107.2 \pm 11.6	44.7 \pm 4.7	5.1 \pm 0.5
RL	13	133.1 \pm 7.8	163.5 \pm 8.3	0.5 \pm 0.1	1.3 \pm 0.6	1.5 \pm 0	93.9 \pm 0.8	46.2 \pm 0.6	5.2 \pm 0.1
ZG	30	62.2 \pm 8.2	51.7 \pm 6.8	0.7 \pm 0.1	9.6 \pm 1.8	1.9 \pm 0.1	28.1 \pm 2.5	29.9 \pm 14.4	2.6 \pm 0.5
PP	30	53.9 \pm 3	72.3 \pm 6.2	0.8 \pm 0.2	15.8 \pm 1.2	1.9 \pm 0.1	21 \pm 0.5	25.2 \pm 2.3	2.3 \pm 0.1
Mean					11.4 \pm 14.3	2.6 \pm 3.5	87.9 \pm 82.2	48.5 \pm 36.4	4.3 \pm 1.9
Eastern Scheldt tidal bay									
DT	30	122.7 \pm 8.3	116.8 \pm 1.5	0.5 \pm 0.1	1.9 \pm 1	0.2 \pm 0.1	28.3 \pm 1.9	18.4 \pm 1	2 \pm 0.1
RK	30	105 \pm 4.3	124.4 \pm 4.6	0.5 \pm 0.1	9.4 \pm 0.8	0.4 \pm 0	21.8 \pm 0.8	15.6 \pm 0.2	1.7 \pm 0.3
ZK'	30	83 \pm 5.2	-	0.7 \pm 0.1	0.5 \pm 0.3	0.5 \pm 0.5	30 \pm 7.2	25.7 \pm 0.3	1.8 \pm 0.6
Mean					4.3 \pm 4.1	0.3 \pm 0.3	26.3 \pm 4.7	19 \pm 3.9	1.9 \pm 0.3

* Porosity in Appels was >1 possibly caused by a sample manipulation error therefore porosity values from Rios-Yunes et al. (2023a) will be used instead

+ Sites AP and ZK were only sampled in the high tidal zone

5.3.3 Incubations and porewater extraction

Each station was visited once during low tide between August - October 2020. Sediment core samples were taken in triplicate for undisturbed nutrient exchange incubations (30 cm long cores, 15 cm inner diameter (\varnothing) filled with sediment to 50 % of the core), and for pore water extraction (30 cm long cores, 10 cm \varnothing). Water (10 L) was collected from nearby the site. All cores were immediately transported to the Royal Netherlands Institute for Sea Research (NIOZ) after collection. Undisturbed incubation cores were filled with the unfiltered ambient water, aerated, and kept in a thermostatic bath at ambient water temperature in a dark controlled-climate room until the next day to acclimatize. The next day, the overlying water was renewed by carefully adding it to each sediment core preventing resuspension, the aeration was stopped, and the cores were closed with a hermetic lid with a central stirring mechanism that ensured the water was continuously homogenized. After closing the cores, the oxygen (O_2) concentration in the overlying water was continuously measured with an oxygen optode (Firesting, Pyroscience). The O_2 measurements were stopped when the concentration reached 70% saturation (~ 6 - 7 h), after which lids were opened, and the overlying water was aerated to continue the incubation. Water samples (5-mL each) were filtered (Chromdis CA 0.45 μm , 25 mm, No. 250425) for analysis of dissolved inorganic nitrogen (NH_4^+ , NO_2^- , NO_3^-), dissolved silicate (DSi) and PO_4^{3-} and were taken at the start of the incubation, at the end of the respiration measurement (6 - 7 h), and after 23, 31 and 48 hours.

The pore water cores were processed immediately after arrival to the NIOZ. The cores were sliced every 0.5 cm from 0 to 3 cm and every 1 cm from 3 to 10 cm inside an anoxic glove bag. Half of each slice was transferred to a centrifuge filter tube with a basket (Chrom Tech, CTF-NYO45-03) fitted with a glass fibre filter (Whatman GF/F, 0.7 μm , 21 mm, WHA1825021). Pore water was extracted by centrifugation (10 min, 5000 rpm). Thereafter the samples were taken to an anoxic glove bag and an aliquot of 500 μL was obtained for NH_4^+ , NO_2^- , NO_3^- , and DSi; and one of 100 μL acidified with 10 μL of 1 M sulfuric acid (Merck, No. 100731) was used for PO_4^{3-} analysis.

5.3.4 Erosion experiment

Erosion experiments were conducted *in-situ* in triplicate at each location (high and low tidal zone) per site. A modified EROMES erosion chamber (37 cm long, 25 cm \varnothing , Appendix 5.2) with an open top and a rotating disc (Kalnejais et al., 2010) was placed on the sediment and inserted down to 15 cm in AP, and down to 10 cm in the other sites. Thereafter, water from the site was carefully added to avoid sediment resuspension. The chamber had a port for water sampling and another for a turbidity sensor which logged NTU values every 10 s (Turner Designs Cyclops 7F submersible sensor interfaced with a Turner Designs DataBank Handheld Datalogger) (Figure 5.2, Appendix 5.2). The turbidity sensor was

calibrated prior to the sampling with 3 calibration standards of 10, 100 and 1000 NTU and one blank following the manufacturer protocols (Turner Designs, n.d.). The rotating disc was calibrated in the laboratory with an Acoustic Doppler Velocimeter (ADV, Nortek Vectrino Profiler) to obtain near-bed flow velocity and shear stress as a function of rotation speed.

The experimental set-up for the erosion experiment and sample collection procedure for nutrients (NH_4^+ , NO_2^- , NO_3^- , DSi and PO_4^{3-}) and suspended sediments is shown in Figure 5.2. Initial water samples (nutrients and suspended sediments) were taken 2 min after the addition of water to account for any instantaneous release of nutrients that may have occurred upon the water addition. Then, the disc rotation was slowly increased until resuspension was detected with the turbidity sensor and erosion could be seen to occur across the entire surface of the core, i.e. the erosion threshold. From this point onwards, the rotation speed was incrementally increased until it was no longer possible to measure turbidity changes with the turbidity sensor, which typically happened at a maximum flow velocity between 0.175 m s^{-1} and 0.203 m s^{-1} . Each rotation speed was held for 17 min allowing for 2 min of stabilization after which three water nutrient samples (5 mL filtered with Chromdis CA filter $0.45 \mu\text{m}$, 25 mm, No. 250425; orange vials in Figure 5.2) were taken with a 5 min interval between them. The suspended sediments were sampled (40 mL) in the last interval (Figure 5.2, blue vial). Maximum erosion was determined when the SS concentration stabilized. Between three to five speed increments were imposed for each replicate. The range of imposed flow velocities was 0 m s^{-1} , 0.067 m s^{-1} , 0.106 m s^{-1} , 0.149 m s^{-1} , 0.175 m s^{-1} , and 0.203 m s^{-1} .

Chapter 5

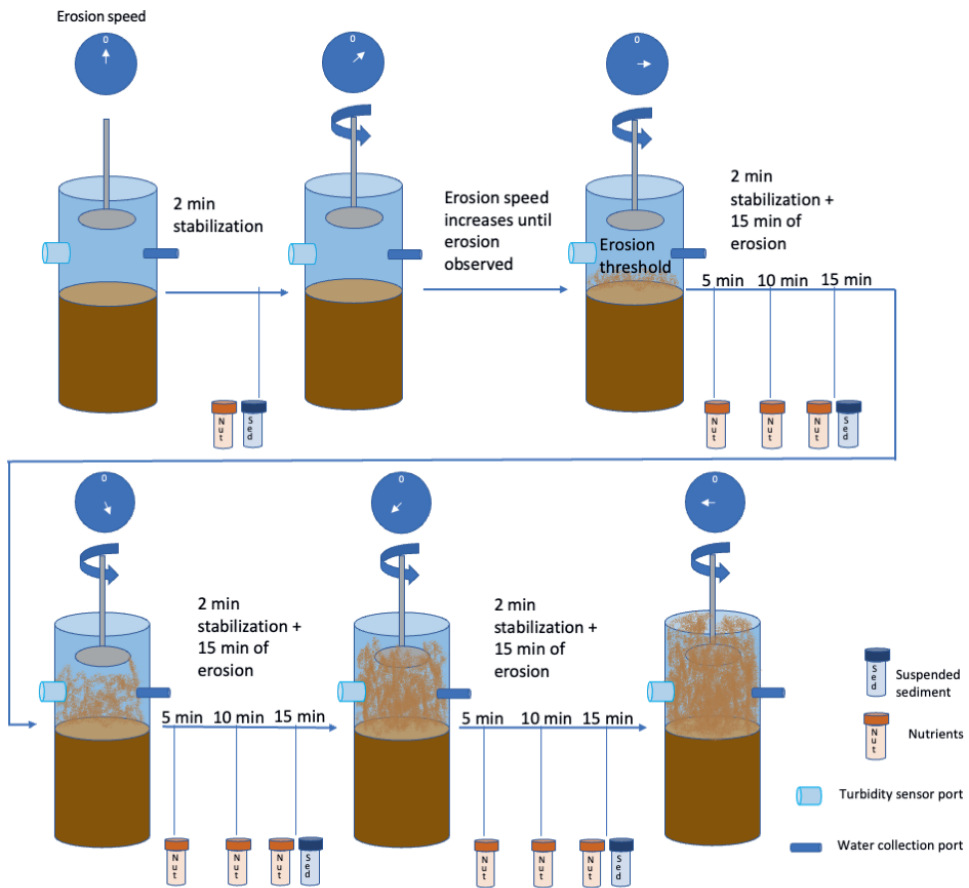


Figure 5.2 Scheme of nutrient and suspended sediment sampling procedure during the erosion experiment. Orange vials correspond with nutrient samples and blue vials to suspended sediment samples. Circles at the top represent increasing speed of the rotator.

5.3.5 Sample analysis

Nutrient samples from the incubations, pore water and erosion experiment were collected in 6 ml plastic vials and stored at -20°C until analysis with a Segmented Flow Analyzer (QuAatro39 AutoAnalyzer with XY-2 Sampler Autosampler, SEAL Analytical) (Jodo et al., 1992). Detection limits were: 0.05 mmol m^{-3} for NH_4^+ and DSi, 0.03 mmol m^{-3} for NO_2^- and PO_4^{3-} and 0.01 mmol m^{-3} for NO_3^- . Sediment-water exchange fluxes of O_2 and inorganic nutrients (NH_4^+ , NO_2^- , NO_3^- , DSi and PO_4^{3-}) were estimated by linear regression of the concentration (mmol m^{-3}) versus time (d). The slope of the regression was multiplied by the height of the overlying water column (m) to obtain the flux in $\text{mmol m}^{-2} \text{ d}^{-1}$. The concentration of suspended sediment was calculated by resuspending the suspended sediment samples and filtering 10 ml of the sample with a pre-weighed GF/F filter

(Whatman). Thereafter, the filters were dried for 48 h at 60° C and weighed. The weight difference was recorded as the suspended sediment weight. A regression between the discrete suspended sediment weight values and the NTU values from the turbidity sensor was made to calculate the suspended sediments concentration (SSC) during the experiment.

5.3.6 Statistical methods and data analysis

Linear models were used to test if sediment grain size or pore water nutrient concentrations could explain nutrient release by erosion. Statistical differences were detected with a t-test when the data distribution was normal, otherwise a Kruskal-Wallis test was used. Nutrient fluxes for each erosion speed were estimated by fitting a linear regression over the concentration versus time (5, 10, 15 minutes), and multiplying the slope of the regression by the height of the overlying water column. The thickness of eroded sediment (m) was calculated from the SSC as:

$$Erosion\ depth = \frac{sp * h}{\rho * (1 - \varphi)}$$

Where sp is the concentration of suspended particles (Kg m^{-3}), h is the height of the water column (m) inside the erosion chamber, ρ is the bulk density of the sediment defined as 2600 kg m^{-3} (Haan et al., 1994) and φ is the sediment porosity of the top 1 cm. From the eroded sediment depth, the total amount of pore water nutrients released into the water ($C_{erosion}$, mmol m^{-2}) was calculated as:

$$C_{erosion} = Concentration_{pw} * Erosion\ depth * \varphi \quad \text{Eq. 12}$$

Where $Concentration_{pw}$ is the concentration of pore water nutrients (mmol m^{-3}) in the top 1 cm of the sediment. The expected water column nutrient concentration (Nut_{exp} , mmol m^{-3}) due to nutrient release from sediment erosion (Eq. 12) and the undisturbed ambient nutrient flux at time t was calculated as:

$$Nut_{exp}(t) = Nut_{bw} + \frac{\int_0^t F_{release} dt + C_{erosion}(t)}{h + Erosion\ depth}$$

Where Nut_{bw} is the nutrient concentration in the water column at the start of the experiment (mmol m^{-3}), and the integral involving $F_{release}$ is the undisturbed nutrient flux (mmol m^{-2}) calculated from the sediment incubation over the duration (d) of the experiment.

Data analysis, visualization and statistical tests were done using R (R Core Team, 2020). Geospatial analysis was conducted with the program QGIS (QGIS Development Team, 2021).

5.4 Results

5.4.1 *Oxygen and nutrient fluxes from undisturbed sediments*

In general, all fluxes (O_2 , NH_4^+ , NO_2^- , NO_3^- , DSi and PO_4^{3-}) showed significant differences between high (_{high}) and low (_{low}) tidal zones (Appendix 5.3) except for RK in the Eastern Scheldt. The O_2 consumption rate in stations in the high tidal zone of the Western Scheldt increased from the freshwater site (AP) ($-42 \pm 5.1 \text{ mmol m}^{-2} \text{ d}^{-1}$) to the sandy brackish station (RL_{high}) ($-73.4 \pm 7.7 \text{ mmol m}^{-2} \text{ d}^{-1}$) and then decreased seawards (PP_{high} $-60.2 \pm 6.4 \text{ mmol m}^{-2} \text{ d}^{-1}$, Table 5.2). All stations except ZG_{high}, showed an efflux (directed out of the sediment) of NH_4^+ (0.8 ± 1.3 to $5.3 \pm 1 \text{ mmol m}^{-2} \text{ d}^{-1}$) and an influx of NO_3^- (-1 ± 0.2 to $-4.6 \pm 0.2 \text{ mmol m}^{-2} \text{ d}^{-1}$, Table 5.2). The freshwater site exhibited an influx of PO_4^{3-} ($-0.2 \pm 0.1 \text{ mmol m}^{-2} \text{ d}^{-1}$) and DSi ($-0.2 \pm 0.2 \text{ mmol m}^{-2} \text{ d}^{-1}$) that became an efflux in the brackish and marine parts of the Western Scheldt. In the low tidal zone O_2 consumption was higher in marine ($> -61.4 \pm 7.5 \text{ mmol m}^{-2} \text{ d}^{-1}$, PP_{low}) than in brackish stations (GBS_{low} and RL_{low}). All stations in the low tidal zone, apart from ZG_{low}, exhibited an influx of NO_3^- that ranged between -0.9 ± 0.1 and $-3.4 \pm 0.3 \text{ mmol m}^{-2} \text{ d}^{-1}$ (Table 5.2). Similarly, an efflux of DSi was observed in all stations (max. $6.5 \pm 0.8 \text{ mmol m}^{-2} \text{ d}^{-1}$, ZG_{low}) except for RL_{low}.

Overall, the flux of PO_4^{3-} in the freshwater site was significantly different from the other sites; and it was the only significantly different flux between the fresh and brackish sites (Appendix 5.4). Fluxes at the brackish sites, GBS and RL, did not differ significantly. However, the flux of NO_3^- and DSi was significantly different between fresh and brackish sites and the marine sites (Appendix 5.4).

In the Eastern Scheldt, the muddy station ZK_{high} had the highest O_2 consumption ($-55.6 \pm 3.45 \text{ mmol m}^{-2} \text{ d}^{-1}$), and the sandy DT_{low} the lowest ($-23.2 \pm 2.8 \text{ mmol m}^{-2} \text{ d}^{-1}$) (Table 5.2). All stations in the Eastern Scheldt tidal bay had an efflux of NH_4^+ which was highest in RK_{high} (max $3.7 \pm 0.7 \text{ mmol m}^{-2} \text{ d}^{-1}$), and an influx of NO_3^- that was greatest in ZK ($-1.4 \pm 0.4 \text{ mmol m}^{-2} \text{ d}^{-1}$). Sandy sites (DT and RK_{high}) exhibited an influx of DSi, while muddy ZK an efflux ($2.5 \pm 0.2 \text{ mmol m}^{-2} \text{ d}^{-1}$). All stations except RK_{high} had an influx of PO_4^{3-} . The flux of NH_4^+ was significantly different between RK and DT (Appendix 5.4). The muddy site ZK exhibited significantly different fluxes of NO_3^- to DT, and DSi to DT and RK.

Between systems, oxygen consumption rates, the efflux of DSi, and the influx of NO_3^- were significantly higher (t-test, $p \leq .05$, Appendix 5.5) in the Western Scheldt (all sites) than in the Eastern Scheldt. Phosphate flux was significantly different (t-test, $p \leq .05$) in the Eastern

Scheldt (net influx) and the WS (net efflux). In contrast, fluxes of NH_4^+ and NO_2^- were not significantly different between systems. Comparing only the marine Western Scheldt sites (ZG and PP) with the Eastern Scheldt, the significant differences in O_2 , NO_3^- , DSi and PO_4^{3-} fluxes were retained (t-test, $p \leq .05$, Appendix 5.6).

Table 5.2 Mean \pm standard deviation of oxygen and nutrient fluxes ($\text{mmol m}^{-2} \text{d}^{-1}$) at the high and low tidal zone locations of the different sites in the Western and Eastern Scheldt. Sites in the Western Scheldt are ordered from upstream to downstream. A negative sign (-) indicates an influx and a positive (+) sign an efflux from the sediment into the water column.

Location	Site	O ₂	NH ₄ ⁺	NO ₂ ⁻	NO ₃ ⁻	DSi	PO ₄ ³⁻
Western Scheldt estuary							
High tidal zone	AP	-42 \pm 5.1	2.6 \pm 0.2	0.1 \pm 0	-4 \pm 0.3	-0.2 \pm 0.2	-0.2 \pm 0.1
	GBS	-49.4 \pm 7.1	0.8 \pm 1.3	0 \pm 0	-2.7 \pm 0.9	2 \pm 0.8	0.2 \pm 0.1
	RL	-73.4 \pm 7.7	3.8 \pm 0.8	0.2 \pm 0	-4.6 \pm 0.2	4.2 \pm 0.7	0.2 \pm 0
	ZG	-68.4 \pm 5.4	-0.1 \pm 0.2	-0.1 \pm 0	0 \pm 1.2	5.2 \pm 0.2	0.1 \pm 0.1
Low tidal zone	PP	-60.2 \pm 6.4	4 \pm 0.3	0.2 \pm 0.1	-1 \pm 0.2	4.9 \pm 0.3	0 \pm 0
	AP	-	-	-	-	-	-
	GBS	-35.8 \pm 11.4	1.4 \pm 0.4	0.1 \pm 0.1	-3.4 \pm 0.3	1.6 \pm 0.7	0.1 \pm 0
	RL	-33.7 \pm 10.9	1.2 \pm 0.7	0 \pm 0	-3 \pm 0.7	-0.7 \pm 0.3	0 \pm 0
Eastern Scheldt tidal bay	ZG	-83.3 \pm 7.4	2.3 \pm 0.5	0 \pm 0	0.9 \pm 0.6	6.5 \pm 0.8	0.1 \pm 0
	PP	-61.4 \pm 7.5	5.3 \pm 1	0.3 \pm 0.1	-0.9 \pm 0.1	4.2 \pm 0.6	0 \pm 0
	DT	-34 \pm 8.4	2.6 \pm 1	0.1 \pm 0	-0.8 \pm 0.4	-0.1 \pm 0.1	-0.1 \pm 0
	RK	-28.3 \pm 0.7	3.7 \pm 0.7	0 \pm 0	-0.7 \pm 0.1	-0.5 \pm 0.1	0 \pm 0
High tidal zone	ZK	-55.6 \pm 3.5	2.4 \pm 0.4	0 \pm 0	-1.4 \pm 0.4	2.5 \pm 0.2	0 \pm 0.1
	DT	-23.2 \pm 2.8	1.1 \pm 0.8	0 \pm 0	-0.5 \pm 0.2	-0.2 \pm 0.1	-0.1 \pm 0
	RK	-35 \pm 2.6	3.3 \pm 0.3	0 \pm 0	-1 \pm 0.1	0.1 \pm 0	0 \pm 0
	ZK	-	-	-	-	-	-

5.4.2 Pore water nutrients

In all pore water profiles, the concentration of NH_4^+ was lowest in the surface 0-1 cm and increased with sediment depth, while the concentration of NO_2^- and NO_3^- was high near the surface and decreased with depth (Figure 5.3 A, B, C, F, G, H, K, L, M, P, Q, R, U, V and W). Most sites of the Western Scheldt showed comparable concentrations of NH_4^+ and NO_2^- except for the freshwater site which had the highest concentration of NH_4^+ (up to 1000 mmol m^{-3}) and NO_2^- , and RL_{low} with the lowest concentration of NH_4^+ . The concentration of NO_3^- in the Western Scheldt sediments varied more between sites and locations, with the highest (ZG_{high}) and the lowest (ZG_{low}) concentrations occurring in the marine section. DSi increased with depth and was similar at all stations, except for RL_{high} which was significantly lower (Wilcoxon rank sum test, $p \leq .05$, Figure 5.3 D, I, N, S and X). In the low tidal zone, the highest concentration of DSi was observed in ZG_{low} and GBS_{low} , and the lowest in RL_{low} . Phosphate concentrations did not exhibit a consistent trend with sediment depth, but the Western Scheldt locations of AP , GBS_{low} , ZG_{high} , and $\text{PP}_{\text{high and low}}$ had subsurface peaks below 2 cm. Overall, the pore water concentration of NH_4^+ and PO_4^{3-} decreased from the fresh to the brackish and the marine parts of the estuary while the concentration of NO_3^- increased.

In the Eastern Scheldt, ammonium also increased with sediment depth with the highest concentration observed in the sandy site RK_{high} and the lowest at RK_{low} (Figure 5.3 AE). NO_3^- was highest in DT_{high} and lowest in RK_{low} (Figure 5.3 AB and AG). The highest concentration of DSi and PO_4^{3-} was observed in RK_{high} reaching over 500 and 300 mmol m^{-3} , respectively. No correlation was found between pore water nutrient concentration and grain size except for DSi ($p \leq .05$, $R^2 = 0.87$) and PO_4^{3-} ($p \leq .05$, $R^2 = 0.67$) in the low tidal zone.

Chapter 5

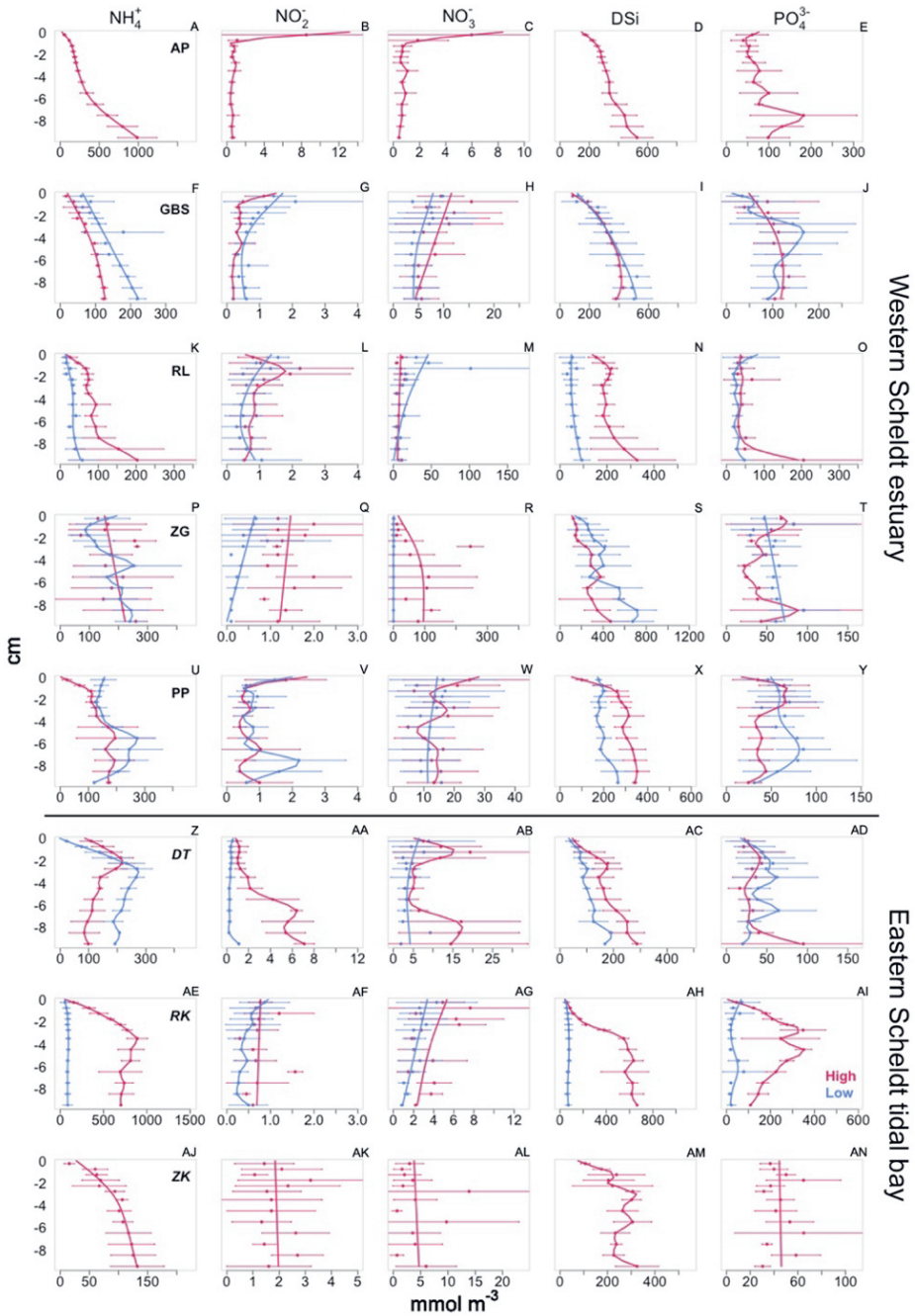


Figure 5.3 Pore water profiles from the high (red) and low (blue) tidal zone from the Western (A to Y) and Eastern Scheldt (W to AN) sites. Dots and horizontal lines represent mean \pm standard deviation of pore water concentration. Vertical line is a smoothed spline. Western Scheldt site are ordered from upstream to downstream. Notice differences in x axis scales.

5.4.3 Sediment resuspension and solute release

A small amount of sediment particles in suspension was visually observed at the beginning of the erosion experiment at all sites, however, this minor resuspension was too low to influence the critical erosion threshold (Appendix 5.7). The freshwater site exhibited the lowest erosion threshold speed ($\leq 0.067 \text{ m s}^{-1}$), while for all other sites the threshold speed fluctuated between 0.106 and 0.149 m s^{-1} . Once the erosion threshold was exceeded, the concentration of suspended particles increased with increasing velocity until the SSC stabilized (Figure 5.4A). However, in the freshwater site the SSC seemed to plateau faster than in other stations like RL and DT where the concentration stabilized towards the end of the experiment (Figure 5.4C and G). In all other stations the SSC increased steadily during the erosion experiment. The SSC and erosion depth observed at the highest erosion speed differed between sites and went from as little as 0.62 Kg m^{-3} , corresponding to 0.25 mm erosion in GBS₂₀₀ (0.203 m s^{-1}) to as much as 33.85 Kg m^{-3} with an erosion depth of 6.1 mm in RL_{high} (0.175 m s^{-1}) (Appendix 5.7).

The erosion of sediments induced nutrient release in most sites, except for PO_4^{3-} in the Eastern Scheldt. In the WS, the freshwater site AP, showed an increase in concentration (blue dots in Figure 5.4 I and Q) of NH_4^+ , NO_2^- that was twice as high as the estimated increase due to release of pore water caused by erosion (grey columns), but for PO_4^{3-} the expected concentration was closer to the observed increase (Figure 5.4Y). In other WS sites (ZG_{high}, and PP_{low}), the observed concentration of NH_4^+ and that of PO_4^{3-} for GBS_{high} and low, RL_{high} and PP_{high} and low was higher than expected from pore water release, while the concentration of NH_4^+ in RL_{high}, ZG_{low} and PP_{high} and PO_4^{3-} in ZG_{low} matched the predicted release from pore water dilution (Figure 5.4).

In the Eastern Scheldt, the observed increase in concentration of NH_4^+ and NO_2^- closely matched the predicted concentrations due to release from pore water nutrients in DT_{high} (grey bars in Figure 5.4 N and V). In contrast, the release of NH_4^+ in DT_{low} and ZK_{high} was lower than predicted by pore water dilution (grey bars in Figure 5.4 AD and O). The locations RK_{high} and low exhibited a sharp increase in the concentration of NH_4^+ and NO_2^- during erosion which was several times higher than expected by pore water release only. Changes in the water column concentration of PO_4^{3-} in the Eastern Scheldt showed an interesting pattern with the concentration sharply decreasing with erosion at all sites and following the opposite direction of the release expected from pore water dilution (Figure 5.4 AD, AE, AF, BC, and BD). No correlation was found between nutrient release and grain size.

Chapter 5

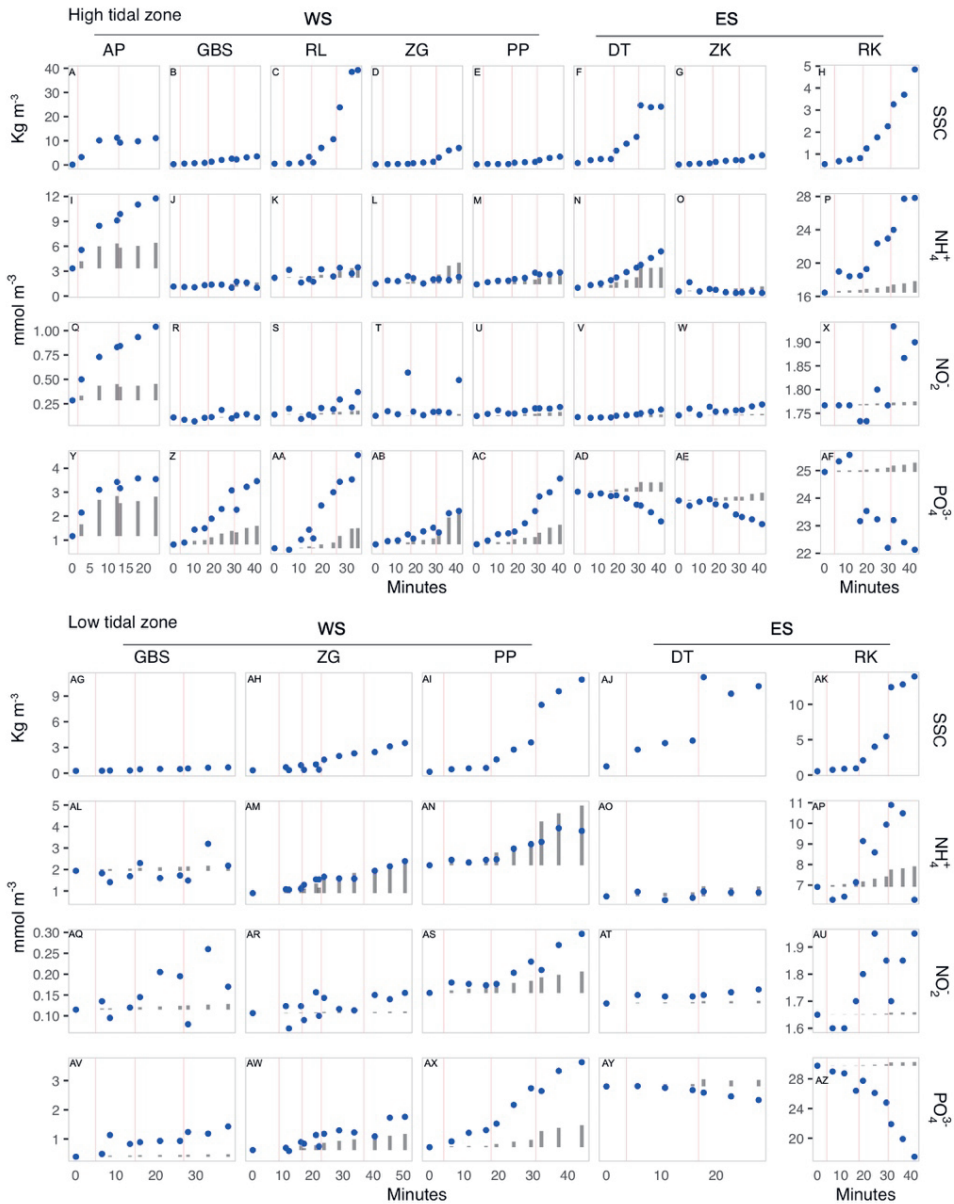


Figure 5.4 Nutrient release and suspended sediment concentration (SSC) changes due to sediment erosion over time in the high (A to AF) and low (AG to AZ) tidal zone locations of the Eastern (ES) and Western Scheldt (WS). All nutrient concentrations expressed in mmol m⁻³. Suspended sediments concentration in Kg m⁻³. Blue dots denote measured nutrient concentrations during the erosion experiment. Grey bars indicate the bottom water concentration at the beginning of the experiment (t₀) plus the predicted increase in concentration solely from dilution of pore water nutrients from the eroded layer of top sediments, as calculated from the suspended particles concentration. Red lines indicate the

moments at which the speed was increased during the experiment. Western Scheldt sites AP, GBS, RL, ZG, and PP are ordered from upstream to downstream sites.

A comparison was made between the undisturbed and the erosion fluxes of NH_4^+ , NO_2^- and PO_4^{3-} to determine the contribution of sediment erosion to the overall nutrient fluxes (Figure 5.5). Sediment erosion had an additive effect on the undisturbed flux when both the undisturbed and the erosion fluxes were an efflux or an influx. In those instances, an hour of erosion fluxes was equivalent to several days of undisturbed PO_4^{3-} , NO_2^- and NH_4^+ fluxes in 93%, 69% and 19% of cases, respectively (Appendix 5.8). Other cases showed an inversion in the direction of the erosion fluxes compared to the undisturbed fluxes. In those instances, an hour of sediment resuspension counterbalanced at least a day of undisturbed fluxes in 95%, 55% and 20% of cases for PO_4^{3-} , NO_2^- and NH_4^+ , respectively (Appendix 5.8).

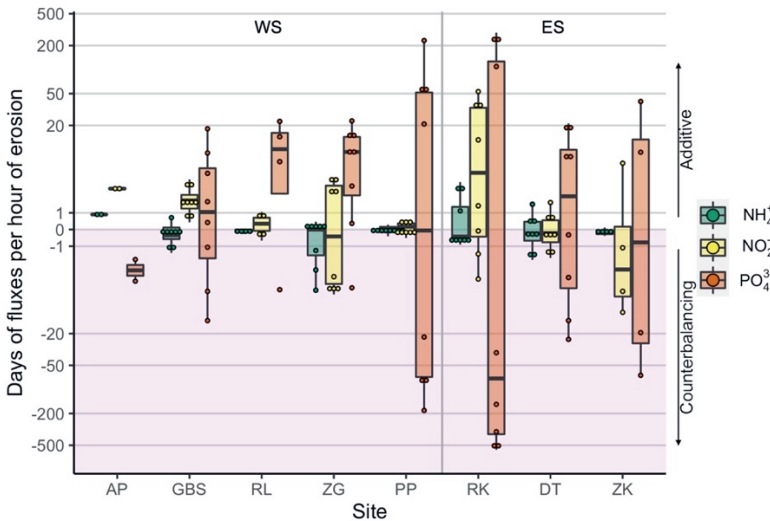


Figure 5.5 Equivalence of one hour of erosion to days of undisturbed fluxes. All replicates of both the high and the low water line locations are pooled together by nutrient per site. The additive effect of erosion on the undisturbed fluxes is shown in the white area with positive values, while the cases with a counterbalancing effect are depicted in the shaded area with negative values. Vertical line separates between WS sites arranged from fresh to marine salinities and sites in the ES. Notice the logarithmic scale in the y axis.

5.5 Discussion

Our results show a differential response to sediment resuspension and nutrient release of adjacent coastal systems. The nutrients ammonium and nitrite responded predictably to sediment erosion by increasing their concentration in both systems. In contrast, the concentration of phosphate increased with nutrient erosion in the estuarine system, but

not in the tidal bay where it decreased. The concentration of nitrate appeared to be unaltered by sediment erosion.

5.5.1 *Physicochemical characteristics*

The WS exhibits the typical characteristics of an “estuarine filter” with a decrease in the concentration of nutrients in the water column from the freshwater area to the mouth (Table 5.1). This gradient has been well documented (Middelburg and Nieuwenhuize, 2000; Soetaert et al., 2006; Rios-Yunes et al., 2023b) and results from the dilution of land runoff in riverine water with seawater (Gilbert et al., 2007), biogeochemical transformations along the estuary (e.g. sorption, denitrification, etc.) (Soetaert et al., 2006; Rios-Yunes et al., 2023b) and uptake by both marine and terrestrial (e.g. adjacent reed marshes) primary producers (Struyf et al., 2005b; Arndt et al., 2009). The Eastern Scheldt is, in contrast, a tidal bay with a single connection with the North Sea via the storm surge barrier. This unilateral tidal exchange though this inlet is reported to cause decreasing concentrations of nutrients and increased water retention towards the eastern section (Jiang et al., 2019). However, we were not able to detect this gradient based on our results.

5.5.2 *Sediment oxygen consumption and undisturbed nutrient fluxes*

Sediment oxygen consumption and nutrient fluxes are indicative of the activity and nature of the biogeochemical processes occurring within the sediment such as OM mineralization, respiration, and primary production. The 'undisturbed' fluxes were measured to determine the activity of the sediment and to compare them with the nutrient fluxes observed during the erosion experiment. Fluxes can be detected as an influx when processes (or organisms) within the sediments consume substances from the water column that are not produced in the sediment, such as oxygen, or when organisms utilize the totality of nutrients released during mineralization plus some nutrients from the water column. Alternatively, an efflux is observed when nutrients released from sedimentary OM mineralization are not entirely consumed by benthic processes but rather escape to the water column via diffusion, bioturbation, and bio-irrigation.

The increase in O₂ consumption along the salinity gradient of the Western Scheldt (Table 5.2) may result from increasing rates of oxygen consuming processes like aerobic respiration and nitrification from fresh to marine areas, as well as changes in the macrofaunal community (Ysebaert et al., 1993; Mestdagh et al., 2020). Nutrient retention also changes through the estuary with freshwater sediments acting as a sink of PO₄³⁻, which is significantly different to all other sites (Appendix 5.4). Similarly, brackish sediments, and to a lesser extent freshwater sediments, exhibit an important influx of NO₃⁻ implying high rates of denitrification (Table 5.2). Nitrogen dynamics in the fresh and brackish areas are different to marine sites (Appendix 5.4). These results are consistent

with a recent analysis of Western Scheldt sediments by Rios-Yunes et al. (2023a), where freshwater sediments were recognized as a sink of phosphate facilitated by sorption to sediments; and brackish sediments were a sink of nitrogen due to enhanced denitrification.

In the Eastern Scheldt, the muddy site of ZK showed the highest oxygen consumption rates, and likely also had higher denitrification rates compared to the other ES sites, as evidenced by the prevalent influx of NO_3^- (Table 5.2). The lower O_2 consumption and smaller fluxes of NO_3^- observed in DT and RK (Table 5.2) may have resulted from their coarser grain sizes that facilitated tidal flushing of OM, limiting mineralization and nitrification (Precht et al., 2004). The influx of NO_3^- in DT was significantly lower than in ZK (Appendix 5.4) suggesting that nitrification may have been lowest in this site.

A comparison of Eastern Scheldt (all sites) and WS (ZG and PP) sites evidenced significantly higher O_2 consumption in the Western Scheldt (Appendix 5.6, t-test, $p \leq 0.05$). Both systems receive autochthonous input from phytoplankton and, from the more dominant, microphytobenthos production, but the Western Scheldt also has a permanent influx of allochthonous OM from rivers and the North Sea which contributes to the supply of OM thereby fuelling higher mineralization rates (mean $68.3 \text{ mmol m}^{-2} \text{ d}^{-1}$). In contrast, the Eastern Scheldt has a small net input of OM from the North Sea, longer residence times, and intense OM grazing in areas with a high biomass of filter-feeders (Jiang et al., 2020b), which results in lower benthic O_2 consumption in the intertidal sites (mean $35.2 \text{ mmol m}^{-2} \text{ d}^{-1}$, Appendix 5.6).

In estuaries, phosphate sorption decreases with increasing salinity and generally, an efflux of phosphate from the sediment is observed in brackish and marine areas (Table 5.2) (Jordan et al., 2008; Rios-Yunes et al., 2023b). The flux of PO_4^{3-} is also influenced by the concentration of phosphate in the water column; the pore water concentration of N, DSi, and sulphur as well as by an interplay between rates of sulphate reduction and concentration, or turnover, of iron oxides (FeOOH) (Caraco et al., 1990; Slomp et al., 1996; Jordan et al., 2008). The significantly different (t-test, $p \leq .05$) PO_4^{3-} fluxes between the marine Eastern Scheldt ($-0.04 \text{ mmol m}^{-2} \text{ d}^{-1}$) and marine sites (PP and ZG) in the Western Scheldt ($0.05 \text{ mmol m}^{-2} \text{ d}^{-1}$, Appendix 5.5) could not have been attributed to the effect of salinity. It was similarly unlikely that the disparities in fluxes were related to differences in concentration of PO_4^{3-} in the water column (Western Scheldt 2.4 mmol m^{-3} and Eastern Scheldt 1.9 mmol m^{-3} , $p \leq .05$; Appendix 5.6), or in the pore water of the upper cm of the sediment (58.8 mmol m^{-3} in the Western Scheldt and 56.0 mmol m^{-3} in the Eastern Scheldt, $p = 0.2$, Appendix 5.5), given the small differences. It is, however, possible that the observed differences are associated with physicochemical processes in the sediment such as sorption-desorption (Jordan et al., 2008), but we are unable to provide a conclusion based on the available data. It is noteworthy that these observations were obtained in the summer-autumn, so it is possible that the dynamics would be different in other seasons.

5.5.3 *Pore water nutrients*

The remineralization of OM releases nutrients (e.g. NH_4^+ , DSi, and PO_4^{3-}) that can be transformed and stored within the sediment or released into the water column (Slomp et al., 1996; Herbert, 1999; Struyf et al., 2005b; Jordan et al., 2008). In the Western Scheldt, the fresh water (AP) and brackish (GBS) sites are within the vicinity of *Phragmites australis* reed marshes which are known to store biogenic silicate (BSi) in the form of phytoliths (Struyf et al., 2005b). The observed accumulation of DSi at depth (Figure 5.3) could be associated with the transfer and burial of reed OM from the marsh to the mudflat and subsequent dissolution of BSi (Struyf et al., 2005b). The decrease in pore water concentration of NH_4^+ and the increase of NO_3^- from the fresh to the brackish and the marine parts of the Western Scheldt estuary (Figure 5.3) may be related to the deeper penetration of oxygen in coarser sediments that promotes nitrification.

In contrast, the decreasing pore water concentration of PO_4^{3-} with increasing salinity is most likely associated with the differential sorption of phosphate to oxidized iron and sediment particles along salinity gradients (Jordan et al., 2008), but it could also be influenced by the presence of silicates, ammonium, iron, and oxygen (Caraco et al., 1990; Tengberg et al., 2003; Morgan et al., 2012), as well as the composition of the sediment particles (Borggaard, 1983). Similar observations on the concentration of pore water nutrients the Western Scheldt have been reported by Rios-Yunes et al. (2023a). It is noteworthy that the WS receives runoff from heavily farmed areas (Gilbert et al., 2007), so it is possible that the high porewater nutrient concentration in upstream sediments could also be associated with the historical accumulation of nutrients from land runoff (Shaughnessy et al., 2019). We are unaware of any existing data reporting on this.

In the Eastern Scheldt, the concentration of NH_4^+ and PO_4^{3-} increases steadily up to ~ 3 cm depth. This may be related to a deeper oxygen penetration depth that promotes OM mineralization within the top 3 cm, possibly facilitated by tidal flushing (Precht et al., 2004) or by bioturbation and bioirrigation (De Borger et al., 2020) in these sites. The low pore water nutrient concentrations observed in RL_{low} (Western Scheldt) and RK_{low} (Eastern Scheldt) may be associated with their coarse sediment grain size as this would allow tidal flushing of solutes (Precht et al., 2004).

5.5.4 *Nutrient release by erosion*

The differences in critical erosion threshold between sites are mostly associated with the intrinsic characteristics of the sediment (e.g. density, grain size, clay and organic matter content etc.) (Shrestha et al., 2001; Tang et al., 2020), but also with the presence of microphytobenthos that can stabilize surface sediment particles by excreting exopolymeric substances (Paterson et al., 2018), and with bioturbation which can

destabilize the sediment matrix (Widdows et al., 2000c, 2000b; Li et al., 2017). Nevertheless, the values obtained in our study were within values observed in other macrotidal systems like the Ems-Dollard, NL (between 0.1 and 0.6 N m⁻²) (Kornman and Deckere, 1998; Dyer et al., 2000), but lower than those of, for example, the Humber estuary, UK (~0.4 N m⁻²) (Amos et al., 1998).

Our field observations revealed that sediment resuspension in muddy sediments happened quickly when the upper unconsolidated layer was eroded. However, the resuspension plateaued with an increasing shear stress speed that failed to erode the consolidated sediment layer at greater depth. The freshwater site of AP in the Western Scheldt is characterized by an unconsolidated sediment layer on the sediment surface. This layer was easily eroded as evidenced by the low critical erosion speed needed to initiate erosion (0.067 m s⁻¹) and the rapid stabilization of the SSC (Figure 5.4). Different to muddier sediments, sites with coarser grain sizes, e.g. RL and DT, produced the highest concentration of suspended sediments (Appendix 5.7). In such sites, sediment resuspension continued until plateauing at higher erosion speeds (Figure 5.4). This stabilization likely occurred because the maximum concentration of particles in suspension was reached, and particle sedimentation was in balance with sediment erosion.

As sediments erode, dissolved solutes in pore water and sediment particles mix into the overlying water changing the concentration of dissolved nutrients NH₄⁺, NO₂⁻ and PO₄³⁻ (Figure 5.4). An increase in nutrient concentrations in the water column may not only indicate a release of pore water nutrients, but also desorption of nutrients. A decrease in concentration is likely associated with the uptake of water column nutrients by sorption to suspended sediment particles or to other nutrients (Kalnejais et al., 2010; Morgan et al., 2012). It could also be caused by biological uptake, but this is unlikely to have occurred in our experiment since its duration was about 1 hour and thus changes caused by biological uptake would have been negligible.

Changes in the concentration of nutrients began slowly but increased with the speed of erosion and the duration of resuspension treatments. This was expected since pore water nutrients were being released, but also because the added particles in the water column had sufficient time to desorb nutrients, similar to findings from Niemistö and Lund-Hansen (2019). Moreover, changes in nutrient concentrations continued despite the apparent stabilization of the SSC (AP, DT, RL in Figure 5.4) further supporting the suggestion that suspension time is a more important factor for nutrient desorption than the number of particles.

In most sites, the nutrient concentration measured in the water column was greater than the expected pore water release from erosion (Figure 5.4). The difference between measured and expected concentration of the different nutrients is likely caused by reactions with the solid phase (i.e. desorption) (Falcão and Vale, 1995; Cabrita et al., 1999;

Chapter 5

Morin and Morse, 1999; Kalnejais et al., 2010; Morgan et al., 2012; Chen et al., 2018). The mismatch between expected input from pore water nutrients release and changes in the overlying water concentration (Figure 5.4) could also be the result of pore water entrainment from deeper layers of the sediment. Nevertheless, this seems implausible. First, because the sediments were rather muddy (except in sandy RL) with low permeability and porewater advection (Precht et al., 2004), and second, because previous reports have not found significant differences in pore water profiles before and after erosion events in fine-grained sediments (Kalnejais et al., 2010).

Changes in the overlying water concentration of ammonium and nitrate have been associated with ammonium oxidation (Niemistö et al., 2018). However, this process was observed after several hours of resuspension and caused the simultaneous increase of nitrates and decrease of NH_4^+ (Niemistö et al., 2018). In our case, it is unlikely that significant ammonium oxidation occurred in the erosion experiment because the duration of each erosion run was shorter than needed for the oxidation reaction to strongly affect ammonium or nitrate concentrations. Nevertheless, if there had been oxidation of NH_4^+ to NO_3^- it is possible we may not have detected it due to the high concentration of NO_3^- in the water column (Table 5.1) compared to pore waters in the surface (Figure 5.3). Other processes that gain relevance over longer periods of sediment resuspension and contribute to nitrogen transformation include ion-exchange reactions, and slow desorption processes (Kalnejais et al., 2010; Niemistö and Lund-Hansen, 2019) as well as biological uptake.

A surprising observation was the differential behaviour of PO_4^{3-} between the Western Scheldt and Eastern Scheldt during the erosion experiment (Figure 5.4). In the Western Scheldt, phosphate was released with increasing erosion speed, at all stations, likely due to pore water addition to the water column combined with desorption. Similar increases in PO_4^{3-} concentration attributed to desorption have been observed in North Sea subtidal sediments (Couceiro et al., 2013), the Boston Harbour, US (Kalnejais et al., 2010) and the Peel-Harvey Estuary, Aus. (Morgan et al., 2012). In contrast, sediment erosion decreased the concentration of phosphate in the water column of ES sites, therefore highlighting sediment resuspension as a possibly important process for PO_4^{3-} removal in this system. A decrease in phosphate with erosion has also been observed in North Sea sediments (Tiano et al., 2021), the Baltic Sea (Tengberg et al., 2003; Niemistö et al., 2018) and Great Bay estuary, US (Percuoco et al., 2015).

The differences in release or sorption of phosphate between the Western Scheldt and the Eastern Scheldt (Figure 5.4) are unlikely to be determined by the origin of their sediments since both systems have a similar geological history. Likewise, salinity can be ignored since the different phosphate dynamics were observed in sites with marine salinities. It is, however, possible that differences in, for example, iron oxide concentration may be the cause. Unfortunately, based on available data it is not possible to confidently determine the source of the different phosphate dynamics due to erosion.

The concentration of NO_3^- and DSi in the overlying water was one to two orders of magnitude higher than in pore waters in the top 1 cm of the sediment. Therefore, it is possible that the high concentrations in the water column masked the dilution of pore water nutrients appearing unaltered by increasing sediment erosion. Our results contrast with studies reporting an increase in overlying water concentrations of NO_3^- and DSi upon sediment resuspension in systems like the Boston harbour, US (Kalnejais et al., 2010), the North Sea (Couceiro et al., 2013) and the Baltic Sea (Niemistö and Lund-Hansen, 2019), but also in the ES (Tiano et al., 2021). The disparity in DSi release between our study and that of Tiano et al. (2021) may result from their resuspension of 3 cm versus the 2 to 6 mm (Appendix 5.6) obtained in our erosion study.

No changes in DSi were detected by solely investigating fluctuations in the overlying water nutrient concentration. Nevertheless, it is possible that an erosion disturbance of > 2 cm depth like those previously reported in the Western Scheldt and Eastern Scheldt (de Vet et al., 2020) may cause DSi release as observed by Tiano et al. (2021) and possibly change the concentration of DSi in the overlying water.

5.5.5 *Relevance of erosion mediated nutrient release*

An erosion event can have an additive or counterbalancing effect on undisturbed nutrient fluxes as was evidenced by the comparison between undisturbed and erosion fluxes (Appendix 5.8). In both the additive and counterbalancing cases, however, the effects of resuspension obtained for PO_4^{3-} were one, and in for example PP and RK, up to three orders of magnitude higher than for NO_2^- and NH_4^+ (Figure 5.5). The larger effects on PO_4^{3-} release from resuspension were observed in PP and RK and are unlikely to be related to grain size characteristics as there was no correlation found between grain size and nutrient release. Instead, they are probably due to a lower exposure to wave action, as both sites are in a sheltered position from the prevailing southwestern wind (de Vet et al., 2020), and/or to the high stability of these sediments as evidenced by their low long-term and daily fluctuations in bed level (Appendix 5.9). It is therefore plausible that the reduced frequency of resuspension events allows for the accumulation of pore water nutrients. These accumulated nutrients can subsequently be exchanged in case of a resuspension event; a similar observation has been reported by Abril et al. (1999). In this respect, it is likely that an erosion event would translate in greater nutrient exchange in sheltered sediments than in exposed areas where sediment resuspension and nutrient exchange are more regular. Moreover, the first erosion event is expected to cause a greater exchange than subsequent ones because each event would mobilize the nutrients stored since the last resuspension event.

The results obtained in the Eastern Scheldt sites DT and ZK can be compared with those of Tiano et al. (2021), who performed similar experiments at these sites. Our results coincide on the overall additive effect of erosion on undisturbed NH_4^+ fluxes in DT and

Chapter 5

ZK, however, they observed a greater effect of erosion on this flux, possibly due to a difference in methodology as they resuspended down to 3 cm depth. Regarding PO_4^{3-} , our observations also agree in that sediment resuspension had an additive effect on the influxes in DT and a counterbalancing one in ZK, however, these effects were higher in our experiment.

The relevance and magnitude of a storm event on intertidal areas erosion would depend on the wind direction and speed (de Vet et al., 2020) as they determine which areas are directly exposed to wave and wind action; the different hydrodynamic forces (Yang et al., 2003) together with duration and period of the tidal cycle (Green and Coco, 2014; de Vet et al., 2020) since they control the intensity of erosion and concentrate the effects of a storm in a certain area; and on the depth of the eroded layer. Other important aspects to be considered are seasonality (Bancon-Montigny et al., 2019) as well as precipitation and run off (Chen et al., 2018) because annual fluctuations may alter the effect of an erosion event; and land use of the surrounding area (Gilbert et al., 2007) as this would greatly affect the concentration of nutrients in terrestrial runoff.

The range of shear stress used in the erosion experiment (0.023 to 0.159 N m^{-2}) was within values observed to cause shallow water sediment resuspension (0.02 to 0.07 N m^{-2}) (Qin et al., 2004; Tang et al., 2020) and to naturally occur in spring tides and storms (0.11 to 0.28 N m^{-2}) (Kalnejais et al., 2007; Percuoco et al., 2015). Nevertheless, our shear stress values were lower than observed for wind dominated flow velocities in the Western Scheldt and Eastern Scheldt ($1.6 - 7 \text{ N m}^{-2}$) (de Vet et al., 2020).

The maximum sediment erosion depth of 6 mm obtained from our experiment (Appendix 5.6) was comparable to values from other studies (Kalnejais et al., 2010; Percuoco et al., 2015), and it was a higher than the daily bed level fluctuations observed in most locations (Appendix 5.9). However, it is noteworthy that a major storm event could erode between 2-3 cm (datasets mentioned in Hu et al. [2021]) to as much as 20 cm of mudflat sediments (Yang et al., 2003; de Vet et al., 2020). This means that our experiment did not recreate a major storm event, but it caused greater erosion than observed from daily fluctuations. Notwithstanding, it is likely that our measurements underestimate the potential nutrient exchange that could occur during a wind dominated erosion event in the Eastern Scheldt and WS because the imposed shear stress was lower than what could naturally occur in these systems (de Vet et al., 2020) and the maximum erosion depth was shallower than observed during major storm events (Hu et al., 2021). Despite this limitation, our results provide a first indication of differences in nutrient release between contrasting coastal systems and sites with different exposure.

To conclude, different nutrient exchange responses to sediment resuspension were detected in adjacent coastal systems with contrasting morphology, but also between sites with varied exposure to wave action. The magnitude of these exchanges generally increased with erosion speed and the duration of the disturbance. For instance,

ammonium and nitrite release could be explained by erosion depth and pore water concentration. In contrast, phosphate release was much higher than predicted by erosion depth and porewater concentration at all estuarine sites, and it was even removed from the overlying water in the tidal bay stations. An erosion nutrient flux can be positive (i.e. additive) or negative (i.e. counterbalancing) compared to the undisturbed flux and comparable to several days of undisturbed fluxes. On this note, local characteristics of the site, such as exposure to wave action, were decisive for the magnitude of this effect with sheltered sites exhibiting a greater contribution in days of fluxes than exposed sites. We have demonstrated that sediment resuspension has the potential to alter the concentration of nutrients in the water column. This information could be used to assess whether algal blooms could occur following an intertidal sediments resuspension event.

5.6 Acknowledgements

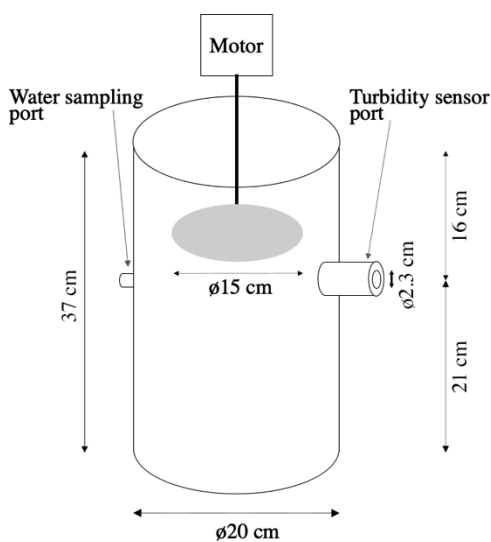
We would like to thank the students Ivory Maast and Zono Heidemans for helping with the collection and processing of samples for this study. This work could not have been done without the help of the NIOZ analytical lab (Peter van Breugel, Yvonne Maas, Jan Peene, Jurian Brasser and more) which processed our sediment and water samples.

5.7 Appendix

Appendix 5.1 Sampling locations coordinates. Sites Appels and Zandkreek were only sampled in the high tidal zone. Elevation (elev.) above normal Amsterdam level (NAP).

	High tidal zone	Elev. (m)	Low tidal zone	Elev. (m)	Tidal range (m)
Western Scheldt estuary					
Appels	51.048320 N, 4.069340 E	-0.8	-	-	3
Groot Buitenschoor	51.3642058 N, 4.2464467 E	1.9	51.3637679 N, 4.2440356 E	0.7	4.5
Rilland	51.3970722 N, 4.1630143 E	1.7	51.395658 N, 4.1636237 E	1.2	4.5
Zuidgors	51.3869205 N, 3.8247581 E	1.8	51.3853995 N, 3.8237443 E	1.2	4
Paulinapolder	51.3510113 N, 3.7200606 E	0.8	51.3522441 N, 3.7217453 E	0.4	4
Eastern Scheldt tidal bay					
Dortsman	51.5650906 N, 4.0267081 E	1.3	51.5640437 N, 4.0248895 E	0.9	3
Ratekaai	51.4411493 N, 4.1738345 E	1.6	51.4421134 N, 4.1716691 E	0.8	3
Zandkreek	51.55298 N, 3.8728884 E	1.0	-	-	3

Appendix 5.2 Diagram of erosion chamber



Appendix 5.3 t-test of significant differences between fluxes measured at high and low tidal zones. Sites Appels and Zandkreek are not included since no samples were collected in the low tidal zone.

Site	Flux mmol m ⁻² d ⁻¹	t statistic	p value
Western Scheldt estuary			
GBS	O ₂	-3.94	<i>p</i> < .05
	PO ₄ ³⁻	-2.87	<i>p</i> < .05
	NO ₃ ⁻	-2.95	<i>p</i> < .05
	NO ₂ ⁻	-2.87	<i>p</i> < .05
	NH ₄ ⁺	-2.85	<i>p</i> < .05
	DSi	-2.83	<i>p</i> < .05
RL	O ₂	-4.12	<i>p</i> < .05
	PO ₄ ³⁻	-2.87	<i>p</i> < .05
	NO ₃ ⁻	-2.97	<i>p</i> < .05
	NO ₂ ⁻	-2.87	<i>p</i> < .05
	NH ₄ ⁺	-2.81	<i>p</i> < .05
	DSi	-2.83	<i>p</i> < .05
ZG	O ₂	-4.79	<i>p</i> < .05
	PO ₄ ³⁻	-2.87	<i>p</i> < .05
	NO ₃ ⁻	-2.86	<i>p</i> < .05
	NO ₂ ⁻	-2.88	<i>p</i> < .05
	NH ₄ ⁺	-2.85	<i>p</i> < .05
	DSi	-2.73	<i>p</i> < .05
PP	O ₂	-4.42	<i>p</i> < .05
	PO ₄ ³⁻	-2.87	<i>p</i> < .05
	NO ₃ ⁻	-2.90	<i>p</i> < .05
	NO ₂ ⁻	-2.87	<i>p</i> < .05
	NH ₄ ⁺	-2.76	<i>p</i> < .05
	DSi	-2.76	<i>p</i> < .05
Eastern Scheldt tidal bay			
RK	O ₂	-2.94	<i>p</i> < .05
	PO ₄ ³⁻	-2.22	0.09
	NO ₃ ⁻	-2.23	0.09
	NO ₂ ⁻	-2.22	0.09
	NH ₄ ⁺	-2.13	0.10
	DSi	-2.22	0.09
DT	O ₂	-3.59	<i>p</i> < .05
	PO ₄ ³⁻	-2.88	<i>p</i> < .05
	NO ₃ ⁻	-2.89	<i>p</i> < .05
	NO ₂ ⁻	-2.87	<i>p</i> < .05
	NH ₄ ⁺	-2.83	<i>p</i> < .05
	DSi	-2.88	<i>p</i> < .05

Appendix 5.4 Significant differences in fluxes between sites, both tidal zones considered per site. "x" indicates significant differences.

	AP GBS	AP RL	AP ZG	AP PP	GBS RL	GBS ZG	GBS PP	RL ZG	RL PP	ZG PP	DT ZK	DT RK	RK ZK
O ₂	-	-	x	-	-	-	-	x	-	-	x	-	x
NH ₄ ⁺	-	-	-	-	-	-	x	-	x	x	-	x	-
NO ₃ ⁻	-	-	x	x	-	x	x	x	x	x	x	-	-
NO ₂ ⁻	-	-	-	-	-	-	x	-	x	x	x	-	-
PO ₄ ³⁻	x	x	x	x	-	-	-	-	-	-	-	-	-
DSi	-	-	x	x	-	x	x	x	x	-	x	-	x

Chapter 5

Appendix 5.5 Mean natural fluxes of all sites in the Eastern Scheldt (ES) and Western Scheldt (WS) and significant differences test. All fluxes were tested with a t-test except DSi due to non-normality of its distribution.

Fluxes	WS	ES	statistic	p value	method
O ₂	56.42±17.29	35.21±12.34	4.43	$p \leq .05$	t-test
NH ₄ ⁺	2.4±1.8	2.6±1.1	0.37	0.71	t-test
NO ₂ ⁻	0.1±0.1	0±0	-1.77	0.09	t-test
NO ₃ ⁻	-2.1±1.9	-0.9±0.4	3.23	$p \leq .05$	t-test
DSi	3.1±2.5	0.4±1.2	8.98	$p \leq .05$	Kruskal-Wallis rank sum test
PO ₄ ³⁻	0.05±0.1	-0.04±0.05	-3.17	$p \leq .05$	t-test

Appendix 5.6 Comparison of mean natural nutrient fluxes, bottom water, and pore water (top 1 cm) nutrient concentration in marine sites of the Western Scheldt (ZG and PP) and sites in the Eastern Scheldt. Statistical differences were determined with a t-test (Welch two sample) for parametric data and with a Kruskal-Wallis rank sum test for non-parametric data.

	WS (ZG and PP)	ES	t statistic	p value	Method	
Fluxes (mmol m ⁻² d ⁻¹)	O ₂	-68.3	-35.2	7.14	$p < .05$	t-test
	NH ₄ ⁺	2.9	2.6	-0.48	0.64	t-test
	NO ₂ ⁻	0.1	0.0	-1.37	0.2	t-test
	NO ₃ ⁻	-0.3	-0.9*	-4.67	$p < .05$	t-test
	DIN	2.7	1.7	-2.65	0.15	t-test
	PO ₄ ³⁻	0.05	-0.04	-4.17	$p < .05$	t-test
	DSi	5.2	0.4	18.6	$p < .05$	Kruskal-Wallis rank sum test
Bottom water (mmol m ⁻³)	NH ₄ ⁺	12.7	4.3	14.9	$p < .05$	Kruskal-Wallis rank sum test
	NO ₂ ⁻	1.9	0.3	18.7	$p < .05$	Kruskal-Wallis rank sum test
	NO ₃ ⁻	24.5	26.3	2.1	0.15	Kruskal-Wallis rank sum test
	DIN	39.1	30.9	14.5	$p < .05$	Kruskal-Wallis rank sum test
	PO ₄ ³⁻	2.4	1.9	17.4	$p < .05$	Kruskal-Wallis rank sum test
	DSi	27.6	19.0	10.2	$p < .05$	Kruskal-Wallis rank sum test
Pore water (mmol m ⁻³)	NH ₄ ⁺	116.5	104.3	1.6	0.2	Kruskal-Wallis rank sum test
	NO ₂ ⁻	1.1	0.9	-0.7	0.5	t-test
	NO ₃ ⁻	10.9	5.7	-1.6	0.1	t-test
	DIN	129.5	110.9	2.7	0.1	Kruskal-Wallis rank sum test
	PO ₄ ³⁻	58.8	45	-1.3	0.2	t-test
DSi	172.1	75.7	-6.6	$p < .05$	t-test	

Appendix 5.7 Erosion threshold (ET) speed (m s⁻¹), maximum erosion speed (MS; m s⁻¹) and equivalent pressure (P; N m⁻²) with corresponding mean suspended sediment concentration (SSC) (Kg m⁻³) and millimetres of sediment erosion per location per site. The low tidal zone location from site RL is not included since it was not possible to conduct the experiment due to the sediment properties. Sites of the Western Scheldt are ordered from upstream to downstream. Sites of the Eastern Scheldt are indicated in italics.

Site	High tidal zone					Low tidal zone			
	ET m s ⁻¹	MS m s ⁻¹	P N m ⁻²	SSC Kg m ⁻³	Erosion depth mm	MS m s ⁻¹	P N m ⁻²	SSC Kg m ⁻³	Erosion depth mm
Western Scheldt estuary									
AP	0.067	0.106	0.045	10.04	3.09				
GBS	0.149	0.203	0.159	2.98	1.67	0.203	0.159	0.62	0.25
RL	0.106	0.175	0.133	33.85	6.1				
ZG	0.106	0.175	0.133	5.37	2.28	0.203	0.159	3.03	1.25
PP	0.149	0.203	0.159	2.76	2.03	0.203	0.159	9.49	2.60
Eastern Scheldt tidal bay									
DT	0.149	0.203	0.159	24.22	4.66	0.175	0.133	10.21	2.05
RK	0.106	0.175	0.133	3.93	0.82	0.175	0.133	13.07	2.56
ZK	0.149	0.203	0.159	3.10	1.19				

Appendix 5.8 Erosion fluxes, natural fluxes, and equivalence of erosion fluxes to natural fluxes in hours for each site and nutrient in the high and low tidal zone. Negative equivalences indicate a reversal of the flux direction.

Site	Nut	Location	Velocity m s ⁻¹	Erosion fluxes mmol m ⁻² h ⁻¹	Undisturbed fluxes mmol m ⁻² d ⁻¹	Days of fluxes in 1 hour of erosion	
Western Scheldt estuary							
AP	NH ₄ ⁺	High	0.067	2.32	2.6	0.89	
			0.106	2.32	2.6	0.89	
	NO ₂ ⁻	High	0.067	0.26	0.08	3.05	
			0.106	0.24	0.08	2.83	
	PO ₄ ³⁻	High	0.067	0.95	-0.23	-4.2	
			0.106	0.44	-0.23	-1.95	
	GBS	NH ₄ ⁺	High	0.106	0.2	0.85	0.24
				0.149	-0.16	0.85	-0.19
		NH ₄ ⁺	High	0.175	-0.38	0.85	-0.45
				0.203	-0.62	0.85	-0.73
NH ₄ ⁺		Low	0.106	-2.09	1.43	-1.46	
			0.149	-0.72	1.43	-0.5	
NH ₄ ⁺		Low	0.175	0.11	1.43	0.08	
			0.203	1	1.43	0.7	
NO ₂ ⁻		High	0.106	-0.09	-0.02	3.99	
			0.149	-0.06	-0.02	2.8	
NO ₂ ⁻	High	0.175	-0.05	-0.02	2.08		
		0.203	-0.03	-0.02	1.3		
NO ₂ ⁻	Low	0.106	0.04	0.1	0.42		
		0.149	0.12	0.1	1.21		
NO ₂ ⁻	Low	0.175	0.17	0.1	1.69		
		0.203	0.22	0.1	2.2		
PO ₄ ³⁻	High	0.106	-2.47	0.18	-13.72		

Chapter 5

Site	Nut	Location	Velocity m s ⁻¹	Erosion fluxes mmol m ⁻² h ⁻¹	Undisturbed fluxes mmol m ⁻² d ⁻¹	Days of fluxes in 1 hour of erosion
			0.149	0.07	0.18	0.41
			0.175	1.61	0.18	8.95
			0.203	3.27	0.18	18.15
			0.106	-0.52	0.09	-5.77
		Low	0.149	-0.1	0.09	-1.07
			0.175	0.16	0.09	1.78
			0.203	0.44	0.09	4.85
			0.106	-1	3.84	-0.26
	NH ₄ ⁺		0.149	-0.46	3.84	-0.12
			0.175	-0.13	3.84	-0.03
			0.203	0.23	3.84	0.06
			0.106	-0.12	0.19	-0.65
RL	NO ₂ ⁻	High	0.149	0.02	0.19	0.11
			0.175	0.11	0.19	0.57
			0.203	0.2	0.19	1.06
			0.106	-1.14	0.21	-5.48
	PO ₄ ³⁻		0.149	1.44	0.21	6.92
			0.175	3	0.21	14.41
			0.203	4.67	0.21	22.48
			0.106	0.64	-0.12	-5.57
		High	0.149	0.33	-0.12	-2.9
			0.175	0.15	-0.12	-1.28
	NH ₄ ⁺		0.203	-0.05	-0.12	0.46
			0.106	-0.22	2.33	-0.1
		Low	0.149	0.19	2.33	0.08
			0.175	0.44	2.33	0.19
			0.203	0.72	2.33	0.31
			0.106	0.53	-0.08	-6.34
		High	0.149	0.43	-0.08	-5.14
			0.175	0.37	-0.08	-4.42
			0.203	0.3	-0.08	-3.64
ZG	NO ₂ ⁻		0.106	0.03	0.01	2.22
		Low	0.149	0.05	0.01	3.13
			0.175	0.05	0.01	3.67
			0.203	0.06	0.01	4.26
			0.106	0.03	0.09	0.35
		High	0.149	0.93	0.09	10.3
			0.175	1.47	0.09	16.31
			0.203	2.06	0.09	22.79
			0.106	-0.34	0.07	-5.17
	PO ₄ ³⁻	Low	0.149	0.21	0.07	3.21
			0.175	0.55	0.07	8.28
			0.203	0.91	0.07	13.73
			0.106	-1.05	3.99	-0.26
		High	0.149	-0.08	3.99	-0.02
			0.175	0.5	3.99	0.13
			0.203	1.13	3.99	0.28
			0.106	-2.12	5.35	-0.4
PP	NH ₄ ⁺	Low	0.149	-0.64	5.35	-0.12
			0.175	0.26	5.35	0.05

Sediment resuspension

Site	Nut	Location	Velocity m s ⁻¹	Erosion fluxes mmol m ⁻² h ⁻¹	Undisturbed fluxes mmol m ⁻² d ⁻¹	Days of fluxes in 1 hour of erosion
			0.203	1.23	5.35	0.23
			0.106	-0.02	0.19	-0.13
		High	0.149	0.03	0.19	0.16
			0.175	0.06	0.19	0.33
	NO ₂ ⁻		0.203	0.1	0.19	0.52
			0.106	-0.15	0.31	-0.5
		Low	0.149	-0.03	0.31	-0.09
			0.175	0.05	0.31	0.16
			0.203	0.13	0.31	0.43
			0.106	-3.41	0.04	-93
		High	0.149	-0.81	0.04	-22.06
			0.175	0.76	0.04	20.83
	PO ₄ ³⁻		0.203	2.46	0.04	67.03
			0.106	-2.79	-0.01	231.35
		Low	0.149	-0.57	-0.01	47.54
			0.175	0.77	-0.01	-63.6
			0.203	2.21	-0.01	-183.29
Eastern Scheldt tidal bay						
			0.106	-3.3	3.69	-0.89
		High	0.149	4.16	3.69	1.13
			0.175	8.67	3.69	2.35
	NH ₄ ⁺		0.203	13.53	3.69	3.66
			0.106	-1.16	3.26	-0.35
		Low	0.149	-1.5	3.26	-0.46
			0.175	-1.7	3.26	-0.52
			0.203	-1.93	3.26	-0.59
			0.106	-0.19	0.05	-3.92
		High	0.149	-0.07	0.05	-1.53
			0.175	0	0.05	-0.08
	NO ₂ ⁻		0.203	0.07	0.05	1.48
			0.106	0.13	0.01	13.15
		Low	0.149	0.32	0.01	30.87
			0.175	0.43	0.01	41.58
			0.203	0.54	0.01	53.12
			0.106	-1.03	0.01	-153.59
		High	0.149	-2.27	0.01	-338.44
			0.175	-3.02	0.01	-450.2
	PO ₄ ³⁻		0.203	-3.83	0.01	-570.57
			0.106	1.71	-0.05	-34.74
		Low	0.149	-5.38	-0.05	109.34
			0.175	-9.67	-0.05	196.46
			0.203	-14.29	-0.05	290.28
			0.106	-5.15	2.6	-1.98
		High	0.149	-1.04	2.6	-0.4
			0.175	1.45	2.6	0.56
	NH ₄ ⁺		0.203	4.12	2.6	1.59
			0.106	-1.32	1.1	-1.2
		Low	0.149	-0.53	1.1	-0.48
			0.175	-0.05	1.1	-0.05

Chapter 5

Site	Nut	Location	Velocity m s ⁻¹	Erosion fluxes mmol m ⁻² h ⁻¹	Undisturbed fluxes mmol m ⁻² d ⁻¹	Days of fluxes in 1 hour of erosion
			0.203	0.46	1.1	0.42
			0.106	-0.06	0.09	-0.67
		High	0.149	0.04	0.09	0.39
			0.175	0.1	0.09	1.03
	NO ₂ ⁻		0.203	0.16	0.09	1.72
			0.106	-0.07	0.04	-1.83
		Low	0.149	-0.04	0.04	-0.99
			0.175	-0.02	0.04	-0.49
			0.203	0	0.04	0.06
			0.106	1.52	-0.06	-23.63
		High	0.149	0.24	-0.06	-3.73
			0.175	-0.53	-0.06	8.3
	PO ₄ ³⁻		0.203	-1.37	-0.06	21.25
			0.106	0.96	-0.07	-13.69
		Low	0.149	0.02	-0.07	-0.31
			0.175	-0.55	-0.07	7.78
			0.203	-1.16	-0.07	16.49
			0.106	0.29	2.37	0.12
	NH ₄ ⁺		0.149	-0.23	2.37	-0.1
			0.175	-0.54	2.37	-0.23
			0.203	-0.88	2.37	-0.37
			0.106	-0.04	-0.01	6.6
ZK	NO ₂ ⁻	High	0.149	0.01	-0.01	-1.1
			0.175	0.04	-0.01	-5.76
			0.203	0.07	-0.01	-10.78
			0.106	1.7	-0.03	-66.69
	PO ₄ ³⁻		0.149	0.5	-0.03	-19.42
			0.175	-0.23	-0.03	9.16

Appendix 5.9 Daily bed-level elevation data measured with acoustic surface elevation dynamic (SED) sensors at all sites, except ZK and AP. Local sediment dynamics were derived from the bed-level data by obtaining surface elevation variance (Z_{var}) and average daily elevation change (δZ_{avg}) values. High values of Z_{var} are indicative of large, long-term (seasonal) changes in the tidal flat elevation, while low values of δZ_{avg} imply limited short-term (daily) changes in the bed-level. For further information refer to the work of Grandjean et al. (2022).


Site	Location	Z_{var}	δZ_{avg} (mm / day)
GBS	High	61	10
	Low	276	6
RL	High	186	28
	Low	227	48
ZG	High	90	4
	Low	1405	15
PP	High	147	5
	Low	319	7
DT	High	4	3
	Low	134	21
RK	High	56	1
	Low	60	1

Appendix A How do estuaries improve water quality?

Adapted from: Annual biogeochemical cycling in intertidal sediments of a restored estuary reveals dependence of N, P, C and Si cycles to temperature and water column properties

Dunia Rios-Yunes; Justin C. Tiano; Dick van Oevelen; Jeroen van Dalen & Karline Soetaert


Published in Science Journal for Kids (2023)



**ENVIRONMENTAL
SCIENCE
JOURNAL
FOR
KIDS**

JUNE 2023

How do estuaries improve water quality?



Authors:
Dunia Rios-Yunes, Justin Tiano,
Dick van Oevelen and others

Associate Editors:
Elitsa Panayotova and
Alexandra Appleton

Abstract

Estuaries are very special. They act like a natural filter that helps clean the water before it enters the ocean. But we don't fully understand how this works and how the processes change throughout the year. So, for a whole year we took samples from various sites along the Western Scheldt estuary. It's a restored estuary that used to be very polluted. The samples were taken from freshwater, marine water, and brackish water. We analyzed them for several nutrients. We wanted to check how the concentration of nutrients changes in different seasons. Thankfully, our results show that the Western Scheldt estuary is healthy! We discovered that each section of water works differently as a filter. We also found out that temperature is a very important factor in how they work.


Introduction

Do you know what an estuary is? It's where the river meets the ocean. It's very special because fresh water mixes with salty marine water. This creates a unique environment where many different organisms can live. **A lot of estuaries help clean the water by trapping pollutants and excess nutrients.** Just like natural filters! This is why it's very important to protect them.

But many estuaries are in danger. We change their habitats when building dams. We also pollute the land and the water we use. When we grow crops, we increase the amounts of nutrients that go into estuaries. This may sound good, but it actually leads to **eutrophication**. Small plants called algae thrive when there are too many nutrients. They grow very quickly and cover the surface of the water. When they die, they fall to the bottom and start to decompose. This takes a lot of oxygen! But when this happens there is not enough oxygen for other plants and animals, so they get sick or die. And climate change affects these ecosystems, too.

Many countries have started to restore estuaries. This may include controlling the nutrients from farms, creating new habitats, or removing dams. **We wanted to see if these**

measures helped to improve the water quality. We also wanted to find out how a restored estuary works. What processes occur there? Do they change in different seasons? How does the salt in the water impact them?



The Western Scheldt estuary in the Netherlands.
Photo: Dunia Rios-Yunes

More free science education resources at www.ScienceJournalForKids.org 1

Methods

To answer these questions, we took samples from the **Western Scheldt estuary** (Fig. 1). It used to be very polluted, but several countries have worked to restore it. The river starts in France, flows through Belgium and the Netherlands, and finally meets the North Sea. The estuary is like a funnel: narrow at the beginning and wider at the end. We took samples for a whole year from different sites:

- where the water is fresh,
- where the water is mostly saltwater (marine), and
- where the water is a mix of fresh and saltwater. This is called **brackish water**.

We took samples from the water and also from the **sediment** on the estuary shore. We **incubated** part of the samples to simulate real-life conditions. We looked for various chemical compounds like **ammonium, nitrates, nitrites, and phosphates**. These nutrients are vital for many plants and animals. We wanted to know what amount of nutrients the sediment exchanges (takes in or releases).

Results

The salinity of the water stayed the same throughout the year at all sites. But the **temperature changed with the seasons**. The concentration of most of the nutrients depended on these temperature changes. The salinity also affected the nutrients' concentrations. For example, ammonium in the freshwater was high in the winter. But in the marine water, it was high during the summer. Oxygen **exchange rates** were highest in the summer, especially at the marine site. Overall, the concentration of nutrients was much higher in the freshwater. Then it started to decrease towards the ocean.

So how do sediments exchange various nutrients at these different sites? On average each year:

Where are the highest oxygen exchange rates?

Figure 2: Exchange rates of oxygen, nitrogen, and phosphorus in the marine, brackish, and freshwater sites. Upward-pointed arrows indicate the nutrients released by the sediment, while downward-pointed arrows indicate the nutrients taken in by the sediment.

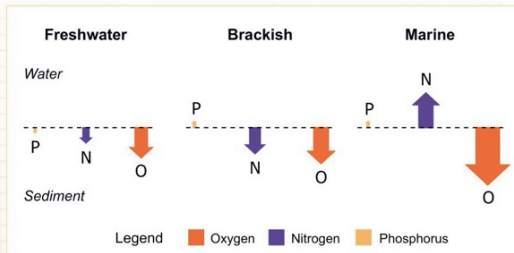
We tested the water's **salinity** (how salty it was) at each site during each month of the year. We also measured the temperature and oxygen levels each month.



Figure 1: Taking sediment samples from the brackish site of the estuary's shore.
Photo: Pieter van Rijswijk

- the freshwater site took in more nitrogen and phosphorus than it released;
- the brackish site took in more nitrogen but released more phosphorus;
- the marine site released more nitrogen and phosphorus than it took in (Fig. 2).

The sediments at the marine and brackish sites were great at **remobilizing** carbon! Plus, sediments removed 11% of the total nitrogen that had entered the estuary. They also removed 15% of the phosphorus.





Discussion

The estuary restoration efforts have been worth it! The estuary used to be very polluted, but now there is no eutrophication. The oxygen levels are not low, either. But what happens at each site of the estuary?

The river washes down water rich in pollutants, nutrients, and **organic matter**. Then comes the estuary. **The first part of the estuary – the freshwater – traps a lot of nitrogen and phosphorus. The brackish and marine sites also trap many**

nutrients, since they cover a larger area. And they are great at breaking down organic matter! The high oxygen exchange rates there show levels of high **microbial activity**. **The warmer it gets, the quicker they break the organic matter down. This is important, as climate change warms the Earth.** We can use this information to better predict what could happen in these unique environments in the future.

Conclusion

You can see now that estuaries are very special. There may not be one where you live, but research some estuaries in nearby regions. What is their condition? How can we help? Remember that it is humans who pollute estuaries! Here are a few ideas:

- Dispose of household (e.g. cooking oil, soaps) and yard chemicals (e.g. fertilizers, pesticides) properly.
- Avoid using toxic pesticides in your garden. Try using natural treatments instead!
- Reduce your waste by using reusable water bottles and food containers. This reduces the amount of trash going to landfills, as well as the amount of litter in natural areas.

Glossary of Key Terms

Ammonium - a form of nitrogen. When animals and plants die in the water, they fall to the bottom and microorganisms start to decompose them. Ammonium is a byproduct of that process (ammonification). Next, other microorganisms turn that into nitrites and then nitrates (nitrification).

Brackish water - a mix of freshwater and saltwater, found in estuaries.

Eutrophication - when lakes and rivers receive too many nutrients (e.g. nitrogen and phosphorus) due to human activities such as agriculture and sewage discharge. Algae use these excess nutrients and grow rapidly. But when they die, microbes use a lot of oxygen to decompose them.

Exchange rates - the rate at which nutrients or oxygen move between two environments; for example, between the water and the sediment.

Incubation - maintain something in conditions that allow it to grow or develop. In our case, we put the water samples in the lab under similar conditions to the natural ones.

Microbial activity - when microorganisms eat, breathe, and grow, they break down organic matter to nutrients. They need a lot of oxygen for that – just like we need oxygen to live and function.

Nitrates and nitrites - forms of nitrogen. They are useful for plant growth (there are nitrates in fertilizers), but when their levels are too high, they lead to harmful overgrowths of algae.

Nutrients - chemical substances that plants and animals need to grow.

Organic matter - matter that comes from organisms; waste from living things and parts of plants and animals that used to be alive. When microorganisms decompose organic matter, they use oxygen and release nutrients.

Phosphates - a form of phosphorus; also important for plant growth and commonly used in fertilizers.

Pollutant - a substance that has negative effects on the water, soil, or air.

Remineralization - the breakdown of organic matter to inorganic forms and nutrients.

Salinity - the saltiness of the water.

Sediment - the bottom of the river, lake, estuary, etc. It consists of rocks, sand, minerals, and organic matter.

Check your understanding

- 1 How does the estuary water change from upstream to downstream?

- 2 What happens to organic matter in the estuary?

- 3 How does eutrophication happen in estuaries and what are the consequences?

- 4 We mentioned some of the ways humans affect estuaries. Can you think of any other human impacts?

- 5 Estuaries act like filters and stop harmful compounds from entering the ocean. With a partner, look up other ways that estuaries are helpful to animals or humans.

REFERENCES

Dunia Rios-Yunes, Justin C. Tiano, Dick van Oevelen, Jeroen van Dalen, and Karlina Soetaert (2023) *Annual biogeochemical cycling in intertidal sediments of a restored estuary reveals dependence of N, P, C and Si cycles to temperature and water column properties*. Estuarine, Coastal and Shelf Science.

<https://www.sciencedirect.com/science/article/pii/S0272771423000173>

NOAA: What is an estuary?

<https://oceanservice.noaa.gov/facts/estuary.html>

Kiddle: Estuary facts for kids

<https://kids.kiddle.co/Estuary>

Acknowledgment:

This article's adaptation was supported by the Royal Netherlands Academy of Arts and Sciences (KNAW).



Appendix A

Summary

Estuaries are unique coastal ecosystems that connect terrestrial and marine areas, providing habitat to several freshwater, brackish, and marine species, both within the sediment and in the water column. The estuarine intertidal mudflats play a crucial role in the remineralization of organic matter, nutrient recycling, and the filtration of pollutants and nutrients from terrestrial sources. Despite their importance, the global extent of mudflats is decreasing due to a range of direct and indirect anthropogenic stressors that include activities such as dumping of dredged material, land reclamation, land-use change, sand starvation, and sea level rise. With the ever-growing human population and the widespread implementation of coastal management and coastal modification measures in response to climate change, the effect of these stressors is expected to increase.

This thesis was motivated by the urgent need to expand our understanding of the present state of biogeochemical dynamics in intertidal mudflats. Our primary aim was to determine the extent to which mudflats contribute to estuarine nutrient retention and how this contribution is influenced by seasonal fluctuations and biological activity. Furthermore, we sought to understand the potential modifications that may occur in the biogeochemical functioning of mudflats as a result of sand starvation and increased sediment resuspension.

Since intertidal and subtidal areas experience distinct daily dynamics, it was necessary to determine the different biogeochemical processes occurring in each zone. We quantified the biogeochemical dynamics in both intertidal and subtidal areas of the Eastern Scheldt tidal bay and discovered that intertidal sediments exhibited higher productivity and removed significantly higher amounts of nutrients compared to subtidal sediments. Conversely, subtidal sediments played a more prominent role in blue carbon storage. The relevance of this study becomes evident when considering the ongoing loss of intertidal areas due to sand starvation and the potential loss resulting from sea level rise. A decline in intertidal area would effectively diminish the nutrient removal capacity of the Eastern Scheldt, compromising its biogeochemical functionality.

Part of our study focused on biogeochemical dynamics and the macrobenthic community of intertidal mudflats in the Western Scheldt estuary. We discovered distinct differences among the fresh, brackish, and marine habitats. The estuarine filter became apparent, with freshwater sediments acting as a sink of phosphorus (P) and nitrogen (N), the brackish sediments as a sink of only N, and the marine as a source of both nutrients. Regarding abiotic and biotic influences on nutrient dynamics, we observed that both the

Summary

local nutrient dynamics and the macrobenthic community were highly influenced by salinity, while temperature exerted an overarching effect on these dynamics as well as on the biological activity. Additionally, the bioturbating and bioirrigating activity of macrofauna played a crucial role in shaping the observed nutrient dynamics at each site, facilitating enhanced OM mineralization and microbial processes.

The sediment of intertidal mudflats serves as a nutrient reservoir; however, occasional disturbances such as sediment resuspension can release porewaters and the nutrients within into the water column. While sediment resuspension is a natural process, our understanding of its influence on nutrient dynamics and nutrient concentrations in coastal waters and sediments remains limited. We investigated the effect of sediment resuspension in mudflats of both the Eastern and Western Scheldt and found that sediment resuspension did indeed release nutrients into the water column. However, the magnitude of this release depended on site exposure and the time elapsed since the last resuspension event. Interestingly, we found consistent differences in the response of phosphate to erosion between the estuary and the tidal bay suggesting that some nutrients may exhibit site-specific responses to sediment resuspension. These findings carry significance as it is anticipated that storm frequency and strength will increase in the coming decades, leading to a greater release of nutrients with potential consequences for nutrient dynamics in coastal systems.

This thesis underscores the critical importance of intertidal mudflats as active centres of biogeochemical transformations and nutrient removal, positioning them as invaluable components for maintaining the functionality of estuarine ecosystems. Moreover, emphasis is made on the potential consequences of the worldwide loss of mudflats on the ecosystem services provided by coastal systems.

Samenvatting

Estuaria vormen unieke kustecosystemen, op de overgang van terrestrische naar mariene gebieden. Daarbij vormt het een habitat voor verschillende zoetwater-, brakwater- en mariene soorten, zowel in de bodem als in de waterkolom. Slikken spelen hierbij een cruciale rol in de remineralisatie van organisch materiaal, de recycling van voedingsstoffen en de filtratie van verontreinigende stoffen en terrestrische voedingsstoffen. Ondanks het belang van slikken neemt de wereldwijde verspreiding af als gevolg van een scala aan directe en indirecte oorzaken, waaronder menselijke activiteiten zoals het storten van baggermateriaal, landaanwinning, veranderingen in het grondgebruik, schaarste aan zand aanvoer en de stijging van de zeespiegel. Met de voortdurende toename van de menselijke bevolking en de wijdverbreide implementatie van kustbeheer- en kustmodificatiemaatregelen als reactie op klimaatverandering, worden deze oorzaken naar verwachting steeds gebruikelijker.

Dit proefschrift werd gemotiveerd door de dringende noodzaak om ons begrip van de huidige toestand van de biogeochemische dynamiek in slikken beter te begrijpen. Het voornaamste doel was om de bijdrage van slikken aan de retentie van voedingsstoffen in estuaria te onderzoeken en hoe deze bijdrage wordt beïnvloed door zowel seizoensfluctuaties als biologische activiteit. Bovendien wilden we inzicht krijgen in mogelijke veranderingen in de biogeochemische werking van slikken als gevolg van zand schaarste en toegenomen erosie van de bodem.

Aangezien intertidale en subtidale gebieden verschillende dagelijkse dynamiek ervaren, is het noodzakelijk om de verschillende biogeochemische processen in elke zone te bepalen. We hebben de biogeochemische dynamiek in zowel intertidale als subtidale gebieden van de Oosterschelde gekwantificeerd en ontdekten dat slikken een hogere productiviteit vertoonden en aanzienlijk meer voedingsstoffen verwijderden dan subtidale gebieden. Daarentegen hebben de subtidale gebieden een belangrijker rol in de opslag van koolstof. De relevantie van dit onderzoek wordt duidelijk wanneer we rekening houden met de voortdurende afname van de intertidale gebieden als gevolg van de zand schaarste in de Oosterschelde en het mogelijke verlies als gevolg van de relatieve stijging van de zeespiegel. Een afname van intertidaal gebied zou de capaciteit om voedingsstoffen te verwijderen aanzienlijk verminderen in de Oosterschelde, met als gevolg een verstoring van de huidige biogeochemische functionaliteit.

Ons onderzoek richtte zich op de biogeochemische dynamiek en de macrobenthische gemeenschap van de slikken in het Westerschelde-estuarium. Hier ontdekten we duidelijke verschillen tussen de zoete, brakke en zoute habitats. Het estuariën

Samenvatting

filtersysteem werd zichtbaar, waarbij het sediment in het zoetwatergedeelte dienstdeed als opslag voor fosfor (P) en stikstof (N), in het brakwatergedeelte alleen als opslag voor N en in het mariene gebied als bron voor beide voedingsstoffen. Met betrekking tot de abiotische en biotische invloeden op de voedingsstoffendynamiek, observeerden we dat zowel de lokale voedingsstoffendynamiek als de macrobenthische gemeenschap sterk werden beïnvloed door het zoutgehalte, terwijl de temperatuur een overkoepelend effect had op de mate van dynamiek en de biologische activiteit. Daarnaast speelden bioturbatie en bioirrigatie van macrofauna een cruciale rol bij de karakteristieken van de waargenomen voedingsstoffendynamiek, wat resulteerde in verbeterde mineralisatie van organisch materiaal en microbiële processen.

Het sediment van slikken fungeert als een voedingsstoffenreservoir, maar wanneer deze af en toe verstoord wordt door erosie evenementen, wordt poriën water en de daarin aanwezige voedingsstoffen in de waterkolom vrijgegeven. Hoewel erosie een natuurlijk proces is, is onze kennis van de invloed ervan op de voedingsstoffendynamiek en -concentraties in kustwateren en sedimenten beperkt. We hebben het effect van erosie van slikken in zowel de Oosterschelde als de Westerschelde onderzocht en ontdekten dat erosie inderdaad voedingsstoffen in de waterkolom vrijgeeft. De omvang van deze afgifte was echter afhankelijk van de blootstelling van de locatie aan wind en de tijd sinds het laatste erosie evenementen. Interessant genoeg vonden we consistente verschillen in de reactie van fosfaat op erosie tussen het estuarium (Westerschelde) en het getijdensysteem (Oosterschelde), wat suggereert dat sommige voedingsstoffen site-specifieke reacties kunnen vertonen op erosie. Deze bevindingen zijn relevant, aangezien verwacht wordt dat stormfrequentie en -intensiteit in de komende decennia zullen toenemen, wat zal leiden tot een grotere afgifte van voedingsstoffen met potentiële gevolgen voor de voedingsstoffendynamiek in kustsystemen.

Dit proefschrift benadrukt het cruciale belang van intertidale gebieden als actieve centra van biogeochemische transformaties en voedingsstoffenverwijdering, waardoor ze een onschatbare component zijn voor het behoud van de functionaliteit van estuariën ecosystemen. Bovendien wordt de nadruk gelegd op de mogelijke gevolgen van het wereldwijde verlies van slikken voor de ecosystemendiensten die worden geleverd door kustsystemen.

Resumen

Los estuarios son ecosistemas costeros únicos que conectan áreas terrestres y marinas y proporcionan hábitat a varias especies de agua dulce, salobre y marina, tanto en el sedimento como en la columna de agua. Las llanuras mareales fangosas de la costa estuarina desempeñan un papel crucial en la remineralización de la materia orgánica, el reciclaje de nutrientes y la filtración de contaminantes y nutrientes provenientes de fuentes terrestres. A pesar de su importancia, la extensión global de las llanuras mareales fangosas está disminuyendo debido a factores antropogénicos directos e indirectos tales como el vertido de material dragado, la reclamación de tierra, el cambio en el uso del suelo, el déficit sedimentario y el aumento del nivel del mar. Con el crecimiento continuo de la población humana y la implementación generalizada de medidas de manejo y modificación costera como respuesta al cambio climático, se espera que el efecto de estos factores detrimentales se intensifique.

Esta tesis fue motivada por la necesidad urgente de ampliar nuestra comprensión del estado actual de las dinámicas biogeoquímicas que ocurren en las llanuras mareales fangosas intermareales. Nuestros objetivos principales fueron determinar la contribución de estas llanuras para la retención de nutrientes estuarinos y entender cómo es que ésta es influida por fluctuaciones estacionales y de actividad biológica. Además, buscamos comprender las posibles modificaciones que podrían ocurrir en el funcionamiento biogeoquímico de estas llanuras a raíz de un déficit sedimentario y un incremento en la resuspensión de sedimentos.

Las áreas intermareales y submareales experimentan dinámicas diarias distintas, por lo que es necesario determinar los diferentes procesos biogeoquímicos que ocurren en cada zona. En este estudio cuantificamos las dinámicas biogeoquímicas en la zona intermareal y submareal de la laguna mareal del Escalda Oriental y descubrimos que los sedimentos intermareales mostraban una mayor productividad y removían cantidades significativamente mayores de nutrientes en comparación con los sedimentos submareales. Por otro lado, los sedimentos submareales desempeñaron un papel más prominente en el almacenamiento de carbono azul. La relevancia de este estudio se evidencia al considerar la pérdida continua de áreas intermareales debido al déficit sedimentario y la pérdida potencial atribuida al aumento del nivel del mar. Por lo tanto, una disminución en el área intermareal causaría una disminución en la capacidad de eliminación de nutrientes del Escalda Oriental, comprometiendo así su funcionalidad biogeoquímica.

Resumen

Nuestro primer estudio se centró en las dinámicas biogeoquímicas y de la comunidad macrobentónica de las llanuras mareales fangosas intermareales en el estuario del Escalda Occidental a lo largo de un año. Diferencias entre los hábitats de agua dulce, salobre y marina fueron observadas y el filtro estuarino se hizo evidente al detectar que los sedimentos de agua dulce fungieron como un sumidero de fósforo (P) y nitrógeno (N), los sedimentos salobres como un sumidero solo de N y los marinos como una fuente de ambos nutrientes. En cuanto a las influencias bióticas y abióticas de las dinámicas de nutrientes entre estos hábitats, observamos que la salinidad influyó las dinámicas locales de nutrientes y a la comunidad macrobentónica, mientras que la temperatura tuvo un efecto general sobre los nutrientes y la actividad biológica. Además, se observó que las actividades de bioturbación y bioirrigación de la macrofauna influyeron las dinámicas de nutrientes locales al promover la mineralización de la materia orgánica y los procesos microbianos.

El sedimento de las llanuras mareales fangosas intermareales sirve como un reservorio de nutrientes; sin embargo, perturbaciones ocasionales como la resuspensión de sedimentos pueden liberar aguas intersticiales y los nutrientes contenidos en ellas hacia la columna de agua. Aunque la resuspensión de sedimentos es un proceso natural, nuestro conocimiento sobre su influencia en las dinámicas de nutrientes y en la concentración de nutrientes en aguas costeras y sedimentos es limitado. Nuestro estudio se enfocó en el efecto de la resuspensión de sedimentos en las llanuras mareales fangosas de la bahía mareal Escalda Oriental y del estuario Escalda Occidental. Observamos que los eventos de resuspensión de sedimentos causaron la liberación de nutrientes hacia la columna de agua. Cabe destacar que la magnitud de esta liberación dependió de la exposición del sitio y el tiempo transcurrido desde el último evento de resuspensión. Curiosamente, encontramos diferencias en la respuesta del fosfato a la resuspensión entre el estuario y la bahía mareal, lo que sugiere que algunos nutrientes pueden exhibir dinámicas específicas del sitio en el que ocurre la resuspensión. Estos hallazgos son significativos, ya que se prevé un aumento en la frecuencia e intensidad de las tormentas costeras dentro de las próximas décadas, lo que conducirá, potencialmente, a una mayor liberación de nutrientes con posibles consecuencias para los ecosistemas costeros.

Esta tesis enfatiza la importancia de las llanuras mareales fangosas intermareales como centros activos de transformaciones biogeoquímicas y retención de nutrientes. Adicionalmente, las posiciona como componentes invaluable de la funcionalidad de los ecosistemas estuarinos y se hace hincapié en las posibles consecuencias que la pérdida de llanuras mareales fangosas puede tener en los servicios ecosistémicos proporcionados por sistemas costeros.

Short Curriculum Vitae

5.8 Education

2016-2018 MSc Marine Coastal Development, Norwegian University of Science and Technology (NTNU), Norway

2010-2014 BSc Biology, National Autonomous University of Mexico (UNAM), Mexico

5.9 Work Experience

2019-present PhD Marine biogeochemistry Royal Netherlands Institute for Sea Research and Utrecht University, The Netherlands

2018 Laboratory technician, Chemistry Department, Norwegian University of Science and Technology, Norway

2017 Coach for new students, Natural Sciences Faculty, Norwegian University of Science and Technology, Norway

2013-2014 Data analyst Marine Informatics Unit (UNINMAR), Sea Sciences and Limnology Institute, National Autonomous University of Mexico, Mexico

5.10 Research expeditions

2022 September R/V Sarmiento de Gamboa, Eurofleets+ Sines, Portuguese Coast

2019 September R/V Pelagia North Sea Research Cruise (64PE45), North Sea

2017 July Sailing for Science Research Cruise, Aegean Sea

5.11 Publications

Rios-Yunes, D., Borrero-Santiago, A. R., Mathew, K.A., Gonzalez, S. V., Ciesielski, T. M., Asimakopoulos, A. G., Ardelan, M. V, 2021. Potential effect of CO₂ seepage at high pressure on the marine organic matter. *International Journal of Greenhouse Gas Control* 106, 103276. <https://doi.org/10.1016/j.ijggc.2021.103276>

Curriculum Vitae

Fontela, M., Abrantes, F., Álvarez-Fernández, M.J., Borges De Sousa, J., Choi Wang, D., Curbelo, D., Fernández-Román, D., Ferreira, F., Fuentes-Lema, A., Gebara, L., Gomes, M., Herman Temu, V., Mega, A., Mendes Renato, Molina, G., Nieto, S., Pereira, H., Pereira, J., Ramalho, S., Relvas, P., **Rios-Yunes, D.**, Voelker, A., 2022. Hydrographic dataset from the Eurofleets+ SINES 2022 research cruise in the Iberian Upwelling System. SEANOE. Data set.

Rios-Yunes, D., Tiano, J.C., van Oevelen, D., van Dalen, J., Soetaert, K., 2023a. Annual biogeochemical cycling in intertidal sediments of a restored estuary reveals dependence of N, P, C and Si cycles to temperature and water column properties. *Estuar Coast Shelf Sci* 108227. <https://doi.org/10.1016/j.ecss.2023.108227>

Rios-Yunes, D., Tiano, J.C., van Rijswijk, P., de Borger, E., van Oevelen, D., Soetaert, K., 2023b. Long-term changes in ecosystem functioning of a coastal bay expected from a shifting balance between intertidal and subtidal habitats. *Cont Shelf Res* 254. <https://doi.org/10.1016/j.csr.2022.104904>

In the pipeline

Rios-Yunes, D.; Beauchard, O.; De Borger, E.; Tramper, A.; Xu, Y.; Ysebaert, T; Soetaert, K. Influence of benthic fauna on intertidal sediment biogeochemistry along the estuarine salinity gradient. (in prep.)

Zhang, T; **Rios-Yunes, D.**; Tian, B.; Liu, Q.; Liu, D.; Soetaert, K.; van der Wal, D. Hyperspectral remote sensing of macrobenthos in the estuarine tidal flat using chlorophyll a and pheophorbide a pigments (in prep.)

Bibliography

- Abril, G., Etcheber, H., le Hir, P., Bassoullet, P., Boutier, B., and Frankignoulle, M. (1999). Oxidic/anoxic oscillations and organic carbon mineralization in an estuarine maximum turbidity zone (The Gironde, France). *Limnol Oceanogr* 44, 1304–1315. doi: 10.4319/lo.1999.44.5.1304.
- Aller, R. C. (1982). "The Effects of Macrobenthos on Chemical Properties of Marine Sediment and Overlying Water," in, 53–102. doi: 10.1007/978-1-4757-1317-6_2.
- Amos, C. L., Brylinsky, M., Sutherland, T. F., O'Brien, D., Lee, S., and Cramp, A. (1998). The stability of a mudflat in the Humber estuary, South Yorkshire, UK. *Geological Society, London, Special Publications* 139, 25–43. doi: 10.1144/GSL.SP.1998.139.01.03.
- An, S., and Gardner, W. (2002). Dissimilatory nitrate reduction to ammonium (DNRA) as a nitrogen link, versus denitrification as a sink in a shallow estuary (Laguna Madre/Baffin Bay, Texas). *Mar Ecol Prog Ser* 237, 41–50. doi: 10.3354/meps237041.
- Andersson, M., Brion, N., and Middelburg, J. (2006). Comparison of nitrifier activity versus growth in the Scheldt estuary - a turbid, tidal estuary in northern Europe. *Aquatic Microbial Ecology* 42, 149–158. doi: 10.3354/ameo42149.
- Arndt, S., Jørgensen, B. B., LaRowe, D. E., Middelburg, J. J., Pancost, R. D., and Regnier, P. (2013). Quantifying the degradation of organic matter in marine sediments: A review and synthesis. *Earth Sci Rev* 123, 53–86. doi: 10.1016/j.earscirev.2013.02.008.
- Arndt, S., Regnier, P., and Vanderborght, J.-P. (2009). Seasonally-resolved nutrient export fluxes and filtering capacities in a macrotidal estuary. *Journal of Marine Systems* 78, 42–58. doi: 10.1016/j.jmarsys.2009.02.008.
- Baeyens, W., van Eck, B., Lambert, C., Wollast, R., and Goeyens, L. (1997). General description of the Scheldt estuary. *Hydrobiologia* 366, 1–14. doi: 10.1023/a:1003164009031.
- Bailey, G., Galanidou, N., Peeters, H., Jöns, H., and Mennenga, M. eds. (2020). *The Archaeology of Europe's Drowned Landscapes*. Cham: Springer International Publishing doi: 10.1007/978-3-030-37367-2.
- Bally, G., Mesnage, V., Deloffre, J., Clarisse, O., Lafite, R., and Dupont, J.-P. (2004). Chemical characterization of porewaters in an intertidal mudflat of the Seine

Bibliography

- estuary: relationship to erosion–deposition cycles. *Mar Pollut Bull* 49, 163–173. doi: 10.1016/j.marpolbul.2004.02.005.
- Bancon-Montigny, C., Gonzalez, C., Delpoux, S., Avenzac, M., Spinelli, S., Mhadhbi, T., et al. (2019). Seasonal changes of chemical contamination in coastal waters during sediment resuspension. *Chemosphere* 235, 651–661. doi: 10.1016/j.chemosphere.2019.06.213.
- Barbier, E. B., Sally, D. H., Chris, K., Evamaria, W. K., Adrian, C. S., and Brian, R. S. (2011). The value of estuarine and coastal ecosystem services. *Ecol Monogr* 81, 169–193. doi: 10.1890/10-1510.1.
- Barsanti, L., and Gualtieri, P. (2020). “Anatomy of *Euglena gracilis*,” in *Handbook of Algal Science, Technology and Medicine* (Elsevier), 61–70. doi: 10.1016/B978-0-12-818305-2.00004-8.
- Bates, D., Mächler, M., Bolker, B., and Walker, S. (2015). Fitting Linear Mixed-Effects Models Using lme4. *J Stat Softw* 67. doi: 10.18637/jss.v067.i01.
- Baugh, T. M., Day, J. W., Hall, C. A. S., Kemp, W. M., Yáñez-Arancibia, A., and Yanez-Arancibia, A. (1990). Estuarine Ecology. *Estuaries* 13, 112. doi: 10.2307/1351438.
- Beauchard, O., Ciutat, A., Gerino, M., Munoz, T., Jacobs, S., Tackx, M., et al. (2012). Spatiotemporal bioturbation patterns in a tidal freshwater marsh. *Estuar Coast Shelf Sci* 96, 159–169. doi: 10.1016/j.ecss.2011.10.026.
- Beauchard, O., Thompson, M. S. A., Ellingsen, K., Piet, G. J., Laffargue, P., and Soetaert, K. (2023). Quantifying sea floor functional biodiversity and vulnerability. *Mar Ecol Prog Ser* 708, 21–43. doi: 10.3354/meps14270.
- Beck, M., Dellwig, O., Liebezeit, G., Schnetger, B., and Brumsack, H.-J. (2008). Spatial and seasonal variations of sulphate, dissolved organic carbon, and nutrients in deep pore waters of intertidal flat sediments. *Estuar Coast Shelf Sci* 79, 307–316. doi: 10.1016/j.ecss.2008.04.007.
- Benitez-Nelson, C. R. (2000). The biogeochemical cycling of phosphorus in marine systems. *Earth Sci Rev* 51, 109–135. doi: 10.1016/S0012-8252(00)00018-0.
- Berthold, M., Zimmer, D., Reiff, V., and Schumann, R. (2018). Phosphorus Contents Revisited After 40 Years in Muddy and Sandy Sediments of a Temperate Lagoon System. *Front Mar Sci* 5. doi: 10.3389/fmars.2018.00305.
- Bianchi, T. S. (2007). *Biogeochemistry of Estuaries*. New York: Oxford University Press.

- Billen, G., Garnier, J., and Rousseau, V. (2005). Nutrient fluxes and water quality in the drainage network of the Scheldt basin over the last 50 years. *Hydrobiologia* 540, 47–67. doi: 10.1007/s10750-004-7103-1.
- Bolker, B. M., Brooks, M. E., Clark, C. J., Geange, S. W., Poulsen, J. R., Stevens, M. H. H., et al. (2009). Generalized linear mixed models: a practical guide for ecology and evolution. *Trends Ecol Evol* 24, 127–135. doi: 10.1016/j.tree.2008.10.008.
- Bonifácio, P., Bourgeois, S., Labrune, C., Amouroux, J. M., Escoubeyrou, K., Buscail, R., et al. (2014). Spatiotemporal changes in surface sediment characteristics and benthic macrofauna composition off the Rhône River in relation to its hydrological regime. *Estuar Coast Shelf Sci* 151, 196–209. doi: 10.1016/j.ecss.2014.10.011.
- Borggaard, O. K. (1983). Effect of Surface Area and Mineralogy of Iron Oxides on Their Surface Charge and Anion-Adsorption Properties. *Clays Clay Miner* 31, 230–232. doi: 10.1346/CCMN.1983.0310309.
- Boudreau, B. P. (1986). Mathematics of tracer mixing in sediments; I, Spatially-dependent, diffusive mixing. *Am J Sci* 286, 161–198. doi: 10.2475/ajs.286.3.161.
- Boudreau, B. P. (1996). The diffusive tortuosity of fine-grained unlithified sediments. *Geochim Cosmochim Acta* 60, 3139–3142. doi: 10.1016/0016-7037(96)00158-5.
- Boynton, W., and Kemp, W. (1985). Nutrient regeneration and oxygen consumption by sediments along an estuarine salinity gradient. *Mar Ecol Prog Ser* 23, 45–55. doi: 10.3354/meps023045.
- Boynton, W. R., Ceballos, M. A. C., Bailey, E. M., Hodgkins, C. L. S., Humphrey, J. L., and Testa, J. M. (2018). Oxygen and Nutrient Exchanges at the Sediment-Water Interface: a Global Synthesis and Critique of Estuarine and Coastal Data. *Estuaries and Coasts* 41, 301–333. doi: 10.1007/s12237-017-0275-5.
- Braeckman, U., Provoost, P., Gribsholt, B., van Gansbeke, D., Middelburg, J., Soetaert, K., et al. (2010a). Role of macrofauna functional traits and density in biogeochemical fluxes and bioturbation. *Mar Ecol Prog Ser* 399, 173–186. doi: 10.3354/meps08336.
- Braeckman, U., Provoost, P., Gribsholt, B., Van Gansbeke, D., Middelburg, J., Soetaert, K., et al. (2010b). Role of macrofauna functional traits and density in biogeochemical fluxes and bioturbation. *Mar Ecol Prog Ser* 399, 173–186. doi: 10.3354/meps08336.
- Braeckman, U., van Colen, C., Guilini, K., van Gansbeke, D., Soetaert, K., Vincx, M., et al. (2014). Empirical evidence reveals seasonally dependent reduction in nitrification in coastal sediments subjected to near future ocean acidification. *PLoS One* 9. doi: 10.1371/journal.pone.0108153.

Bibliography

- Breitburg, D., Levin, L. A., Oschlies, A., Grégoire, M., Chavez, F. P., Conley, D. J., et al. (2018). Declining oxygen in the global ocean and coastal waters. *Science (1979)* 359. doi: 10.1126/science.aam7240.
- Brion, N., Andersson, M., Elskens, M., Diaconu, C., Baeyens, W., Dehairs, F., et al. (2008). Nitrogen cycling, retention and export in a eutrophic temperate macrotidal estuary. *Mar Ecol Prog Ser* 357, 87–99. doi: 10.3354/meps07249.
- Brion, N., Verbanck, M. A., Bauwens, W., Elskens, M., Chen, M., and Servais, P. (2015). Assessing the impacts of wastewater treatment implementation on the water quality of a small urban river over the past 40 years. *Environmental Science and Pollution Research* 22, 12720–12736. doi: 10.1007/s11356-015-4493-8.
- Bulmer, R. H., Stephenson, F., Jones, H. F. E., Townsend, M., Hillman, J. R., Schwendenmann, L., et al. (2020). Blue Carbon Stocks and Cross-Habitat Subsidies. *Front Mar Sci* 7. doi: 10.3389/fmars.2020.00380.
- Burdon, D., Callaway, R., Elliott, M., Smith, T., and Wither, A. (2014). Mass mortalities in bivalve populations: A review of the edible cockle *Cerastoderma edule* (L.). *Estuar Coast Shelf Sci* 150, 271–280. doi: 10.1016/j.ecss.2014.04.011.
- Byun, C., Lee, S. H., and Kang, H. (2019). Estimation of carbon storage in coastal wetlands and comparison of different management schemes in South Korea. *J Ecol Environ* 43. doi: 10.1186/s41610-019-0106-7.
- Cabrita, M. T., Catarino, F., and Vale, C. (1999). The effect of tidal range on the flushing of ammonium from intertidal sediments of the Tagus estuary, Portugal. *Oceanologica Acta* 22, 291–302. doi: 10.1016/S0399-1784(99)80053-X.
- Cadée, G. C. (1979). Sediment reworking by the polychaete *Heteromastus filiformis* on a tidal flat in the Dutch Wadden Sea. *Netherlands Journal of Sea Research* 13, 441–456. doi: 10.1016/0077-7579(79)90017-6.
- Canfield, D. E., and Thamdrup, B. (2009). Towards a consistent classification scheme for geochemical environments, or, why we wish the term ‘suboxic’ would go away. *Geobiology* 7, 385–392. doi: 10.1111/j.1472-4669.2009.00214.x.
- Caraco, N., Cole, J., and Likens, GeneE. (1990). A comparison of phosphorus immobilization in sediments of freshwater and coastal marine systems. *Biogeochemistry* 9, 277–290. doi: 10.1007/BF00000602.
- Chen, M. S., Wartel, S., Lavkulich, L. M., Baeyens, W., Goeyens, L., and Brion, N. (2007). Organic matter and dissolved inorganic nitrogen distributions in estuarine muddy deposits. *Aquat Ecosyst Health Manag* 10, 69–85. doi: 10.1080/14634980701211896.

- Chen, N., Krom, M. D., Wu, Y., Yu, D., and Hong, H. (2018). Storm induced estuarine turbidity maxima and controls on nutrient fluxes across river-estuary-coast continuum. *Science of The Total Environment* 628–629, 1108–1120. doi: 10.1016/j.scitotenv.2018.02.060.
- Clavier, J., Boucher, G., Chauvaud, L., Fichez, R., and Chifflet, S. (2005). Benthic response to ammonium pulses in a tropical lagoon: implications for coastal environmental processes. *J Exp Mar Biol Ecol* 316, 231–241.
- Cook, P., Butler, E., and Eyre, B. (2004). Carbon and nitrogen cycling on intertidal mudflats of a temperate Australian estuary. I. Benthic metabolism. *Mar Ecol Prog Ser* 280, 25–38. doi: 10.3354/meps280025.
- Costanza, R., de Groot, R., Sutton, P., van der Ploeg, S., Anderson, S. J., Kubiszewski, I., et al. (2014). Changes in the global value of ecosystem services. *Global Environmental Change* 26, 152–158. doi: 10.1016/j.gloenvcha.2014.04.002.
- Couceiro, F., Fones, G. R., Thompson, C. E. L., Statham, P. J., Sivyer, D. B., Parker, R., et al. (2013). Impact of resuspension of cohesive sediments at the Oyster Grounds (North Sea) on nutrient exchange across the sediment–water interface. *Biogeochemistry* 113, 37–52. doi: 10.1007/s10533-012-9710-7.
- Cowan, J., Pennock, J., and Boynton, W. (1996). Seasonal and interannual patterns of sediment-water nutrient and oxygen fluxes in Mobile Bay, Alabama (USA):regulating factors and ecological significance. *Mar Ecol Prog Ser* 141, 229–245. doi: 10.3354/meps141229.
- Cox, T. J. S., Maris, T., Soetaert, K., Conley, D. J., van Damme, S., Meire, P., et al. (2009). A macro-tidal freshwater ecosystem recovering from hypereutrophication: the Schelde case study. *Biogeosciences* 6, 2935–2948. doi: 10.5194/bg-6-2935-2009.
- Daggers, T. D., Oevelen, D., Herman, P. M. J., Boschker, H. T. S., and Wal, D. (2020). Spatial variability in macrofaunal diet composition and grazing pressure on microphytobenthos in intertidal areas. *Limnol Oceanogr* 65, 2819–2834. doi: 10.1002/lno.11554.
- Dahl, E. (1956). Ecological Salinity Boundaries in Poikilohaline Waters. Available at: <https://about.jstor.org/terms>.
- Dairain, A., Maire, O., Meynard, G., Richard, A., Rodolfo-Damiano, T., and Orvain, F. (2020). Sediment stability: can we disentangle the effect of bioturbating species on sediment erodibility from their impact on sediment roughness? *Mar Environ Res* 162. doi: 10.1016/j.marenvres.2020.105147.

Bibliography

- De Backer, A., Van Ael, E., Vincx, M., and Degraer, S. (2010). Behaviour and time allocation of the mud shrimp, *Corophium volutator*, during the tidal cycle: a laboratory study. *Helgol Mar Res* 64, 63–67. doi: 10.1007/s10152-009-0167-6.
- de Backer, A., van Coillie, F., Montserrat, F., Provoost, P., van Colen, C., Vincx, M., et al. (2011). Bioturbation effects of *Corophium volutator*: Importance of density and behavioural activity. *Estuar Coast Shelf Sci* 91, 306–313. doi: 10.1016/j.ecss.2010.10.031.
- de Borger, E., Braeckman, U., and Soetaert, K. (2021). Rapid organic matter cycling in North Sea sediments. *Cont Shelf Res* 214, 104327. doi: 10.1016/j.csr.2020.104327.
- De Borger, E., Tiano, J., Braeckman, U., Ysebaert, T., and Soetaert, K. (2020). Biological and biogeochemical methods for estimating bioirrigation: a case study in the Oosterschelde estuary. *Biogeosciences* 17, 1701–1715. doi: 10.5194/bg-17-1701-2020.
- de Vet, P. L. M., van Prooijen, B. C., Colosimo, I., Steiner, N., Ysebaert, T., Herman, P. M. J., et al. (2020). Variations in storm-induced bed level dynamics across intertidal flats. *Sci Rep* 10, 12877. doi: 10.1038/s41598-020-69444-7.
- Decleyre, H., Heylen, K., van Colen, C., and Willems, A. (2015). Dissimilatory nitrogen reduction in intertidal sediments of a temperate estuary: Small scale heterogeneity and novel nitrate-to-ammonium reducers. *Front Microbiol* 6. doi: 10.3389/fmicb.2015.01124.
- Dedieu, K., Rabouille, C., Gilbert, F., Soetaert, K., Metzger, E., Simonucci, C., et al. (2007). Coupling of carbon, nitrogen and oxygen cycles in sediments from a Mediterranean lagoon: A seasonal perspective. *Mar Ecol Prog Ser* 346, 45–59. doi: 10.3354/meps07031.
- Deltares (2013). Tidal Phenomena in the Scheldt Estuary, part 2. Available at: <https://www.vnsc.eu/uploads/2014/02/g-7-tidal-phenomena-in-the-scheldt-estuary-part-2-v2-o.pdf>.
- Deng, L., Meile, C., Fiskal, A., Bölsterli, D., Han, X., Gajendra, N., et al. (2022). Deposit-feeding worms control subsurface ecosystem functioning in intertidal sediment with strong physical forcing. *PNAS Nexus* 1. doi: 10.1093/pnasnexus/pgac146.
- Dipper, F. (2022). “The seawater environment and ecological adaptations,” in *Elements of Marine Ecology* (Elsevier), 37–151. doi: 10.1016/B978-0-08-102826-1.00002-8.
- Dixit, S. (2003). Predicting benthic fluxes of silicic acid from deep-sea sediments. *J Geophys Res* 108, 3334. doi: 10.1029/2002JC001309.
- Douglas, T. J., Schuerholz, G., and Juniper, S. K. (2022). Blue Carbon Storage in a Northern Temperate Estuary Subject to Habitat Loss and Chronic Habitat Disturbance:

- Cowichan Estuary, British Columbia, Canada. *Front Mar Sci* 9. doi: 10.3389/fmars.2022.857586.
- Dounas, C., Davies, I., Triantafyllou, G., Koulouri, P., Petihakis, G., Arvanitidis, C., et al. (2007). Large-scale impacts of bottom trawling on shelf primary productivity. *Cont Shelf Res* 27, 2198–2210. doi: 10.1016/j.csr.2007.05.006.
- Dyer, K. R. (1998). The typology of intertidal mudflats. *Geol Soc Spec Publ* 139, 11–24. doi: 10.1144/GSL.SP.1998.139.01.02.
- Dyer, K. R., Christie, M. C., Feates, N., Fennessy, M. J., Pejrup, M., and van der Lee, W. (2000). An Investigation into Processes Influencing the Morphodynamics of an Intertidal Mudflat, the Dollard Estuary, The Netherlands: I. Hydrodynamics and Suspended Sediment. *Estuar Coast Shelf Sci* 50, 607–625. doi: 10.1006/ecss.1999.0596.
- Dzialowski, A. R., Wang, S. H., Lim, N. C., Beury, J. H., and Huggins, D. G. (2008). Effects of sediment resuspension on nutrient concentrations and algal biomass in reservoirs of the Central Plains. *Lake Reserv Manag* 24, 313–320. doi: 10.1080/07438140809354841.
- Eyre, B. D., Ferguson, A. J. P., Webb, A., Maher, D., and Oakes, J. M. (2011). Denitrification, N-fixation and nitrogen and phosphorus fluxes in different benthic habitats and their contribution to the nitrogen and phosphorus budgets of a shallow oligotrophic sub-tropical coastal system (southern Moreton Bay, Australia). *Biogeochemistry* 102, 111–133. doi: 10.1007/s10533-010-9425-6.
- Fagherazzi, S., Viggato, T., Vieillard, A. M., Mariotti, G., and Fulweiler, R. W. (2017). The effect of evaporation on the erodibility of mudflats in a mesotidal estuary. *Estuar Coast Shelf Sci* 194, 118–127. doi: 10.1016/j.ecss.2017.06.011.
- Falcão, M., and Vale, C. (1995). Tidal flushing of ammonium from intertidal sediments of Ria Formosa, Portugal. *Netherlands Journal of Aquatic Ecology* 29, 239–244. doi: 10.1007/BF02084221.
- Falcão, M., and Vale, C. (1998). “Sediment—water exchanges of ammonium and phosphate in intertidal and subtidal areas of a mesotidal coastal lagoon (Ria Formosa),” in *Oceans, Rivers and Lakes: Energy and Substance Transfers at Interfaces* (Dordrecht: Springer Netherlands), 193–201. doi: 10.1007/978-94-011-5266-2_16.
- Fang, X., Mestdagh, S., Ysebaert, T., Moens, T., Soetaert, K., and Van Colen, C. (2019). Spatio-temporal variation in sediment ecosystem processes and roles of key biota in the Scheldt estuary. *Estuar Coast Shelf Sci* 222, 21–31. doi: 10.1016/j.ecss.2019.04.001.
- Fauchald, K., and Jumars, P. A. (1979). The diet of worms: A study of polychaete feeding guilds. *Oceanography and Marine Biology: An Annual Review* 17, 193–284.

Bibliography

- Fenchel, T. M. (1978). The ecology of micro- and meiobenthos. doi: 10.2307/2096745.
- Feuillet-Girard, M., Gouleau, D., Blanchard, G., and Joassard, L. (1997). Nutrient fluxes on an intertidal mudflat in Marennes-Oléron Bay, and influence of the emersion period. *Aquat Living Resour* 10, 49–58. doi: 10.1051/alr:1997005.
- Flanders Environment Agency (n.d.). Flanders Environment Agency. Available at: <https://www.waterinfo.be/Themas#item=waterkwaliteit/fysische parameters>.
- Flanders Environment Agency (n.d.). Geoloket. Available at: <http://geoloket.vmm.be/Geoviews/> [Accessed October 20, 2021b].
- Flemish Government (n.d.). Kaartencatalogus. Available at: <https://www.waterinfo.be/kaartencatalogus> [Accessed October 10, 2021].
- Fong, P. P. (1987). Particle-Size Utilization in the Introduced Polychaete *Neanthes succinea* in San Francisco Bay. *Pac Sci* 41.
- Fong, P. P. (1991). The effects of salinity, temperature, and photoperiod on epitokal metamorphosis in *Neanthes succinea* (Frey et Leuckart) from San Francisco Bay. *J Exp Mar Biol Ecol* 149, 177–190. doi: 10.1016/0022-0981(91)90044-W.
- Foss, P., Guillard, R. R. L., and Liaaen-Jensen, S. (1984). Prasincoxanthin—a chemosystematic marker for algae. *Phytochemistry* 23, 1629–1633. doi: 10.1016/S0031-9422(00)83455-X.
- Fox-Kemper, B., Hewitt, H. T., Xiao, C., Aðalgeirsdóttir, G., Drijfhout, S. S., Edwards, T. L., et al. (2021). “Ocean, Cryosphere and Sea Level Change,” in *Climate Change 2021: The Physical Science Basis. Contribution of Working Group I to the Sixth Assessment Report of the Intergovernmental Panel on Climate Change*, eds. V. MassonDelmotte, P. Zhai, A. Pirani, S. L. Connors, C. Péan, S. Berger, et al. (Cambridge University Press).
- François, F., Poggiale, J.-C., Durbec, J.-P., and Stora, G. (1997). A New Approach for the Modelling of Sediment Reworking Induced by a Macrobenthic Community. *Acta Biotheor* 45, 295–319. doi: 10.1023/A:1000636109604.
- Friedrichs, C. T. (2011). “Tidal Flat Morphodynamics,” in *Treatise on Estuarine and Coastal Science* (Elsevier), 137–170. doi: 10.1016/B978-0-12-374711-2.00307-7.
- Gerritsen, H. (2005). What happened in 1953? The Big Flood in the Netherlands in retrospect. *Philosophical Transactions of the Royal Society A: Mathematical, Physical and Engineering Sciences* 363, 1271–1291. doi: 10.1098/rsta.2005.1568.
- Giere, O. (2006). Ecology and Biology of Marine Oligochaeta – an Inventory Rather than another Review. *Hydrobiologia* 564, 103–116. doi: 10.1007/s10750-005-1712-1.

- Giere, O., and Pfannkuche, O. (1982). "Biology and ecology of marine oligochaeta, a review," in *Oceanography and Marine Biology, Volume 20*, ed. H. Barnes (CRC Press). doi: 10.1201/9781482267228.
- Gilbert, A., Schaafsma, M., de Nocker, L., Liekens, I., and Broekx, S. (2007). Case study status report Scheldt river basin. doi: 10.1.1.713.9579.
- Gogina, M., Lipka, M., Woelfel, J., Liu, B., Morys, C., Böttcher, M. E., et al. (2018). In Search of a Field-Based Relationship Between Benthic Macrofauna and Biogeochemistry in a Modern Brackish Coastal Sea. *Front Mar Sci* 5. doi: 10.3389/fmars.2018.00489.
- Grandjean, T. J., de Smit, J. C., van Belzen, J., Fivash, G. S., van Dalen, J., Ysebaert, T., et al. (2022). Morphodynamic signatures derived from daily surface elevation dynamics can explain the morphodynamic development of tidal flats. *Water Science and Engineering*. doi: 10.1016/j.wse.2022.11.003.
- Green, M. O., and Coco, G. (2014). Review of wave-driven sediment resuspension and transport in estuaries. *Reviews of Geophysics* 52, 77–117. doi: 10.1002/2013RG000437.
- Haan, C. T., Barfield, B. J., and Hayes, J. C. (1994). "Sediment Properties and Transport," in *Design Hydrology and Sedimentology for Small Catchments* (Elsevier), 204–237. doi: 10.1016/B978-0-08-057164-5.50011-6.
- Harley, C. D. G., Hughes, A. R., Hultgren, K. M., Miner, B. G., Sorte, C. J. B., Thornber, C. S., et al. (2006). The impacts of climate change in coastal marine systems. *Ecol Lett* 9, 228–241. doi: 10.1111/j.1461-0248.2005.00871.x.
- Harrison, S. J., and Phizacklea, A. P. (1987). Vertical temperature gradients in muddy intertidal sediments in the Forth estuary, Scotland. *Limnol Oceanogr* 32, 954–963. doi: 10.4319/lo.1987.32.4.0954.
- Heip, C. H. R. (1989). The ecology of the estuaries of Rhine, Meuse and Scheldt in the Netherlands. in (European Marine Biology Symposia).
- Heip, C. H. R., Goosen, N. K., Herman, P. M. J., Kromkamp, J. C., Middelburg, J. J., and Soetaert, K. E. R. (1995). Production and consumption of biogenic particles in temperate tidal estuaries. Available at: <https://www.researchgate.net/publication/37934497>.
- Heip, C. H. R., Herman, P. M. J., Middelburg, J. J., Moodley, L., Soetaert, K. E. R., and Ysebaert, T. (2005). "The ecology of estuarine intertidal flats-the example of the Westerschelde," in, ed. J. G. Wilson (Royal Irish Academy). Available at: <https://www.researchgate.net/publication/241863791>.

Bibliography

- Herbert, R. (1999). Nitrogen cycling in coastal marine ecosystems. *FEMS Microbiol Rev* 23, 563–590. doi: 10.1016/S0168-6445(99)00022-4.
- Hilmi, N., Chami, R., Sutherland, M. D., Hall-Spencer, J. M., Lebleu, L., Benitez, M. B., et al. (2021). The Role of Blue Carbon in Climate Change Mitigation and Carbon Stock Conservation. *Frontiers in Climate* 3. doi: 10.3389/fclim.2021.710546.
- Hofmann, A. F., Soetaert, K., and Middelburg, J. J. (2008). Nitrogen and carbon dynamics in the Scheldt estuary at the beginning of the 21st century; a modelling study. *Biogeosciences Discussions* 5, 83–161. doi: 10.5194/bgd-5-83-2008.
- Hopkinson, C. S., Giblin, A. E., Tucker, J., and Garritt, R. H. (1999). Benthic Metabolism and Nutrient Cycling along an Estuarine Salinity Gradient. *Estuaries* 22, 863. doi: 10.2307/1353067.
- Hu, Z., Willemsen, P. W. J. M., Borsje, B. W., Wang, C., Wang, H., van der Wal, D., et al. (2021). Synchronized high-resolution bed-level change and biophysical data from 10 marsh–mudflat sites in northwestern Europe. *Earth Syst Sci Data* 13, 405–416. doi: 10.5194/essd-13-405-2021.
- Hutchins, D. A., and Capone, D. G. (2022). The marine nitrogen cycle: new developments and global change. *Nat Rev Microbiol* 20, 401–414. doi: 10.1038/s41579-022-00687-z.
- IUCN (2021). Blue Carbon. Available at: <https://www.iucn.org/resources/issues-briefs/blue-carbon> [Accessed December 14, 2021].
- Jiang, L., Gerkema, T., Idier, D., Slangen, A. B. A., and Soetaert, K. (2020a). Effects of sea-level rise on tides and sediment dynamics in a Dutch tidal bay. *Ocean Science* 16, 307–321. doi: 10.5194/os-16-307-2020.
- Jiang, L., Gerkema, T., Kromkamp, J. C., van der Wal, D., Carrasco De La Cruz, P. M., and Soetaert, K. (2020b). Drivers of the spatial phytoplankton gradient in estuarine–coastal systems: generic implications of a case study in a Dutch tidal bay. *Biogeosciences* 17, 4135–4152. doi: 10.5194/bg-17-4135-2020.
- Jiang, L., Soetaert, K., and Gerkema, T. (2019). Decomposing the intra-annual variability of flushing characteristics in a tidal bay along the North Sea. *J Sea Res* 155, 101821. doi: 10.1016/j.seares.2019.101821.
- Jickells, T., Andrews, J., Samways, G., Sanders, R., Malcolm, S., Sivyver, D., et al. (2000). Nutrient fluxes through the Humber estuary - Past, present and future. *Ambio* 29, 130–135. doi: 10.1579/0044-7447-29.3.130.
- Jodo, M., Kawamoto, K., Tochimoto, M., and Coverly, S. C. (1992). Determination of nutrients in seawater by segmented–flow analysis with higher analysis rate and

- reduced interference on ammonia. *Journal of Automatic Chemistry* 14, 163–167. doi: 10.1155/S1463924692000300.
- Jordan, T. E., Cornwell, J. C., Boynton, W. R., and Anderson, J. T. (2008). Changes in phosphorus biogeochemistry along an estuarine salinity gradient: The iron conveyor belt. *Limnol Oceanogr* 53, 172–184. doi: 10.4319/lo.2008.53.1.0172.
- Jørgensen, B., and Sørensen, J. (1985). Seasonal cycles of O₂, NO₃⁻ and SO₄²⁻ reduction in estuarine sediments: the significance of an NO₃⁻ reduction maximum in spring. *Mar Ecol Prog Ser* 24, 65–74. doi: 10.3354/meps024065.
- Joye, S. B., and Paerl, H. W. (1993). “Nitrogen Fixation and Denitrification in the Intertidal and Subtidal Environments of Tomales Bay, California,” in *Biogeochemistry of Global Change* (Boston, MA: Springer US), 633–653. doi: 10.1007/978-1-4615-2812-8_35.
- Kalnejais, L. H., Martin, W. R., and Bothner, M. H. (2010). The release of dissolved nutrients and metals from coastal sediments due to resuspension. *Mar Chem* 121, 224–235. doi: 10.1016/j.marchem.2010.05.002.
- Kalnejais, L. H., Martin, W. R., Signell, R. P., and Bothner, M. H. (2007). Role of Sediment Resuspension in the Remobilization of Particulate-Phase Metals from Coastal Sediments. *Environ Sci Technol* 41, 2282–2288. doi: 10.1021/es061770z.
- Kamatani, A. (1982). Dissolution rates of silica from diatoms decomposing at various temperatures. *Mar Biol* 68, 91–96. doi: 10.1007/BF00393146.
- Kang, C.-K., Park, H. J., Choy, E. J., Choi, K.-S., Hwang, K., and Kim, J.-B. (2015). Linking Intertidal and Subtidal Food Webs: Consumer-Mediated Transport of Intertidal Benthic Microalgal Carbon. *PLoS One* 10, e0139802. doi: 10.1371/journal.pone.0139802.
- Kemp, W. M., Sampou, P., Caffrey, J., Mayer, M., Henriksen, K., and Boynton, W. R. (1990). Ammonium recycling versus denitrification in Chesapeake Bay sediments. *Limnol Oceanogr* 35, 1545–1563. doi: 10.4319/lo.1990.35.7.1545.
- Khalil, K., Laverman, A. M., Raimonet, M., and Rabouille, C. (2018). Importance of nitrate reduction in benthic carbon mineralization in two eutrophic estuaries: Modelling, observations, and laboratory experiments. *Mar Chem* 199, 24–36. doi: 10.1016/j.marchem.2018.01.004.
- Khalil, K., Raimonet, M., Laverman, A. M., Yan, C., Andrieux-Loyer, F., Viollier, E., et al. (2013). Spatial and Temporal Variability of Sediment Organic Matter Recycling in Two Temperate Eutrophicated Estuaries. *Aquat Geochem* 19, 517–542. doi: 10.1007/s10498-013-9213-8.

Bibliography

- Koch, M. S., Maltby, E., Oliver, G. A., and Bakker, S. A. (1992). Factors controlling denitrification rates of tidal mudflats and fringing salt marshes in south-west England. *Estuar Coast Shelf Sci* 34, 471–485. doi: 10.1016/S0272-7714(05)80118-0.
- Kornman, B. A., and Deckere, E. M. G. T. de (1998). Temporal variation in sediment erodibility and suspended sediment dynamics in the Dollard estuary. *Geological Society, London, Special Publications* 139, 231–241. doi: 10.1144/GSL.SP.1998.139.01.19.
- Kownacki, A., and Szarek-Gwiazda, E. (2022). The Impact of Pollution on Diversity and Density of Benthic Macroinvertebrates in Mountain and Upland Rivers. *Water (Switzerland)* 14. doi: 10.3390/w14091349.
- Krauss, K. W., Noe, G. B., Duberstein, J. A., Conner, W. H., Stagg, C. L., Cormier, N., et al. (2018). The Role of the Upper Tidal Estuary in Wetland Blue Carbon Storage and Flux. *Global Biogeochem Cycles* 32, 817–839. doi: 10.1029/2018GB005897.
- Kristensen, E. (1988). Factors influencing the distribution of nereid polychaetes in Danish coastal waters. *Ophelia* 29, 127–140. doi: 10.1080/00785326.1988.10430824.
- Kristensen, E., and Kostka, J. E. (2005). “Macrofaunal burrows and irrigation in marine sediment: Microbiological and biogeochemical interactions,” in, 125–157. doi: 10.1029/CE060p0125.
- Kristensen, E., Penha-Lopes, G., Delefosse, M., Valdemarsen, T., Quintana, C., and Banta, G. (2012). What is bioturbation? The need for a precise definition for fauna in aquatic sciences. *Mar Ecol Prog Ser* 446, 285–302. doi: 10.3354/meps09506.
- Kromkamp, J., and Peene, J. (1995a). Possibility of net phytoplankton primary production in the turbid Schelde Estuary (SW Netherlands). *Mar Ecol Prog Ser* 121, 249–259. doi: 10.3354/meps121249.
- Kromkamp, J., and Peene, J. (1995b). Possibility of net phytoplankton primary production in the turbid Schelde Estuary (SW Netherlands). *Mar Ecol Prog Ser* 121, 249–259. doi: 10.3354/meps121249.
- Kuijper, K., and Lescinski, J. (2013). Data-analysis water levels, bathymetry Western Scheldt. doi: <https://www.vnsc.eu/uploads/2014/02/g-5-data-analysis-water-levels-bathymetry-western-scheldt-v2-o.pdf>.
- Laffoley, D., Baxter, J. M., Thevenon, F., and Oliver, J. (2014). The Significance and Management of Natural Carbon Stores in the Open Ocean. Gland, Switzerland.
- Lam, P., and Kuypers, M. M. M. (2011). Microbial nitrogen cycling processes in oxygen minimum zones. *Ann Rev Mar Sci* 3, 317–345. doi: 10.1146/annurev-marine-120709-142814.

- Lamarque, B., Deflandre, B., Galindo Dalto, A., Schmidt, S., Romero-Ramirez, A., Garabetian, F., et al. (2021). Spatial Distributions of Surface Sedimentary Organics and Sediment Profile Image Characteristics in a High-Energy Temperate Marine RiOMar: The West Gironde Mud Patch. *J Mar Sci Eng* 9, 242. doi: 10.3390/jmse9030242.
- Lam-Gordillo, O., Huang, J., Barceló, A., Kent, J., Mosley, L. M., Welsh, D. T., et al. (2022). Restoration of benthic macrofauna promotes biogeochemical remediation of hostile sediments; An in-situ transplantation experiment in a eutrophic estuarine-hypersaline lagoon system. *Sci Total Environ* 833, 155201. doi: 10.1016/j.scitotenv.2022.155201.
- Laverock, B., Gilbert, J. A., Tait, K., Osborn, A. M., and Widdicombe, S. (2011). Bioturbation: impact on the marine nitrogen cycle. *Biochem Soc Trans* 39, 315–320. doi: 10.1042/BST0390315.
- Lawson, D. S., Hurd, D. C., and Pankratz, H. S. (1978). Silica dissolution rates of decomposing phytoplankton assemblages at various temperatures. *Am J Sci* 278, 1373–1393. doi: 10.2475/ajs.278.10.1373.
- Legendre, P., and Legendre, L. (2012). *Numerical Modelling*. 3rd ed. Oxford: Elsevier Science & Technology.
- Legendre, P., Oksanen, J., and ter Braak, C. J. F. (2011). Testing the significance of canonical axes in redundancy analysis. *Methods Ecol Evol* 2, 269–277. doi: 10.1111/j.2041-210X.2010.00078.x.
- Lessin, G., Artioli, Y., Almroth-Rosell, E., Blackford, J. C., Dale, A. W., Glud, R. N., et al. (2018). Modelling Marine Sediment Biogeochemistry: Current Knowledge Gaps, Challenges, and Some Methodological Advice for Advancement. *Front Mar Sci* 5, 1–8. doi: 10.3389/fmars.2018.00019.
- Li, B., Cozzoli, F., Soissons, L. M., Bouma, T. J., and Chen, L. (2017). Effects of bioturbation on the erodibility of cohesive versus non-cohesive sediments along a current-velocity gradient: A case study on cockles. *J Exp Mar Biol Ecol* 496, 84–90. doi: 10.1016/j.jembe.2017.08.002.
- Liu, C., Hou, L., Liu, M., Zheng, Y., Yin, G., Dong, H., et al. (2020). In situ nitrogen removal processes in intertidal wetlands of the Yangtze Estuary. *J Environ Sci (China)* 93, 91–97. doi: 10.1016/j.jes.2020.03.005.
- López-Romero, E., Verdin, F., Eynaud, F., Culioli, C., Hoffmann, A., Huchet, J.-B., et al. (2021). Human settlement and landscape dynamics on the coastline south of the

Bibliography

- Gironde estuary (SW France): A multi-proxy approach. *The Journal of Island and Coastal Archaeology*, 1–22. doi: 10.1080/15564894.2021.1880505.
- Loucaide, S., Cappelle, P. van, and Behrends, T. (2008). Dissolution of biogenic silica from land to ocean: Role of salinity and pH. *Limnol Oceanogr* 53, 1614–1621. doi: 10.4319/lo.2008.53.4.1614.
- Magalhães, C., Bordalo, A., and Wiebe, W. (2002). Temporal and spatial patterns of intertidal sediment-water nutrient and oxygen fluxes in the Douro River estuary, Portugal. *Mar Ecol Prog Ser* 233, 55–71. doi: 10.3354/meps233055.
- Magni, P., and Montani, S. (2006). Seasonal patterns of pore-water nutrients, benthic chlorophyll a and sedimentary AVS in a macrobenthos-rich tidal flat. *Hydrobiologia* 571, 297–311. doi: 10.1007/s10750-006-0242-9.
- Malone, T. C., and Newton, A. (2020). The Globalization of Cultural Eutrophication in the Coastal Ocean: Causes and Consequences. *Front Mar Sci* 7. doi: 10.3389/fmars.2020.00670.
- Maris, T., and Meire, P. (2017). OMES rapport 2016. Onderzoek naar de gevolgen van het Sigmaphan, baggeractiviteiten en havenuitbreiding in de Zeeschelde op het milieu. Antwerpen.
- Mateus, M., Mateus, S., and Baretta, J. W. (2008). “Basic concepts of estuarine ecology,” in *Perspectives on Integrated Coastal Zone Management in South America*, eds. J. W. Baretta, M. Mateus, and R. Neves (IST Press).
- Mayer, T. D., and Jarrell, W. M. (2000). Phosphorus sorption during iron (II) oxidation in the presence of dissolved silica. *Water Res* 34, 3949–3956. doi: 10.1016/S0043-1354(00)00158-5.
- McCann, L. D., and Evin, L. A. (1989). Oligochaete influence on settlement, growth and reproduction in a surface-deposit-feeding polychaete. *J Exp Mar Biol Ecol* 131, 233–253. doi: 10.1016/0022-0981(89)90115-9.
- Meire, P., Ysebaert, T., van Damme, S., van den Bergh, E., Maris, T., and Struyf, E. (2005). The Scheldt estuary: A description of a changing ecosystem. *Hydrobiologia* 540, 1–11. doi: 10.1007/s10750-005-0896-8.
- Mermillod-Blondin, F., Rosenberg, R., François-Carcaillet, F., Norling, K., and Mauclair, L. (2004). Influence of bioturbation by three benthic infaunal species on microbial communities and biogeochemical processes in marine sediment. *Aquatic Microbial Ecology* 36, 271–284. doi: 10.3354/ameo36271.

- Mestdagh, S., Fang, X., Soetaert, K., Ysebaert, T., Moens, T., and van Colen, C. (2020). Seasonal variability in ecosystem functioning across estuarine gradients: The role of sediment communities and ecosystem processes. *Mar Environ Res* 162, 105096. doi: 10.1016/j.marenvres.2020.105096.
- Meysman, F., Middelburg, J., and Heip, C. (2006). Bioturbation: a fresh look at Darwin's last idea. *Trends Ecol Evol* 21, 688–695. doi: 10.1016/j.tree.2006.08.002.
- Michalopoulos, P., Aller, R. C., and Reeder, R. J. (2000). Conversion of diatoms to clays during early diagenesis in tropical, continental shelf muds. *Geology* 28, 1095. doi: 10.1130/0091-7613(2000)28<1095:CODTCD>2.0.CO;2.
- Middelburg, J. J., Duarte, C. M., and Gattuso, J.-P. (2005). "Respiration in coastal benthic communities," in *Respiration in Aquatic Ecosystems* (Oxford University Press), 206–224. doi: 10.1093/acprof:oso/9780198527084.003.0011.
- Middelburg, J. J., Klaver, G., Nieuwenhuize, J., Markuse, R. M., Vlug, T., and van der Nat, F. J. W. A. (1995a). Nitrous oxide emissions from estuarine intertidal sediments. *Hydrobiologia* 311, 43–55. doi: 10.1007/BF00008570.
- Middelburg, J. J., Klaver, G., Nieuwenhuize, J., and Vlug, T. (1995b). Carbon and nitrogen cycling in intertidal sediments near Doel, Scheldt Estuary. *Hydrobiologia* 311, 57–69. doi: 10.1007/BF00008571.
- Middelburg, J. J., Klaver, G., Nieuwenhuize, J., Wielemaker, A., de Haas, W., Vlug, T., et al. (1996). Organic matter mineralization in intertidal sediments along an estuarine gradient. *Mar Ecol Prog Ser* 132, 157–168.
- Middelburg, J. J., and Nieuwenhuize, J. (2000). Uptake of dissolved inorganic nitrogen in turbid, tidal estuaries. *Mar Ecol Prog Ser* 192, 79–88. doi: 10.3354/meps192079.
- Morgan, B., Rate, A. W., and Burton, E. D. (2012). Water chemistry and nutrient release during the resuspension of FeS-rich sediments in a eutrophic estuarine system. *Sci Total Environ* 432, 47–56. doi: 10.1016/j.scitotenv.2012.05.065.
- Morin, J., and Morse, J. W. (1999). Ammonium release from resuspended sediments in the Laguna Madre estuary. *Mar Chem* 65, 97–110. doi: 10.1016/S0304-4203(99)00013-4.
- Mortimer, R. J. G., Krom, M. D., Watson, P. G., Frickers, P. E., Davey, J. T., and Clifton, R. J. (1999). Sediment-water exchange of nutrients in the intertidal zone of the Humber estuary, UK. *Mar Pollut Bull* 37, 261–279. doi: 10.1016/S0025-326X(99)00053-3.

Bibliography

- Morys, C., Forster, S., and Graf, G. (2016). Variability of bioturbation in various sediment types and on different spatial scales in the southwestern Baltic Sea. 557, 31–49. doi: 10.3354/meps11837.
- Murray, N. J., Phinn, S. R., DeWitt, M., Ferrari, R., Johnston, R., Lyons, M. B., et al. (2019). The global distribution and trajectory of tidal flats. *Nature* 565, 222–225. doi: 10.1038/s41586-018-0805-8.
- Muylaert, K., van Nieuwerburgh, L., Sabbe, K., and Vyverman, W. (2002). Microphytobenthos communities in the freshwater tidal to brackish reaches of the Schelde estuary (Belgium). *Belgian Journal of Botany* 135, 15–26. Available at: <http://www.jstor.org/stable/20794495> [Accessed October 20, 2022].
- Nielsen, A., Eriksen, N., Iversen, J., and Riisgård, H. (1995). Feeding, growth and respiration in the polychaetes *Nereis diversicolor* (facultative filter-feeder) and *N. virens* (omnivorous)-a comparative study. *Mar Ecol Prog Ser* 125, 149–158. doi: 10.3354/meps125149.
- Niemistö, J., Kononets, M., Ekeröth, N., Tallberg, P., Tengberg, A., and Hall, P. O. J. (2018). Benthic fluxes of oxygen and inorganic nutrients in the archipelago of Gulf of Finland, Baltic Sea – Effects of sediment resuspension measured in situ. *J Sea Res* 135, 95–106. doi: 10.1016/j.seares.2018.02.006.
- Niemistö, J., and Lund-Hansen, L. C. (2019). Instantaneous Effects of Sediment Resuspension on Inorganic and Organic Benthic Nutrient Fluxes at a Shallow Water Coastal Site in the Gulf of Finland, Baltic Sea. *Estuaries and Coasts* 42, 2054–2071. doi: 10.1007/s12237-019-00648-5.
- Nienhuis, P. H., and Smaal, A. C. (1994). “The Oosterschelde estuary, a case-study of a changing ecosystem: an introduction,” in *The Oosterschelde Estuary (The Netherlands): a Case-Study of a Changing Ecosystem* (Dordrecht: Springer Netherlands), 1–14. doi: 10.1007/978-94-011-1174-4_1.
- NSW Department of Planning and Environment (2021). Why are estuaries important. Available at: <https://www.environment.nsw.gov.au/topics/water/estuaries/about-estuaries/why-estuaries-are-important> [Accessed November 9, 2022].
- Ogilvie, B. G., and Mitchell, S. F. (1998). Does sediment resuspension have persistent effects on phytoplankton? Experimental studies in three shallow lakes. *Freshw Biol* 40, 51–63. doi: 10.1046/j.1365-2427.1998.00331.x.
- Oksanen, J., Guillaume Blanchet, F., Friendly, M., Kindt, R., Legendre, P., McGlenn, D., et al. (2020). Vegan: community ecology package. Available at: <https://CRAN.R-project.org/package=vegan> [Accessed April 22, 2022].

- OSPAR (2008a). Assessment of the environmental impact of land reclamation. London, UK Available at: https://qsr2010.ospar.org/media/assessments/p00368_Land_Reclamation.pdf [Accessed November 8, 2022].
- OSPAR (2008b). Literature Review on the Impacts of Dredged Sediment Disposed at Sea. London, UK Available at: <https://www.ospar.org/documents?v=7119> [Accessed November 8, 2022].
- Pastor, L., Deflandre, B., Viollier, E., Cathalot, C., Metzger, E., Rabouille, C., et al. (2011). Influence of the organic matter composition on benthic oxygen demand in the Rhône River prodelta (NW Mediterranean Sea). *Cont Shelf Res* 31, 1008–1019. doi: 10.1016/j.csr.2011.03.007.
- Pastuszak, M., Conley, D. J., Humborg, C., Witek, Z., and Sitek, S. (2008). Silicon dynamics in the Oder estuary, Baltic Sea. *Journal of Marine Systems* 73, 250–262. doi: 10.1016/j.jmarsys.2007.10.013.
- Paterson, D. M., Hope, J. A., Kenworthy, J., Biles, C. L., and Gerbersdorf, S. U. (2018). Form, function and physics: the ecology of biogenic stabilisation. *J Soils Sediments* 18, 3044–3054. doi: 10.1007/s11368-018-2005-4.
- Paytan, A., and McLaughlin, K. (2007). The oceanic phosphorus cycle. *Chem Rev* 107, 563–576. doi: 10.1021/cr0503613.
- Pearson, T. H., and Rosenberg, R. (1977). Macrobenthic succession in relation to organic enrichment and pollution of the marine environment. *Oceanography and Marine Biology* 16, 229–311.
- Pelegri, S., Nielsen, L., and Blackburn, T. (1994). Denitrification in estuarine sediment stimulated by the irrigation activity of the amphipod *Corophium volutator*. *Mar Ecol Prog Ser* 105, 285–290. doi: 10.3354/meps105285.
- Pelegri, S. P., and Blackburn, T. H. (1994). Bioturbation effects of the amphipod *Corophium volutator* on microbial nitrogen transformations in marine sediments. *Mar Biol* 121, 253–258. doi: 10.1007/BF00346733.
- Percuoco, V. P., Kalnejais, L. H., and Officer, L. v. (2015). Nutrient release from the sediments of the Great Bay Estuary, N.H. USA. *Estuar Coast Shelf Sci* 161, 76–87. doi: 10.1016/j.ecss.2015.04.006.
- Peterson, M. S., and Ross, S. T. (1991). Dynamics of littoral fishes and decapods along a coastal river-estuarine gradient. *Estuar Coast Shelf Sci* 33, 467–483. doi: 10.1016/0272-7714(91)90085-P.

Bibliography

- Piebler, M. F., and Smyth, A. R. (2011). Habitat-specific distinctions in estuarine denitrification affect both ecosystem function and services. *Ecosphere* 2, art12. doi: 10.1890/ES10-00082.1.
- Precht, E., Franke, U., Polerecky, L., and Huettel, M. (2004). Oxygen dynamics in permeable sediments with wave-driven pore water exchange. *Limnol Oceanogr* 49, 693–705. doi: 10.4319/lo.2004.49.3.0693.
- QGIS Development Team (2021). QGIS Geographic Information System. Available at: <https://www.qgis.org/>.
- Qin, B., Hu, W., Gao, G., Luo, L., and Zhang, J. (2004). Dynamics of sediment resuspension and the conceptual schema of nutrient release in the large shallow Lake Taihu, China. *Chinese Science Bulletin* 49, 54. doi: 10.1360/03wdo174.
- Queirós, A. M., Birchenough, S. N. R., Bremner, J., Godbold, J. A., Parker, R. E., Romero-Ramirez, A., et al. (2013). A bioturbation classification of European marine infaunal invertebrates. *Ecol Evol* 3, 3958–3985. doi: 10.1002/ece3.769.
- Quintana, C. O., Tang, M., and Kristensen, E. (2007). Simultaneous study of particle reworking, irrigation transport and reaction rates in sediment bioturbated by the polychaetes *Heteromastus* and *Marenzelleria*. *J Exp Mar Biol Ecol* 352, 392–406. doi: 10.1016/j.jembe.2007.08.015.
- R Core Team (2020). R: A Language and environment for statistical computing.
- Raffaelli, D., Emmerson, M., Solan, M., Biles, C., and Paterson, D. (2003). Biodiversity and ecosystem processes in shallow coastal waters: an experimental approach. *J Sea Res* 49, 133–141. doi: 10.1016/S1385-1101(02)00200-9.
- Reed, D. J., Davidson-arnott, R., and Perillo, G. M. E. (2009). “Estuaries, coastal marshes, tidal flats and coastal dunes,” in *Geomorphology and Global Environmental Change*, eds. O. Slaymaker, T. Spencer, and C. Embleton-Hamann (Cambridge University Press), 130–157.
- Reuss, N. (2005). Sediment pigments as biomarkers of environmental change. *Ph.D. thesis*.
- Richard, A., Orvain, F., Morelle, J., Romero-Ramirez, A., Bernard, G., Paulin-Henricksson, S., et al. (2023). Impact of Sediment Bioturbation on Microphytobenthic Primary Producers: Importance of Macrobenthic Functional Traits. *Ecosystems*. doi: 10.1007/s10021-022-00817-x.
- Riedl, R. J., Huang, N., and Machan, R. (1972). The subtidal pump: a mechanism of interstitial water exchange by wave action. *Mar Biol* 13, 210–221. doi: 10.1007/BF00391379.

- Rijkswaterstaat (2016). Ecotopenkaarten. *ecotopenkaart_oosterschelde_2016*. Available at: <https://maps.rijkswaterstaat.nl/gwproj55/index.html?viewer=Ecotopen.Webviewer> [Accessed January 12, 2022].
- Rijkswaterstaat (n.d.). National Georegister. Available at: <https://www.nationaalgeoregister.nl/geonetwork/srv//dut/catalog.search#/home> [Accessed October 15, 2021a].
- Rijkswaterstaat (n.d.). Rijkswaterstaat Waterinfo. *Nutriënten en eutrofiëringsparameters-OW*. Available at: <https://waterinfo.rws.nl/> [Accessed August 2, 2022b].
- Rijkswaterstaat (n.d.). Rijkswaterstaat Waterinfo. Available at: <https://waterinfo.rws.nl/> [Accessed September 25, 2020c].
- Rios-Yunes, D., Grandjean, T., di Primio, A., Tiano, J., Bouma, T. J., van Oevelen, D., et al. (2023a). Sediment resuspension enhances nutrient exchange in intertidal mudflats. *Front Mar Sci* 10. doi: 10.3389/fmars.2023.1155386.
- Rios-Yunes, D., Tiano, J. C., van Oevelen, D., van Dalen, J., and Soetaert, K. (2023b). Annual biogeochemical cycling in intertidal sediments of a restored estuary reveals dependence of N, P, C and Si cycles to temperature and water column properties. *Estuar Coast Shelf Sci* 282, 108227. doi: 10.1016/j.ecss.2023.108227.
- Rios-Yunes, D., Tiano, J. C., van Rijswijk, P., De Borger, E., van Oevelen, D., and Soetaert, K. (2023c). Long-term changes in ecosystem functioning of a coastal bay expected from a shifting balance between intertidal and subtidal habitats. *Cont Shelf Res* 254, 104904. doi: 10.1016/j.csr.2022.104904.
- Rivera-Ingraham, G. A., and Lignot, J.-H. (2017). Osmoregulation, bioenergetics and oxidative stress in coastal marine invertebrates: raising the questions for future research. *Journal of Experimental Biology* 220, 1749–1760. doi: 10.1242/jeb.135624.
- Rocha, C., and Cabral, A. P. (1998). The Influence of Tidal Action on Porewater Nitrate Concentration and Dynamics in Intertidal Sediments of the Sado Estuary. *Estuaries* 21, 635. doi: 10.2307/1353301.
- Rönn, C., Bonsdorff, E., and Nelson, W. G. (1988). Predation as a mechanism of interference within infauna in shallow brackish water soft bottoms; experiments with an infauna predator, *Nereis diversicolor* O.F. Müller. *J Exp Mar Biol Ecol* 116, 143–157. doi: 10.1016/0022-0981(88)90052-4.
- Rossi, F., Gribsholt, B., Middelburg, J., and Heip, C. (2008). Context-dependent effects of suspension feeding on intertidal ecosystem functioning. *Mar Ecol Prog Ser* 354, 47–57. doi: 10.3354/meps07213.

Bibliography

- Ruttenberg, K. C. (2019). "Phosphorus Cycle," in *Encyclopedia of Ocean Sciences* (Elsevier), 447–460. doi: 10.1016/B978-0-12-409548-9.10807-3.
- Rysgaard, S., Risgaard-Petersen, N., Niels Peter, S., Kim, J., and Lars Peter, N. (1994). Oxygen regulation of nitrification and denitrification in sediments. *Limnol Oceanogr* 39, 1643–1652. doi: 10.4319/lo.1994.39.7.1643.
- Rysgaard, S. S., Thastum, P., Dalsgaard, T., Christensen, P. B., Sloth, N. P., and Rysgaard, S. S. (1999). Effects of Salinity on NH₄⁺ Adsorption Capacity, Nitrification, and Denitrification in Danish Estuarine Sediments. *Estuaries* 22, 21. doi: 10.2307/1352923.
- Sagemann, J., Skowronek, F., Dahmke, A., and Schulz, H. D. (1996). Pore-water response on seasonal environmental changes in intertidal sediments of the Weser Estuary, Germany. *Environmental Geology* 27, 362–369. doi: 10.1007/s002540050070.
- Sajilata, M. G., Singhal, R. S., and Kamat, M. Y. (2008). The Carotenoid Pigment Zeaxanthin—A Review. *Compr Rev Food Sci Food Saf* 7, 29–49. doi: 10.1111/j.1541-4337.2007.00028.x.
- Schallenberg, M., and Burns, C. W. (2004). Effects of sediment resuspension on phytoplankton production: teasing apart the influences of light, nutrients and algal entrainment. *Freshw Biol* 49, 143–159. doi: 10.1046/j.1365-2426.2003.01172.x.
- Schimek, C., Stadnichuk, I. N., Knaust, R., and Wehrmeyer, W. (1994). Detection of chlorophyll *c*₁ and magnesium-2,4-divinylpheoporphyryl *a*₅ monomethylester in cryptophytes. *J Phycol* 30, 621–627. doi: 10.1111/j.0022-3646.1994.00621.x.
- Serôdio, J., and Paterson, D. M. (2021). "Role of Microphytobenthos in the Functioning of Estuarine and Coastal Ecosystems," in 1–13. doi: 10.1007/978-3-319-71064-8_11-1.
- Seys, J., Vincx, M., and Meire, P. (1999). Spatial distribution of oligochaetes (Clitellata) in the tidal freshwater and brackish parts of the Schelde estuary (Belgium). *Hydrobiologia* 406, 119–132. doi: 10.1023/A:1003751512971.
- Sharp, J. H., Pennock, J. R., Church, T. M., Tramontano, J. M., and Cifuentes, L. A. (1984). "The estuarine interaction of nutrients, organics, and metals: a case study in the Delaware estuary," in *The Estuary As a Filter* (Elsevier), 241–258. doi: 10.1016/B978-0-12-405070-9.50017-7.
- Shaughnessy, A. R., Sloan, J. J., Corcoran, M. J., and Hasenmueller, E. A. (2019). Sediments in Agricultural Reservoirs Act as Sinks and Sources for Nutrients over Various Timescales. *Water Resour Res* 55, 5985–6000. doi: 10.1029/2018WR024004.
- Shrestha, P. L., Kaluarachchi, I. D., Anid, P. J., Blumberg, A. F., and DiToro, D. M. (2001). Cohesive Sediment Resuspension: Experimentation and Analysis. in *Bridging the*

- Gap* (Reston, VA: American Society of Civil Engineers), 1–8. doi: 10.1061/40569(2001)258.
- Slomp, C. P. (2011). “Phosphorus Cycling in the Estuarine and Coastal Zones,” in *Treatise on Estuarine and Coastal Science* (Elsevier), 201–229. doi: 10.1016/B978-0-12-374711-2.00506-4.
- Slomp, C. P., Epping, E. H. G., Helder, W., and Raaphorst, W. van (1996). A key role for iron-bound phosphorus in authigenic apatite formation in North Atlantic continental platform sediments. *J Mar Res* 54, 1179–1205. doi: 10.1357/0022240963213745.
- Smaal, A. C., and Nienhuis, P. H. (1992). The eastern Scheldt (The Netherlands), from an estuary to a tidal bay: A review of responses at the ecosystem level. *Netherlands Journal of Sea Research* 30, 161–173. doi: 10.1016/0077-7579(92)90055-J.
- Smaal, A. C., Schellekens, T., van Stralen, M. R., and Kromkamp, J. C. (2013). Decrease of the carrying capacity of the Oosterschelde estuary (SW Delta, NL) for bivalve filter feeders due to overgrazing? *Aquaculture* 404–405, 28–34. doi: 10.1016/j.aquaculture.2013.04.008.
- Small, C., Nicholls, R. J., Smallt, C., and Nichollst, R. J. (2003). A Global Analysis of Human Settlement in Coastal Zones. *Source: Journal of Coastal Research* 19, 584–599. doi: 10.2307/4299200.
- Small, N., Munday, M., and Durance, I. (2017). The challenge of valuing ecosystem services that have no material benefits. *Global Environmental Change* 44, 57–67. doi: 10.1016/j.gloenvcha.2017.03.005.
- Smeaton, C., and Austin, W. E. N. (2022). Quality Not Quantity: Prioritizing the Management of Sedimentary Organic Matter Across Continental Shelf Seas. *Geophys Res Lett* 49. doi: 10.1029/2021GL097481.
- Soetaert, K., and Herman, P. M. J. (1995a). Carbon flows in the Westerschelde estuary (The Netherlands) evaluated by means of an ecosystem model (MOSES). *Hydrobiologia* 311, 247–266. doi: 10.1007/BF00008584.
- Soetaert, K., and Herman, P. M. J. (1995b). Nitrogen dynamics in the Westerschelde estuary (SW Netherlands) estimated by means of the ecosystem model MOSES. *Hydrobiologia* 311, 225–246. doi: 10.1007/BF00008583.
- Soetaert, K., Herman, P. M. J., and Kromkamp, J. (1994a). Living in the twilight: estimating net phytoplankton growth in the Westerschelde estuary (The Netherlands) by

Bibliography

- means of an ecosystem model (MOSES). *J Plankton Res* 16, 1277–1301. doi: 10.1093/plankt/16.10.1277.
- Soetaert, K., Herman, P. M. J., and Middelburg, J. J. (1996a). A model of early diagenetic processes from the shelf to abyssal depths. *Geochim Cosmochim Acta* 60, 1019–1040. doi: 10.1016/0016-7037(96)00013-0.
- Soetaert, K., Herman, P. M. J., Middelburg, J. J., Heip, C., deStigter, H. S., van Weering, T. C. E., et al. (1996b). Modelling ²¹⁰Pb-derived mixing activity in ocean margin sediments: Diffusive versus nonlocal mixing. *J Mar Res* 54, 1207–1227. doi: 10.1357/0022240963213808.
- Soetaert, K., Herman, P. M. J., and Scholten, H. (1992). Moses: model of the Scheldt estuary: ecosystem model development under SENECA.
- Soetaert, K., Middelburg, J. J., Heip, C., Meire, P., van Damme, S., and Maris, T. (2006). Long-term change in dissolved inorganic nutrients in the heterotrophic Scheldt estuary (Belgium, The Netherlands). in *Limnology and Oceanography* (American Society of Limnology and Oceanography Inc.), 409–423. doi: 10.4319/lo.2006.51.1_part_2.0409.
- Soetaert, K., Petzoldt, T., and Meysman, F. (2010). marelac: Tools for Aquatic Sciences.
- Soetaert, K., and Provoost, P. (2016). Turbo: Bioturbation and profile models.
- Soetaert, K., Vincx, M., Wittoeck, J., Tulkens, M., and Van Gansbeke, D. (1994b). Spatial Patterns of Westerschelde Meiobenthos. *Estuar Coast Shelf Sci* 39, 367–388. doi: 10.1006/ecss.1994.1070.
- Statham, P. J. (2012a). Nutrients in estuaries — An overview and the potential impacts of climate change. *Science of The Total Environment* 434, 213–227. doi: 10.1016/j.scitotenv.2011.09.088.
- Statham, P. J. (2012b). Nutrients in estuaries - An overview and the potential impacts of climate change. *Science of the Total Environment* 434, 213–227. doi: 10.1016/j.scitotenv.2011.09.088.
- Stauber, J. L., Chariton, A., and Apte, S. (2016). “Global Change,” in *Marine Ecotoxicology* (Elsevier), 273–313. doi: 10.1016/B978-0-12-803371-5.00010-2.
- Stratmann, T., van Oevelen, D., Martínez Arbizu, P., Wei, C.-L., Liao, J.-X., Cusson, M., et al. (2020). The BenBioDen database, a global database for meio-, macro- and megabenthic biomass and densities. *Sci Data* 7, 206. doi: 10.1038/s41597-020-0551-2.

- Struyf, E., and Conley, D. J. (2009). Silica: an essential nutrient in wetland biogeochemistry. *Front Ecol Environ* 7, 88–94. doi: 10.1890/070126.
- Struyf, E., Dausse, A., van Damme, S., Bal, K., Gribsholt, B., Boschker, H. T. S. S., et al. (2006). Tidal marshes and biogenic silica recycling at the land-sea interface. *Limnol Oceanogr* 51, 838–846. doi: 10.4319/l0.2006.51.2.0838.
- Struyf, E., van Damme, S., Gribsholt, B., and Meire, P. (2005a). Freshwater marshes as dissolved silica recyclers in an estuarine environment (Schelde estuary, Belgium). *Hydrobiologia* 540, 69–77. doi: 10.1007/s10750-004-7104-0.
- Struyf, E., van Damme, S., Gribsholt, B., Middelburg, J., and Meire, P. (2005b). Biogenic silica in tidal freshwater marsh sediments and vegetation (Schelde estuary, Belgium). *Mar Ecol Prog Ser* 303, 51–60. doi: 10.3354/meps303051.
- Struyf, E., van Damme, S., and Meire, P. (2004a). Possible effects of climate change on estuarine nutrient fluxes: A case study in the highly nutrified Schelde estuary (Belgium, the Netherlands). *Estuar Coast Shelf Sci* 60, 649–661. doi: 10.1016/j.ecss.2004.03.004.
- Struyf, E., Van Damme, S., and Meire, P. (2004b). Possible effects of climate change on estuarine nutrient fluxes: a case study in the highly nutrified Schelde estuary (Belgium, The Netherlands). *Estuar Coast Shelf Sci* 60, 649–661. doi: 10.1016/j.ecss.2004.03.004.
- Swan, B. K., Watts, J. M., Reifel, K. M., and Hurlbert, S. H. (2007). Role of the polychaete *Neanthes succinea* in phosphorus regeneration from sediments in the Salton Sea, California. in *Hydrobiologia*, 111–125. doi: 10.1007/s10750-006-0298-6.
- Swaney, D. P., Hong, B., Ti, C., Howarth, R. W., and Humborg, C. (2012). Net anthropogenic nitrogen inputs to watersheds and riverine N export to coastal waters: a brief overview. *Curr Opin Environ Sustain* 4, 203–211. doi: 10.1016/j.cosust.2012.03.004.
- Syvitski, J. P. M. M., Vörösmarty, C. J., Kettner, A. J., and Green, P. (2005). Impact of humans on the flux of terrestrial sediment to the global coastal ocean. *Science (1979)* 308, 376–380. doi: 10.1126/science.1109454.
- Tang, C., Li, Y., He, C., and Acharya, K. (2020). Dynamic behaviour of sediment resuspension and nutrients release in the shallow and wind-exposed Meiliang Bay of Lake Taihu. *Science of The Total Environment* 708, 135131. doi: 10.1016/j.scitotenv.2019.135131.
- Tartowski, S. L., and Howarth, R. W. (2013). “Nitrogen, Nitrogen Cycle,” in *Encyclopedia of Biodiversity* (Elsevier), 537–546. doi: 10.1016/B978-0-12-384719-5.00098-8.

Bibliography

- Tee, H. S., Waite, D., Lear, G., and Handley, K. M. (2021). Microbial river-to-sea continuum: gradients in benthic and planktonic diversity, osmoregulation and nutrient cycling. *Microbiome* 9, 190. doi: 10.1186/s40168-021-01145-3.
- ten Brinke, W. B. M. (1994). "Hydrodynamic and geomorphological changes in the tidal system," in *The Oosterschelde Estuary (The Netherlands): a Case-Study of a Changing Ecosystem* (Dordrecht: Springer Netherlands), 15–16. doi: 10.1007/978-94-011-1174-4_2.
- Tengberg, A., Almroth, E., and Hall, P. (2003). Resuspension and its effects on organic carbon recycling and nutrient exchange in coastal sediments: in situ measurements using new experimental technology. *J Exp Mar Biol Ecol* 285–286, 119–142. doi: 10.1016/S0022-0981(02)00523-3.
- Terai, H., Goto, N., and Mitamura, O. (2000). Seasonal variation in primary production of microphytobenthos at the Isshiki intertidal flat in Mikawa Bay. *Limnology (Tokyo)* 1, 133–138. doi: 10.1007/s102010070019.
- Thamdrup, B., and Dalsgaard, T. (2002). Production of N₂ through anaerobic ammonium oxidation coupled to nitrate reduction in marine sediments. *Appl Environ Microbiol* 68, 1312–1318. doi: 10.1128/AEM.68.3.1312-1318.2002.
- Thoms, F., Burmeister, C., Dippner, J. W., Gogina, M., Janas, U., Kendzierska, H., et al. (2018). Impact of Macrofaunal Communities on the Coastal Filter Function in the Bay of Gdansk, Baltic Sea. *Front Mar Sci* 5. doi: 10.3389/fmars.2018.00201.
- Thouzeau, G., Grall, J., Clavier, J., Chauvaud, L., Jean, F., Leynaert, A., et al. (2007). Spatial and temporal variability of benthic biogeochemical fluxes associated with macrophytic and macrofaunal distributions in the Thau lagoon (France). *Estuar Coast Shelf Sci* 72, 432–446. doi: 10.1016/j.ecss.2006.11.028.
- Tiano, J. C., de Borger, E., O'Flynn, S., Cheng, C. H., van Oevelen, D., and Soetaert, K. (2021). Physical and electrical disturbance experiments uncover potential bottom fishing impacts on benthic ecosystem functioning. *J Exp Mar Biol Ecol* 545, 151628. doi: 10.1016/j.jembe.2021.151628.
- Tiano, J. C., Witbaard, R., Bergman, M. J. N., van Rijswijk, P., Tramper, A., van Oevelen, D., et al. (2019). Acute impacts of bottom trawl gears on benthic metabolism and nutrient cycling. *ICES Journal of Marine Science* 76, 1917–1930. doi: 10.1093/icesjms/fszo60.
- Toussaint, E., De Borger, E., Braeckman, U., De Backer, A., Soetaert, K., and Vanaverbeke, J. (2021). Faunal and environmental drivers of carbon and nitrogen cycling along a permeability gradient in shallow North Sea sediments. *Science of The Total Environment* 767, 144994. doi: 10.1016/j.scitotenv.2021.144994.

- Tréguer, P. J., and de La Rocha, C. L. (2013). The World Ocean Silica Cycle. *Ann Rev Mar Sci* 5, 477–501. doi: 10.1146/annurev-marine-121211-172346.
- Tréguer, P., Nelson, D. M., van Bennekom, A. J., DeMaster, D. J., Leynaert, A., and Quéguiner, B. (1995). The Silica Balance in the World Ocean: A Reestimate. *Science (1979)* 268, 375–379. doi: 10.1126/science.268.5209.375.
- Turner Designs (n.d.). S-0243 Cyclops-7 or 7F Calibration Using Liquid Dye Standards. Available at: <http://docs.turnerdesigns.com/t2/doc/tech-notes/S-0243.pdf> [Accessed February 28, 2023].
- Underwood, G. J. C., and Kromkamp, J. (1999). Primary Production by Phytoplankton and Microphytobenthos in Estuaries. *Adv Ecol Res* 29, 93–153. doi: 10.1016/S0065-2504(08)60192-0.
- Underwood, G., Phillips, J., and Saunders, K. (1998). Distribution of estuarine benthic diatom species along salinity and nutrient gradients. *Eur J Phycol* 33, 173–183. doi: 10.1080/09670269810001736673.
- Usui, T., Koike, I., and Ogura, N. (1998). Tidal Effect on Dynamics of Pore Water Nitrate in Intertidal Sediment of a Eutrophic Estuary. *J Oceanogr* 54.
- van Colen, C., Rossi, F., Montserrat, F., Andersson, M. G. I., Gribsholt, B., Herman, P. M. J., et al. (2012). Organism-Sediment Interactions Govern Post-Hypoxia Recovery of Ecosystem Functioning. *PLoS One* 7, e49795. doi: 10.1371/journal.pone.0049795.
- van Damme, S., Struyf, E., Maris, T., Ysebaert, T., Dehairs, F., Tackx, M., et al. (2005). Spatial and temporal patterns of water quality along the estuarine salinity gradient of the Scheldt estuary (Belgium and The Netherlands): results of an integrated monitoring approach. *Hydrobiologia* 540, 29–45. doi: 10.1007/s10750-004-7102-2.
- van den Meersche, K., Soetaert, K., and Middelburg, J. J. (2011). Plankton dynamics in an estuarine plume: A mesocosm ^{13}C and ^{15}N tracer study. *Mar Ecol Prog Ser* 429, 29–43. doi: 10.3354/meps09097.
- van den Meersche, K., van Rijswijk, P., Soetaert, K., and Middelburg, J. J. (2009). Autochthonous and allochthonous contributions to mesozooplankton diet in a tidal river and estuary: Integrating carbon isotope and fatty acid constraints. *Limnol Oceanogr* 54, 62–74. doi: 10.4319/lo.2009.54.1.0062.
- van der Zee, C., Roelvros, N., and Chou, L. (2007). Phosphorus speciation, transformation and retention in the Scheldt estuary (Belgium/The Netherlands) from the freshwater tidal limits to the North Sea. *Mar Chem* 106, 76–91. doi: 10.1016/j.marchem.2007.01.003.

Bibliography

- van Hoven, W. (1975). Aspects of the Respiratory Physiology and Oxygen Preferences of Four Aquatic Oligochaetes (Annelida). *Zoologica Africana* 10, 29–44. doi: 10.1080/00445096.1975.11447490.
- van Leeuwe, M. A., Visser, R. J. W., and Stefels, J. (2014). The pigment composition of *Phaeocystis antarctica* (Haptophyceae) under various conditions of light, temperature, salinity, and iron. *J Phycol* 50, 1070–1080. doi: 10.1111/jpy.12238.
- van Zanten, E., and Adriaanse, L. A. (2008). Verminderd getij, verkenning naar mogelijkheden om het verlies van platen, slikken en schorren in de Oosterschelde te beperken. Available at: https://puc.overheid.nl/rijkswaterstaat/doc/PUC_132565_31/#:~:text=De%20Oosterschelde%20blijft%20veranderen, bekend%20als%20de%20'zandhonger'. [Accessed April 4, 2022].
- Vanderborght, J.-P., Folmer, I. M., Aguilera, D. R., Uhrenholdt, T., and Regnier, P. (2007). Reactive-transport modelling of C, N, and O₂ in a river–estuarine–coastal zone system: Application to the Scheldt estuary. *Mar Chem* 106, 92–110. doi: 10.1016/j.marchem.2006.06.006.
- VanKoningsveld, M., Mulder, J. P. M., Stive, M. J. F., VanDerValk, L., and VanDerWeck, A. W. (2008). Living with Sea-Level Rise and Climate Change: A Case Study of the Netherlands. *J Coast Res* 242, 367–379. doi: 10.2112/07A-0010.1.
- Vejre, H., Jensen, F. S., and Thorsen, B. J. (2010). Demonstrating the importance of intangible ecosystem services from peri-urban landscapes. *Ecological Complexity* 7, 338–348. doi: 10.1016/j.ecocom.2009.09.005.
- Wallmann, K. (2010). Phosphorus imbalance in the global ocean? *Global Biogeochem Cycles* 24, n/a-n/a. doi: 10.1029/2009GB003643.
- Wang, Z. B., Vandenbruwaene, W., Taal, M., and Winterwerp, H. (2019). Amplification and deformation of tidal wave in the Upper Scheldt Estuary. *Ocean Dyn* 69, 829–839. doi: 10.1007/s10236-019-01281-3.
- Weng, L., van Riemsdijk, W. H., and Hiemstra, T. (2012). Factors Controlling Phosphate Interaction with Iron Oxides. *J Environ Qual* 41, 628–635. doi: 10.2134/jeq2011.0250.
- Wetsteyn, L. P. M. J., Duin, R. N. M., Kromkamp, J., Latuhihin, M. J., Peene, J., Power, A., et al. (2003). Verkenning draagkracht Oosterschelde. Rijksinstituut voor Kust en Zee/RIKZ Available at: https://www.researchgate.net/publication/230578453_Verkenning_draagkracht_Oosterschelde [Accessed February 16, 2022].

- Wetsteyn, L. P. M. J., and Kromkamp, J. C. (1994). Turbidity, nutrients and phytoplankton primary production in the Oosterschelde (The Netherlands) before, during and after a large-scale coastal engineering project (1980–1990). *Hydrobiologia* 282–283, 61–78. doi: 10.1007/BF00024622.
- Widdows, J., and Brinsley, M. (2002). Impact of biotic and abiotic processes on sediment dynamics and the consequences to the structure and functioning of the intertidal zone. *J Sea Res* 48, 143–156. doi: 10.1016/S1385-1101(02)00148-X.
- Widdows, J., Brinsley, M., Salkeld, P., and Lucas, C. (2000a). Influence of biota on spatial and temporal variation in sediment erodability and material flux on a tidal flat (Westerschelde, The Netherlands). *Mar Ecol Prog Ser* 194, 23–37. doi: 10.3354/meps194023.
- Widdows, J., Brinsley, M., Salkeld, P., and Lucas, C. (2000b). Influence of biota on spatial and temporal variation in sediment erodability and material flux on a tidal flat (Westerschelde, The Netherlands). *Mar Ecol Prog Ser* 194, 23–37. doi: 10.3354/meps194023.
- Widdows, J., Brown, S., Brinsley, M. D., Salkeld, P. N., and Elliott, M. (2000c). Temporal changes in intertidal sediment erodability: influence of biological and climatic factors. *Cont Shelf Res* 20, 1275–1289. doi: 10.1016/S0278-4343(00)00023-6.
- Williams, B. A., Watson, J. E. M., Beyer, H. L., Klein, C. J., Montgomery, J., Runting, R. K., et al. (2022). Global rarity of intact coastal regions. *Conservation Biology* 36. doi: 10.1111/cobi.13874.
- Wolff, W. J. (1973). The estuary as a habitat an analysis of data on the soft-bottom macrofauna of the estuarine area of the rivers Rhine, Meuse and Scheldt.
- Wollast, R., and Peters, J. J. (1978). “Biogeochemical properties of an estuarine system: the River Scheldt,” in *Biogeochemistry of estuarine sediments*, ed. Goldberg E.D. (Paris: UNESCO), 279–293.
- Woodward, F. I. (2007). Global primary production. *Current Biology* 17, R269–R273. doi: 10.1016/j.cub.2007.01.054.
- Woth, K., Weisse, R., and von Storch, H. (2006). Climate change and North Sea storm surge extremes: an ensemble study of storm surge extremes expected in a changed climate projected by four different regional climate models. *Ocean Dyn* 56, 3–15. doi: 10.1007/s10236-005-0024-3.
- Yamada, S., and D’Elia, C. (1984). Silicic acid regeneration from estuarine sediment cores. *Mar Ecol Prog Ser* 18, 113–118. doi: 10.3354/meps018113.

Bibliography

- Yang, S.-L., Friedrichs, C. T., Shi, Z., Ding, P.-X., Zhu, J., and Zhao, Q.-Y. (2003). Morphological response of tidal marshes, flats and channels of the Outer Yangtze River mouth to a major storm. *Estuaries* 26, 1416–1425. doi: 10.1007/BF02803650.
- Yilmaz, C., and Gökmen, V. (2016). “Chlorophyll,” in *Encyclopedia of Food and Health* (Elsevier), 37–41. doi: 10.1016/B978-0-12-384947-2.00147-1.
- Yoshino, K., Tsugeki, N. K., Amano, Y., Hayami, Y., Hamaoka, H., and Omori, K. (2012). Intertidal bare mudflats subsidize subtidal production through outwelling of benthic microalgae. *Estuar Coast Shelf Sci* 109, 138–143. doi: 10.1016/j.ecss.2012.05.021.
- Ysebaert, T., Herman, P. M. J., Meire, P., Craeymeersch, J., Verbeek, H., and Heip, C. H. R. (2003a). Large-scale spatial patterns in estuaries: Estuarine macrobenthic communities in the Schelde estuary, NW Europe. *Estuar Coast Shelf Sci* 57, 335–355. doi: 10.1016/S0272-7714(02)00359-1.
- Ysebaert, T., Herman, P. M. J., Meire, P., Craeymeersch, J., Verbeek, H., and Heip, C. H. R. (2003b). Large-scale spatial patterns in estuaries: estuarine macrobenthic communities in the Schelde estuary, NW Europe. *Estuar Coast Shelf Sci* 57, 335–355. doi: 10.1016/S0272-7714(02)00359-1.
- Ysebaert, T., Meire, P., Coosen, J., and Essinik, K. (1998). Zonation of intertidal macrobenthos in the estuaries of Schelde and Ems. *Aquat Ecol* 32, 53–71. doi: 10.1023/A:1009912103505.
- Ysebaert, T., Meire, P., Maes, D., and Buijs, J. (1993). The benthic macrofauna along the estuarine gradient of the Schelde estuary. *Netherlands Journal of Aquatic Ecology* 27, 327–341. doi: 10.1007/BF02334796.
- Ysebaert, T., van der Hoek, D.-J., Wortelboer, R., Wijsman, J. W. M., Tangelder, M., and Nolte, A. (2016). Management options for restoring estuarine dynamics and implications for ecosystems: A quantitative approach for the Southwest Delta in the Netherlands. *Ocean Coast Manag* 121, 33–48. doi: 10.1016/j.ocecoaman.2015.11.005.
- Zapata, M., Rodríguez, F., and Garrido, J. (2000). Separation of chlorophylls and carotenoids from marine phytoplankton: a new HPLC method using a reversed phase C8 column and pyridine-containing mobile phases. *Mar Ecol Prog Ser* 195, 29–45. doi: 10.3354/meps195029.
- Zhang, J. Z., and Huang, X. L. (2011). Effect of temperature and salinity on phosphate sorption on marine sediments. *Environ Sci Technol* 45, 6831–6837. doi: 10.1021/es200867p.

Zhou, Z., Bouma, T. J., Fivash, G. S., Ysebaert, T., van IJzerloo, L., van Dalen, J., et al. (2022). Thermal stress affects bioturbators' burrowing behaviour: A mesocosm experiment on common cockles (*Cerastoderma edule*). *Science of The Total Environment* 824, 153621. doi: 10.1016/j.scitotenv.2022.153621.

Zwarts, L., Blomert, A.-M., Bos, D., and Sikkema, M. (n.d.). Exploitation of intertidal flats in the Oosterschelde by estuarine birds A&W report 1657.



